THE ISOCYANOARENE MOTIF IN ORGANOMETALLIC CRYSTAL ENGINEERING AND NEW AZULENE-BASED ORGANOMETALLICS

By

John Joseph Meyers, Jr.

Submitted to the graduate degree program in the Department of Chemistry and the Graduate Faculty of the University of Kansas in partial fulfillment of the requirements for the degree of Doctor of Philosophy.

_____

Dr. Mikhail V. Barybin, Chairperson

_____

Dr. Cindy L. Berrie

_____

Dr. Timothy A. Jackson

_____

Dr. Shenqiang Ren

_____

Dr. Susan M. Williams

Date Defended: May 13, 2013

The Dissertation Committee for John J. Meyers, Jr.

certifies that this is the approved version of the following dissertation:

THE ISOCYANOARENE MOTIF IN ORGANOMETALLIC CRYSTAL ENGINEERING AND NEW AZULENE-BASED ORGANOMETALLICS

_____

Dr. Mikhail V. Barybin, Chairperson

Date approved: May 31, 2013

Abstract

Isocyanides (:C≡N-R) and their metal complexes play an important role in many areas including synthetic organic chemistry, catalysis, diagnostic medicine, as well as surface, polymer, and materials sciences. The rich chemistry of isocyanides stems from the tunability of the molecular and electronic structure through variations of the substituent R. Isocyanides represent a rather versatile class of ligands and can accommodate metal ions in both high and low oxidation states upon complexation. Isocyanoarene derivatives have been shown to be effective in the design of charge transport materials (e.g., molecular wires). In addition, di- and other polyisocyanoarenes have been employed as building blocks in the coordination chemistry of polynuclear organometallics. In the past decade, Barybin *et al*. have developed the chemistry of electron-rich compounds and materials that incorporate isocyanoarene ligands featuring nonbenzenoid aromatic azulenyl and η^5-cyclopendadienyl substituents. In this Dissertation, isocyanide-terminated benzenoid and nonbenzenoid arenes as well as the organometallic complexes thereof are discussed.

Chapter I constitutes a review of recent developments in the chemistry of isocyanoarenes as ligands in low-valent organometallics. Particular emphases are placed on (1) isocyanometalates (isocyanide complexes of metals in negative oxidation states), (2) low-coordinate complexes of extremely bulky isocyanoarenes, and (3) the chemistry of nonbenzenoid isocyanoarenes.

The first part of Chapter II is dedicated to the chemistry of an unusual supramolecular charge-transfer ensemble ($[Cp_2Co]_2[\{(OC)_5V\}_2(\mu\text{-}CNC_6Me_4NC)])_\infty$ (Cp = cyclopentadienyl) held together via synergistic π-stacking and contact-ion interactions. This three-dimensional, porous framework features channels capable of housing linear molecules such as acetonitrile, carbon dioxide, etc., and offers new opportunities in organometallic crystal engineering. The

second part of Chapter II describes preliminary studies on the interaction of the novel 2-isocyano-1,3-dimethylazulene ligand with sub-valent metal ions (e.g., Co(I-) and Fe(II-)).

Chapter III of this Dissertation describes the syntheses and coordination chemistry of the polar, linear 2-isocyano-1,3-diethoxycarbonyl-2',6-biazulene ligand and related species. Detailed electrochemical and spectroscopic studies of these novel ligands and their low-valent homoleptic complexes shed light on electron delocalization between the azulenic/biazulenic π-systems and electron-rich metal ions mediated by the isocyanide junction.

In Chapter IV, synthetic studies toward a family of azulene-based metal-organic frameworks are described. Two-dimensional, rectangular metal-organic frameworks were formed by bridging {Cp*ClIr(III)} corner fragments (Cp* = pentamethylcyclopentadienyl) with either asymmetric 2,6-diisocyanoazulenic or symmetric 2,2'-diisocyano-6,6'-biazulenic ditopic edge units. 16-Electron metal carbonyl units, namely $[Cr(CO)_5]$, were employed as end caps to control orientation of the molecular dipole of 2,6-diisocyano-1,3-diethoxycarbonylazulene within tetrametallic molecular frameworks.

Acknowledgments

First and foremost, I am eternally indebted to my research mentor for none of this would have been possible without him. Misha, you taught, encouraged, listened, supported, and inspired throughout our time together. You have played such a large role in my personal and professional development for which I will never be able to repay you. If, as a professor, I possess only a fraction of your teaching and mentoring abilities, I know I will be able to greatly impact the lives of future students. I look forward to our life-long friendship and will always remember what you have so generously done.

I would like to thank the Department of Chemistry at KU for providing the facilities for my research as well as the opportunities and funding to further my teaching experience. Thank you to the entire faculty who contributed to my graduate education. To Dr. Justin Douglas and Sarah Neuenswander, your expertise and discussions in regard to NMR spectroscopy provided me experience and understanding integral to my work at KU. Many thanks go to Dr. Victor Day and Dr. Doug Powell (University of Oklahoma) for their expertise with X-ray crystallographic experiments. Furthermore, I am grateful for funding awarded to Misha from the NSF (CHE-0548212 and CHE-1214102) and the DuPont Young Professor Award that fueled my research.

A special thank you is owed to Dr. Timothy Jackson and Dr. Roderick Black. Dr. Jackson, you taught every graduate inorganic course I ever took at KU and I truly appreciate your insight over the years (and for allowing me to use your lab equipment). I am honored to have been able to learn from you in many different settings and that you could be on my committee. Dr. Black, the insight and encouragement in regard to teaching, research, and life gave me an oft needed uplifting to persevere. I also want to thank Dr. Cindy Berrie, Dr. Shenqiang Ren, and Dr. Susan Williams for agreeing to serve on my committee. Your support is greatly appreciated.

Mom and Dad, thank you for always pushing me to succeed. Your stress on education, as well as constant encouragement and understanding, led me to where I am today. Kat, your high expectations for me were great motivation. I appreciate every one of those weekly math and spelling quizzes from when I was younger. To AM, Uncle Mark, Gram, and Pop, I owe you for always supporting me through all of the hard times. Also, I am fortunate to have such great in-laws (especially you, Tank) who stood by us and understood when Rachael moved to Kansas.

Unwinding outside of the lab would not have been possible without my friends: Carl, Megan, Tom, Cassie, Jen, Dan, Igor, Nathan, Alex, and anyone else I may have unintentionally forgotten. I am thankful to have shared our time together in Kansas. Steve, Adam, and Mark have been great friends for a long time. To my friends from the Jackson group (Dom, James, and Gayan), you were all a big part of my graduate career. Of course, the Barybin group would not be what it is without many people leaving their mark. I owe Sasha for sharing with me many synthetic tips (and starting materials!) when I first started that gave me a great foundation for my research. Thank you to my past and current lab mates (Andy, Kolbe, Tiffany, Toshi, Rodi, Mason, and Erin) for the friendship, fun, and laughs. I will always consider you to be my close friends. Dave, you made my graduate school experience something special and you will always be my "brother from another mother." Brad, you were my best man at our wedding for a reason. Our friendship is invaluable to me and I know we will be a large part of each other's lives.

To my wife Rachael, whatever I can say or write does no justice in expressing how much you truly mean to me. You have stood by me every step of the way and I would not have made it this far without your constant support, encouragement, and love. I must be the luckiest man alive for you to be with me. You are a fantastic person, friend, and wife. I look forward to spending the rest of our lives together. I love you.

Table of Contents

List of Tables

List of Figures

List of Schemes

CHAPTER I

Renaissance of Isocyanoarenes as Ligands in Low-Valent Organometallics

Portions of this work have been reproduced from:

Barybin, M. V.; Meyers, Jr., J. J.; Neal, B. M. Renaissance of Isocyanoarenes as Ligands in Low-Valent Organometallics. In *Isocyanide Chemistry - Applications in Synthesis and Material Science*. Nenajdenko, V. G., Ed. Wiley–VCH: Weinheim, **2012**; pp 493-529. ISBN: 978-3-527-33043-0.

I.1 Historical Perspective

The birth of isocyanide coordination chemistry can be traced back to 1869 (Alfred Werner was only three years old at that time!), when Gautier isolated several compounds of the composition "Ag(CNR)(CN)".[1] Gautier recognized correctly that the extraordinarily repulsive odor generated upon treatment of silver cyanide with organohalides was not associated with the formation of organonitriles as had been previously thought by Meyer[2] and Lieke[3], but rather with the production of species isomeric to nitriles. Ninety years later, an impressively large number of homoleptic (i.e., binary) isocyanide complexes involving metals of the Cr, Mn, Fe, Co, Ni, and Cu triads were featured in Malatesta's monograph "Isocyanide Complexes of Metals."[4] The analogy between carbon monoxide (:C≡O) and isocyanides (:C≡N-R) as ligands became apparent well before the introduction of Hoffmann's concept of isolobal relationships.[5] Efforts toward accessing isocyanide congeners of various metal carbonyls, particularly those containing highly electron-rich metal centers such as carbonylmetalates[6], continue to this date.

In his 1959 review[4], Malatesta emphasized the complete lack of isocyanidemetalates (i.e., isocyanide complexes of metals in sub-zero oxidation states) that would be analogous to carbonylmetalates such as $[Fe(CO_4)]^{2-}$, $[Co(CO)_4]^-$, and $[Rh(CO_4)]^-$ already known at that time.[6] He also commented on the fact that group 4 and 5 transition metals "did not show any tendency to form complexes with isocyanides," and pointed at the absence of zero-valent isocyanide complexes of the elements with odd atomic numbers. It took many years to begin filling the above gaps in the isocyanide coordination chemistry. Indeed, $Co_2(CNR)_8$ (R = ^{t}Bu, 2,6-xylyl, mesityl), the first zero-valent isocyanide complexes of an odd-numbered transition metal were obtained in 1977[7], the first binary isocyanide adduct of a group 5 metal, $[V(CN^tBu)_6]^{2+}$, was reported in 1980[8], and the initial homoleptic isocyanidemetalate, $[Co(CNXyl)_4]^-$ (Xyl = 2,6-xylyl

or 2,6-dimethylphenyl), was isolated in 1989[9]. While no homoleptic isocyanide complexes of group 4 transition metals are yet known, several group 4 heteroleptic species, including $CpTi(CNXyl)_4E$ (E = I, $SnPh_3$, and $SnMe_3$), have been described.[10]

The up-to-date list of isolable binary isocyanide complexes of transition metals is compiled in Table I.1. The italicized entries correspond to a few species[11] that had been known, but omitted from a similar table of neutral and cationic binary isocyanide complexes published in 1998[12], whereas bolded entries reflect new types of complexes established since 1998. No distinction between mono- versus polydentate or terminal versus bridging isocyanide ligands is provided in Table I.1. For example, a mononuclear complex featuring three η^2-bound diisocyanide ligands would be represented as $M(CNR)_6$ while a dinuclear complex with six terminal and two μ_2-bridging isocyanide ligands would be shown as $M_2(CNR)_8$. As Table I.1 clearly illustrates, the old paradigm that isocyanide ligands are greatly inferior to CO in accommodating zero- and, especially, sub-valent metals has been shattered.

Table I.1 Homoleptic isocyanide complexes of transition metals isolated to date.

Group 5	6	7	8	9	10	11
$[V(CNR)_6]^-$	$Cr(CNR)_6$	$[Mn(CNR)_5]^-$	**$[Fe(CNR)_4]^{2-}$**	$[Co(CNR)_4]^-$	**$Ni(CNR)_3$**	$[Cu(CNR)_4]^+$
$V(CNR)_6$	$[Cr(CNR)_6]^+$	$[Mn(CNR)_6]^+$	$Fe(CNR)_5$	**$Co(CNR)_4$**	$Ni(CNR)_4$	**$[Cu_2(CNRNC)_3]^{2+}$**
$[V(CNR)_6]^+$	$[Cr(CNR)_6]^{2+}$	*$[Mn(CNR)_6]^{2+}$*	$Fe_2(CNR)_9$	$Co_2(CNR)_8$	$Ni_4(CNR)_7$	
$[V(CNR)_6]^{2+}$	$[Cr(CNR)_6]^{3+}$		*$[Fe(CNR)_6]^{2+}$*	**$[Co(CNR)_4]^+$**	$[Ni(CNR)_4]^{2+}$	
	$[Cr(CNR)_7]^{2+}$			$[Co(CNR)_5]^+$	*$Ni_4(CNR)_6$*	
				$[Co(CNR)_5]^{2+}$		
				$[Co_2(CNR)_{10}]^{2+}$		
$[Nb(CNR)_6]^-$	$[Mo(CNR)_6]$	*$[Tc(CNR)_6]^+$*	$Ru(CNR)_5$	*$Rh_2(CNR)_8$*	**$Pd(CNR)_2$**	$[Ag(CNR)_2]^+$
$[Nb(CNR)_7]^+$	$[Mo(CNR)_7]^{2+}$		$Ru_2(CNR)_9$	$[Rh(CNR)_4]^+$	$Pd_3(CNR)_6$	*$[Ag(CNR)_4]^+$*
			$[Ru(CNR)_6]^{2+}$	$[Rh_2(CNR)_8]^{2+}$	$[Pd(CNR)_4]^{2+}$	
			$[Ru_2(CNR)_{10}]^{2+}$	$[Rh_2(CNRNC)_4]^{2+}$	$[Pd_2(CNR)_6]^{2+}$	
					$[Pd_3(CNR)_8]^{2+}$	
$[Ta(CNR)_6]^-$	$W(CNR)_6$	$[Re(CNR)_6]^+$	$Os(CNR)_5$	$[Ir(CNR)_4]^+$	$Pt_3(CNR)_6$	$[Au(CNR)_2]^+$
$[Ta(CNR)_7]^+$	$[W(CNR)_7]^{2+}$		*$[Os(CNR)_6]^{2+}$*		$Pt_7(CNR)_{12}$	
			$[Os_2(CNR)_{10}]^{2+}$		$[Pt(CNR)_4]^{2+}$	
					$[Pt_2(CNR)_6]^{2+}$	

Unlike carbon monoxide, which has a dipole moment of only 0.12 Debye[13], organic isocyanides are quite polar substances. For instance, the dipole moment of CNPh is 3.44 Debye.[13] Given that the dominant resonance form of a typical isocyanide with a hydrocarbon substituent R places the negative charge on the terminal carbon atom ($^-$:C≡N$^+$–R), isocyanide ligands are considered stronger σ-donors and weaker π-acceptors compared to CO. In other words, the so-called σ-donor/π-acceptor ratio of an isocyanide ligand is significantly higher than that of carbon monoxide.[14] This argument has been frequently used to explain why isocyanides may not be as suitable for stabilizing electron rich metal ions as is CO. The two reactions shown in Scheme I.1 are certainly consistent with the above reasoning.[8b, 15]

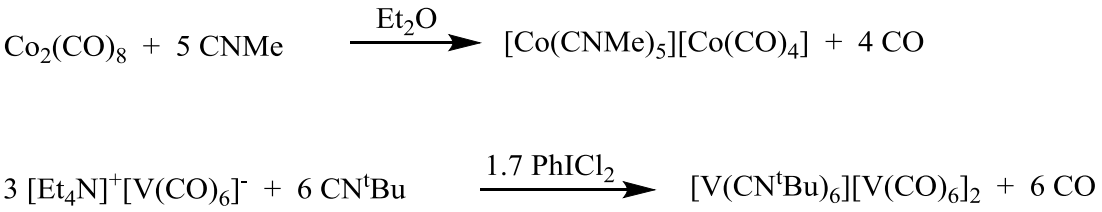

Scheme I.1

In general, aryl isocyanides (CNAr) are better at accommodating low-valent metals than alkyl isocyanides, presumably due to the possibility of delocalization of back-donated electron density into the aromatic ring as described by the resonance contribution M=C=N$^+$=Ar$^-$. However, Lentz *et al*. provided convincing X-ray structural as well as ^{13}C NMR and IR spectroscopic evidence that certain isocyanide ligands with fluorinated substituents are very strong π-acceptors.[16] In particular, $CNCF_3$, which unfortunately has very poor thermal stability in the condensed phase, appears to be on par with (if not more powerful than) CO in terms of its π-accepting ability.

The remarkable versatility of isocyanide ligands compared to CO can be nicely illustrated by the recently crystallographically characterized series of complexes $[Ta(CNXyl)_7]^+$,

$[Ta(CNXyl)_6I]$, $[Ta(CNXyl)_5(NO)]$, *cis*-$[Ta(CNXyl)_4(NO)_2]^+$, and $[Ta(CNXyl)_6]^-$.[17] While $[Ta(CO)_6]^-$ is well known[18], the carbonyl analogues $[Ta(CO)_7]^+$, $[Ta(CO)_6I]$, $[Ta(CO)_5(NO)]$ and $[Ta(CO)_4(NO)_2]^+$ do not exist. To be fair though, $[Ta(CNR)_5]^{3-}$, an isocyanide congener of $[Ta(CO)_5]^{3-}$,[6, 19] is not (yet) known either. A quantitative testimony to the electronic flexibility of 2,6-xylyl isocyanide is provided in Figure I.1, which compares the ^{13}C NMR and vibrational signatures of the CNXyl ligands in four octahedral, formally Ta(-I) complexes to those of free CNXyl. The isocyanide ligands in $[Ta(CNXyl)_4(NO)_2]^+$ serve essentially as σ-donors, whereas those in $[Ta(CNXyl)_6]^-$ clearly behave as powerful π-acceptors.[17]

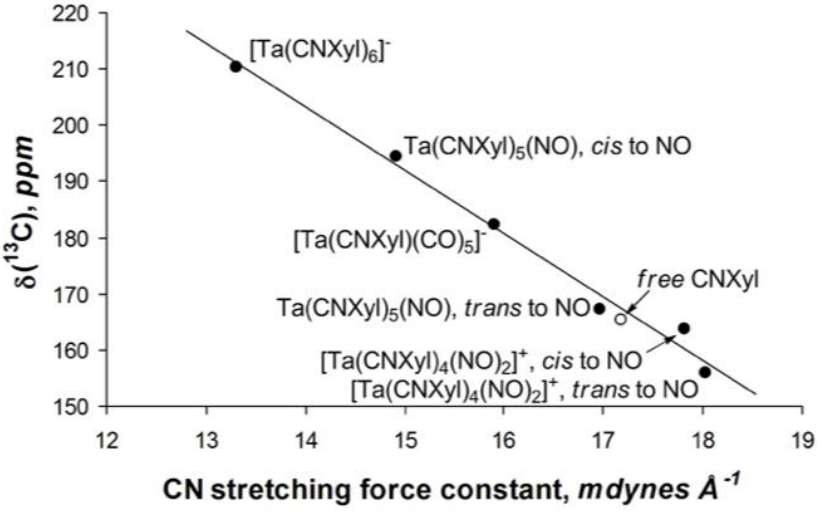

Figure I.1 ^{13}C NMR chemical shifts for the ligating carbon atom of CNXyl plotted against the corresponding C-N stretching force constants for $[Ta(CNXyl)_6]^-$, $Ta(CNXyl)_5(NO)$, $[Ta(CNXyl)(CO)_5]^-$, and $[Ta(CNXyl)_4(NO)_2]^-$. The open circle refers to the properties of the uncomplexed CNXyl ligand. Xyl = 2,6-dimethylphenyl. Adapted with permission from Ref. 17; Copyright 2007 American Chemical Society.

During the past decade, the number of commercially available isocyanides has doubled to reach about 25, of which only 5 are classified as aryl isocyanides (Sigma-Aldrich®: 2,6-dimethylphenyl isocyanide, 4-methoxyphenyl isocyanide, 2-naphthyl isocyanide, 2-chloro-6-methylphenyl isocyanide, and 1,4-phenylene diisocyanide). The surge has undoubtedly been

driven by the growing demands for new substrates in the combinatorial drug discovery research that employs isocyanide-based multicomponent reactions (MCR).[20]

The coordination chemistry of isocyanides, including polydentate versions thereof, has been at the heart of numerous fundamental and practical advances in organic and organometallic syntheses, catalysis, diagnostic medicine, as well as in surface, polymer, and materials sciences. A number of excellent reviews dealing with these topics are available.[14, 20-25] This Chapter addresses recent breakthroughs in the chemistry of isocyanidemetalates and related electron-rich complexes. In addition, it highlights the coordination chemistry of the recently emerged families of unusual isocyanoarene ligands that feature either nonbenzenoid substituents or extremely sterically encumbered benzenoid substituents.

I.2 Isocyanidemetalates and Related Low-Valent Complexes

I.2.1 Introduction

This section highlights the chemistry of binary isocyanidemetalates documented to date which include species containing Co(-I), Fe(-II), Mn(-I), V(-I), Nb(-I), and Ta(-I) metal centers. Redox-related, higher valent congeners thereof and a few currently known non-homoleptic isocyanidemetalates are accounted for as well. Notably, all isolable isocyanidemetalates contain *aryl* isocyanide ligands and can be viewed as the isocyanide analogues of the long-established carbonylmetalates $[Co(CO)_4]^-$, $[Fe(CO)_4]^{2-}$, $[Mn(CO)_5]^-$, and $[M(CO)_6]^-$ (M = V, Nb, Ta).[6] The isocyanidemetalate counterparts of the highly reduced anions $[Ti(CO)_6]^{2-}$, $[Cr(CO)_5]^{2-}$, $[V(CO)_5]^{3-}$, $[Co(CO)_3]^{3-}$, $[Mn(CO)_4]^{3-}$, $[Cr(CO)_4]^{4-}$, and their second and third row equivalents[6] have yet to be discovered, if they can be accessible at all.

I.2.2 Four-Coordinate Isocyanidemetalates and Redox-Related Complexes

In 1989, Cooper and Warnock reported synthesis of the initial binary isocyanidemetalate, namely $[Co(CNXyl)_4]^-$ (Figure I.2), through substitution of all four ethylene ligands in the labile anion $[Co(C_2H_4)_4]^-$ and later developed additional elegant routes to $[Co(CNXyl)_4]^-$ involving reductions of Cp_2Co, $Co_2(CNXyl)_8$, or $[Co(CNXyl)_5]^+$ (Scheme I.2).[9,33] Complex $[Co(CNXyl)_4]^-$ undergoes electrophilic addition upon treatment with Ph_3SnCl to form five-coordinate $Co(CNXyl)_4(SnPh_3)$. The nature of the "Co(-I)" intermediate(s) generated via potassium naphthalenide reduction of Cp_2Co remains unclear. It might be related, at least to some degree, to that of polyarenecobaltates(I-) described by Ellis and co-workers (Figure I.3).[34] Notably, $[Co(\eta^4\text{-anthracene})_2]^-$ reacts cleanly with CNXyl to afford $[Co(CNXyl)_4]^-$ (Scheme I.3) .[34b]

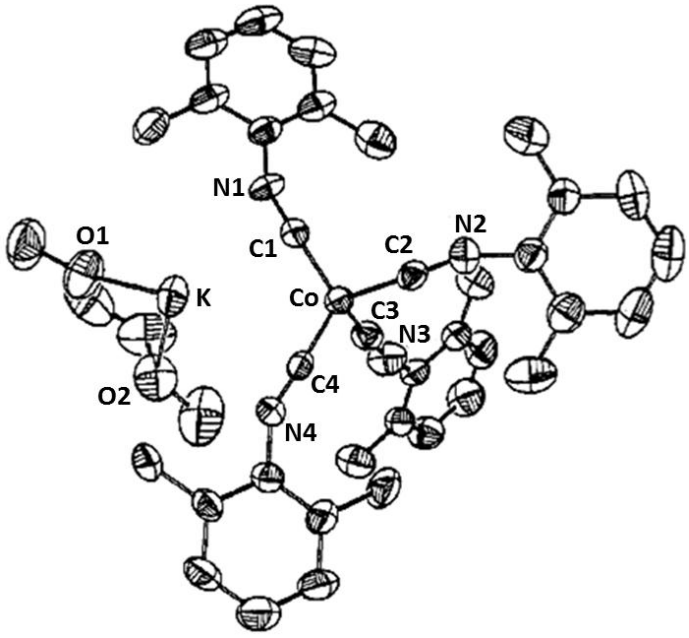

Figure I.2 ORTEP diagram for $[K(DME)][Co(CNXyl)_4]$. Hydrogen atoms are omitted. Adapted with permission from Ref. 9; Copyright 1994 American Chemical Society.

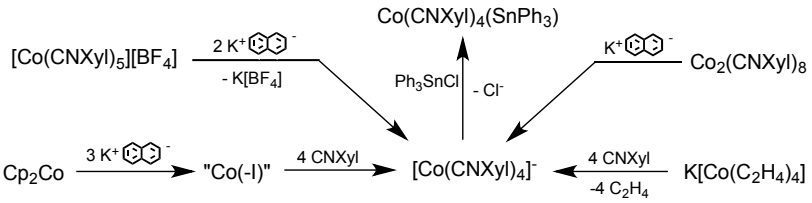

Scheme I.2

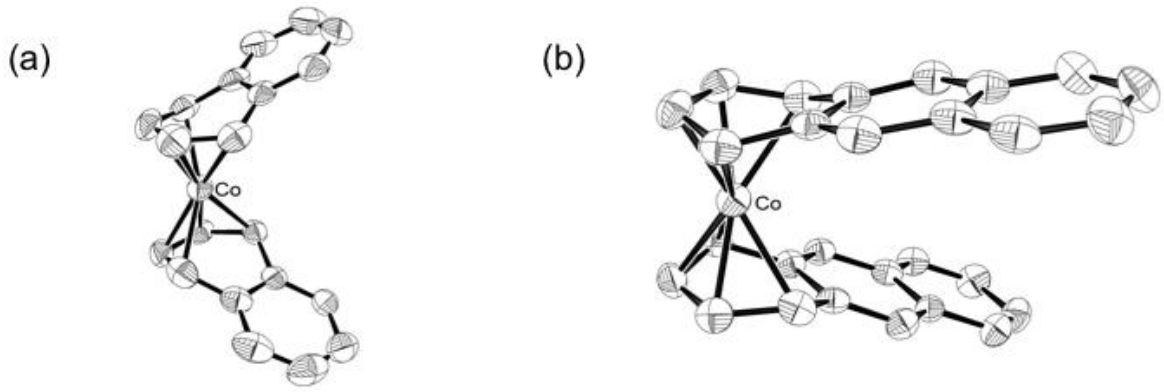

Figure I.3 ORTEP diagrams for (a) $[Co(\eta^4\text{-naphthalene})_2]^-$ anion in "triple salt" $[K(18\text{-crown-}6)]_3[Co(\eta^4\text{-}C_{10}H_8)_2][Co(\eta^4\text{-}C_{10}H_8)_2(\eta^2\text{-}C_2H_4)_2]$ and (b) the $[Co(\eta^4\text{-anthracene})_2]^-$ anion in $[K(18\text{-crown-}6)(THF)_2][Co(\eta^4\text{-}C_{14}H_{10})]$ generated using the ORTEP-3 program from CIF data in Ref. 34. Hydrogen atoms are omitted.

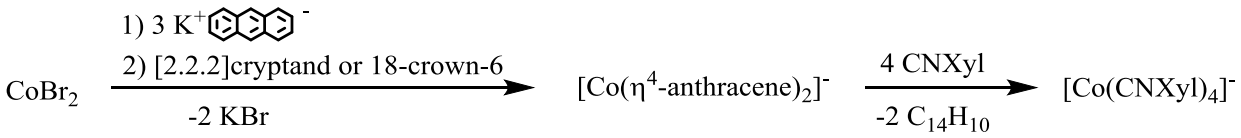

Scheme I.3

Recently, Figueroa *et al*. introduced coordination chemistry of two remarkably bulky aryl isocyanide ligands $CNAr^{Mes2}$ and $CNAr^{Dipp2}$ that are based on the *m*-terphenyl scaffold (Figure I.4).[35] Reduction of CoI_2 with sodium amalgam in the presence of $CNAr^{Mes2}$ afforded $[Co(CNAr^{Mes2})_4]^-$, an extremely sterically encumbered congener of $[Co(CNXyl)_4]^-$ (Scheme I.4).[36] The $[Co(CNAr^{Mes2})_4]^-$ and $[Co(CNXyl)_4]^-$ anions exhibit ν_{NC} bands at 1821 and 1815 cm^{-1}, respectively, in their IR spectra, which is consistent with strong back-bonding interaction between the formally Co(-I) centers and the isocyanide ligands in these complexes. The

crystallographically characterized salts $[Ph_3PNPPh_3][Co(CNAr^{Mes2})_4]$ (Figure I.5a) and $[K(DME)][Co(CNXyl)_4]$ (Figure I.2) have essentially identical average Co-C and C-NR bond distances, as well as very similar average C-N-C angles (Table I.2). However, substantial variability in C-N-C bending occurs among the individual ligands in $[K(DME)][Co(CNXyl)_4]$ due to perturbation of the anion's geometry by close cation-anion interactions.[33]

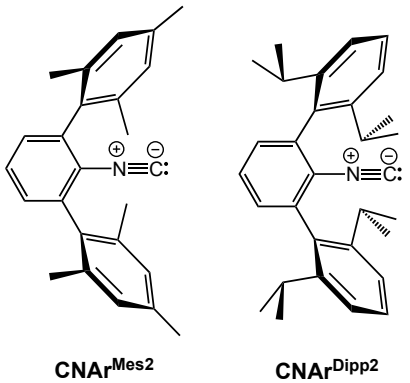

Figure I.4 Bulky *m*-terphenyl isocyanides $CNAr^{Mes2}$ (left) and $CNAr^{Dipp2}$ (right) synthesized by Figureoa *et al*.[35]

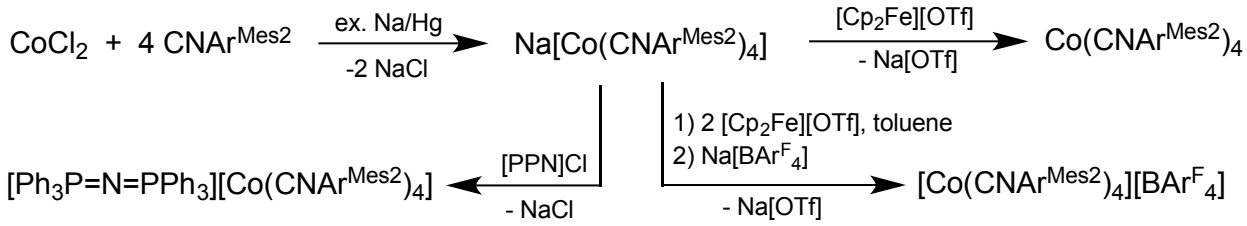

Scheme I.4

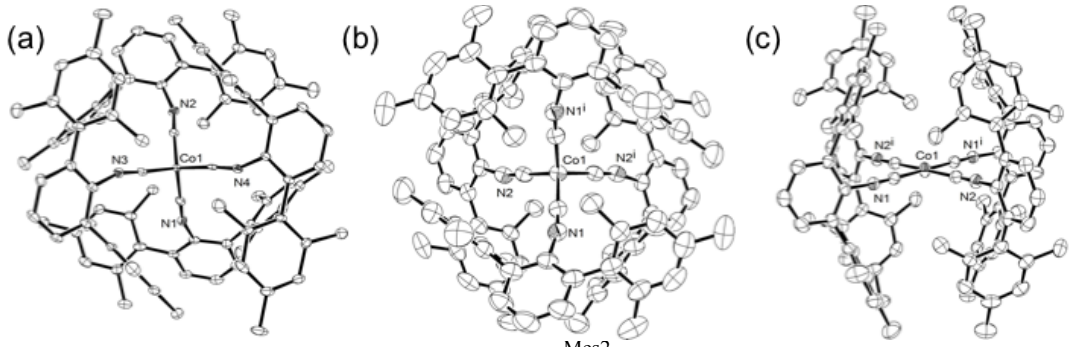

Figure I.5 ORTEP diagrams for (a) the $[Co(CNAr^{Mes2})_4]^-$ anion in $[Ph_3PNPPh_3][Co(CNAr^{Mes2})_4]$, (b) $Co(CNAr^{Mes2})_4$, and (c) the cation $[Co(CNAr^{Mes2})_4]^+$ in $[Co(CNAr^{Mes2})_4][B([3,5\text{-}(CF_3)_2C_6H_3)_4]$ generated using the ORTEP-3 program from CIF data in Ref. 36. Hydrogen atoms are omitted.

Table I.2 Selected IR spectroscopic and X-ray structural data[a] for CNXyl, $CNAr^{Mes2}$ and series of binary isocyanide complexes of Co, Fe, Mn, V, Nb, and Ta containing metal centers in various oxidation states.

Compound	ν_{NC} (cm^{-1})	M-C bond length (Å)	C-NR bond length (Å)	C-N-C angle (°)	Reference
CNXyl	2117	-	1.160(3)	179.4(2)	40
$CNAr^{Mes2}$	2120	-	1.158(3)	178.1(3)	35a
$[Co(CNAr^{Mes2})_4]^+$	2085	1.863(0)	1.168(0)	170.8(3)	36
$[Co(CNAr^{Mes2})_4]$	1941	1.828(2)	1.180(4)	166(1)	36
$[Co(CNAr^{Mes2})_4]^-$	1821	1.784(5)	1.207(8)	158(3)	36
$[Co(CNXyl)_4]^-$	1815	1.79(2)	1.20(2)	156(7)	36
$[Fe(CNXyl)_4]^{2-}$	1675	1.765(3)	1.237(7)	144(3)	38
$[Mn(CNXyl)_5]^-$	1920, 1710	1.80(5)	1.21(2)	151(8)	11a
$[V(CN^tBu)_6]^{2+}$	2197	2.10(1)	1.14(2)	178(1)	8b
$[V(CNXyl)_6]^+$	2033	2.07(2)	1.169(6)	173(2)	53
$[V(CNXyl)_6]$	1939	2.026(7)	1.186(5)	163(4)	53
$[V(CNXyl)_6]^-$	1823	1.98(3)	1.20(2)	158(10)	53
$[Nb(CNXyl)_6]^-$	1820	2.141(3)	1.191(4)	157.0(3)	17
$[Ta(CNXyl)_7]^+$	2029	2.15(1)	1.17(1)	173(5)	17
$[Ta(CNXyl)_6]^-$	1824	2.127(3)	1.199(4)	155.7(3)	17

a NUMBERS IN PARENTHESES ARE THE STANDARD DEVIATIONS FROM THE MEAN.

The similarity between the above two isocyanidecobaltates(-I) ends when their oxidation chemistry is considered. Indeed, oxidation of the $[Co(CNXyl)_4]^-$ anion produces the dimer $Co_2(CNXyl)_8$ while its mono-valent homoleptic analogue is the five-coordinate cation $[Co(CNXyl)_5]^+$.[33] However, one-electron oxidation of $[Co(CNAr^{Mes2})_4]^-$ affords zero-valent, mononuclear, paramagnetic $Co(CNAr^{Mes2})_4$ (Figure I.5b, Scheme I.4).[36] This stable analogue of the non-isolable "$Co(CO)_4$" radical exhibits intriguing temperature-dependent changes in its X-ray structural and EPR spectroscopic characteristics. Moreover, two-electron oxidation of $[Co(CNAr^{Mes2})_4]^-$ in a non-coordinating solvent medium gives the 16-electron, diamagnetic, square-planar cation $[Co(CNAr^{Mes2})_4]^+$ (Figure I.5c). This is in marked contrast to the related $[Co(CO)_4]^+$ cation detected in the gas phase, which is believed to be C_{2v}-symmetric and paramagnetic.[37] Within the series $[Co(CNAr^{Mes2})_4]^z$, the average Co-C bond shortens, the average C-NR bond lengthens, and the average C-N-C angle becomes more bent upon reducing the charge z from +1 to -1 due to the increase in the extent of back-bonding (Table I.2).

Soon after describing $[Co(CNXyl)_4]^-$, Cooper *et al*. presented convincing, albeit circumstantial, evidence that supported the possibility of accessing binary isocyanidemetalate dianions.[11e] Four-electron reduction of $Ru(CNR)_4Cl_2$ (R = Xyl, ^{t}Bu) with potassium naphthalenide at -78 °C in THF produced very thermally unstable species that were formulated as isocyanideruthenates(-II), $[Ru(CNR)_4]^{2-}$, based on their oxidative addition reactivity with several electrophiles, including Ph_3SnCl.[11e] Fifteen years later, Ellis and Brennessel reduced in-situ-generated $Fe(CNXyl)_4Br_2$ following the above reaction protocol to isolate complex $K_2[Fe(CNXyl)_4]$, which afforded *trans*-$[Fe(CNXyl)_4(SnPh_3)_2]$ upon treatment with Ph_3SnCl (Scheme I.5, Figure I.6).[38] *Trans*-$[Fe(CN^tBu)_4(SnPh_3)_2]$ was prepared from the non-isolable intermediate $[Fe(CN^tBu)_4]^{2-}$ as well. The dianion $[Fe(CNXyl)_4]^{2-}$ was crystallographically

characterized as a salt with two $[K[2.2.2.]cryptand]^+$ cations (Figure I.6a) and remains the sole isolable isocyanidemetalate(-II) known to date. It constitutes the isocyanide analogue of the oldest carbonylmetalate $[Fe(CO)_4]^{2-}$ (often referred to as "Collman's reagent") initially prepared by Hieber and Leutert in 1931.[39]

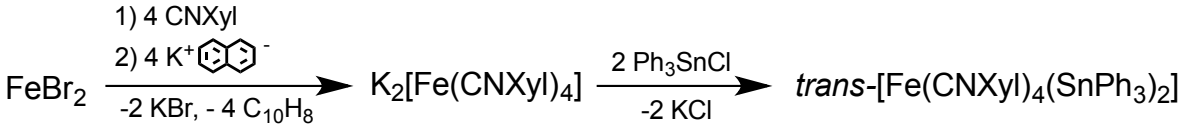

Scheme I.5

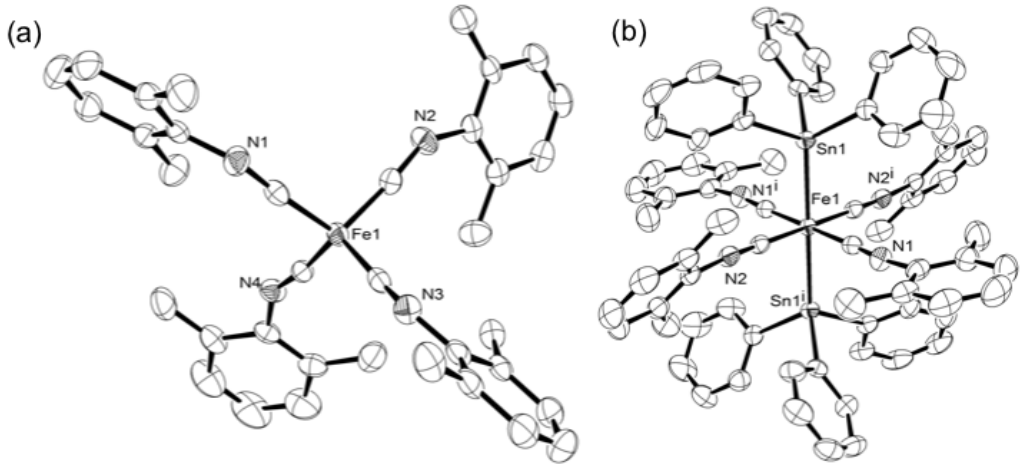

Figure I.6 ORTEP diagram for (a) the $[Fe(CNXyl)_4]^{2-}$ dianion in $[K([2.2.2]cryptand)]_2[Fe(CNXyl)_4]$ and (b) *trans*-$[Fe(CNXyl)_4(SnPh_3)_2]$ generated using the ORTEP-3 program from CIF data in Ref. 38. Hydrogen atoms are omitted.

The CNXyl ligands in $[Fe(CNXyl)_4]^{2-}$ feature the most bent average C-N-C angle (144(3)°), the longest average isocyanide C-N bond distance (1.237 Å), and the lowest energy ν_{NC} infrared signature (1675 cm^{-1} in THF) documented for any terminal isocyanide ligand in a binary metal complex (Table I.2). For "free" CNXyl, the corresponding parameters are: <(C-N-C) = 179.4°, d(C≡NXyl) = 1.160(3) Å, and ν_{NC} = 2117 cm^{-1} (in THF).[40] Also interesting is the fact that the average Fe-C bond distance in $[Fe(CNXyl)_4]^{2-}$ is only 0.02 Å longer than that in $[Fe(CO)_4]^{2-}$.[41] Thus, the isocyanide ligands in $[Fe(CNXyl)_4]^{2-}$ behave as very powerful π-

acceptors and experience an extremely large extent of back-bonding, as may be represented by the resonance contribution "Fe=C=N-Xyl."

I.2.3 Five-Coordinate Isocyanidemetalates

In contrast to a variety of five-coordinate carbonylmetalates $[M(CO)_5]^-$, $[M(CO)_5]^{2-}$, and $[M(CO)_5]^{3-}$ that contain group 7, 6, or 5 metal ions, respectively[6], only one homoleptic isocyanidemetalate, namely $[Mn(CNXyl)_5]^-$, has been reported to date[11a]. As summarized in Scheme I.6, Cooper and co-workers accessed quite thermally sensitive $K[Mn(CNXyl)_5]$ by employing potassium naphthalenide reduction of $ClMn(CNXyl)_5$ and initially established its nature as a binary isocyanide complex of Mn(-I) through its reaction with Ph_3SnCl. The successful isolation of the crystallographically characterized salt [K(18-crown-6)(DME)][$Mn(CNXyl)_5$] must be credited to remarkable technical skills of the researchers as samples had to be maintained at temperatures below -30 °C, including any manipulations during the reaction workup. The anion $[Mn(CNXyl)_5]^-$ features trigonal bipyramidal (tbp) geometry (Figure I.7), with the axial CNXyl ligands being on average 16° less bent than the CNXyl ligands in the equatorial positions. The latter fact is consistent with the expectation that π-acceptor ligands in the equatorial sites of a tbp complex should engage in more effective back-bonding than those in the axial sites.

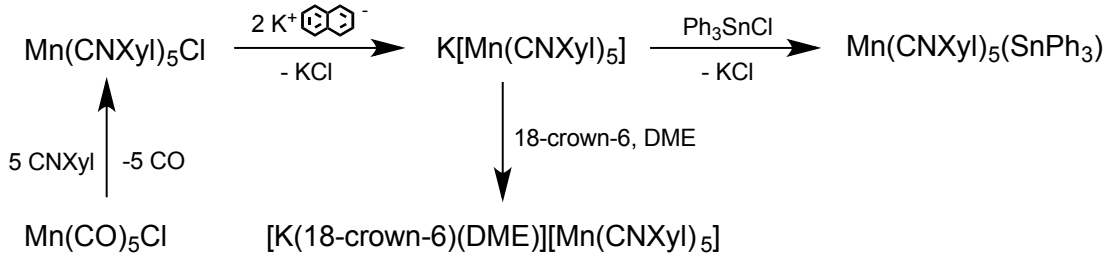

Scheme I.6

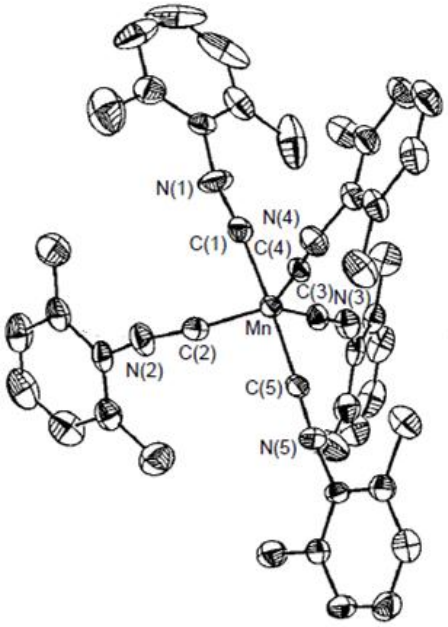

Figure I.7 ORTEP diagram for the anion in $[K(DME)][Mn(CNXyl)_5]$.[11a] Hydrogen atoms are omitted. Adapted by permission of The Royal Society of Chemistry.

Despite the straightforward reactivity of $[Mn(CNXyl)_5]^-$ toward Ph_3SnCl, its interactions with MeI, EtI, and $MeOSO_2CF_3$ proved to be quite different from what might had been expected based on the known reactions of $[Mn(CO)_5]^-$ with such organic electrophiles. The Mn(I) alkylation products were isolated in low to mediocre yields and featured new bidentate ligands formed via double isocyanide/alkyl insertion.[42]

Very recently, Figueroa *et al*. discovered the golden mean of the robust reactivity characteristics of $[Mn(CO)_5]^-$ and the steric/electronic tunability at the metal center that can be provided by isocyanide ligands. Treatment of $BrMn(CO)_5$ with the bulky *m*-terphenyl isocyanides $CNAr^{Mes2}$ or $CNAr^{Dipp2}$ shown in Figure I.4 followed by two-electron reduction of the corresponding Mn(I) substitution products gave mixed carbonyl/isocyanidemanganates(-I) $[Mn(CO)_2(CNAr^{Mes2})_3]^-$ or $[Mn(CO)_3(CNAr^{Dipp2})_2]^-$ in 20% and 47% yields, respectively (Scheme I.7).[43] Given that CO is certainly a stronger π-acid than the $CNAr^{Mes2}$ ligand, the axial placement of both carbonyl ligands in $[Mn(CO)_2(CNAr^{Mes2})_3]^-$ (Figure I.8a) must be forced by

the steric requirements of the three bulky Ar^{Mes2} substituents in the complex. In contrast, the three CO ligands in the tbp anion $[Mn(CO)_3(CNAr^{Dipp2})_2]^-$ occupy equatorial sites (Figure I.8b), which is favorable both sterically and electronically.[44]

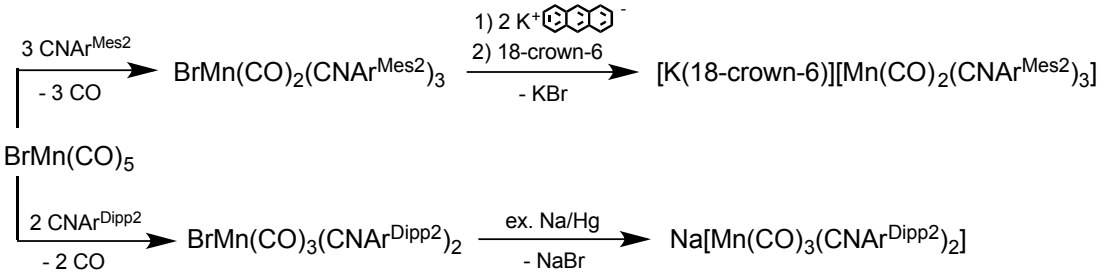

Scheme I.7

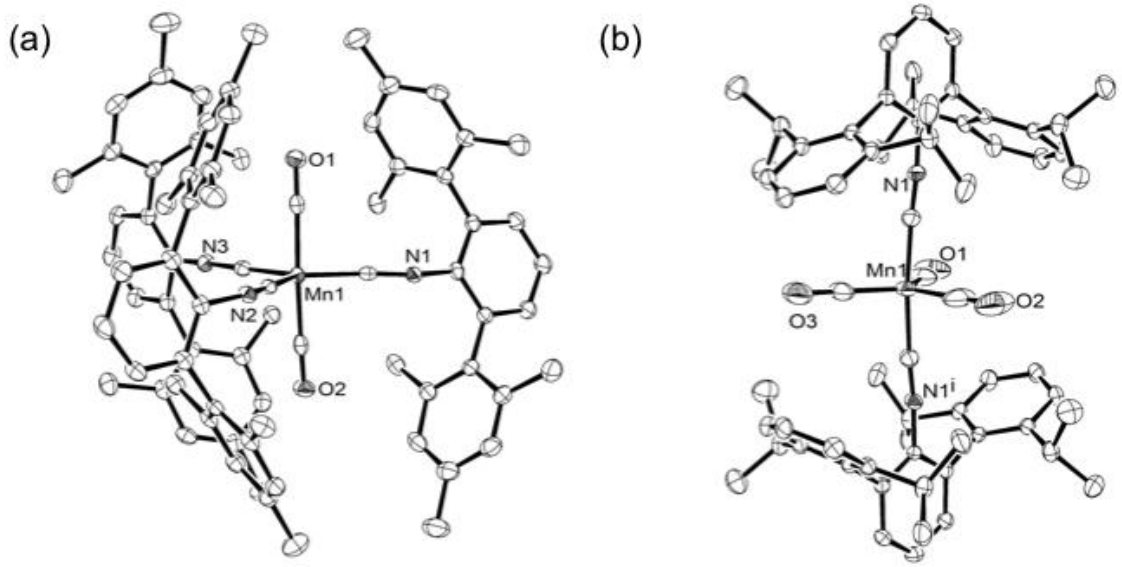

Figure I.8 ORTEP diagrams for (a) the $[Mn(CNAr^{Mes2})_3(CO)_2]^-$ anion in $[K(18\text{-crown-}6)(DME)][Mn(CO)_2(CNAr^{Dipp2})_3]$ and (b) the $[Mn(CO)_3(CNAr^{Dipp2})_2]^-$ anion in $[K(NCMe)_2][Mn(CO)_3(CNAr^{Dipp2})_2]$ generated using the ORTEP-3 program from CIF data in Ref. 44. Hydrogen atoms are omitted.

Treatment of $[Mn(CO)_3(CNAr^{Dipp2})_2]^-$ with HCl and MeI cleanly afforded *mer*-,*trans*-$HMn(CO)_3(CNAr^{Dipp2})_2$ and *mer*,*trans*-$MeMn(CO)_3(CNAr^{Dipp2})_2$, respectively. This reactivity profile is similar to that of $[Mn(CO)_5]^-$ but not $[Mn(CNXyl)_5]^-$.[43] The reactions of $[Mn(CO)_3(CNAr^{Dipp2})_2]^-$ with $MeSiCl_3$ and $SnCl_2$ gave *mer*,*trans*-

$(Cl_2\{Me\}Sn)Mn(CO)_3(CNAr^{Dipp2})$ and *mer,trans*-$ClSnMn(CO)_3(CNAr^{Dipp2})$, respectively. The latter metallostannylene complex is particularly intriguing as its Sn center does not carry a bulky substituent.[43]

I.2.4 Six-Coordinate Isocyanidemetalates and Redox-Related Complexes

Binary hexacoordination in mononuclear isocyanidemetalate complexes with an 18-electron count at the metal center can, in principle, be accommodated in two scenarios: $[M(CNR)_6]^-$ (M = V, Nb, Ta) or $[M(CNR)_6]^{2-}$ (M = Ti, Zr, Hf). These would be analogous to the well-established group 5 monoanionic $[M(CO)_6]^-$ (M = V, Nb, Ta) or group 4 dianionic $[M(CO)_6]^{2-}$ (M = Ti, Zr, Hf) species, respectively.[6] No group 4 transition metal complexes with the metal center having a formally negative oxidation number and containing at least one isocyanide ligand are currently known although a few higher valent group 4 metal complexes featuring up to four descrete isocyanide ligands have been described.[10] Earlier examples of isolable, isocyanide-containing group 5 metalates included $[V(CO)_5(CNR)]^-$ (R = Me, C_6H_{11}, ^tBu, ^nBu, Ph)[45], $[M(CO)_5(CN^tBu)]^-$ (M = Nb, Ta)[19, 46], and $[M(CO)(CNMe)(dmpe)_2]^-$ (M = Nb, Ta)[47], all of which contain only one isocyanide ligand. More recently, the synthesis of the anion $[Ta(CO)_5(CNXyl)]^-$ has been reported as well (Scheme I.8).[17b] In addition, complexes *cis*-$[V(NO)_2(CN^tBu)_4]^+$,[48] $CpV(NO)_2(CN^tBu)$,[49] and $VX(NO)_2(CNR)_3$ (R = ^tBu, X = Cl; R = ^iPr, X = Br, Cl; R = C_6H_{11}, X = Br, I)[50] that have vanadium centers in -1 formal oxidation state have been reported in the 1980s.

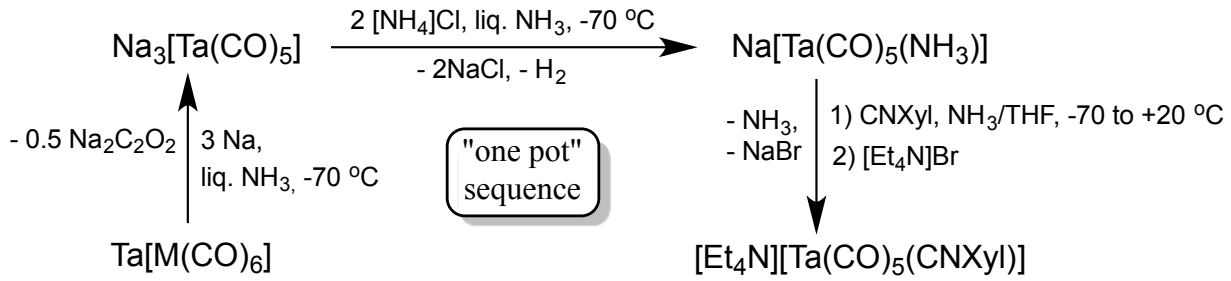

Scheme I.8

The scarcity of group 4 and 5 metal isocyanides may be related to the fact that early transition metal complexes usually exhibit relatively high coordination numbers and can induce reductive C-C coupling of isocyanide ligands.[29, 51] While almost all reported cases of such reductive coupling reactions involve alkyl isocyanides, at least one example of reductively coupled aryl isocyanide ligands (CNXyl) has been documented (Figure I.9).

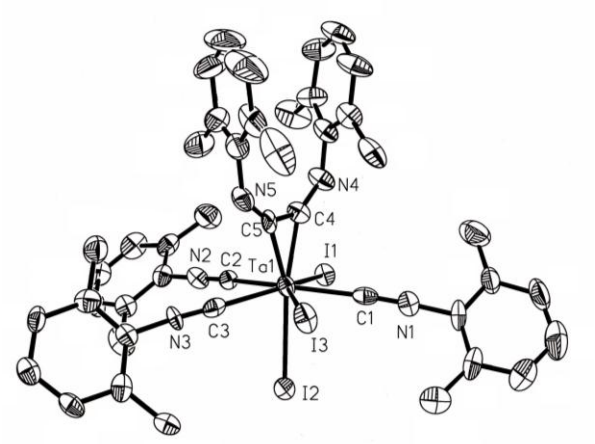

Figure I.9 ORTEP diagram for $Ta(CNXyl)_3(Xyl(H)NC{\equiv}CN(H)Xyl)I_3$. Hydrogen atoms are omitted. Adapted with permission from Ref. 52.

At the turn of the 20th century, Ellis and Barybin isolated the first homoleptic isocyanide complex of vanadium(0), $V(CNXyl)_6$ (Figure I.10a), by substituting both naphthalene rings in labile $V(\eta^6\text{-}C_{10}H_7R)_2$ (R = H, Me) (Scheme I.9).[52] This thermally stable isocyanide analogue of very sensitive $V(CO)_6$[53] undergoes either one-electron reduction to form binary isocyanovanadate(-I) $[V(CNXyl)_6]^-$ (Figure I.10b) or one-electron oxidation to afford

$[V(CNXyl)_6]^+$ (Figure I.10c). The homoleptic series $[V(CNXyl)_6]^{1+,0,1-}$ can also be accessed from $V(CO)_6$ as summarized in Scheme I.10.[52b] Unlike $Co(CNAr^{Mes2})_4$,[36] the paramagnetic, 17-electron species $V(CNXyl)_6$ is EPR-silent, but exhibits sharp resonances in its ^1H and ^{13}C NMR spectra. The paramagnetic, low-spin d^4 complex $[V(CNXyl)_6]^+$ gives sharp ^1H and ^{13}C NMR resonances as well.[52b] The ^1H paramagnetic shifts for both $V(CNXyl)_6$ and $[V(CNXyl)_6]^+$ are essentially "contact" in origin and indicate unpaired spin delocalization into the π-systems of the 2,6-xylyl substituents.

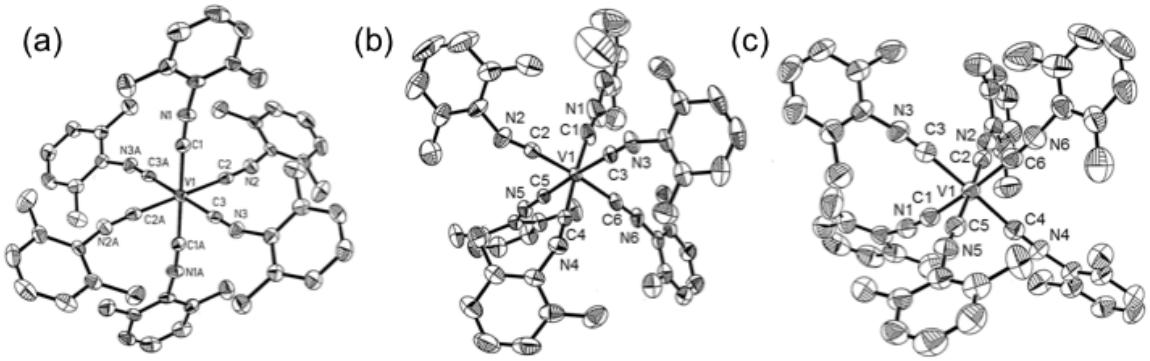

Figure I.10 ORTEP diagrams for (a) $V(CNXyl)_6$, (b) the $[V(CNXyl)_6]^-$ anion in $Cs[V(CNXyl)_6]$, and (c) the $[V(CNXyl)_6]^+$ cation in $[V(CNXyl)_6][PF_6]$. Hydrogen atoms are omitted. Adapted with permission from Ref. 53b; Copyright 2000 American Chemical Society.

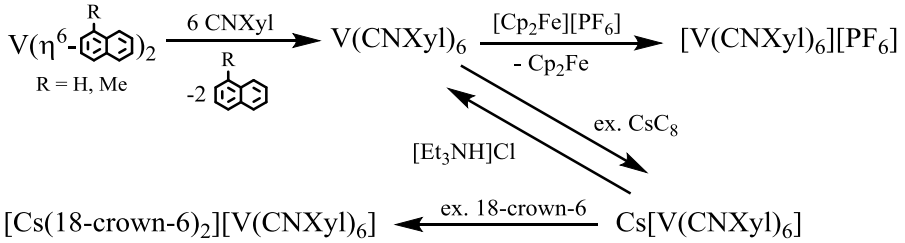

Scheme I.9

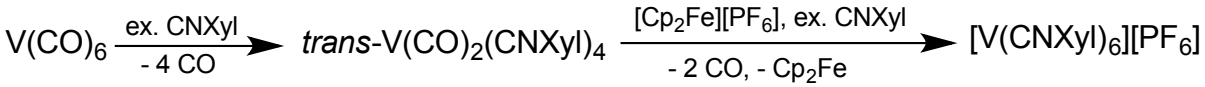

Scheme I.10

The energies of the ν_{NC} bands in the IR spectra of $[V(CNXyl)_6]^z$ (z = +1, 0, -1) are well below that for the free CNXyl ligand, which indicates a substantial extent of back-bonding even in the cation $[V(CNXyl)_6]^+$ (Table I.2). The trends in V-C and C-NXyl bond distances, C-N-C angles, as well as ν_{NC} energies for $[V(CNXyl)_6]^z$ (z = +1, 0, -1) and $[V(CN^tBu)]^{2+}$ are apparent from the corresponding data in Table I.2 and can be explained by increasing the extent of V(dπ)→CNR(π*) back-bonding upon decreasing the oxidation number of the metal ion.

The niobium and tantalum congeners of the isocyanidevanadate(-I) $[V(CNXyl)_6]^-$ were accessed by Ellis, Barybin and coworkers via sequential treatment of solutions of $[M(CO)_6]^-$ (M = Nb, Ta) with I_2 and CNXyl, followed by 2-electron reduction of the resulting seven-coordinate complex $M(CNXyl)_6I$ with excess CsC_8 (Scheme I.11) to yield $Cs[M(CNXyl)_6]$ (Figure I.11a).[17] Oxidative decarbonylation of $[M(CO)_6]^-$ with 2 equiv of $Ag[BF]_4$ in the presence of CNXyl cleanly afforded homoleptic cationic complexes $[M(CNXyl)_7]^+$ (Scheme I.11). Unlike paramagnetic six-coordinate $[V(CNXyl)_6]^+$, the Nb and Ta cations $[M(CNXyl)_7]^+$ are diamagnetic and contain seven discrete CNXyl ligands (Figure I.11b). Interestingly, the CNXyl ligands support direct nitrosylation of $[M(CO)_6]^-$ (M = Nb, Ta) with 2 equiv of $[NO][BF_4]$ to give *cis*-$[M(NO)_2(CNXyl)_4]^+$ (Scheme I.11).[17] Even though *cis*-$[M(NO)_2(CNXyl)_4]^+$ formally contain Nb(-I) and Ta(-I) centers, the CNXyl ligands in these complexes behave primarily as σ-donors to accommodate two linear NO ligands, which are extremely powerful π-acceptors. Treatment of $Ta(CNXyl)_6I$ with Diazald®, a mild source of NO^+, afforded mono-nitrosyl complex $Ta(CNXyl)_6(NO)$ (Scheme I.11).[17]

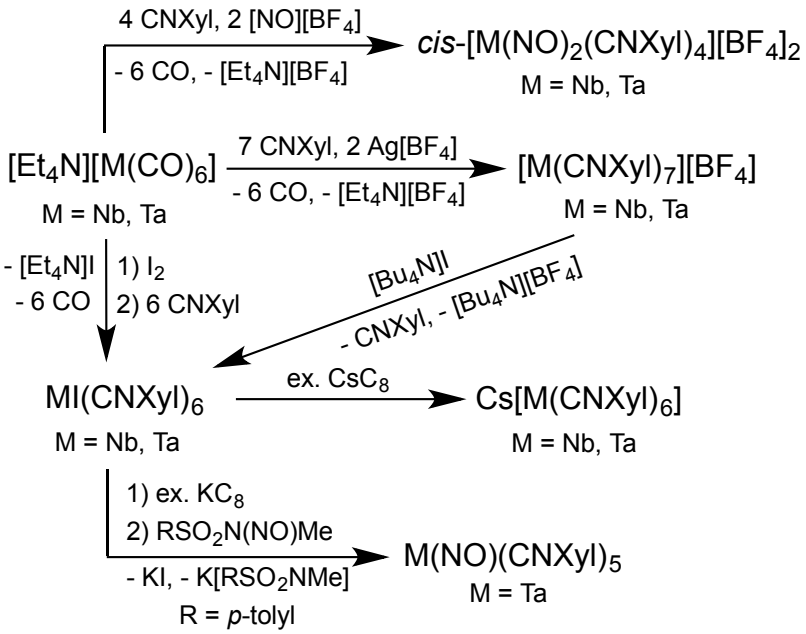

Scheme I.11

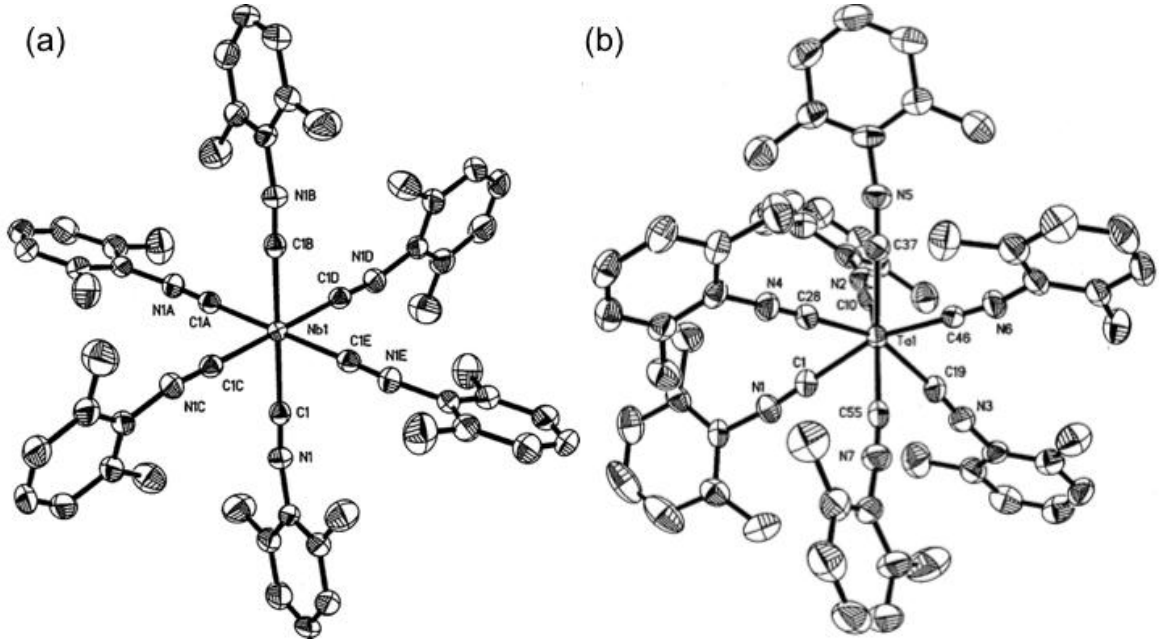

Figure I.11 ORTEP diagrams for (a) the $[Nb(CNXyl)_6]^-$ anion in $Cs[Nb(CNXyl)_6]$ and (b) the $[Ta(CNXyl)_7]^+$ cation in $[Ta(CNXyl)_7][BF_4]$. Hydrogen atoms are omitted. Adapted with permission from Ref. 17b; Copyright 2007 American Chemical Society.

While isocyanidemetalate(-1) analogues of long-established $[M(CO)_6]^-$ (M = V, Nb, Ta)[6] have finally been discovered, the existence of thermally stable $[V(CNXyl)_6]^+$, $[M(CNXyl)_7]^+$ (M = Nb, Ta), $M(CNXyl)_6I$ (M = Nb, Ta), *cis*-$[M(NO)_2(CNXyl)_4]^+$ (M = Nb, Ta), *cis*-

$[V(NO)_2(CN^tBu)_4]^+$ and $Ta(NO)(CNXyl)_5$, for which no carbonyl equivalents can be obtained, clearly underscores remarkable electronic versatility of 2,6-xylylisocyanide compared to CO as a ligand.

I.3 Coordination Chemistry of Nonbenzenoid Isocyanoarenes

I.3.1 Isocyanoazulenes

With the exception of isocyanoferrocene, all isocyanoarenes known until the early 2000's possessed benzenoid aryl substituents.[21] Recently, we have established a new class of isocyanoarenes incorporating the nonbenzenoid aromatic system of azulene.[21] Azulene is an unusual hydrocarbon composed of fused 5- and 7-membered rings (Figure I.12). Figure I.13 shows isocyanoazulene compounds, together with their corresponding abbreviations, reported by the Barybin group to date.[55-59] Given the polar nature of the azulenic scaffold (Figure I.12), these species can be considered stable derivatives of the hypothetical isocyanocyclopentadienide anion or isocyanotropylium cation.[21] The isocyanoazulenes in Figure I.13 are all crystalline substances that exhibit good thermal stability (except CN^6Az and CN^2Az^{CN}) and can be considered air-stable for practical purposes.

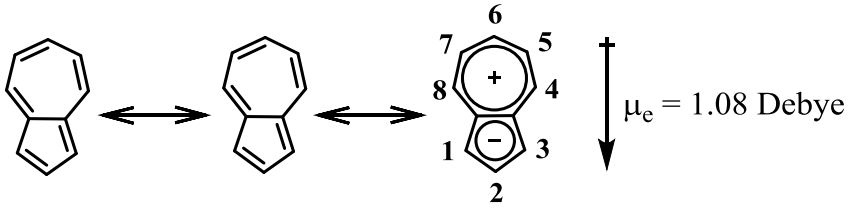

Figure I.12 The resonance forms of azulene emphasizing the polar nature and numbering scheme of the azulenic scaffold. Adapted with permission from Ref. 21.

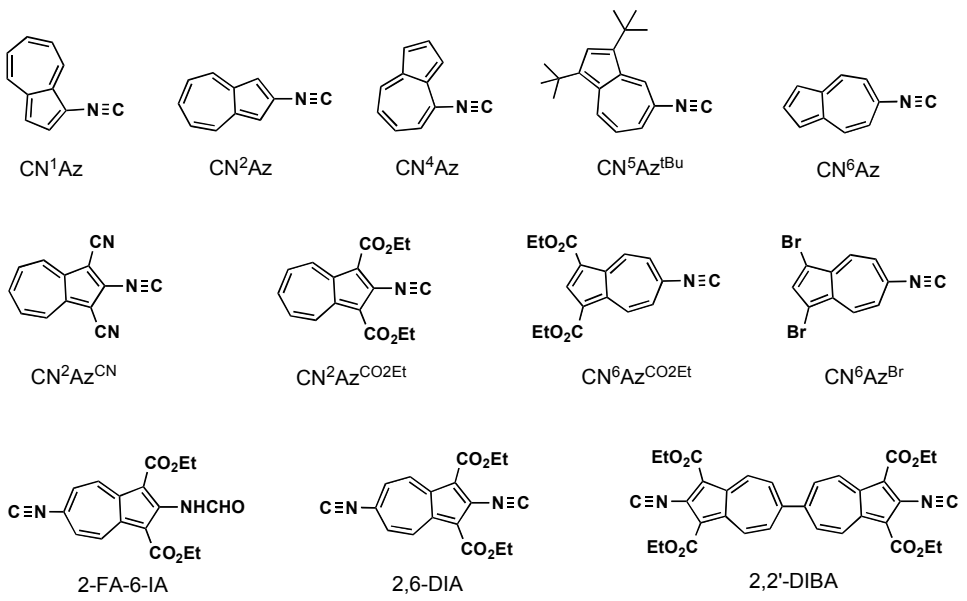

Figure I.13 Structures and the corresponding abbreviations of the isocyanoazulene derivatives known to date.

As shown in Figure I.14a, the frontier molecular orbitals of azulene have complementary density distributions, so the general reactivity profile of the azulenic scaffold is governed by the rules summarized in Figure I.14b. Notably, preparation of 2-substituted azulenes almost always requires having an appropriate substituent in place before closing the azulenic ring due to the quite unreactive nature of the C-H bond at the 2-position of the azulenic framework. The "parent" isocyanoazulenes CN^1Az, CN^4Az, CN^6Az, as well as the di-*t*-butyl derivative CN^5Az^{tBu}, can all be accessed regioselectively from azulene itself.[21, 56]

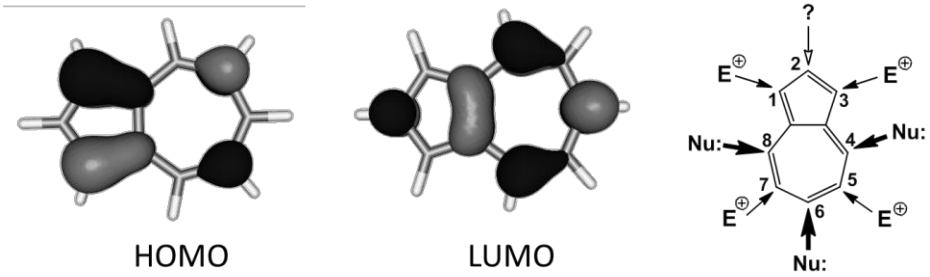

Figure I.14 (a) Lowest unoccupied molecular orbital (LUMO) and highest occupied molecular orbital (HOMO) of azulene. (b) Sites of nucleophilic (Nu:) and electrophilic (E^+) attacks of the azulenic scaffold as general strategies for its functionalization. Adapted with permission from Ref. 21.

I.3.2 Organometallic η^5-Isocyanocyclopentadienides

The currently known transition metal-stabilized η^5-isocyanocyclopentadienide ligands, along with their corresponding abbreviations used in this chapter, are shown in Figure I.15. While the first reports on the synthesis of isocyanoferrocene and two of its complexes $(CNFc)Cr(CO)_5$ and *cis*-$[(CNFc)_2Fe(CO)_4]$ appeared in the late 1980s, the chemistry of this redox-active, nonbenzenoid isocyanoarene ligand had remained idle until 2002,[60] presumably due to the rather tedious and inefficient procedures for the preparation of its precursor H_2NFc available at the time.[21] Indeed, depending on the synthetic route chosen, CNFc could be obtained in only 0.6 - 5% overall yields starting from ferrocene.[21]

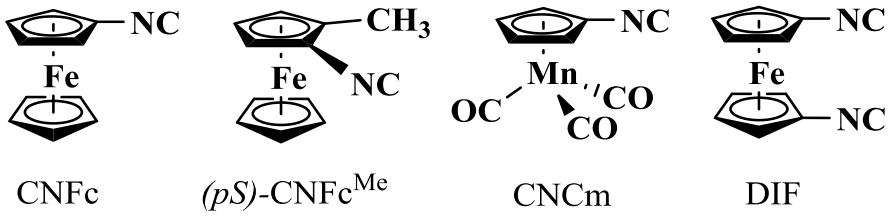

Figure I.15 Structures and the corresponding abbreviations of the η^5-bound isocyanocyclopentadienide ligands reported to date.

After a few greatly improved syntheses of aminoferrocene had been published at the turn of the 20th century,[61-63] the Barybin group developed a highly reproducible procedure for the preparation of isocyanoferrocene that affords CNFc in a 38% overall yield based on the starting ferrocene.[60] Previously unknown isocyanocymantrene, CNCm, was synthesized from commercial cymantrene, $CpMn(CO)_3$, in a 45% overall yield through a convenient three-step reaction sequence.[64] In addition, a planar-chiral version of isocyanoferrocene, namely $(_pS)$-1-isocyano-2-methylferrocene, was recently isolated in an enantiomerically pure form and characterized crystallographically as an adduct with PdI_2 (Figure I.16).[65] Finally, an efficient

synthesis of 1,1'-diisocyanoferrocene, DIF, from 1,1'-ferrocenedicarboxylic acid was reported by Hessen and van Leusen in 2001.[63]

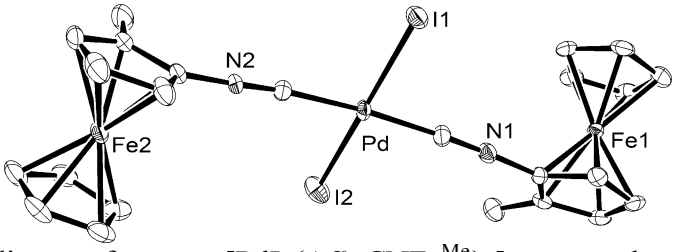

Figure I.16 ORTEP diagram for *trans*-[$PdI_2\{(_pS)$-$CNFc^{Me}\}_2$] generated using the ORTEP-3 program from CIF data in Ref. 65. Hydrogen atoms are omitted.

I.3.3 Homoleptic Complexes of Nonbenzenoid Isocyanoarenes

The coordination chemistry of azulene and its derivatives has been dominated by multi-hapto interactions of the azulenic scaffold with transition metal centers that disrupt the aromaticity of the azulenic nucleus.[21, 66] Our interest in the family of isocyanoazulenes originated from the quest for metal-organic systems in which the azulenic core is electronically coupled to an electron-rich metal atom or ion while retaining its aromatic character. Because of the cylindrical symmetry of its π-system, the isocyanide group appeared to be an attractive choice as a π-conducting junction. Treatment of $Cr(\eta^6$-naphthalene$)_2$, a storable source of atomic chromium, with six equivalents of various isocyanoazulenes, including CN^1Az, CN^2Az, CN^4Az, CN^5Az^{tBu}, and CN^6Az, afforded the corresponding binary complexes $Cr(CNR)_6$ that feature six discrete isocyanoazulene ligands. The monocationic versions thereof were prepared via oxidation of the neutral complexes with, for example, AgX (X = BF_4, SbF_6).

The isomeric, low-spin d^5 complexes $[Cr(CN^xAz)_6]^+$ (x = 1, 2, 4, or 6) (Figure I.17) give interesting ^1H and ^{13}C NMR patterns that suggest unpaired electron spin delocalization from the Cr(I) center into the π*-systems of the azulenyl substituents by means of back-bonding to the isocyanide junction.[56] For instance, Figure I.18a displays the ^1H NMR spectrum of

$[Cr(CN^1Az)_6]^+$ that features substantial paramagnetic shifts of the ^1H resonances with respect to its diamagnetic, low-spin d^6 analogue $Cr(CN^1Az)_6$. These paramagnetic shifts are essentially "contact" in origin because of the octahedral symmetry of the cation. The ^1H NMR peaks for the hydrogen atoms 2, 5, and 7 of the azulenic frameworks in $[Cr(CN^1Az)_6]^+$ are shifted upfield, which suggests the presence of unpaired electron spin density in the p-orbitals of the corresponding carbon atoms. This phenomenon is nicely illustrated by the DFT-generated pictures of the "t_{2g}"-like molecular orbitals of $[Cr(CN^1Az)_6]^+$ (Figure I.18b) that clearly show contributions from the p-orbitals of the carbon atoms 2, 5, and 7, as well as $Cr(d\pi)\rightarrow CN^1Az(p\pi^*)$ back-bonding interactions between the Cr(I)-center and the isocyanide junctions. The ^1H NMR pattern in Figure I.18a can also be rationalized by considering a simple valence-bond description of back-bonding in $[Cr(CN^1Az)_6]^+$, as illustrated in Figure I.18c.

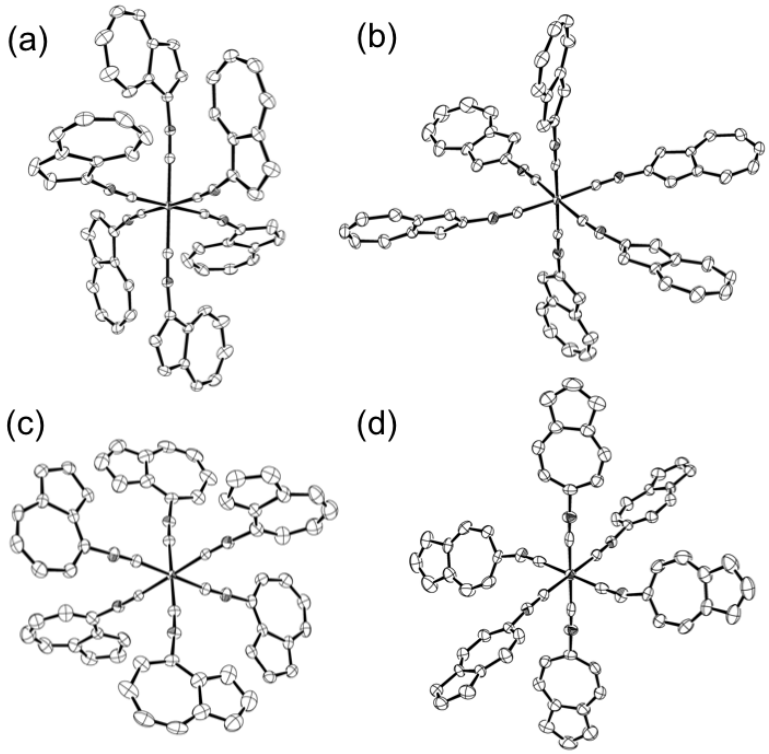

Figure I.17 ORTEP diagrams for the isomeric cations in (a) $[Cr(CN^1Az)_6][V(CO)_6]$, (b) $[Cr(CN^2Az)_6][BF_4]$, (c) $[Cr(CN^4Az)_6][SbF_6]$, and (d) $[Cr(CN^6Az)_6][BF_4]$. Hydrogen atoms are omitted. Adapted with permission from Ref. 21.

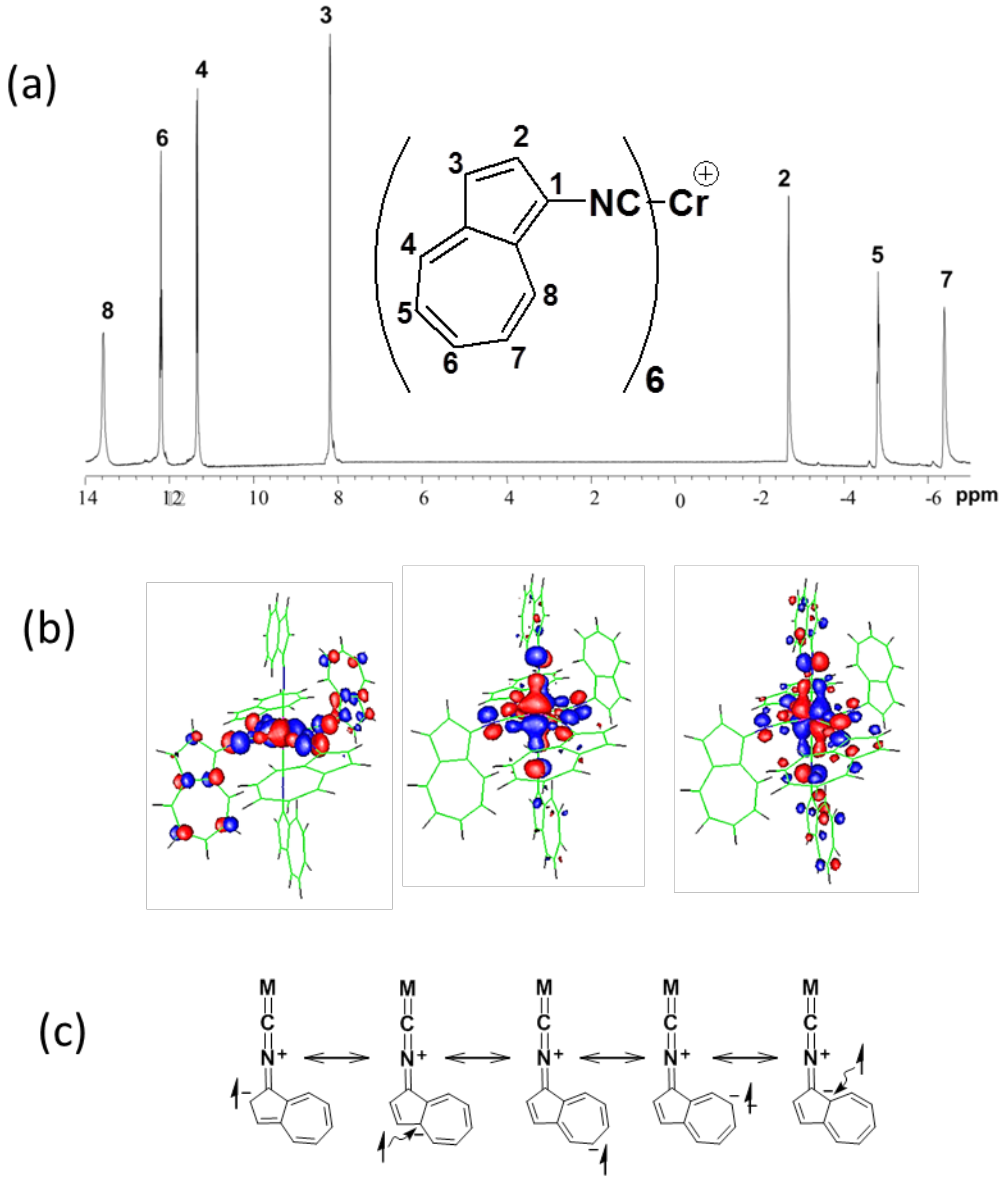

Figure I.18 (a) ^{1}H NMR spectrum of $[Cr(CN^{1}Az)_6][V(CO)_6]$ in CD_2Cl_2 at 25 °C. (b) The "t_{2g}"-like set of the highest occupied MO's for the low-spin d^5 complex $[Cr(CN^{1}Az)_6]^{+}$ adapted with permission from Ref. 56; Copyright 2005 American Chemical Society. (c) Resonance description of unpaired spin delocalization in $[Cr(CN^{1}Az)_6]^{+}$ through $Cr(d\pi)\rightarrow CN^{1}Az(p\pi^*)$ back-bonding.

The air-stable homoleptic, heptanuclear complexes of CNFc and CNCm were isolated for chromium in three different oxidation states: $[Cr(CNR)_6]^{0,1+,2+}$ (Figure I.19).[64] Akin to the series $[Cr(CNR)_6]^{0,1+,2+,3+}$,[67, 68] $[V(CNXyl)_6]^{1-,0,1+}$,[53b] and $[Co(CNAr^{Mes2})_6]^{1-,0,1+}$,[36] for $[Cr(CNFc)_6]^{0,1+,2+}$

the average M-C bond elongates, the average C-NR distance decreases, and the average C-N-C angle widens upon successive oxidation of the metal center (Tables I.2 and I.3).[64]

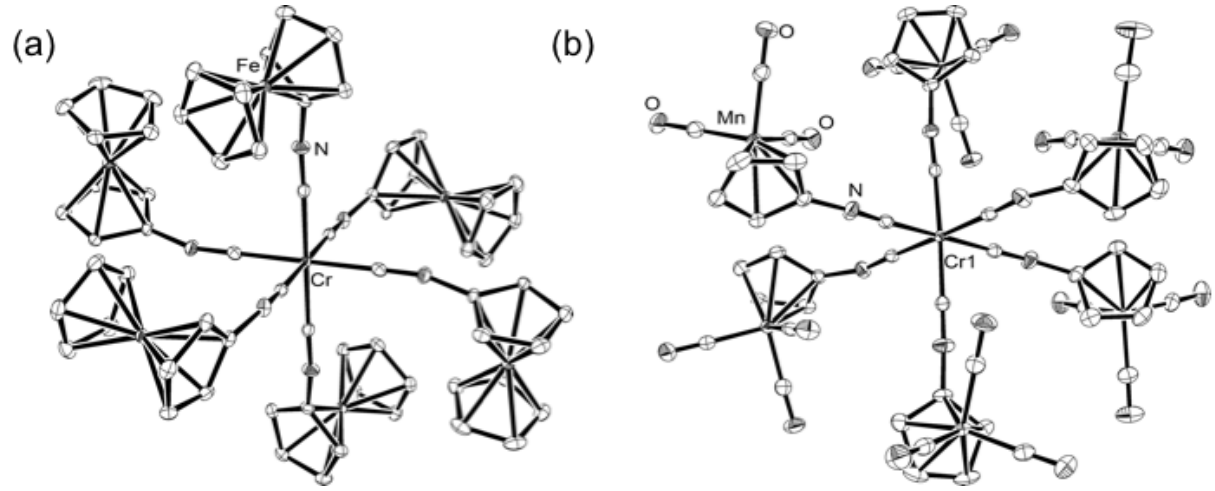

Figure I.19 ORTEP diagrams for (a) $Cr(CNFc)_6$ and (b) $Cr(CNCm)_6$ generated using the ORTEP-3 program from CIF data in Ref. 64. Hydrogen atoms are omitted.

Table I.3 Selected IR spectroscopic and X-ray[a] structural data for binary isocyanide complexes of chromium that contain CNPh, CNFc, or CNCm ligands.

Complex	ν_{NC} (cm^{-1})	Cr-C bond length (Å)	C-NR bond length (Å)	C-N-C angle (°)	Reference
$[Cr(CNPh)_6]^{3+}$	2205	2.07(1)	1.139(5)	172(3)	67
$[Cr(CNPh)_6]^{2+}$	2139	2.014(5)	1.158(5)	177(1)	67
$[Cr(CNPh)_6]^{+}$	2056	1.98(1)	1.159(5)	177(1)	67
$Cr(CNPh)_6$	1950	1.938(3)	1.176(4)	173.7(2)	68
$[Cr(CNFc)_6]^{2+}$	2131	2.019(17)	1.150(5)	175(3)	64
$[Cr(CNFc)_6]^{+}$	2053	1.972(13)	1.160(3)	171(4)	64
$Cr(CNFc)_6$	1971	1.937(7)	1.178(5)	162(4)	64
$Cr(CNCm)_6$	1947	1.93(2)	1.18(1)	162(14)	64

a NUMBERS IN PARENTHESES ARE THE STANDARD DEVIATIONS FROM THE MEAN

It is instructive to consider the extensive data in Table I.4, which contains the values of the half-wave potentials for the reversible redox couples $[Cr(CNR_6)]^{0/1+}$ and $[Cr(CNR_6)]^{1+/2+}$ and essentially constitutes a quantitative electrochemical measure of the σ-donor/π-acceptor ratios of various isocyanide ligands. From Table I.4, it is evident that the electron richness of the metal center in zero-valent $Cr(CN^4Az)_6$ is practically the same as that in the mono-valent $[Cr(CN^1Az)_6]^+$. According to this Table, the isocyanoazulenes CN^4Az and CN^6Az appear to have the lowest σ-donor/π-acceptor ratios amongst any known isocyanide with a purely hydrocarbon substituent.[21]

Table I.4 Half-wave $E_{1/2}$ redox potentials (in volts versus Cp_2Fe/Cp_2Fe^+) for $[Cr(CNR)_6]^{z/z+1}$ couples in $CH_2Cl_2/[^nBu_4N][PF_6]$.

	Substituent R										
Couple		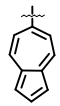	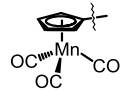	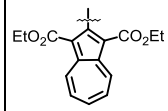	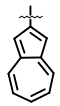		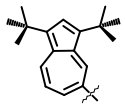				
$[Cr(CNR)_6]^{0/1+}$	-0.44	-0.49	-0.53	-0.67	-0.69	-0.83	-0.87	-0.97	-0.98	-1.03	-1.54
$[Cr(CNR)_6]^{1+/2+}$	0.02	-0.03	-0.04	-0.14	-0.16	-0.21	-0.29	-0.35	-0.42	-0.32	-0.77
Reference	56	56	64	71	56	70	56	64	56	71	69
	σ–donor/π–acceptor ratio increases →										

Even though the electronic characteristics of isocyanoferrocene as a ligand have been thought to be comparable to those of CNMe based on similarities of the electrochemical behavior of $(OC)_5Cr(CNFc)$ and $(OC)_5Cr(CNMe)$,[72, 73] as well as the fact that the Hammett constants for the Fc and Me substituents are identical,[74] the σ-donor/π-acceptor ratio of CNFc is clearly closer to that of CNPh rather than an alkyl isocyanide. The DFT analysis of isocyanoferrocene suggested that its LUMO and LUMO+2 are well-suited for delocalizing π-back-bonded electron density beyond the isocyanide junction upon coordination to an electron-rich metal center.[60, 64] In addition, the CNCm ligand is a substantially more powerful π-acceptor than CNFc, so the σ-donor/π-acceptor behavior of an η^5-isocyclopentadienide can indeed be tuned by varying the nature of the metal unit coordinated to its five-membered ring.

I.3.4 Bridging Nonbenzenoid Isocyanoarenes

In 2005, Chisholm, Barybin, Dalal and co-workers demonstrated through a series of UV-Vis-NIR, EPR, cyclic voltammetry, and DFT studies of the 2,6-azulene-dicarboxylate bridge linking M-M quadruply-bonded units (M = Mo, W) that the π*-system of the 2,6-azulenic scaffold is exceptionally well-suited for supporting charge delocalization between electron reservoirs.[75] Shortly thereafter, the first mono-and dinuclear complexes of 2,6-DIA with $[M(CO)_5]$ (M = Cr, W) fragments were reported.[57] The M(dπ)→2,6-DIA(pπ*) charge transfer in these complexes occurs in the visible range due to the quite low energy of 2,6-DIA's LUMO.

Interestingly, the energy of the M(dπ)→2,6-DIA(pπ*) charge transfer band observed for the mononuclear complexes $(OC)_5M(\eta^1$-2,6-DIA) (M = Cr, W) does not depend on which end of the asymmetric 2,6-DIA ligand is coordinated to the metal pentacarbonyl moiety (Figure I.20). In addition, binucleation of mononuclear species $(OC)_5M(\eta^1$-2,6-DIA) to form $[(OC)_5M]_2(\mu$-

η^1:η^1-2,6-DIA) (M = Cr, W) is accompanied by a substantial red-shift in the M(dπ)→2,6-DIA(pπ*) charge transfer band (Figure I.20), indicating that the entire π*-system of 2,6-DIA, not just its isocyanide junctions, is involved in the M(dπ)→2,6-DIA(pπ*) charge transfer. In the case of the tungsten system, this red shift is much greater than that observed earlier by Bennett *et al.*[76] for the analogous 1,4-diisocyanobenzene-bridged system (Table I.5).

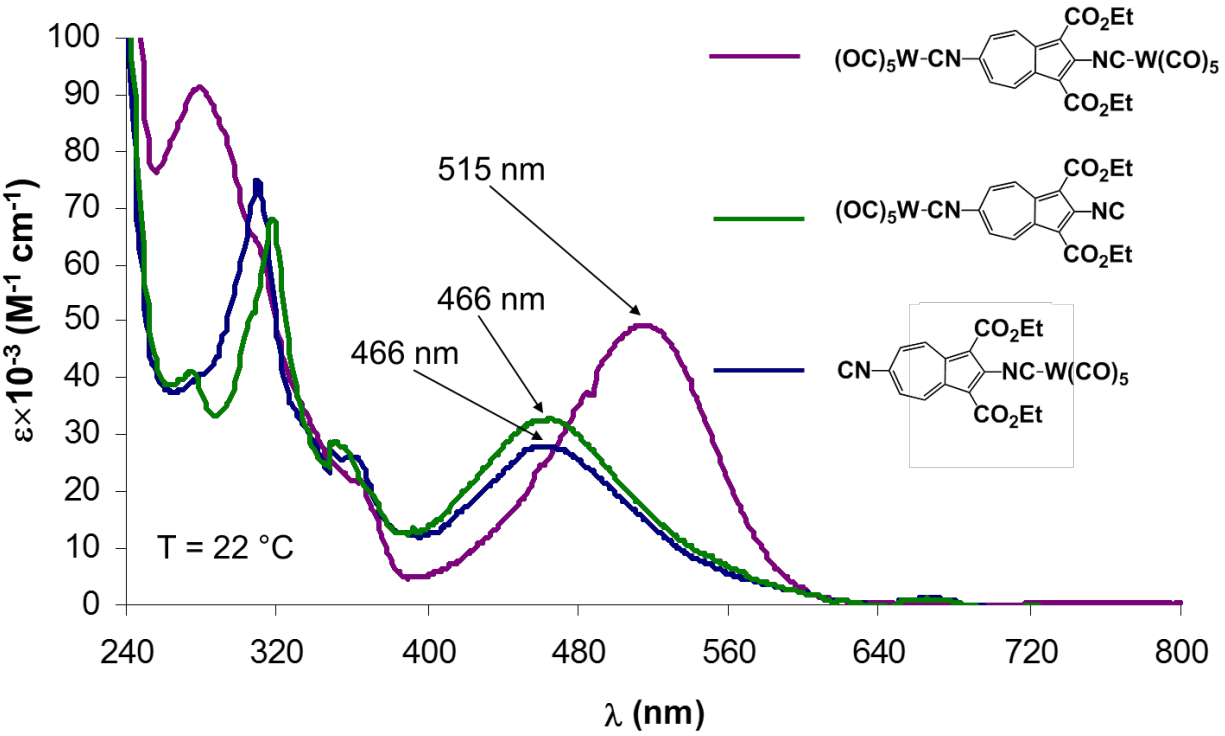

Figure I.20 UV-Vis spectra of $[(OC)_5W]_2(\mu\text{-}\eta^1\text{:}\eta^1\text{-2,6-DIA})$ and two isomeric mononuclear complexes $[(OC)_5W](\eta^1\text{-2,6-DIA})$ in CH_2Cl_2. Adapted with permission from Ref. 57; Copyright 2006 American Chemical Society.

Table I.5 Red-shifts in energy of the metal-to-ligand charge transfer (MLCT) that occur upon binucleation of 2,6-diisocyano-1,3-diethoxycarbonylazulene (2,6-DIA) or 1,4-diisocyanobenzene (DIB) ligands.

Binucleation process	ΔE_{MLCT} (cm^{-1})	Reference
$(OC)_5Cr(\eta^1\text{-2,6-DIA}) \rightarrow [(OC)_5Cr]_2(\mu\text{-}\eta^1\text{:}\eta^1\text{-2,6-DIA})$	1650	57
$(OC)_5W(\eta^1\text{-2,6-DIA}) \rightarrow [(OC)_5W]_2(\mu\text{-}\eta^1\text{:}\eta^1\text{-2,6-DIA})$	2042	57
$(OC)_5W(\eta^1\text{-DIB}) \rightarrow [(OC)_5W]_2(\mu\text{-}\eta^1\text{:}\eta^1\text{-DIB})$	1221	76

While optimizing the synthesis of 2,6-DIA, we noticed that the dehydration of the 2-formamido terminus in 2,6-diformamido-1,3-diethoxycarbonylazulene proceeds significantly slower than that of the 6-formamido end, which allowed for the preparation of the 2-formamido-6-isocyanoazulene derivative 2-FA-6-IA (Figure I.13) in a highly regioselective manner (Scheme I.12). This, in turn, permitted regioselective heterobimetallic complexation of the 2,6-DIA linker via stepwise installation and coordination of its isocyanide termini, as illustrated in Scheme I.12. Switching the order of addition of the two $M(CO)_5(THF)$ reactants in Scheme I.12 afforded the isomeric binuclear product featuring interchanged Cr/W sites (Figure I.21).[21, 57]

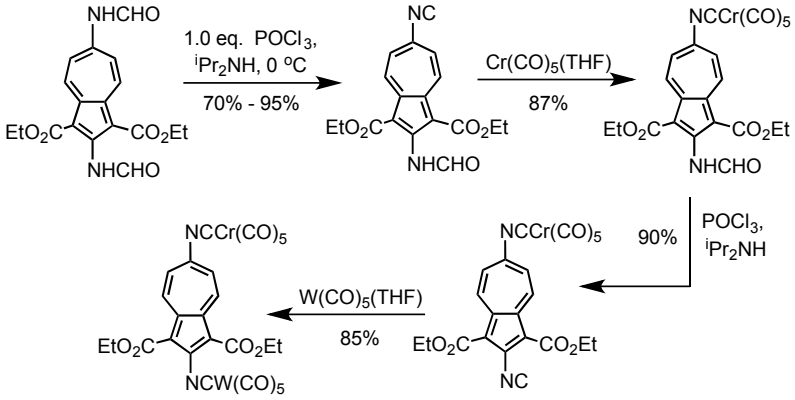

Scheme I.12

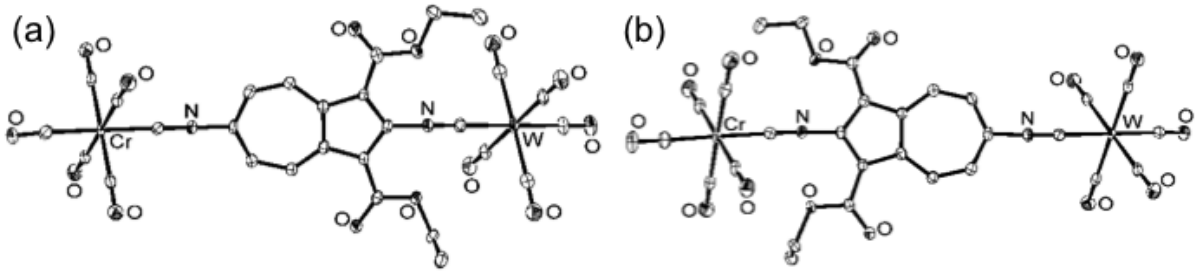

Figure I.21 ORTEP diagrams for two isomeric heterobimetallic complexes $[(OC)_5W](\mu\text{-}\eta^1\text{:}\eta^1\text{-}2,6\text{-DIA})[Cr(CO)_5]$. Hydrogen atoms are omitted. Adapted with permission from Ref. 21.

In 2010, synthesis of the first linear 2,2'-diisocyano-6,6'-biazulenyl linker (2,2'-DIBA, Figure I.13) was accomplished via an unexpected "one-pot" homocoupling of 2-amino-6-bromo-

1,3-diethoxycarbonylazulene followed by standard formylation and dehydration procedures.[58] This molecule exhibits reversible two-electron reduction to form a singlet dianion. The long axis of 2,2'-DIBA, which is the only structurally characterized biazulenyl derivative known, spans more than 17 Å (Figure I.22). Similar to 2,6-DIA, 2,2'-DIBA readily coordinates to metal fragments, such as $[W(CO)_5]$, via its isocyanide termini.

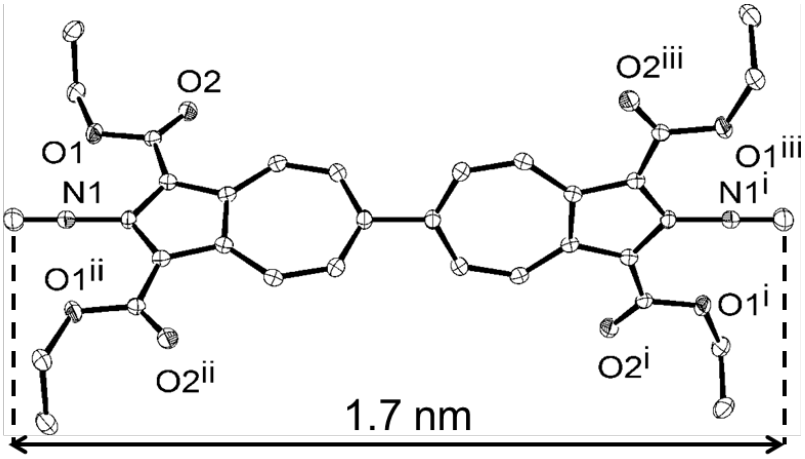

Figure I.22 ORTEP diagram for 2,2'-DIBA generated using the ORTEP-3 program from CIF data in Ref. 58. Hydrogen atoms are omitted.

The coordination chemistry of 1,1'-diisocyanoferocene (DIF) has been recently established by Siemeling and co-workers. The structurally characterized complexes of this redox-active ditopic isocyanide ligand include $[(OC)_5Cr]_2(\mu\text{-DIF})$,[77, 78] $[Ag_2(\mu\text{-DIF})]^{2+}$,[79] paddle-wheel-like $[Cu_2(\mu\text{-DIF})_3]^{2+}$ (Figure I.23a),[80] and $[(ClAu)_2(\mu\text{-DIF})]_\infty$ (Figure I.23b)[77, 78]. The latter structure constitutes an intriguing model for understanding self-assembly of DIF on gold surfaces.[77, 78] Adducts of DIF with a few Au(I) acetylides are also known.[78, 81]

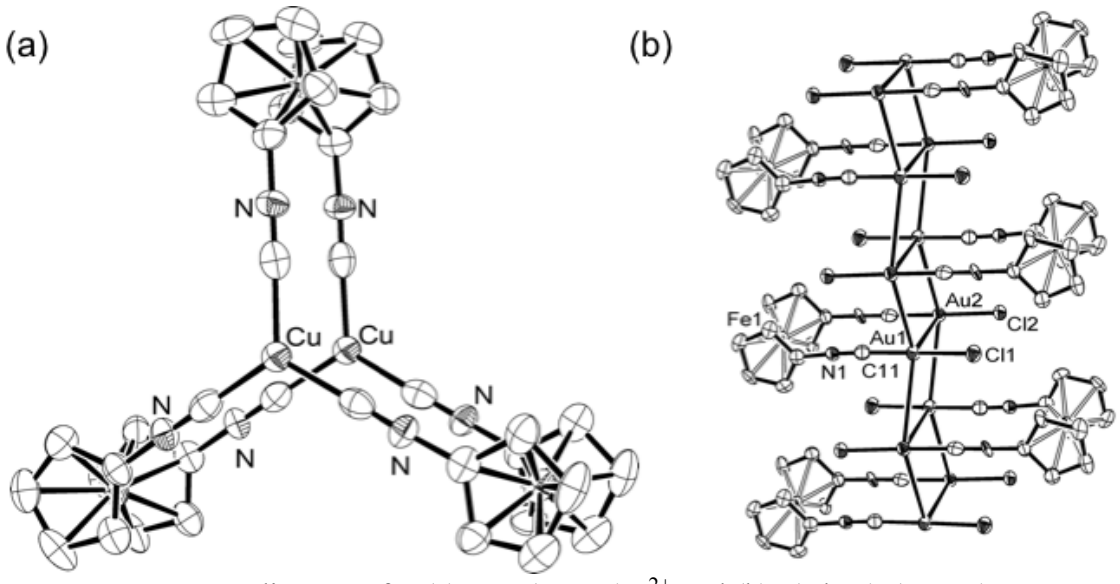

Figure I.23 ORTEP diagrams for (a) $[Cu_2(\mu\text{-DIF})_3]^{2+}$ and (b) $[(ClAu)_2(\mu\text{-DIF})]_\infty$ generated using the ORTEP-3 program from CIF data in Refs. 77, 80. Hydrogen atoms are omitted.

I.4 Conclusions and Outlook

In this Chapter, we addressed several relatively recent developments in the transition metal chemistry of isocyanoarenes. The discovery of isolable isocyanidemetalates and related low-valent complexes significantly narrowed a long-standing fundamental gap in the coordination chemistry of CNR and CO ligands at the electron-rich extreme. It is now apparent that isocyanoarene ligands with hydrocarbon substituents R can behave not only as powerful π-acceptors, but also adjust their σ-donor/π-acceptor characteristics in a wide continuous range to accommodate electronic requirements at the metal center. The recently emerged bulky isocyanoarenes, such as $CNAr^{Mes2}$ and $CNAr^{Dipp2}$, are destined to bring revolutionary changes to the landscape of modern coordination and organometallic chemistry of isocyanides, including applications in catalysis. The unprecedented low-valent, low-coordinate complexes, such as $[Co(CNAr^{Mes2})_4]^z$,[36] $Ni(CNAr^{Dipp2})_3$,[82] and $Pd(CNAr^{Dipp2})_2$[83] exhibit unique reactivity patterns and are the most profound examples of capitalizing on the steric variability of the substituent R in a CNR ligand. The families of isocyanoazulenes and η^5-bound isocyanocyclopentadienides

(including planar-chiral versions thereof) provide yet another dimension for expanding electronic and steric versatilities of an isocyanoarene ligand in coordination and surface chemistry. The linear, isocyanide-terminated 2,6-azulenic and biazulenic frameworks constitute intriguing new platforms for developing azulene-based nanoarchitectures for applications in functional organic electronics.

I.5 References

1 Gautier, A. *Justus Liebigs Ann. Chem.* **1869**, *151*, 239-244.

2 Meyer, E. *J. Prak. Chem.* **1856**, *68*, 279-295.

3 Lieke, W. *Justus Liebigs Ann. Chem.* **1859**, *112*, 316-321.

4 Malatesta, L. Isocyanide complexes of metals. In *Progress in Inorganic Chemistry*, Volume 1; Cotton, F.A., Ed.; John Wiley & Sons: Hoboken, NJ, 1959; pp. 283-379.

5 Hoffmann, R. *Angew. Chem. Int. Ed. Eng.* **1982**, *21*, 711-724.

6 (a) Ellis, J.E. *Organometallics* **2003**, *22*, 3322-3338; (b) Ellis, J.E. *Inorg. Chem.* **2006**, *45*, 3167-3186; (c) Ellis, J.E. *Inorg. Chem.* **2006**, *45*, 5710-5710.

7 (a) Barker, G.K.; Galas, A.M.R.; Green, M.; Howard, J.A.K.; Stone, F.G.A.; Turney, T.W.; Welch, A.J.; Woodward, P. *J. Chem. Soc., Chem. Comm.* **1977**, 256-258; (b) Yamamoto, Y., Yamazaki, H. *Inorg. Chem.* **1978**, *17*, 3111-3114.

8 (a) Silverman, L.D.; Dewan, J.C.; Giandomenico, C.M.; Lippard, S.J. *Inorg. Chem.* **1980**, *19*, 3379-3383; (b) Silverman, L.D.; Corfield, P.W.R.; Lippard, S.J. *Inorg. Chem.* **1981**, *20*, 3106-3109.

9 Warnock, G.F.; Cooper, N.J. *Organometallics* **1989**, *8*, 1826-1827.

10 Allen, J.M.; Ellis, J.E. *J. Organomet. Chem.* **2008**, *693*, 1536-1542.

11 (a) $[Mn(CNR)_5]^-$: Utz, T.L.; Leach, P.A.; Geib, S.J.; Cooper, N.J. *Chem. Comm.* **1997**, 847-848; (b) $[Mn(CNR)_6]^{2+}$: Mann, K.R.; Cimolino, M.; Geoffroy, G.L.; Hammond, G.S.; Orio, A.A.; Albertin, G.; Gray, H.B. *Inorg. Chim. Acta* **1976**, *16*, 97-101; (c) $[Tc(CNR)_6]^+$: Abrams, M.J.; Davison, A.; Jones, A.G.; Costello, C.E.; Pang, H. *Inorg. Chem.* **1983**, *22*, 2798-2800; (d) $[Fe(CNR)_6]^{2+}$: Bonati, F.; Minghetti, G. *J. Organomet. Chem.* **1970**, *22*, 183-194; (e) $[Ru(CNR)_4]^{2-}$: Corella, J.A.; Thompson, R.L.; Cooper, N.J. *Angew. Chem. Int. Ed. Eng.* **1992**, *31*, 83-84; (f) $[Ru(CNR)_6]^{2+}$ and $[Os(CNR)_6]^{2+}$: Tetrick, S.M.; Walton, R.A. *Inorg. Chem.* **1985**, *24*, 3363-3366; (g) $Rh_2(CNR)_8$: Yamamoto, Y.; Yamazaki, H. (1984) *Bull. Chem. Soc. Jpn.* **1984**, *57*, 297-298; (h) $Ni_4(CNR)_6$: Muetterties, E.L.; Band, E.; Kokorin, A.; Pretzer, W.R.; Thomas, M.G. *Inorg. Chem.* **1980**, *19*, 1552-1560; (i) $[Ag(CNR)_4]^+$: Pierce, J.L.; Wigley, D.E.; Walton, R.A. *Organometallics **1982***, *1*, 1328-1331.

12 Weber, L. *Angew. Chem. Int. Ed. Eng.* **1998**, *37*, 1515-1517.

13 Hammick, D.L.; New, R.C.A.; Sidgwick, N.V.; Sutton, L.E. *J. Chem. Soc.* **1930**, 1876-1887.

14 Triechel, P.M. *Adv. Organomet. Chem.* **1973**, *11*, 21-86.

15 Sacco, A. *Gazz*. *Chim*. *Ital*. **1953**, *83*, 632-636.

16 (a) Lentz, D. Organometallic chemistry of fluorinated isocyanides. In *Inorganic Fluorine Chemistry: Toward the 21st Century*; Thrasher, J.S., Strauss, S.H., Eds; American Chemical Society: Washington, D.C., 1994; pp. 265-285; (b) Lentz, D. *Angew*. *Chem*. *Int*. *Ed*. *Eng*. **1994**, *33*, 1315-1331.

17 (a) Barybin, M.V.; Young, Jr., V.G.; Ellis, J.E. *J*. *Am*. *Chem*. *Soc*. **1999**, *121*, 9237-9238; (b) Barybin, M.V.; Brennessel, W.W.; Kucera, B.E.; Minyaev, M.E.; Sussman, V.J.; Young, V.G.; Ellis, J.E. *J*. *Am*. *Chem*. *Soc*. **2007**, *129*, 1141-1150.

18 Ellis, J.E.; Warnock, G.F.; Barybin, M.V.; Pomije, M.K. *Chem*. *Eur*. *J*. **1995**, *1*, 521-527.

19 Warnock, G.F.P.; Sprague, J.; Fjare, K.L.; Ellis, J.E. *J*. *Am*. *Chem*. *Soc*. **1983**, *105*, 672-672.

20 Dömling, A. *Chem*. *Rev*. **2006**, *106*, 17-89.

21 Barybin, M.V. *Coord*. *Chem*. *Rev*. **2010**, *254*, 1240-1252.

22 Harvey, P.D.; Clément, S.; Knorr, M.; Husson, J. Luminescent organometallic coordination polymers built on isocyanide bridging ligands. In *Macromolecules Containing Metal and Metal-like Elements*, *Volume 10: Photophysics and Photochemistry of Metal-Containing Polymers*, 1st edn; Aziz, A.S. A.-E., Carraher, Jr., C.E., Harvey, P.D., Pittman, Jr., C.U., Zeldin, M. Eds.; John Wiley & Sons: Hoboken, 2010; pp. 45-87.

23 Lazar, M.; Angelici, R.J. Isocyanide binding modes on metal surfaces and in metal complexes. In *Modern Surface Organometallic Chemistry*; Basset, J.-M., Psaro, R., Roberto, D., Ugo, R. Eds.; Wiley-VCH: Weinheim, 2009; pp. 513–556.

24 Heimel, G.; Romaner, L.; Zojer, E.; Bredas, J.-L. *Acc*. *Chem*. *Res*. **2008**, *41*, 721-729.

25 Puddephatt, R.J. *Coord*. *Chem*. *Rev*. **2001**, *216–217*, 313-332.

26 Nakano, T.; Okamoto, Y. *Chem*. *Rev*. **2001**, *101*, 4013-4038.

27 Hong, S.; Reifenberger, R.; Tian, W.; Datta, S.; Henderson, J.; Kubiak, C.P. *Superlattices Microstruct*. **2001**, *28*, 289-303.

28 Sharma, V.; Piwnica-Worms, D. *Chem*. *Rev*. **1999**, *99*, 2545-2560.

29 Lippard, S.; Carnahan, E. *Acc*. *Chem*. *Res*. **1993**, *26*, 90-97.

30 Hahn, F.E. *Angew*. *Chem*. *Int*. *Ed*. *Eng*. **1993**, *32*, 650-665.

31 Singleton, E.; Oosthuizen, H.E. *Adv*. *Organomet*. *Chem*. **1983**, *22*, 209-310.

32 Yamamoto, Y. *Coord*. *Chem*. *Rev*. **1980**, *32*, 193-233.

33 Leach, P.A.; Geib, S.J.; Corella, J.A.; Warnock, G.F.; Cooper, N.J. *J*. *Am*. *Chem*. *Soc*. **1994**, *116*, 8566-8574.

34 (a) Brennessel, W.W.; Young, V.G.; Ellis, J.E. *Angew*. *Chem*. *Int*. *Ed*. **2006**, *45*, 7268-7271; (b) Brennessel, W.W.; Young, V.G.; Ellis, J.E. *Angew*. *Chem*. *Int*. *Ed*. **2002**, *41*, 1211-1215.

35 (a) Fox, B.J.; Sun, Q.Y.; DiPasquale, A.G.; Fox, A.R.; Rheingold, A.L.; Figueroa, J.S. *Inorg*. *Chem*. **2008**, *47*, 9010-9020; (b) Ditri, T.B.; Fox, B.J.; Moore, C.E.; Rheingold, A.L.; Figueroa, J.S. *Inorg*. *Chem*. **2009**, *48*, 8362-8375.

36 Margulieux, G.W.; Weidemann, N.; Lacy, D.C.; Moore, C.E.; Rheingold, A.L.; Figueroa, J.S. *J*. *Am*. *Chem*. *Soc*. **2010**, *132*, 5033-5035.

37 Ricks, A.M.; Bakker, J.M.; Douberly, G.E.; Duncan, M. *J*. *Phys*. *Chem*. *A* **2009**, *113*, 4701-4708.

38 Brennessel, W.W.; Ellis, J.E. *Angew*. *Chem*. *Int*. *Ed*. **2007**, *46*, 598-600.

39 Hieber, W.; Leutert, F. *Ber*. *Dtsch*. *Chem*. *Ges*. **1931**, *64*, 2832-2839.

40 Mathieson, T.; Schier, A.; Schmidbaur, H. *J*. *Chem*. *Soc*., *Dalton Trans*. **2001**, 1196-1200.

41 Chin, H.B.; Bau, R. *J*. *Am*. *Chem*. *Soc*. **1976**, *98*, 2434-2439.

42 Utz, T.L.; Leach, P.A.; Geib, S.J.; Cooper, N.J. *Organometallics* **1997**, *16*, 4109-4114.

43 Stewart, M.A.; Moore, C.E.; Ditri, T.B.; Labios, L.A.; Rheingold, A.L.; Figueroa, J.S. *Chem*. *Comm*. **2011**, *47*, 406-408.

44 Rossi, A.R.; Hoffmann, R. *Inorg*. *Chem*. **1975**, *14*, 365-374.

45 (a) Ellis, J.E.; Fjare, K.L. *Organometallics* **1982**, *1*, 898-903; (b) Ihmels, K.; Rehder, D. *Organometallics* **1985**, *4*, 1340-1347.

46 (a) Ellis, J.E.; Fjare, K.L.; Warnock, G.F. *Inorg*. *Chim*. *Acta* **1995**, *240*, 379-384; (b) Barybin, M.V.; Ellis, J.E.; Pomije, M.K.; Tinkham, M.L.; Warnock, G.F. *Inorg*. *Chem*. **1998**, *37*, 6518-6527.

47 Carnahan, E.M.; Lippard, S.J. *J*. *Am*. *Chem*. *Soc*. **1992**, *114*, 4166-4174.

48 Herberhold, M.; Trampisch, H. *Inorg*. *Chim*. *Acta* **1983**, *70*, 143-146.

49 Herberhold, M.; Trampisch, H. *Z*. *Naturforsch*. **1982**, *37b*, 614-619.

50 Naeumann, F.; Rehder, D. *Z. Naturforsch.* **1984**, *39b*, 1654-1661.

51 Collazo, C.; Rodewald, D.; Schmidt, H.; Rehder, D. *Organometallics* **1996**, *15*, 4884-4887.

52 Barybin, M.V. Novel chemistry of low-valent early transition metal complexes. Ph.D. Dissertation, University of Minnesota, Minneapolis, MN, 1999.

53 (a) Barybin, M.V.; Young, V.G.; Ellis, J.E. *J. Am. Chem. Soc.* **1998**, *120*, 429-430; (b) Barybin, M.V.; Young, V.G.; Ellis, J.E. *J. Am. Chem. Soc.* **2000**, *122*, 4678-4691.

54 Natta, G.; Ercoli, R.; Calderazzo, F.; Alberola, A.; Corradini, P.; Allegra, G. *Atti Accad. Naz. Lincei Cl. Sci. Fis. Mat. Nat.* **1959**, *27*, 107-112.

55 Robinson, R.E.; Holovics, T.C.; Deplazes, S.F.; Lushington, G.H.; Powell, D.R.; Barybin, M.V. *J. Am. Chem. Soc.* **2003**, *125*, 4432-4433.

56 Robinson, R.E.; Holovics, T.C.; Deplazes, S.F.; Powell, D.R.; Lushington, G.H.; Thompson, W.H.; Barybin, M.V. *Organometallics* **2005**, *24*, 2386-2397.

57 Holovics, T.C.; Robinson, R.E.; Weintrob, E.; Toriyama, M.; Lushington, G.H.; Barybin, M.V. *J. Am. Chem. Soc.* **2006**, *128*, 2300-2309.

58 Maher, T.R.; Spaeth, A.D.; Neal, B.M.; Berrie, C.L.; Thompson, W.H.; Day, V.W.; Barybin, M.V. *J. Am. Chem. Soc.* **2010**, *132*, 15924-15926.

59 Neal, B.M.; Vorushilov, A.S.; DeLaRosa, A.M.; Robinson, R.E.; Berrie, C.L.; Barybin, M. V. *Chem. Comm.* **2011**, *47*, 10803-10805.

60 Barybin, M.V.; Holovics, T.C.; Deplazes, S.F.; Lushington, G.H.; Powell, D.R.; Toriyama, M. *J. Am. Chem. Soc.* **2002**, *124*, 13668-13669.

61 Bildstein, B.; Malaun, M.; Kopacka, H.; Wurst, K.; Mitterböck, M.; Ongania, K.-H.; Opromolla, G.; Zanello, P. *Organometallics* **1999**, *18*, 4325-4336.

62 Kavallieratos, K.; Hwang, S.; Crabtree, R.H. *Inorg. Chem.* **1999**, *38*, 5184-5186.

63 van Leusen, D.; Hessen, B. *Organometallics* **2001**, *20*, 224-226.

64 Holovics, T.C.; Deplazes, S.F.; Toriyama, M.; Powell, D.R.; Lushington, G.H.; Barybin, M.V. *Organometallics* **2004**, *23*, 2927-2938.

65 McGinnis, D.M.; Deplazes, S.F.; Barybin, M.V. *J. Organomet. Chem.* **2011**, *696*, 3939-3944.

66 Churchill, M.R. Transition Metal Complexes of Azulene and Related Ligands. In *Progress in Inorganic Chemistry*, Volume 11; Lippard, S.J., Ed.; John Wiley & Sons: Hoboken, NJ,1970; pp. 53-98.

67 Bohling, D.A.; Mann, K.R. *Inorg*. *Chem*. **1984**, *23*, 1426-1432.

68 Ljungström, E. *Acta Chem*. *Scand*. **1978**, *32A*, 47-50.

69 Mialki, W.S.; Wigley, D.E.; Wood, T.E.; Walton, R.A. *Inorg*. *Chem*. **1982,** *21*, 480-485.

70 (a) Bullock, J.P.; Mann, K.R. *Inorg*. *Chem*. **1989**, *28*, 4006-4011; (b) Treichel, P.M.; Essenmacher, G.J. *Inorg*. *Chem*. **1976**, *15*, 146-150.

71 Deplazes, S.F. Ligand design, coordination, and electrochemistry of nonbenzenoid aryl isocyanides. Ph.D. Dissertation, University of Kansas, Lawrence, KS, 2008.

72 El-Shihi, T.; Siglmüller, F.; Herrmann, R.; Fernanda, M.; Carvalho, N.N.; Pombeiro, A.J.L. *J*. *Organomet*. *Chem*. **1987**, *335*, 239-247.

73 El-Shihi, T.; Siglmüller, F.; Herrmann, R.; Fernanda, M.; Carvalho, N.N.; Pombeiro, A.J.L. *Port*. *Electrochim*. *Acta* **1987**, *5*, 179-184.

74 Nexmeyanov, A.N.; Perovalova, E.G.; Gubin, S.P.; Grandberg, K.I.; Kozlovsky, A.G. *Tetrahedron Lett*. **1966**, *22*, 2381-2387.

75 Barybin, M.V.; Chisholm, M.H.; Dalal, N.; Holovics, T.H.; Patmore, N.J.; Robinson, R.E.; Zipse, D.J. *J*. *Am*. *Chem*. *Soc*. **2005**, *127*, 15182-15190.

76 Grubisha, D.S.; Rommel, J.S.; Lane, T.M.; Tysoe, W.T.; Bennett, D.W. *Inorg*. *Chem*. **1992**, *31*, 5022-5027.

77 Siemeling, U.; Rother, D.; Bruhn, C.; Fink, H.; Weidner, T.; Träger, F.; Rothenberger, A.; Fenske, D.; Priebe, A.; Maurer, J.; Winter, R. *J*. *Am*. *Chem*. *Soc*. **2005**, *127*, 1102-1103.

78 Siemeling, U.; Rother, D.; Bruhn, C. *Organometallics* **2008**, *27*, 6419-6426.

79 Weidner, T.; Ballav, N.; Zharnikov, M.; Priebe, A.; Long, N.J.; Winter, R.; Rothenberger, A.; Fenske, D.; Rother, D.; Bruhn, C.; Fink, H.; Siemeling, U. *Chem*. *Eur*. *J*. **2008**, *14*, 4346-4360.

80 Siemeling, U.; Klapp, L.R.R.; Bruhn, C. *Z*. *Anorg*. *Allg*. *Chem*. **2010**, *636*, 539-542.

81 Siemeling, U.; Rother, D.; Bruhn, C. *Chem*. *Comm*. **2007**, *41*, 4227-4229.

82 Emerich, B.M.; Moore, C.E.; Fox, B.J.; Rheingold, A.L.; Figueroa, J.S. *Organometallics* **2011**, *30*, 2598-2608.

83 Labios, L.A.; Millard, M.D.; Rheingold, A.L.; Figueroa, J.S. *J*. *Am*. *Chem*. *Soc*. **2009**, *131*, 11318-11319.

CHAPTER II

Isocyanometalates in Organometallic Crystal Engineering and Preliminary Studies Involving Isocyanoazulene Complexes of Sub-Valent Metal Ions

Portions of this work have been published in:

Maher, T. R.; Meyers, Jr., J. J.; Spaeth, A. D.; Lemley, K. R.; Barybin, M. V. "Diisocyanoarene-linked Pentacarbonylvanadate(I-) Ions as Building Blocks in a Supramolecular Charge-Transfer Framework Assembled through Noncovalent π-π and Contact Ion Interactions," *Dalton Trans*. **2012**, *41*, 7845.

II.1 Introduction

Linear diisocyanoarenes have been employed extensively as building blocks in the coordination chemistry of organometallic materials and as charge transport mediators for nanotechnological applications.[1] Advances in organometallic crystal engineering critically rely on the use of noncovalent phenomena, such as π-stacking, hydrogen bonding, and charge transfer interactions, to assemble novel supramolecular materials.[2] Our group's interest in the chemistry of low-valent, diisocyanoarene-bridged organometallics[3] has led to the exploration of the possibility of incorporating metallocene and metal carbonyl complexes, which are arguably the two most ubiquitous motifs in organometallic chemistry, into new charge-transfer coordination platforms featuring conjugated linear diisocyanoarene linkers.

The reactivity profile of $V(CO)_6$, the only isolable odd-electron binary metal carbonyl, has been largely limited to one-electron reduction or disproportionation in the presence of donor ligands/solvents to give $[V(CO)_6]^-$.[4] A few interactions of $V(CO)_6$ with phosphines have led to mixed zero-valent substitution products.[5] In addition, Ellis *et al*. have shown that $V(CO)_6$ reacts with excess CNXyl (Xyl = 2,6-dimethylphenyl or xylyl) to afford neutral *trans*-$V(CO)_2(CNXyl)_4$.[6] While several group 5 mononuclear species $[M(CO)_5(CNR)]^-$ (R = Me, Ph, Cy, ^{t}Bu, ^{i}Pr, CH_2CO_2Et) have been prepared from the labile complexes $[M(CO)_5L]^-$ by the groups of Ellis (L = NH_3)[7] and Rehder (L = DMSO)[8] via ligand exchange, no X-ray structural data on such complexes are available. An unusual supramolecular ensemble containing a hitherto unknown diisocyanoarene-bridged, sub-valent bimetallic framework is reported on, which is accessible either from $V(CO)_6$ or $[V(CO)_6]^-$. Three synthetic routes to the unusual supramolecular complex $([Cp_2Co]_2[\{(OC)_5V\}_2(\mu\text{-}1,4\text{-}CNC_6Me_4NC)])_\infty$, which was crystallographically characterized, are presented.

Aromatic ligands are known to delocalize electron density within their π-system and are attractive due to variability of this delocalization through substitution. As mentioned in Section I.2, benzenoid isocyanoarenes such as xylyl isocyanide, CNXyl (Xyl = 2,6-dimethylbenzene), and *m*-terphenyl isocyanide, $CNAr^{Mes2}$ (Ar^{Mes2} = 2,6-bis(2,4,6-trimethylbenzyl)benzene)[9], have been used to access metalates, or homoleptic organometallic complexes featuring sub-valent metal centers. An ever growing collection of homoleptic, or binary, metalates of general formula $[M(CNXyl)_X]^Z$ has been realized in the past 20 years. Specific examples include $[Co(CNXyl)_4]^-$,[10] $[Mn(CNXyl)_5]^-$,[11] $[M(CNXyl)_6]^-$ (M = V[12], Nb, Ta[13]), $[Ru(CNXyl)_4]^{2-}$,[14] and $[Fe(CNXyl)_4]^{2-}$ [15]. To date, there are no published examples of binary metalates featuring a nonbenzenoid isocyanoarene.

Azulene is an aromatic hydrocarbon featuring fused five- and seven-membered rings (Figure II.1). Due to its nonbenzenoid nature, azulene possesses unique properties. For example, azulene has a dipole moment of 1.08 D despite the absence of any polar bonds. The highest occupied molecular orbital (HOMO) and lowest unoccupied molecular orbital (LUMO) of this molecule are complementary in terms of orbital density distribution (Figure I.14). This complimentary molecular orbital nature allows for tuning of the HOMO-LUMO gap via substitution and, consequently, tuning of physicochemical properties.[16]

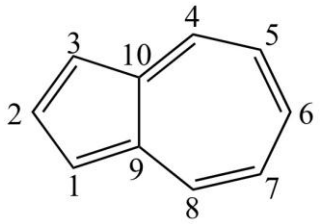

Figure II.1 The molecular structure and numbering scheme of azulene.

In the case of binary metalates, isocyanoazulene[17] would be an ideal aromatic ligand in which to delocalize extra electron density from an electron-rich metal. First, the aromatic delocalization energy of azulene is approximately one-fifth the energy of benzene (azulene, 4.2 kcal/mol; benzene, 20.0 kcal/mol).[18] Second, the isocyanide functionality has been proven to be a suitable junction group between an aromatic ligand and a metal center due to its ability to partake in σ-donation (useful in forming M-C bonds and stabilizing electron-poor metal centers) and, more importantly, π-accepting (useful in strengthening the M-C bond and stabilizing electron-rich metal centers). Figure II.2 demonstrates σ-donation of the lone pair of the isocyanide carbon atom from a σ* orbital (with respect to the CN bond) and π-accepting through a π-backbond from a M(dπ) orbital to the vacant pπ* orbital of the isocyanide group. Third, while azulene chemistry is arguably dominated[3a] by 1,3-functionalization, a 2-functionalized azulene presents as an attractive option for electron delocalization. The substituent on an even-numbered carbon atom will allow for interaction of the vacant LUMO as opposed to the occupied HOMO of the azulene motif of the azulene motif with the metal center through the isocyanide junction group. Transfer of the electron density from the sub-valent metal center to the π-system of the 2-isocyanoazulene, then, is (1) achievable through the M(dπ)-C≡N(pπ*) π-backbond and (2) should be more favorable in a homoleptic azulene metalate than a homoleptic benzenoid metalate due to the low aromatic delocalization energy and vacant LUMO of azulene. The design, synthesis, and implementation of a nonbenzenoid isocyanoarene, namely 2-isocyano-1,3-dimethylazulene, in stabilizing sub-valent metal centers is discussed.

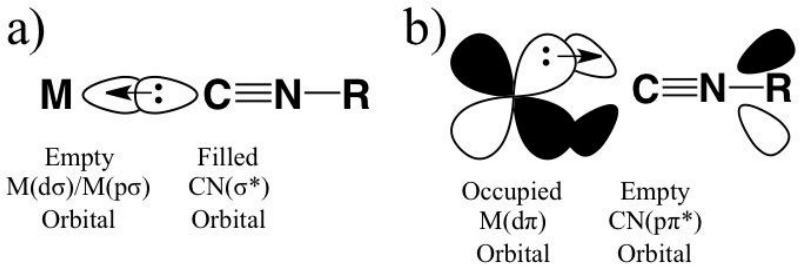

Figure II.2 The a) σ-donation and b) π-accepting modes of metal-isocyanide interactions.

II.2 Work Described in Chapter II

Described in this Chapter is the chemistry of the unusual supramolecular complex $([Cp_2Co]_2[\{(OC)_5V\}_2(\mu\text{-}1,4\text{-}CNC_6Me_4NC)])_\infty$. This crystallographically characterized framework is held together via synergistic contact-ion pairs and π-stacking interactions and includes the first sub-valent organometallic motif featuring a diisocyanoarene linker. In addition, the synthesis and characterization of 2-isocyano-1,3-dimethylazulene, which may be regarded as a nonbenzenoid analog of 2,6-xylyl isocyanide, are presented. Initial studies involving complexation of this new nonbenzenoid isocyanoarene with sub-valent metal ions are discussed as well.

II.3 Experimental Section

II.3.1 General Procedures, Starting Materials and Equipment.

Unless specified otherwise, all operations were performed under an atmosphere of 99.5% argon further purified by passage through columns of activated BASF catalyst and molecular sieves. All connections involving the gas purification systems were made of glass, metal, or other materials impermeable to air. Solutions were transferred via stainless steel needles (cannulas) whenever possible. Standard Schlenk techniques were employed with a double manifold vacuum line. Both CH_3CN and CD_3CN, as well as CH_2Cl_2 and CD_2Cl_2, were distilled over CaH_2. Diethyl ether and THF were distilled from Na/benzophenone. Triethylamine was distilled from NaOH. Heptane and pentane were distilled from Na/benzophenone dissolved in a minimum amount of diglyme. DMSO was distilled over P_2O_5. Following purification, all solvents, including deuterated solvents, were stored under argon.

Infrared spectra were recorded on a PerkinElmer Spectrum 100 FTIR spectrometer with samples sealed in 0.1 mm NaCl cells or between NaCl disks. NMR samples were analyzed on Bruker Avance 400 or 500 spectrometers. ^{1}H and ^{13}C NMR chemical shifts are given with reference to residual solvent resonances relative to $SiMe_4$. ^{51}V NMR chemical shifts are referenced to neat $VOCl_3$. A solution of $[Et_4N][V(CO)_6]$ in CD_3CN was used as an external ^{51}V NMR reference ($\delta(^{51}V)$ = -1955.0 ppm vs. neat $VOCl_3$). ^{14}N NMR chemical shifts are referenced to liquid NH_3 at 25 °C. A solution of N,N-dimethylformamide in CD_2Cl_2 was used as an external ^{14}N NMR reference ($\delta(^{14}N)$ = 103.8 ppm vs. liquid NH_3 at 25 °C). UV-vis spectra were recorded in CH_2Cl_2 or CH_3CN at 24 °C using a CARY 100 spectrophotometer.

Cyclic voltammetry (CV) experiments on *ca*. 2×10^{-3} M solutions of **2.1a**, **2.1b**, and **2.2** in CH_3CN were conducted at room temperature using an EPSILON (Bioanalytical Systems Inc.,

West Lafayette, IN) electrochemical workstation. The electrochemical cell was placed in an argon-filled Vacuum Atmospheres dry-box. Tetrabutylammonium hexafluorophosphate (0.1 M solution in CH_3CN) was used as a supporting electrolyte. Cyclic voltammograms were recorded at 22 ± 2 °C using a three component system consisting of a platinum working electrode, a platinum wire auxiliary electrode, and a glass encased non-aqueous silver/silver chloride reference electrode. The reference Ag/Ag^+ electrode was monitored with the ferrocenium/ferrocene couple. IR compensation was achieved before each CV run by measuring the uncompensated solution resistance followed by incremental compensation and circuit stability testing. Background cyclic voltammograms of the electrolyte solution were recorded before adding the analytes. The half-wave potentials ($E_{1/2}$) were determined as averages of the cathodic and anodic peak potentials of reversible/partially reversible couples and are referenced to the external FcH^+/FcH couple.[19]

Melting points are uncorrected and were determined for samples in capillary tubes sealed under argon. Elemental analyses were carried out by Desert Analytics (now Columbia Analytical Services), Tucson, Arizona.

Compounds $V(CO)_6$,[4] $[Et_4N][V(CO)_6]$,[20] $[Cp_2Co][V(CO)_6]$,[21] $[Cp_2Co][BF_4]$,[22] 1,4-CNC_6Me_4NC,[23] CNXyl (Xyl = 2,6-dimethylphenyl),[24] 2-amino-1,3-diethoxycarbonylazulene,[25] and acetic-formic anhydride[26] were prepared according to literature procedures. Complex $[Et_4N][V(CO)_5(DMSO)]$, generated in THF by the method of Rehder,[27] was used *in situ*. Other reagents were obtained from commercial sources and used as received. Red-Al® (sodium bis(methoxyethoxy)aluminumhydride) and cryptand[2.2.2] (4,7,13,16,21,24-Hexaoxa-1,10-diazabicyclo[8.8.8]hexacosane; CAS: 23978-09-8) were stored under argon. Initial studies involving **2.1a**, **2.1b**, and **2.2** were performed by Dr. Tiffany R. Maher of the Barybin group.[28]

II.3.2 Synthesis of $[Et_4N]_2[\{(OC)_5V\}_2(\mu\text{-}CNC_6Me_4NC)]$ (2.1a).

A yellow solution of $[Et_4N][V(CO)_6]$ (0.3466 g, 0.9924 mmol) and DMSO (0.4 mL, 5.6 mmol) in 80 mL of THF was irradiated using a Hanovia Hg 450 W immersion lamp for 4 hrs at 22 °C with stirring. 1,4-Diisocyanodurene (0.0914g, 0.4962 mmol) dissolved in 20 mL of THF was added to the above solution and the mixture was stirred for 15 hrs. Then, the reaction mixture was concentrated to about 20 mL and stirred for an additional 2-hour period. Pentane (30mL) was added to the reaction flask and the mixture was vigorously stirred for 30 min. An oily dark red precipitate formed, which was washed with toluene (2×20 mL). The toluene washings were carefully removed via cannula. After addition of 50 mL of pentane with stirring, the solution/slurry was filtered. The filter-cake was dissolved in THF. This THF solution was filtered; the filtrate was layered with 150 mL of pentane and stored at -35 °C for 3 hrs. The magenta precipitate was filtered off, washed with pentane (2×10 mL) and dried at 10^{-2} torr to provide **2.1a** (0.2523 g, 0.3052 mmol) in a 62% yield as a free-flowing magenta solid. Mp 82-84 °C. Anal. Calcd. for $C_{38}H_{52}N_4O_{10}V_2$: C, 55.21; H, 6.34; N, 6.78. Found: C, 54.18; H, 6.30; N, 7.14. IR (CH_3CN): ν_{CN} 2061 w, ν_{CO} 1951 m, 1831 vs cm^{-1}. ^1H NMR (500 MHz, CD_3CN, 25°C): δ 1.20 (t, 24H, CH_2CH_3, $^3J_{H\text{-}H}$ = 7 Hz), 2.32 (s, 12H, CH_3), 3.16 (q, 16H, CH_2CH_3, $^3J_{H\text{-}H}$ = 7 Hz) ppm. $^{13}C\{^1H\}$ NMR (125 MHz, CD_3CN, 25°C): δ 7.7 (CH_2CH_3), 16.4 (CH_3), 53.2 (CH_2CH_3) ppm. ^{51}V NMR (131.6 MHz, CD_3CN, 25°C): δ -1903.9 ppm; two ^{13}CO satellite doublets of the relative intensities 4:1 were also observed at -1904.2 ppm with $^1J(^{13}C\text{-}^{51}V)$ = 116.8 Hz and -1903.9 ppm with $^1J(^{13}C\text{-}^{51}V)$ = 167.5 Hz, respectively, as well a $C^{18}O$ satellite singlet at -1904.0 ppm. UV-Vis (CH_3CN, λ_{max} ($\varepsilon\times10^{-3}$ M^{-1} cm^{-1}), 24 °C): 489 (1.02) nm.

II.3.3 Synthesis of $[Cp_2Co]_2[\{(OC)_5V\}_2(\mu\text{-}CNC_6Me_4NC)]$ (2.1b) from $V(CO)_6$.

A colorless solution of diisocyanodurene, 1,4-CNC_6Me_4NC (0.0716 g, 0.3886 mmol), in 100 mL of heptane was added to a cold (-70°C) canary yellow solution of hexacarbonylvanadium(0) (0.1702 g, 0.7772 mmol) in 200 mL of heptane in the dark with stirring. The reaction mixture was stirred at -70°C for 2 hours while acquiring a pale tangerine color and then warmed to 0°C. FTIR of the solution/slurry in the ν_{CN} and ν_{CO} regions indicated essentially complete consumption of the starting materials. Then, an orange-brown solution of cobaltocene (0.1470 g, 0.7772 mmol) in 20 mL of CH_2Cl_2 was transferred to the reaction mixture in one portion at 0 °C and the mixture was vigorously stirred for 30 min. The resulting dark solid was filtered off, washed with CH_2Cl_2 (100 mL) and pentane (50 mL), recrystallized from CH_3CN/Et_2O, and dried at 10^{-2} torr to afford dark violet, nearly black, **2.1b** (0.3020 g, 0.3198 mmol) in a 73% yield. Compound **2.1b** decomposes without melting at 138˚C. Anal. Calcd. for $C_{42}H_{32}Co_2N_2O_{10}V_2$: C, 53.41; H, 3.42; N, 2.97. Found: C, 52.89; H, 3.60; N, 3.38. IR (CH_3CN): ν_{CN} 2041 w br, ν_{CO} 1926 m br, 1847 s sh, 1839 vs, 1824 m sh cm^{-1}. UV-vis (CH_3CN, λ_{max} ($\varepsilon\times10^{-3}$ M^{-1} cm^{-1}), 24 °C): 484 (3.23) nm.

II.3.4 Cation metathesis of 2.1a to 2.1b.

A mixture of cobaltocenium tetrafluoroborate (0.0818 g, 0.2963 mmol) and **2.1a** (0.1225 g, 0.1482 mmol) was dissolved in 80 mL of CH_2Cl_2. The resulting solution was stirred at 22 °C for 48 h to form a dark violet precipitate. After addition of *less* than 100 mL of heptane, the solid was filtered off, washed with 50 mL of heptane, and dried at 10^{-2} torr. Recrystallization from CH_3CN/Et_2O (20/150 mL) followed by drying of the product at 10^{-2} torr afforded a 53% yield of **2.1b** (0.0738g 0.0781 mmol), which was spectroscopically (FTIR, ^1H NMR) identical to *bona fide* **2.1b** described above.

II.3.5 Synthesis of 2.1b from $[Cp_2Co][V(CO)_6]$.

A solution of $[Cp_2Co][V(CO)_6]$ (0.1573 g, 0.3855 mmol) and DMSO (0.2 mL, 2.8 mmol) in 80 mL of THF was irradiated using a Hanovia Hg 450 W immersion lamp for 4 h at 22 °C with stirring. Then, the red-orange reaction mixture was concentrated to about 20 mL under vacuum. 1,4-Diisocyanodurene (0.0355g, 0.1927 mmol) dissolved in 20 mL of THF was added to the above concentrated solution. The mixture was stirred for 10 hrs, concentrated to about 10 mL, and stirred for an additional 8-hour period. An oily black precipitate formed. Pentane (30 mL) was added to the reaction flask and the mixture was vigorously stirred for 30 min. Then, 20 mL of toluene was added with stirring, and the solution/slurry was allowed to settle. The solution was carefully removed by cannula, and the residue was washed with toluene (2×20 mL). The resulting dark violet, nearly black solid was washed with 50 mL of pentane and then triturated with an additional 50 mL of pentane. Filtration followed by drying at 10^{-2} torr provided crude **2.1b** as a dark violet powder. Recrystallization of this solid from CH_3CN/Et_2O gave microcrystalline **2.1b** (0.0572g, 0.0606 mmol) in a 31% yield. The product was spectroscopically (FTIR, NMR) identical to *bona fide* **2.1b** described above.

II.3.6 Synthesis of $[Cp_2Co][V(CO)_5(CNXyl)]$ (2.2).

A colorless solution of 2,6-dimethylphenyl isocyanide (0.1970 g, 1.5019 mmol), in 70 mL of heptane was added to a yellow-green solution of hexacarbonylvanadium(0) (0.3325 g, 1.5183 mmol) in 100 mL of heptane at room temperature. The reaction mixture rapidly acquired a mustard color. After stirring for 2 h, an orange-brown solution of cobaltocene (0.3234 g, 1.7100 mmol) was added to the reaction mixture at 22 °C to result in the formation of dark aqua-colored slurry. This mixture was stirred for 1 hr and then filtered. The filter-cake was washed with heptane (2×30 mL) and recrystallized from THF/Et_2O to afford microcrystalline dark

turquoise (bluish green) **2.2** (0.5425 g, 1.0610 mmol) in two crops in a 71% combined yield. Mp 104-106 °C (dec). Anal. Calcd. for $C_{18}H_{19}CoNO_5V$: C, 56.38; H, 3.75; N, 2.74. Found: C, 56.43; H, 4.01; N, 2.61. IR (CH_3CN): ν_{CN} 2053 w, ν_{CO} 1943 m, 1849 s sh, 1837 vs cm^{-1}. ^1H NMR (400 MHz, CD_3CN, 21 °C): δ 2.36 (s, 6H, C*H*$_3$), 5.35 (s, 10H, C_5H_5), 7.02 (t, 1H, *p*-H, $^3J_{H-H}$ = 8 Hz), 7.05 (d, 2H, *m*-H, $^3J_{H-H}$ = 8 Hz) ppm. $^{13}C\{^1H\}$ NMR (100 MHz, CD_3CN, 21°C): δ 19.1 (*C*H_3), 88.9 (C_5H_5), 126.7, 128.6, 134.4 (aromatic *C*) ppm. UV-vis (CH_3CN, λ_{max} ($\varepsilon \times 10^{-3}$ M^{-1} cm^{-1}), 24 °C): 483 (1.75) nm.

II.3.7 Synthesis of 2-formamido-1,3-dimethylazulene (2.3).

A solution of Red-Al® (2.50 mL, 8.74 mmol) in toluene was added to a cold (0°C) solution of 2-amino-1,3-diethoxycarbonylazulene (0.2513 g, 0.874 mmol) in 25 mL of toluene over a period of 1 h. The reaction mixture was stirred for 15 h at 70°C, at which point the reaction flask was opened to air and its content was poured slowly into a beaker containing 50 mL of 10% aqueous NaOH. After 15 min of stirring to quench any remaining Red-Al®, the organic layer was separated and the aqueous fraction was extracted with Et_2O (1 × 30 mL). The organic fractions were combined, dried over anhydrous $MgSO_4$, and filtered. All solvent was removed from the filtrate in vacuo. The resulting dark red residue was dissolved in a minimum amount of CH_2Cl_2 and added to a freshly prepared mixture of formic acid (3.50 mL) and acetic-formic anhydride (2.95 mL). After stirring for 1.5 h, all volatiles were removed on a rotary evaporator and the resultant residue was treated with 100 mL of 10% aqueous $NaHCO_3$ with stirring to quench any remaining anhydride or acid. After extraction of the aqueous phase with CH_2Cl_2 (2 × 20 mL), the organic fractions were combined and dried over anhydrous $MgSO_4$. Filtration followed by solvent removal from the filtrate on a rotary evaporator produced a dark residue, which was subjected to column chromatography on silica gel using 15% Et_2O in

CH_2Cl_2. A blue band was collected, which gave **2.3** (0.0945 g, 0.474 mmol) as a blue powder in a 55% yield after solvent removal and drying. Mp: 178-181°C. ^{1}H NMR (400 MHz, $CDCl_3$, 25 °C), two rotamers with respect to the C-N bond: δ 2.53, 2.60 (s, 6H, CH_3), 7.05, 7.12 (t, 2H, $H^{5,7}$, $^3J_{HH}$ = 10 Hz), 7.41, 8.08 (s{cis}/d{trans}, 1H, NH, $^3J_{HH}$ = 10 Hz), 7.48, 7.51 (t, 1H, H^6, $^3J_{HH}$ = 10 Hz), 8.15 (d, 2H, $H^{4,8}$, $^3J_{HH}$ = 10 Hz), 8.55, 8.70 (s{cis}/d{trans}, 1H, CHO, $^3J_{HH}$ = 11 Hz) ppm. ^{13}C{^{1}H} NMR (125.8 MHz, $CDCl_3$, 25 °C): δ 10.5, 10.6 (CH$_3$), 115.8, 118.4, 121.7, 122.4, 132.5, 133.1, 135.4, 135.9, 136.3, 136.9, 140.6, 141.2 (azulenic C), 159.0, 164.2 (CHO) ppm.

II.3.8 Synthesis of 2-isocyano-1,3-dimethylazulene (2.4).

Excess phosphorous oxychloride (0.243 mL, 2.61 mmol) was added to a solution of **2.3** (0.450 g, 2.26 mmol) and freshly distilled triethylamine (7.86 mL) in 50 mL of dry CH_2Cl_2 at room temperature. The reaction mixture was stirred for 0.5 h and then quenched with 100 mL of 10% aqueous $NaHCO_3$. The organic layer was separated and the aqueous phase was extracted with CH_2Cl_2 (3 × 30 mL). The organic fractions were combined, dried over anhydrous $MgSO_4$, and filtered. Solvent removal from the filtrate in vacuo left a green microcrystalline product, which was subjected to column chromatography on silica gel using neat CH_2Cl_2. A blue band was collected and afforded green crystalline **2.4** (0.379 g, 2.09 mmol) in a 93% yield following solvent removal and drying. **2.4** can be further purified via recrystallization from hexanes. Mp: 99-101°C. Anal. Calcd for $C_{13}H_{11}N$: C, 86.15; H, 6.12; N, 7.73. Found: C, 85.53; H, 5.90; N, 7.77. IR (CH_2Cl_2): ν_{CN} 2115 cm^{-1}. ^{1}H NMR (400 MHz, $CDCl_3$, 25 °C): δ 2.64 (s, 6H, CH_3), 7.09 (t, 2H, $H^{5,7}$, $^3J_{HH}$ = 9.8 Hz), 7.55 (t, 1H, H^6, $^3J_{HH}$ = 9.8 Hz), 8.18 (d, 2H, $H^{4,8}$, $^3J_{HH}$ = 9.8 Hz) ppm. ^{13}C{^{1}H} NMR (125.8 MHz, $CDCl_3$, 25 °C): 10.1 (CH$_3$), 120.2, 122.7, 134.8, 135.7, 139.2 (azulenic C), 170.7 (CN) ppm. ^{14}N NMR (36.2 MHz, $CDCl_3$, 25 °C): 172.3 ppm. UV-vis

(CH_2Cl_2, λ (log ε)): 732 (2.34), 671 (2.68), 624 (2.70), 354 (3.81), 338 (3.68), 298 (4.71), 290 (4.80), 242 (4.26) nm.

II.3.9 Synthesis of $Co(2.4)_4I_2$ (2.5).

THF (50 mL) was added to a solid mixture of **2.4** (0.2210 g, 1.213 mmol) and CoI_2 (0.0942 g, 0.301 mmol). After the reaction mixture was stirred for 3 h, the green suspension was filtered and washed with THF (3 × 5 mL). Drying at 10^{-2} torr provided **2.5** (0.252 g, 0.242 mmol) as a green powder in a 81% yield. IR (Nujol): ν_{CN} 2156 cm^{-1}.

II.3.10 Synthesis of [K(crypt[2.2.2])][$Co(2.4)_4$] (2.6).

Potassium metal (0.0236 g, 0.604 mmol) and naphthalene (0.0853 g, 0.666 mmol) were stirred in 25 mL of THF for 3 h to provide a green solution of potassium naphthalenide, which was subsequently cooled to -78 °C. This solution was transferred to a green suspension of **2.5** (0.200 g, 0.193 mmol) in 100 mL of THF, also cooled to -78 °C. A solution of cryptand[2.2.2] (0.0795 g, 0.211 mmol) in 10 mL of THF was then added and the reaction mixture was allowed to stir for 16 h while warming to room temperature. The reaction mixture was filtered through a medium porosity frit to give a blue filtrate. The filtercake was washed with THF until the washings were colorless. The filtrate solution was then concentrated and pentane (90 mL) was added to precipitate the product. The solid was filtered off and washed sequentially with pentane (1 × 80 mL) and Et_2O (1 × 80 mL). Following drying, **2.6** was recovered as a dark blue powder. IR (THF): ν_{CN} 1842 br cm^{-1}.

II.3.11 Alternate synthesis of 2.6.

A green suspension of **2.5** was produced by stirring CoI_2 (0.0837 g, 0.268 mmol) and **2.4** (0.2000 g, 1.104 mmol) in 100 mL of THF for 4 h at room temperature. Potassium metal

(0.0329 g, 0.841 mmol) and naphthalene (0.1189 g, 0.9277 mmol) were stirred in 25 mL of THF for 4 h in a separate flask to provide a green solution of potassium naphthalenide. After both solutions were subsequently cooled to -78 °C, the potassium naphthalenide solution was transferred via cannula to the suspension of **2.5.** A solution of cryptand[2.2.2] (0.1058 g, 0.2810 mmol) in 10 mL of THF was then added to the resulting mixture. The blue reaction mixture was allowed to stir for 16 h while warming to room temperature and then filtered through a medium porosity frit to remove any salt byproducts. Following precipitate washing with THF until the washings were colorless, the solution was concentrated and pentane (100 mL) was added to the filtrate to precipitate the product. The solution was decanted using a cannula and the precipitate was further washed with pentane (2 × 10 mL) and Et_2O (2 × 10 mL). Following drying at 10^{-2} torr for 1 h, a dark blue powder of **2.6** (0.2490 g, 0.2076 mmol) was recovered in a 78% yield. The product was spectroscopically (FTIR) identical to *bona fide* **2.6** described above.

II.3.12 Synthesis of $[K(crypt[2.2.2])]_2[Fe(2.4)_4]$ (2.7).

A green suspension of Fe(2-isocyano-1,3-dimethylazulene)$_4Br_2$ was produced by stirring $FeBr_2$ (0.0476 g, 0.221 mmol) and **2.4** (0.1603 g, 0.8845 mmol) in 100 mL of THF for 4 h at room temperature as judged by FTIR (ν_{CN} (THF) = 2132, 2111, 2098 cm^{-1}). Potassium metal (0.0350 g, 0.895 mmol) and naphthalene (0.1263 g, 0.9854 mmol) were stirred in 25 mL of THF for 4 h in a separate flask to provide a green solution of potassium naphthalenide. After both solutions were subsequently cooled to -78 °C, the potassium naphthalenide solution was transferred via cannula to the Fe(2-CN-1,3-Me Az)$_4Br_2$ solution. A solution of cryptand[2.2.2] (0.1686 g, 0.4478 mmol) in 10 mL of THF was then added to the resulting mixture. The blue reaction mixture was allowed to stir for 16 h while warming to room temperature and then filtered through a medium porosity frit to remove any salt byproducts. Following washing of

the filtercake with THF until the washings were colorless, the filtrate was concentrated and pentane (150 mL) was added to it to precipitate the product. The solution was decanted using a cannula and the precipitate was further washed with pentane (2 × 10 mL) and Et_2O (4 × 10 mL). Following drying, **2.7** (0.2641 g, 0.1634 mmol) was recovered as a black powder in a 74% yield. IR (THF): ν_{CN} 1672 br cm^{-1}.

II.4 Results and Discussion

II.4.1 A Diisocyanoarene-Bridged, Sub-Valent Bimetallic Framework in Organometallic Crystal Engineering

Treatment of *in situ* generated $[Et_4N][V(CO)_5(DMSO)]$[8] with 0.5 equivalents of 1,4-diisocyanodurene (1,4-diisocyano-2,3,5,6-tetramethylbenzene) in THF at ambient temperature afforded a dark red solution, from which air- and moisture sensitive, magenta-colored $[Et_4N]_2[\{(OC)_5V\}_2(\mu\text{-}CNC_6Me_4NC)]$ (**2.1a**) was isolated in a *ca*. 60% yield (Scheme II.1). The ν_{CO}/ν_{CN} region of the infrared spectrum of **2.1a** in CH_3CN (Figure II.3) is qualitatively similar to those previously observed for several mononuclear complexes $[Et_4N][M(CO)_5(CNR)]$ M = (V[7,8], Ta[13b]) and constitutes a "classic" example of a pattern expected for a $[M(CO)_5(CNR)]^z$ motif with essentially perfect local C_{4v} symmetry.[29] The ν_{CO} bands at 1951 (m) and 1831 (vs) cm^{-1} correspond to the A_1^{cis} and *E* stretching modes, respectively, of the CO ligands positioned *cis* to the isocyanide groups in **2.1a**. The remaining allowed ν_{CO} band of A_1 symmetry that arises primarily from stretching of the carbonyl ligands *trans* to the isocyanides is obscured by the very intense *E* band, as is the case for many other $[V(CO)_5L]^-$ anions not engaged in contact ion interactions with the accompanying cations.[29] The importance of $V(d\pi) \rightarrow$ diisocyanodurene($p\pi^*$) interaction in **2.1a** is nicely corroborated by a 57 cm^{-1} depression in ν_{CN} upon complexation of the free 1,4-CNC_6Me_4NC linker (ν_{CN} = 2118 cm^{-1} in CH_3CN).

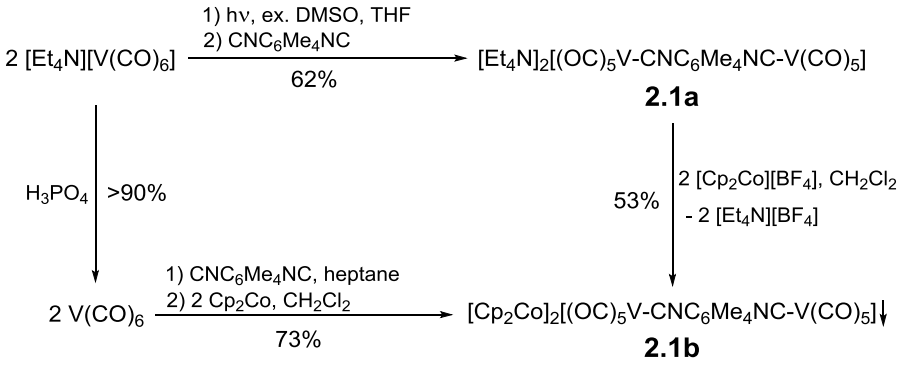

Scheme II.1

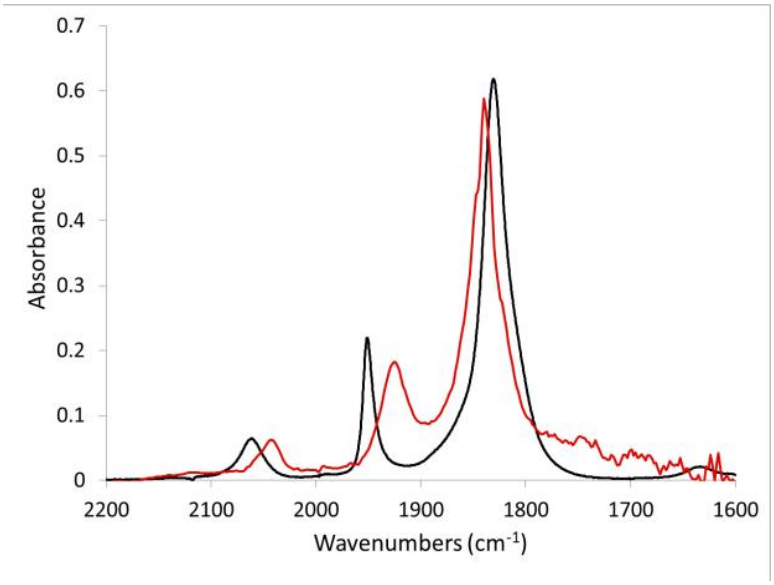

Figure II.3 Infrared spectra of **2.1a** (black) and **2.1b** (red) in CH_3CN.

The electronic spectrum of **2.1a** in CH_3CN in the visible region (Figure II.4) features an intense vanadium-to-diisocyanodurene charge transfer absorption (λ_{max} = 489 nm). This charge transfer band exhibits positive solvatochromism[30] and undergoes a 736 cm^{-1} hipsochromic shift upon changing the solvent from CH_3CN to significantly less polar CH_2Cl_2.

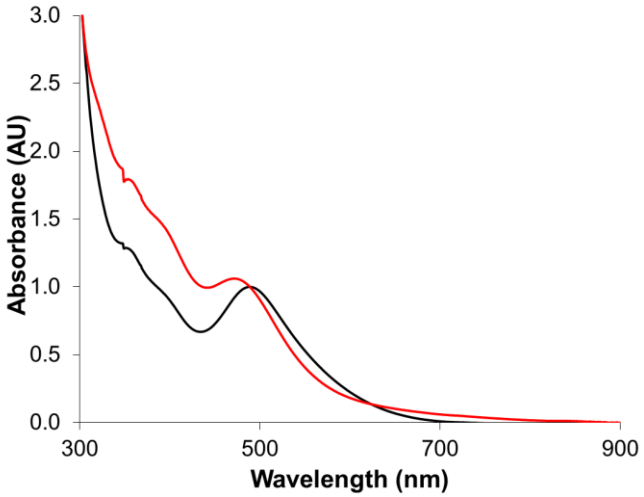

Figure II.4 UV-Vis spectra of **2.1a** in CH_2Cl_2 (red) and CH_3CN (black) at 25 °C.

The ^{51}V NMR (132 MHz) spectrum of **2.1a** in CD_3CN at 25 °C shows a singlet resonance at -1903.9 ppm[31] versus neat $VOCl_3$. This main peak is accompanied by two ^{13}CO satellite doublets of relative intensities 4:1 at -1904.2 ppm with $^1J(^{13}C\text{-}^{51}V) = 116.8$ Hz and -1903.9 ppm with $^1J(^{13}C\text{-}^{51}V) = 167.5$ Hz, respectively, as well as by a weak singlet at -1904.0 ppm due to the $C^{18}O$-containing isotopomer (Figure II.5). These observations nicely parallel Rehder's earlier findings[32] that the ^{51}V NMR pattern for $[V(CO)_6]^-$ features distinguishable resonances for the minor isotopomers $[V(CO)_5(^{13}CO)]^-$ and $[V(CO)_5(C^{18}O)]^-$. Both of these are slightly shifted upfield from the main peak at -1955 ppm because of the different deshielding effects of the $^{12}C^{16}O$, $^{13}C^{16}O$ and $^{12}C^{18}O$ ligands on the ^{51}V nucleus (Figure II.6).

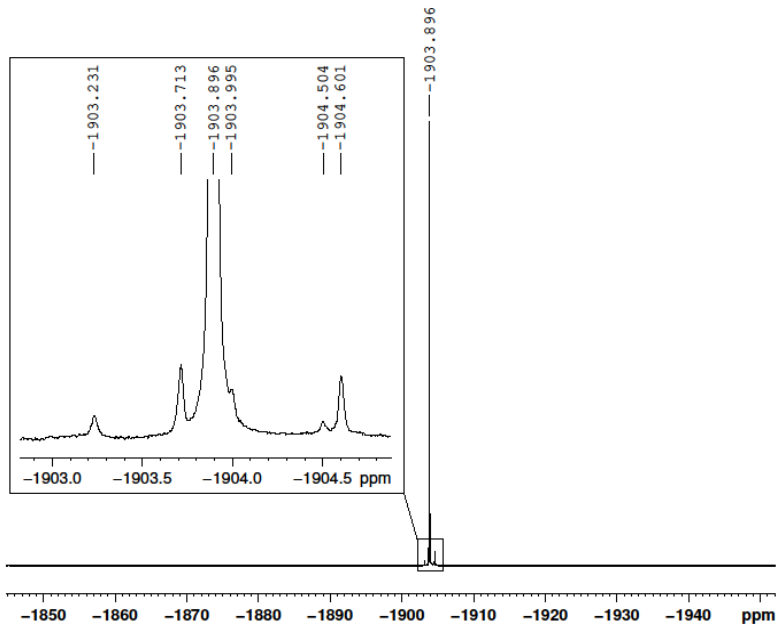

Figure II.5 ^{51}V NMR (131.6 MHz, CD_3CN, 25°C) spectrum of **2.1a** in CD_3CN at 25 °C referenced to neat $VOCl_3$.

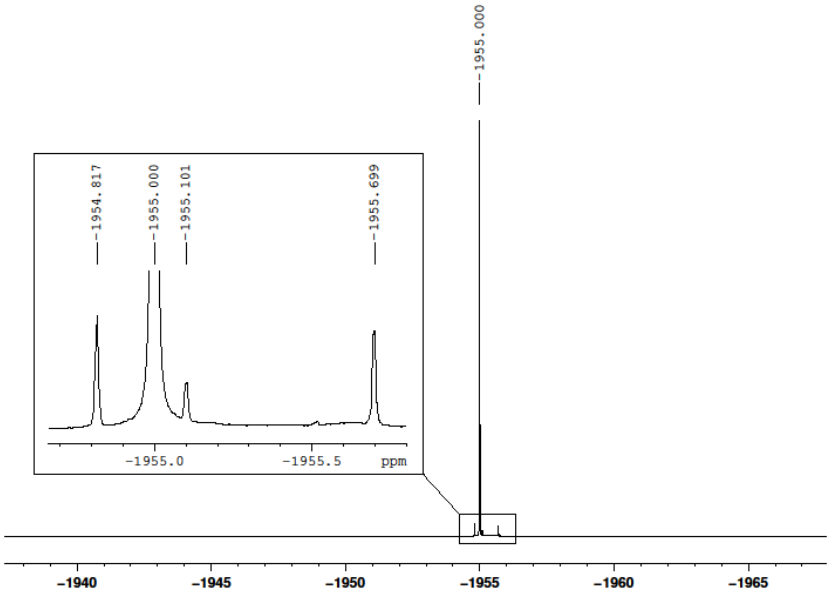

Figure II.6 ^{51}V NMR (131.6 MHz, CD_3CN, 25°C) spectrum of $[Et_4N][V(CO)_6]$ in CD_3CN at 25 °C referenced to neat $VOCl_3$.

Cation metathesis of **2.1a** with $[Cp_2Co][BF_4]$ in CH_2Cl_2 was driven by precipitation of $[Cp_2Co]_2[\{(OC)_5V\}_2(\mu\text{-}CNC_6Me_4NC)]$ (**2.1b**) from the reaction mixture (Scheme II.1). It is important to note that photolysis of $[Cp_2Co][V(CO)_6]$[33] in the presence of excess DMSO proved sluggish and afforded only a 30% yield of **2.1b** upon treating the intermediate $[Cp_2Co][V(CO)_5(DMSO)]$ with 0.5 equivalents of 1,4-CNC_6Me_4NC (Scheme II.2). Our preferred route to compound **2.1b** involves addition of 1,4-diisocyanodurene to 2 equivalents of $V(CO)_6$ in heptane at -70 °C followed by reduction of the presumed thermally unstable, zero-valent intermediate $[\{V(CO)_5\}_2(\mu\text{-}1,4\text{-}CNC_6Me_4NC)]$ with 2 equivalents of cobaltocene in CH_2Cl_2 to afford **2.1b** in a good yield (Scheme II.1). Since **2.1b** is only very sparingly soluble in CH_2Cl_2 or THF, its samples are easily freed from any $[Cp_2Co][V(CO)_6]$ impurity by washing the product with either of these solvents. Employing the above protocol, $[Cp_2Co][V(CO)_5(CNXyl)]$ (**2.2**), which may be viewed as a mononuclear congener of **2.1b**, was also accessed (Scheme II.3).

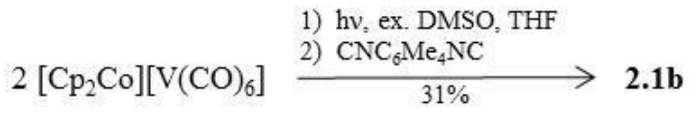

Scheme II.2

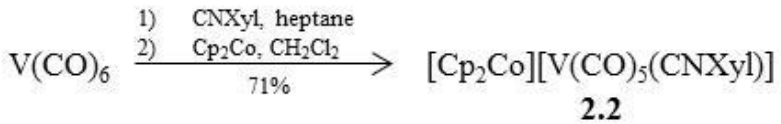

Scheme II.3

The air- and light sensitive complex **2.1b** is modestly soluble in acetonitrile and can be recrystallized from CH_3CN/Et_2O to afford dark violet, nearly black microcrystalline solid. The single crystal X-ray analysis of **2.1b** confirmed its nature as a charge transfer salt between

[{V(CO)$_5$}$_2$(μ-1,4-CNC$_6$Me$_4$NC)] and two cobaltocene units. **2.1b** crystallizes in the tetragonal space group $P4_2/n$. Only a half of the V_2-dianion and one $[Cp_2Co]^+$ cation are crystallographically independent. As illustrated in Figure II.7, the aromatic moieties of the 1,4-diisocyanodurene linker undergo π-stacking aggregation[34] with intercentroid distances between the six-membered rings being 3.58 Å. Such noncovalent π-π interactions form arrays of perfectly staggered [{V(CO)$_5$}$_2$(μ-1,4-CNC$_6$Me$_4$NC)]$^{2-}$ dianions that are insulated from one another by layers of the $[Cp_2Co]^+$ cations. The arrangement of the cobaltocenium ions within the structure of **2.1b** creates well-defined channels with a solvent accessible volume of 102 Å^3 (Figure II.7).[35] These channels appear to be populated by disordered CH_3CN molecules of crystallization.

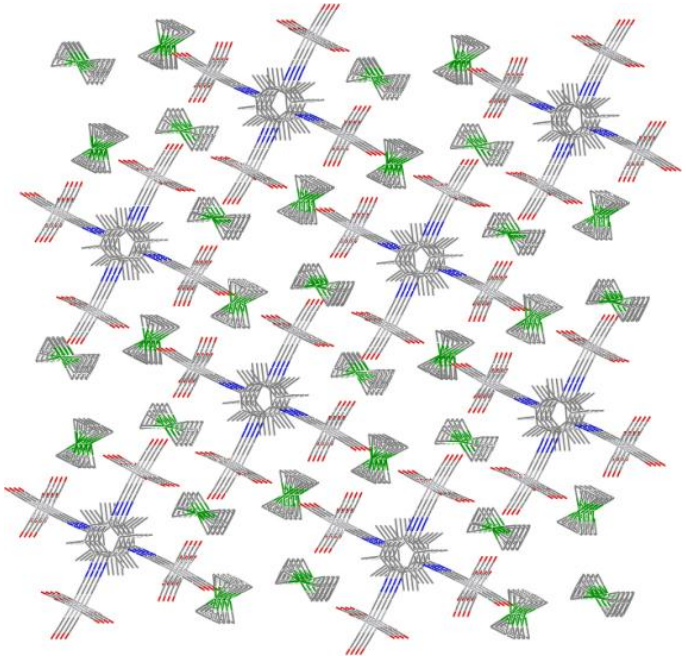

Figure II.7 The supramolecular framework of **2.1b**.

The molecular structure of the V_2-dianion within **2.1b** features slightly distorted octahedral coordination around the V(I-) centers (Figure II.8). For **2.1b**, the C1-N1 distance is 0.010 Å longer while the N1-C2 bond is 0.017 Å shorter compared to corresponding parameters

documented for free 1,4-CNC_6Me_4NC.[36] Albeit small, both of the above differences are statistically significant according to the 3σ criterion and reflect significant V(dπ) → CNC_6Me_4NC(pπ*) back-bonding interaction. Due to the *trans*-influence of the isocyanide ligand, which has a greater σ-donor/π-acceptor ratio than CO, the V-C10 bond is notably shorter while the C10-O10 bond is longer than the V-C and C-O distances, respectively, documented for all other V-C-O units in **2.1b**. The $[Cp_2Co]^+$ cations in **2.1b** exhibit the Co-C bond lengths of 2.022(3) – 2.037(3) Å and the Co–Cp(centroid) distances of 1.63 Å (Figure II.9), which are typical of other cobaltocenium salts.[37]

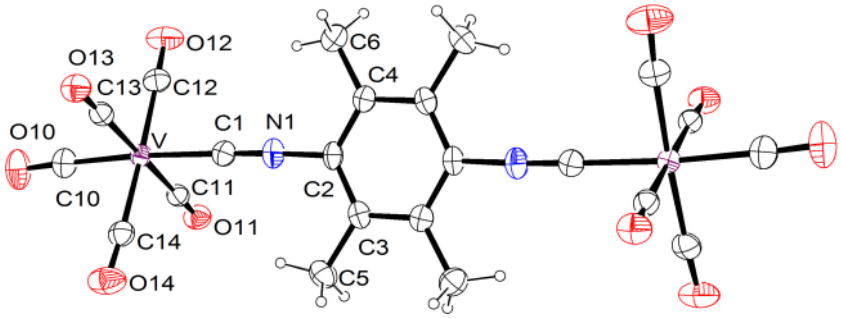

Figure II.8 Molecular structure of the V_2-dianion in **2.1b** (50% thermal ellipsoids). Selected bond distances (Å) and angles (°): V-C1 2.027(2), V-C10 1.919(3), V-C11 1.967(3), V-C12 1.953(3), V-C13 1.960(3), V-C14 1.959(3), C1-N1 1.173(3), N1-C2 1.388(3), C10-O10 1.174(3), C11-O11 1.145(3), C12-O12 1.155(3), C13-O13 1.146(3), C14-O14 1.148(3), V-C1-N1 178.9(2), C1-N1-C2 177.7(3).

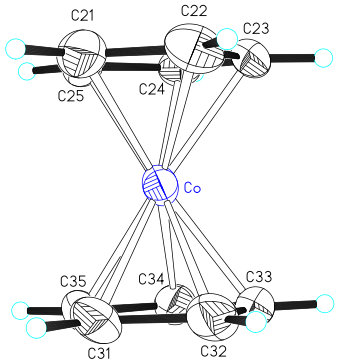

Figure II.9 Thermal ellipsoid plot for the cobaltocenium cations in **2.1b**.

While a satisfactory crystallographic analysis of the charge-transfer salt $[Cp_2Co][V(CO)_6]$ proved impossible in the past due to "massive disorder of $[V(CO)_6]^-$ in the crystal,"[38] the well-ordered framework of **2.1b** now allows detailed geometric appreciation of the interionic interactions between the cobaltocenium and carbonylvanadate(I-) ions in the solid state. The X-ray structure of **2.1b** shows multiple cation-anion contacts at or under 4 Å. These contacts, depicted in Figure II.11, are somewhat shorter than the CO···Co (4.29 Å) and CO···Cp(centroid) (3.91 Å) nonbonded interactions documented by Kochi and Bockman for the contact ion pair $[Cp_2Co]^+[Co(CO)_4]^-$.[39] Each of the pentacarbonylvanadate(I-) moieties in **2.1b** displays close interactions with four cobaltocenium units at distances $d_{Co(A)-V}$ = 5.38 Å, $d_{Co(B)-V}$ = 5.53 Å, $d_{Co(C)-V}$ = 5.73 Å, and $d_{Co(D)-V}$ = 6.48 Å (Figure II.11). Interestingly, ultrafast infrared transient absorption spectroscopy experiments by Spears *et al*. revealed two different electron transfer rates for the $Cp_2Co \mid V(CO)_6$ contact ion pair.[40] These authors' Density Functional Theory (DFT) calculations suggested two distinct stable geometries for $[Cp_2Co]^+ \mid [V(CO)_6]^-$: one with two oxygen atoms lying in the cleft between the two Cp rings at d_{Co-V} = 5.4 Å and the other featuring two oxygen atoms contacting the top of a cyclopentadienyl moiety at d_{Co-V} = 6.1 Å (Figure II.10).[40] Very similar interactions are clearly recognizable in Figure II.11 for **2.1b** ($d_{Co(A)-V}$ = 5.38 Å and $d_{Co(D)-V}$ = 6.48 Å, respectively) and involve the *cis*-CO ligands. In addition, two other cation-anion contacts at $d_{Co(B)-V}$ = 5.73 Å and $d_{Co(C)-V}$ = 5.53 Å place the corresponding $[Cp_2Co]^+$ cations in close proximity of the *trans*-CO ligands (Figure II.11), which experience the greatest extent of back-bonding from the V(I-) centers.

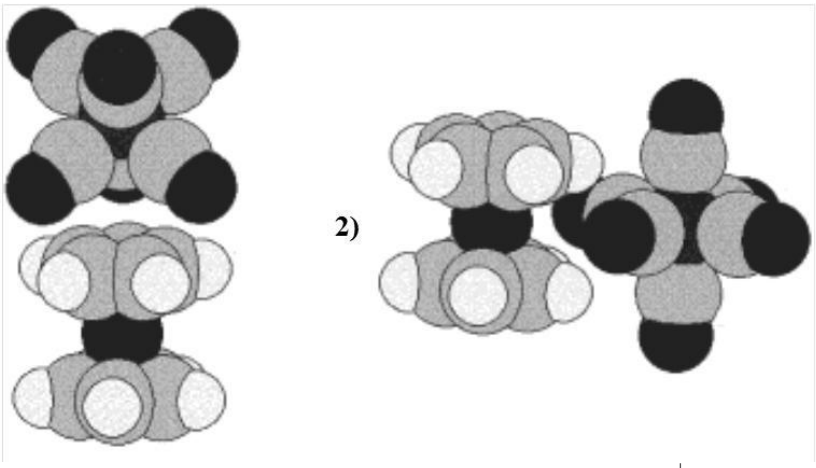

Figure II.10 DFT predicted geometries of the contact ion pair $[Cp_2Co]^+$ | $[V(CO)_6]^-$ predicted by Spears *et al*. showing the oxygen atoms of the carbonyl groups 1) interacting with the top of the Cp ring and 2) lying in the cleft of the Cp rings.[40]

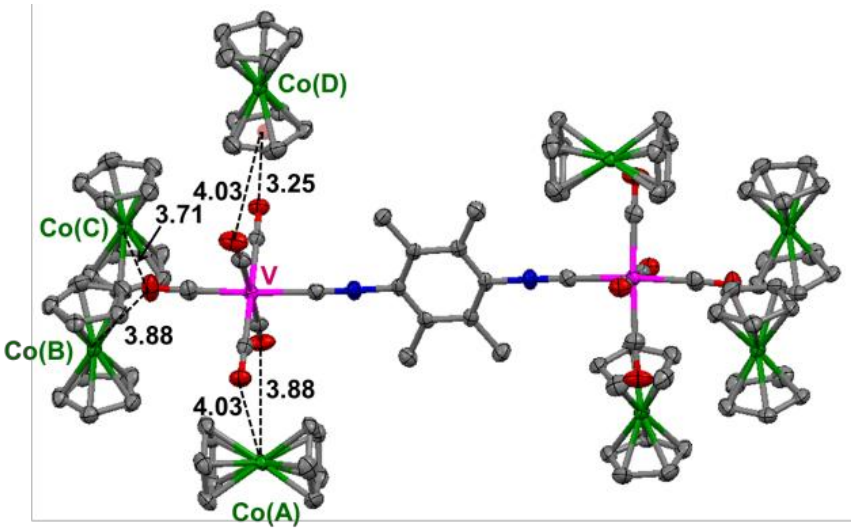

Figure II.11 A fragment of the structure of **2.1b** showing interionic contacts (in Å). All hydrogen atoms are omitted for clarity.

In addition to a reversible $Co^{II/III}$ wave, the cyclic voltammograms of **2.1b** (Figure II.12a) and **2.2** (Figure II.12b) in CH_3CN feature two vanadium-centered processes $V^{I-/0}$ and $V^{0/I}$, both of which are only partially reversible presumably due to instability of the oxidized vanadium species in CH_3CN (*cf*. fast disproportionation of $V(CO)_6$ in donor solvents[4]). The V(I-)→V(0) oxidation for **2.1a**, **2.b** and **2.2** occurs at substantially lower potentials with respect to the

corresponding process for the $[V(CO)_6]^-$ ion (Table II.1).[41,42] Also, the V_2-dianion in **2.1a**,**b** is 60 mV harder to oxidize than the $[V(CO)_5(CNXyl)]^-$ anion in **2.2**. This is consistent with a lower σ-donor/π-acceptor ratio for the 1,4-diisocyanodurene ligand compared to CNXyl.

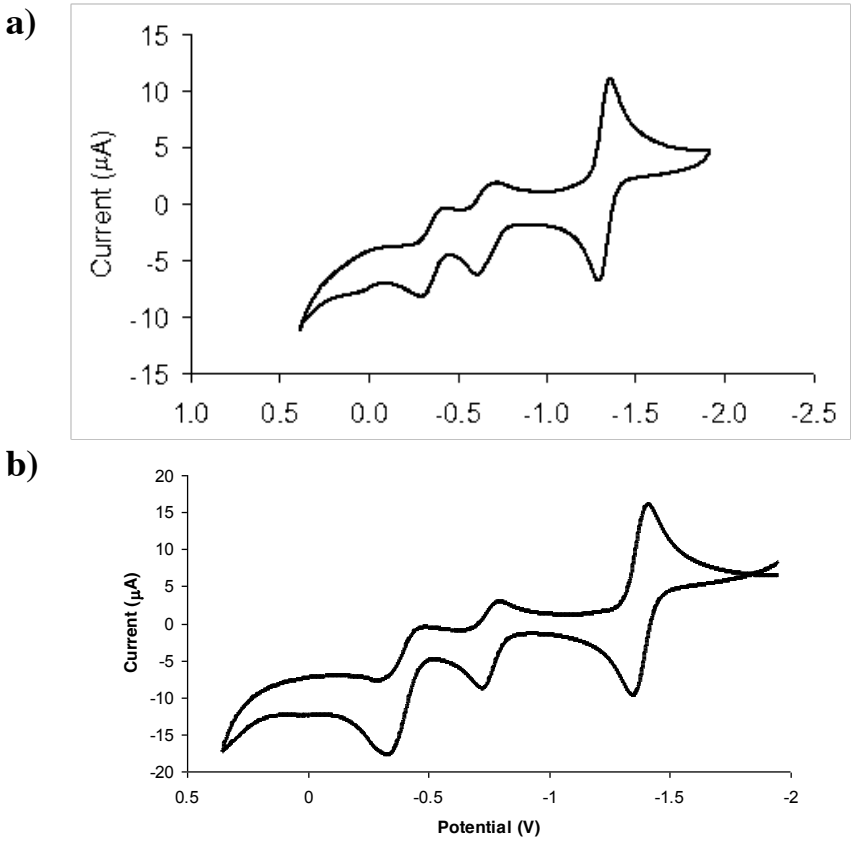

Figure II.12 Cyclic voltammogram for a) **2.1b** and b) **2.2** in CH_3CN at 22 °C at 100 mV/s. Potentials are referenced to the $Cp_2Fe^{0/+}$ couple.

Table II.1 Half-wave potentials (in Volts) for **2.1a**, **2.1b**, **2.2**, and $[V(CO)_6]^-$.[a]

	$E_{1/2}(V^{-I/0})$	$E_{1/2}(V^{0/I})$	$E_{1/2}(Co^{II/III})$	Solvent
2.1a	-0.69	-0.38	-	CH_3CN
2.1b	-0.69	-0.39	-1.35	CH_3CN
2.2	-0.75	-0.38	-1.35	CH_3CN
$[Cp_2Co][V(CO)_6]$	-0.35		-1.32	CH_3CN
$[Na(diglyme)_2][V(CO)_6]$[b]	-0.36	0.06	-	Acetone[b]

[a]Potentials vs. $Cp_2Fe^{0/+}$. [b]Ref. 41.

The IR pattern for **2.1b** in acetonitrile shows broader and more structured bands in the ν_{CO}/ν_{CN} region compared to **2.1a** (Figure II.3). The shoulders at 1847 and 1824 cm^{-1}, that accompany a more intense peak at 1839 cm^{-1}, probably correspond to the B_1 and A_1^{trans} ν_{CO} modes, respectively, the former being IR-forbidden under perfect C_{4v} symmetry. This may suggest perturbation of the dianion's C_{4v} geometry[29] in **2.1b** by contact ion pairing (CIP), e.g., akin to those shown in Figure II.11, even in this polar solvent.

In contrast to **2.1a**, no significant solvatochromism of the vanadium-to-diisocyanodurene charge transfer absorption (λ_{max} = 484 nm) was documented for **2.1b** (Figure II.13), thereby suggesting limited solvent accessibility of the V_2-dianion in **2.1b** compared to that in **2.1a**. Interestingly, a relatively weak shoulder at $\lambda_{max} \approx 738$ nm, which is obscured by the low energy tail of the very intense metal-to-diisocyanodurene charge transfer band, was observed for **2.1b** (Figure II.13). This shoulder is tentatively assigned as an interionic charge transfer band involving the vanadate(I-) anions and the cobaltocenium cations in **2.1b**. For the $[Cp_2Co]^+[V(CO)_6]^-$ ion pair, such interionic charge transfer occurs at *ca*. 620 nm in CH_2Cl_2 (Figure II.14).[38] The lower energy of the interionic charge transfer for **2.1b** versus $[Cp_2Co]^+[V(CO)_6]^-$ correlates[38] nicely with ≈300 mV smaller difference between the $E_{1/2}$ redox potentials of the V(I-) donor and the Co(III) acceptor ions documented for the former (Table II.1).

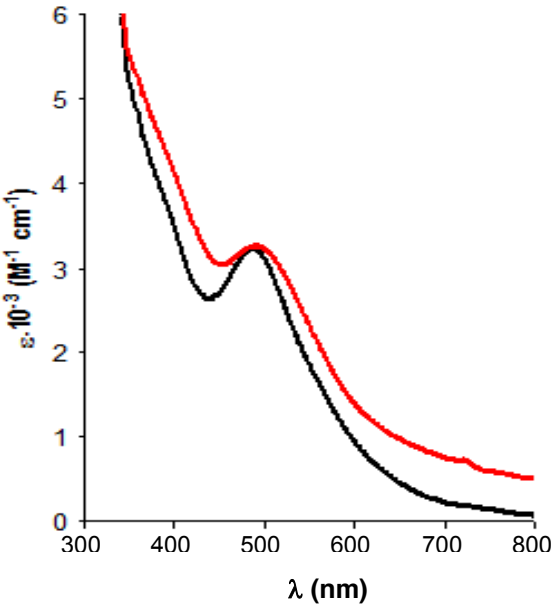

Figure II.13 UV-Vis spectra of **2.1b** in CH_2Cl_2 (red) and CH_3CN (black) at 24 °C.

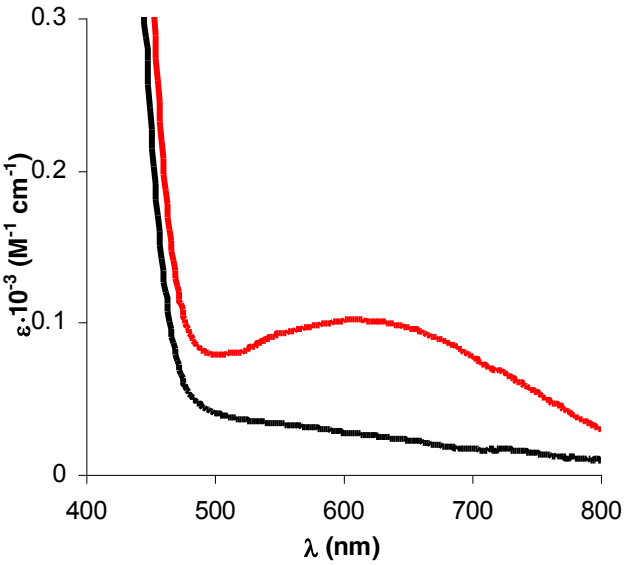

Figure II.14 Electronic absorption spectra (visible region) of $[Cp_2Co][V(CO)_6]$ in CH_2Cl_2 (red) and CH_3CN (black) at 24 °C. The vanadium-to-cobalt contact ion pair charge transfer occurs at λ_{max} = 620 nm in CH_2Cl_2.[38]

II.4.2 2-Isocyano-1,3-dimethylazulene, a Nonbenzenoid Aromatic Analogue of 2,6-Xylyl Isocyanide, and Preliminary Studies of Its Complexation with Sub-Valent Metal Ions

The nonbenzenoid analog of CNXyl can be synthesized from 2-amino-1,3-diethoxycarbonylazulene as shown in Scheme II.4. This starting material is subjected to relatively harsh reducing conditions at 70 °C for a period of 15 hours. Red-Al®, sodium bis(2-methoxyethoxy)aluminumhydride, is a superior reducing agent over, for example, $LiAlH_4$ due to its ability to be dissolved in organic solvents (Red-Al® is commercially available in a toluene solution), decreased sensitivity to air and moisture, and selectivity due to sterically encumbering methoxyethoxy substituents, which help target the ester functional groups on the azulene instead of the azulene moiety itself. The 2-amino-1,3-dimethylazulene intermediate is isolable as a pure (confirmed by ^{1}H NMR) red oil via column chromatography, but is best immediately formylated with acetic-formic anhydride. Following the formylation and quenching, the 2-formamido-1,3-dimethyl azulene (**2.3**) can be purified via column chromatography to give a blue, fluffy powder in a 55% yield over two steps. Both the ^{1}H and ^{13}C NMR spectra show two overlapping, but discernible, sets of resonances. This is due to the *trans* (major) and *cis* (minor) rotational isomers of the formamide functional group. This is opposed to the case of 2-formamido-1,3-diethoxycarbonylazulene where only one set of signals is present in the ^{1}H NMR spectrum due to restricted rotation about the formamide bond by hydrogen bonding between the N-H subunit of the formamide with the C=O subunit of the ester functionalities.[1a]

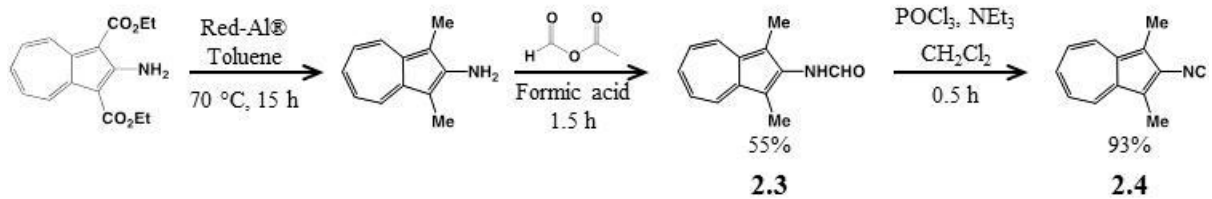

Scheme II.4

The dehydration of **2.3** with phosphorous oxychloride yields the target 2-isocyano-1,3-dimethylazulene (**2.4**) in a 93% yield. Following quenching and subjecting the product to column chromatography, **2.4** can be further purified via recrystallization from hexanes yielding dark green crystals. While the IR spectrum of **2.4** confirm the presence of an isocyanide, ν_{CN} (CH_2Cl_2) = 2115 cm^{-1}, the ^{1}H and ^{13}C NMR spectra confirm this recrystallization provides pure product. The ^{14}N NMR spectrum of **2.4** in CD_2Cl_2 shows a single resonance at 172 ppm, which is similar to the corresponding value of 175 ppm observed for 2-isocyanoazulene.[43] While the commercially available CNXyl ligand (Figure II.15) has been demonstrated to stabilize sub-valent metal ions[44], it has a disagreeable odor and tends to decompose or rearrange over time like most isocyanoarenes. On the other hand, compound **2.4** possesses only a slight and inoffensive odor, has a great solubility profile (being soluble in many common organic solvents), and is stable under ambient conditions for extended periods of time making it an attractive candidate for the stabilization of extremely electron-rich metal centers.

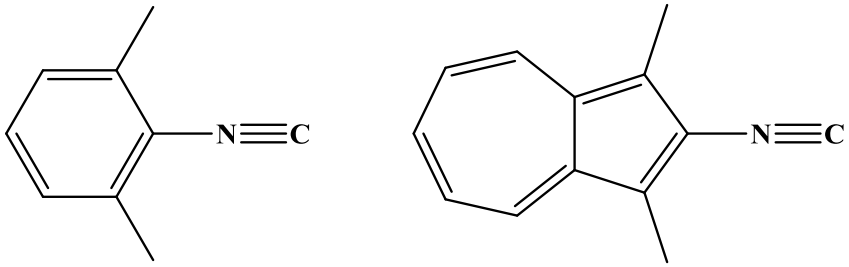

Figure II.15 Molecular structures of CNXyl (left) and **2.4** (right).

The slow evaporation of a CH_2Cl_2 solution of **2.4** provided X-ray diffraction quality crystals (Figure II.16). Compound **2.4** crystallizes in the orthorhombic space group *Pbca* with one molecule in the asymmetric unit. Selected geometric and spectroscopic data are provided in Table II.2 and compared to the benzenoid analogue, CNXyl. The C≡N bond distances in **2.4** and CNXyl are identical at 1.161 Å. The N-C(arene) bond distances are similar at 1.394 Å and 1.401

Å, respectively. More importantly, the distances from the carbon atom of the methyl substituents to the isocyano carbon atom are 3.805 Å and 3.515 Å for **2.4** and CNXyl, respectively. It is well known that isocyanides bound to low-valent metals, especially crowded metal centers, can undergo reductive coupling.[45,46] The methyl substituents in this case may act as steric "guards" to prevent reductive coupling from taking place in high-coordinate, low-valent complexes of these ligands. In addition, both **2.4** (ν_{CN} = 2115 cm^{-1}) and CNXyl (ν_{CN} = 2117 cm^{-1}) have similar CN stretching frequencies in CH_2Cl_2. As a result, **2.4** may prove to be a suitable structural replacement for CNXyl in accessing isocyanometalate complexes.

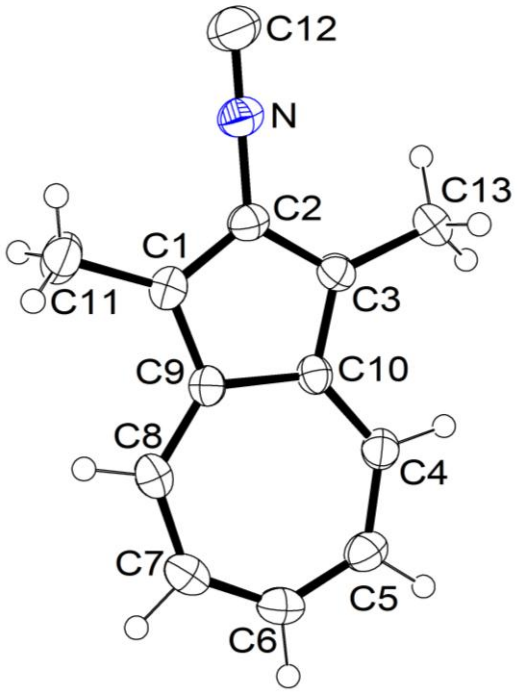

Figure II.16 ORTEP diagram of **2.4** (50% thermal ellipsoids).

Table II.2 Comparison of metric and spectroscopic parameters of **2.4** and CNXyl[47].

Parameter	**2.4**	CNXyl
C≡N bond distance (Å)	1.161(2)	1.160(3)
N-Ar bond distance (Å)	1.394(2)	1.399(2)
Me-C(isocyanide) distance (Å)	3.805(3)	3.533(3)
ν_{CN} in CH_2Cl_2 (cm^{-1})	2115	2117

To access a cobaltate(-I) ion, or cobalt metalate(-I), four equivalents of isocyanide **2.4** were stirred in the presence of CoI_2 in THF under argon (Scheme II.5). Over the course of 5 hours, the blue, clear solution (indicative of uncomplexed **2.4)** turned into a green slurry, presumably due to the formation $Co(\mathbf{2.4})_4I_2$ (**2.5**). Given the composition of **2.5**, either the *cis*- or *trans*-isomer could be formed. Following the work up of this complexation reaction, **2.5** was recovered in an 81% yield and its IR spectrum (in Nujol mull due to poor solubility) revealed a band at 2156 cm^{-1}, which was assigned as a CN stretching frequency. The appearance of only one band indicates the *trans*-isomer is formed as the *cis*-isomer would have displayed more than one band in the IR spectrum as a result of its lower symmetry. The isocyanide stretching observed in **2.5** is in good agreement with similar complexes such as $Co(CNPh)_4I_2$ (ν_{CN} = 2182 cm^{-1}).[48] This 41 cm^{-1} shift to higher energy (Figure II.17) is in accord with the isocyanoazulenes acting as σ-donors to stabilize a relatively high-valent Co(II) metal center. The lone pair on the carbon atom of the isocyanide motif has somewhat antibonding character with respect to the C≡N bond. Upon complexation, the donation of this lone pair to the metal center strengthens the C≡N bond, thereby requiring a higher energy to induce the C≡N vibration.

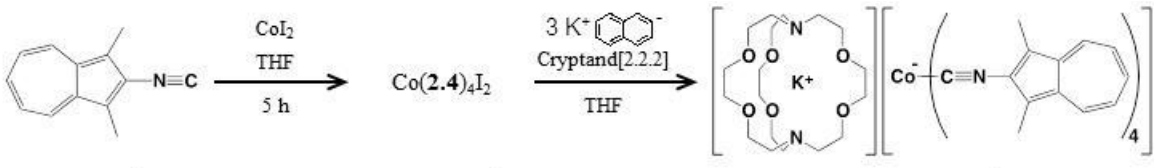

ν_{CN} = 2115 cm^{-1} — **2.4**

ν_{CN} = 2156 cm^{-1} — **2.5**

ν_{CN} = 1842 cm^{-1} — **2.6**

Scheme II.5

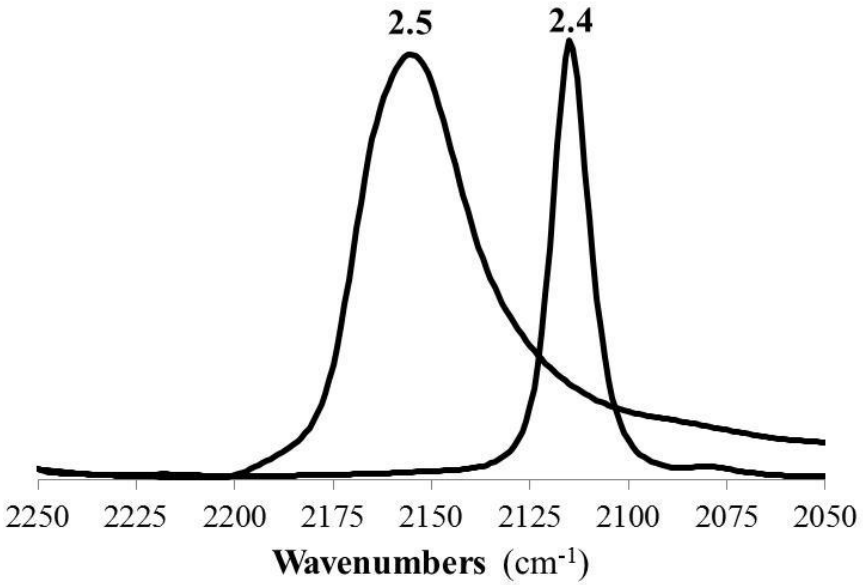

Figure II.17 Infrared spectra of **2.4** in CH_2Cl_2 and **2.5** in Nujol mull.

The reduction of **2.5** (Scheme II.5) in THF with three equivalents of potassium naphthalenide ($Co^{II} \rightarrow Co^{I-}$) at -78 °C, followed by the addition of the K^+-sequestering cryptand[2.2.2] reagent, yielded the desired cobaltate [K(crypt[2.2.2])][Co(**2.4**)$_4$] (compound **2.6**) as a dark blue powder in a 78% yield. Alternatively, the Co(II) intermediate **2.5** does not need to be isolated. Potassium naphthalenide can also be added directly to a suspension of **2.5** generated *in situ* to yield **2.6**. Both routes provide the same material as confirmed spectroscopically by FTIR.

The solid-state FTIR spectrum (in Nujol mull) of **2.6** shows a broad band attributed to CN stretching at 1746 cm^{-1} as well as a weak band at 1985 cm^{-1}. The IR spectrum of this compound in solution (THF) shows a broad band centered at 1842 cm^{-1}. This CN stretching frequency constitutes a 273 cm^{-1} shift to lower energy relative to the uncomplexed ligand indicating an extensive extent of π-backdonation from the formally Co(I-) center into the isocyanoazulene(pπ*) orbitals. This observed value is in good agreement with Cooper's original

isocyanocobaltate[10], [K(DME)][Co(CNXyl)$_4$] (Figure I.2), which displayed one broad CN stretch at 1815 cm^{-1}, and Figueroa's cobaltate[49] [Ph$_3$PNPPh$_3$][Co(CNAr^{Mes2})$_4$] (Figure I.5), which displayed one broad CN stretch at 1821 cm^{-1}. This similarity in stretching frequencies signifies that nonbenzenoid, azulene-based isocyanoarenes can be used in addition to benzenoid isocyanoarenes to stabilize sub-valent metal centers.

To reduce cation-π interactions, cryptand[2.2.2] was added shortly after the reduction was initiated to sequester K$^+$ cations. Figueroa *et al*. showed these cation-π interactions can reduce the local symmetry of the metal center from tetrahedral and confound the IR spectrum.[49] Indeed, the sodium salt Na[Co(CNAr^{Mes2})$_4$] (Figure II.18) exhibits three intense CN stretching bands at 1903, 1821, and 1761 cm^{-1}. Through cation metathesis with [Ph$_3$PNPh$_3$]Cl, the interfering Na$^+$ cation was replaced with the noncoordinating [Ph$_3$PNPh$_3$]$^+$ cation. The removal of the cation-π interactions restored local tetrahedral symmetry about the metal center, which was confirmed by the presence of only one ν_{CN} band at 1821 cm^{-1} in THF.[49]

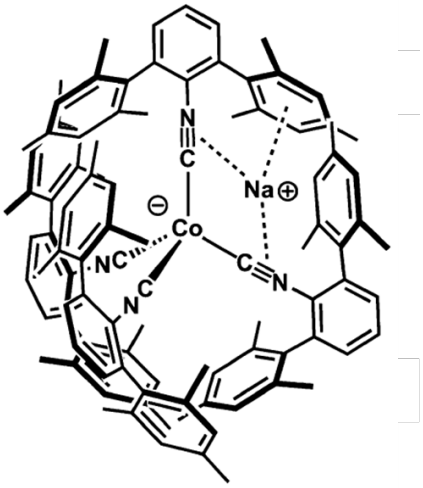

Figure II.18 Figueroa's isocyanocobaltate(I-) complex Na[Co(CNAr^{Mes2})$_4$] featuring cation-π interactions of the Na$^+$ cation with the isocyanide and mesityl π-systems of the cobaltate anion.[49]

Any excess electron density transferred from the metal center to the π-system of the isocyanoarene is delocalized via the M(dπ)-Isocyanoazulene(pπ*) backbond. Addition of electron density into this antibonding orbital weakens the bond and decreases the energy required to induce a vibration. The energy of the CN stretching in **2.6** (ν_{CN} = 1842 cm^{-1}) is similar to the cobaltates of Cooper *et al*. (ν_{CN} = 1815 cm^{-1})[10] and Figueroa *et al*. (ν_{CN} = 1821 cm^{-1})[49].

The ^{1}H NMR spectrum of **2.6** exhibits three aromatic resonances and one aliphatic resonance due to the 1,3-dimethylazulene moiety as well as three resonances (a singlet and two doublets of doublets) due to the cryptand[2.2.2]. Problematically, the ratio of the ^{1}H environments deduced from the integration of the corresponding NMR resonances suggests presence of excess cryptand[2.2.2]; however, **2.6** is extremely air- and moisture sensitive and the sample could have degraded somewhat prior to spectrum acquisition.

To expand the application of **2.4** in electron-rich organometallics, a Fe(II-) metalate was synthesized (Scheme II.6). Four equivalents of **2.4** were stirred with one equivalent of $FeBr_2$ in THF at room temperature under argon. A green suspension developed after stirring for 4 hours. An FTIR analysis of the in situ mixture revealed three bands attributed to CN stretching at 2132, 2111, and 2098 cm^{-1}. This product was formulated as a mixture of the *cis*- and *trans*-isomers of Fe(**2.4**)$_4Br_2$ as suggested by the multiple bands observed in the FTIR spectrum. The analogous $Fe(CNXyl)_4Br_2$ was produced by Ellis *et al*. in a similar fashion and reported to consist of a mixture of *cis*- and *trans*-isomers.[15]

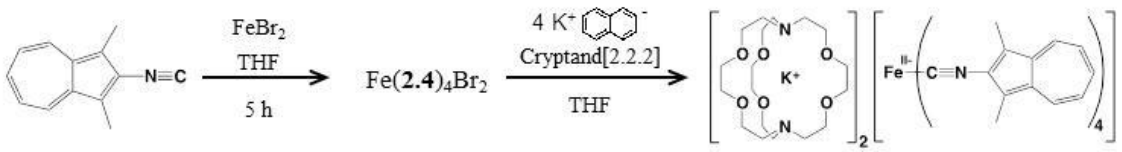

ν_{CN} = 2115 cm^{-1} — ν_{CN} = 2132, 2111, 2098 cm^{-1} — ν_{CN} = 1672 cm^{-1}

2.4 — **2.7**

Scheme II.6

The reduction of the Fe(II)-isocyanoazulene complex to **2.7** was performed similarly to the reduction of **2.5**. The addition of four equivalents of potassium naphthalenide ($Fe^{2+} \rightarrow Fe^{2-}$), followed by the addition of two equivalents of cryptand[2.2.2], to the suspension of Fe(**2.4**)$_4$Br$_2$ produced the proposed [K(crypt[2.2.2])]$_2$[Fe(**2.4**)$_4$] (compound **2.7**) in a 74% yield. This reaction was accompanied by a color change from green starting material to blue **2.7**. While characterization of this extremely sensitive complex was difficult, a solution IR (in THF) of the crude reaction mixture was obtained. The FTIR spectrum shows a broad band centered at 1672 cm^{-1}, which is in line with the ν_{CN} value of 1675 cm^{-1} obtained by Ellis *et al*. for their structurally characterized [K(crypt[2.2.2])]$_2$[Fe(CNXyl)$_4$].[15] This dramatic 443 cm^{-1} depression in ν_{CN} for **2.7** relative to the uncomplexed ligand suggests extensive π-backdonation from the formally Fe(II-) metal center to the π* system of the isocyanoazulene ligands. Unfortunately further characterization of compound **2.7** by the author of this Dissertation was hampered by extreme air-sensitivity of the complex.

II.5 Conclusions and Outlook

In the first part of this Chapter, the supramolecular ensemble $([Cp_2Co]_2[\{(OC)_5V\}_2(\mu\text{-}1,4\text{-}CNC_6Me_4NC)])_\infty$, which is held together via synergistic π-stacking and Co^{III}/V^{I-} contact ion interactions, was described. This unusual platform will offer new opportunities in organometallic crystal engineering.[2] The above unique 3-dimensional framework features pores suitable for housing a variety of linear molecules, such as acetonitrile, CO_2, etc. The dianion $[\{(OC)_5V\}_2(\mu\text{-}1,4\text{-}CNC_6Me_4NC)]^{2-}$ constitutes the first sub-valent organometallics incorporating a diisocyanoarene linker. It will be interesting to determine how the 3-D structure of **2.1b** is affected upon replacing the cobaltocenium cations with decamethylcobaltocenium cations and/or employing the 1,4-diisocyanobenzene linker in place of 1,4-diisocyanodurene. Other modifications to the structures of the metallocenium cation and the aromatic ring of the bridge may be envisioned as well. Our immediate further studies, however, are aimed at detailed understanding of interionic association and photochemistry of **2.1a,b** in solution.

The successful synthesis of 2-isocyano-1,3-dimethylazulene, which exhibits better thermal and air stability than its benzenoid analogue CNXyl, paves the way for developing organometallic chemistry of isocyanoazulenes at the electron-rich extreme. Indeed, the preliminary studies highlighted in this Dissertation indicate that **2.4** appears to be compatible with highly reduced metal ions such as Co(I-) and Fe(II-). While the homoleptic complexes of **2.4** with Co(I-) and Fe(II-) proved to be extremely air-sensitive, the possibility of their isolation is certainly feasible. Certainly, additional experiments to isolate and further characterize these species are necessary. Moreover, heteroleptic variants of the above species (e.g., featuring mixed CO/**2.4** ligand environments) are attractive for the design of new compounds and materials exhibiting low-energy interionic charge transfer akin to that found for **2.1b** and **2.2**.

II.6 References

1 (a) Holovics, T. H.; Robinson, R. E.; Weintrob, E. C.; Toriyama, M.; Lushington, G. H.; Barybin, M. V. *J*. *Am*. *Chem*. *Soc*. **2006**, *128*, 2300. (b) DuBose, D. L.; Robinson, R. E.; Holovics, T. C.; Moody, D. R.; Weintrob, E. C.; Berrie, C. L.; Barybin, M. V. *Langmuir* **2006**, *22*, 4599.

2 Braga, D.; Grepioni, F.; Desiraju, G. R. *Chem*. *Rev*. **1998**, ***98***, 1375.

3 (a) Barybin, M. V. *Coord*. *Chem*. *Rev*. **2010**, *254*, 1240. (b) Maher, T. R.; Spaeth, A. D.; Neal, B. M.; Berrie, C. L.; Thompson, W. H.; Day, V. W.; Barybin, M. V. *J*. *Am*. *Chem*. *Soc*. **2010**, *132*, 15924-15926.

4 Liu, X.;Ellis, J. E. *Inorg*. *Synth*. **2004**, *34*, 96.

5 Selected examples: (a) Shi, Q. Z.; Richmond, T. G.; Trogler, W. C.; Basolo, F. *J*. *Am*. *Chem*. *Soc*. **1984**, *106*, 71. (b) Ellis, J. E.; Faltynek, R. A.; Rochfort, G. L.; Stevens, R. E.; Zank, G. A. *Inorg*. *Chem*. **1980**, *19*, 1082. (c) Hieber W.; Winter, E. *Chem*. *Ber*. **1964**, *97*, 1037.

6 Barybin, M. V.; Young, Jr., V. G.; Ellis, J. E. *J*. *Am*. *Chem*. *Soc*. **2000,** *122*, 4678.

7 Ellis, J. E.; Fjare, K. L. *Organometallics* **1982**, *1*, 898.

8 Ihmels, K.; Rehder, D. *Organometallics* **1985**, *4*, 1340.

9 (a) Fox, B. J.; Sun, Q. Y.; DiPasquale, A. G.; Fox, A. R.; Rheingold, A. L.; Figueroa, J. S. *Inorg*. *Chem*. **2008**, *47*, 9010-9020; (b) Ditri, T. B.; Fox, B. J.; Moore, C. E.; Rheingold, A. L.; Figueroa, J. S. *Inorg*. *Chem*. **2009**, *48*, 8362-8375.

10 Warnock, G.F.; Cooper, N.J. *Organometallics* **1989**, *8*, 1826-1827.

11 Utz, T. L.; Leach, P. A.; Geib, S. J.; Cooper, N. J. *Chem*. *Commun*. **1997**, 847-848.

12 (a) Barybin, M. V.; Young, V. G.; Ellis, J. E. *J*. *Am*. *Chem*. *Soc*. **1998**, *120*, 429-430; (b) Barybin, M. V.; Young, V. G.; Ellis, J. E. *J*. *Am*. *Chem*. *Soc*. **2000**, *122*, 4678-4691.

13 (a) Barybin, M. V.; Young, Jr.; V. G., Ellis, J. E. *J*. *Am*. *Chem*. *Soc*. **1999**, *121*, 9237-9238; (b) Barybin, M. V.; Brennessel, W. W.; Kucera, B. E.; Minyaev, M. E.; Sussman, V. J.; Young, V. G.; Ellis, J. E. *J*. *Am*. *Chem*. *Soc*. **2007**, *129*, 1141-1150.

14 Corella, J. A.; Thompson, R. L.; Cooper, N. J. *Angew*. *Chem*. *Int*. *Ed*. **1992**, *31*, 83-84

15 Brennessel, W. W.; Ellis, J. E. *Angew*. *Chem*. *Int*. *Ed*. **2007**, *46*, 598-600.

16 Liu, R. S. H. *J*. *Chem*. *Ed*. **2002**, *79*, 183-185.

17 See Section I.3 of this Dissertation for further reading.

18 Dewar, M. J. S. The Molecular Orbital Theory of Organic Chemistry; McGraw-Hill: New York, 1969.

19 Connelly, N. G.; Geiger, W. *Chem*. *Rev*. **1996**, *96*, 877.

20 Barybin, M. V.; Pomije, M. K.; Ellis, J. E. *Inorg*. *Chim*. *Acta* **1998**, *269*, 58.

21 Calderazzo, F.; Pampaloni, G.; Zanazzi, P. F. *Chem*. *Ber*. **1986**, *119*, 2796.

22 Cotton, F. A.; Daniels L. M.; Wilkinson, C. C. *Acta Cryst*. *E* **2001**, *57*, m529.

23 Swanson, S. A.; McClain, R.; Lovejoy, K. S.; Alamdari, N. B.; Hamilton J. S.; Scott, J. C . *Langmuir* **2005**, *21*, 5034.

24 Ugi, I.; Fetzer, U.; Eholzer, U.; Knupfer H.; Offermann, K. *Angew*. *Chem*. *Int*. *Ed*. *Engl*. **1965**, *4*, 472.

25 Takase, K.; Nozoe, T.; Nakazawa, T.; Fukuda, S. *Tetrahedron* **1971**, *27*, 3357-3368.

26 Krimen, K. I. *Org*. *Synth*. **1970**, *50*, 1-3.

27 Ihmels K.; Rehder, D. *J*. *Organomet*. *Chem*. **1983**, *232*, 151.

28 Maher, T. R. Design of Novel Electron-Rich Organometallic Frameworks Involving Metal-Isocyanide Junctions. Ph.D. Dissertation, University of Kansas, Lawrence, KS, 2009.

29 Darensbourg, M. Y. *Prog*. *Inorg*. *Chem*. **1985**, *33*, 221

30 Reichardt, C. *Chem*. *Rev*. **1994**, *94*, 2319.

31 *Cf*. δ(51V) = -1901 ppm for $[Et_4N][V(CO)_5(CNiPr)]$ in MeCN: ref. 7.

32 Rehder, D. *Coord*. *Chem*. *Rev*. **2008**, *252*, 2209.

33 Calderazzo, F.; Pampaloni, G.; Pelizzi, G.; Vitali, F. *Organometallics* **1988**, *7*, 1083.

34 Coates, G. W.; Dunn, A. R.; Henling, L. M.; Dougherty D. A.; Grubbs, R. H. *Angew*. *Chem*. *Int*. *Ed*. *Engl*. **1997**, *36*, 248.

35 Van der Sluis, P.; Spek, A. L. *Acta Cryst*. *A* **1990**, *46*, 194.

36 Zeller, M.; Hunter, A. D.; Perrine, C. L. *Acta Cryst*. *E* **2003**, *59*, o1655.

37 For example: (a) Migliori, J. M.; Reiff, W. M.; Arif, A. M.; Miller, J. S. *Inorg*. *Chem*. **2004**, *43*, 6875. (b) Andrews, C. G.; Macdonald, C. L. B. *Acta Cryst*. *E* **2005**, *61*, m2103.

38 Kochi, J. K.; Bockman, T. M. *J*. *Am*. *Chem*. *Soc*. **1989**, *111*, 4669.

39 Bockman, T. M.; Kochi, J. K. *J*. *Am*. *Chem*. *Soc*. **1988**, *110*, 1294.

40 (a) Spears, K. G.; Shang, H. *J*. *Phys*. *Chem*. *A* **2000**, *104*, 2668. (b) Martin, T. W.; Homoelle, B. J.; Spears, K. G. *J*. *Phys*. *Chem*. *A* **2002**, *106*, 1152. (c) Sando G. M.; Spears, K. G. *J*. *Phys*. *Chem*. *A* **2004,** *108*, 1290.

41 (a) Bond, A. M.; Colton, R.; Mahon P. J.; Snook, G. A. *J*. *Phys*. *Chem*. *B* **1998**, *102*, 1229. (b) Bond, A. M.; Colton, R. *Inorg*. *Chem*. **1976**, *15*, 2036.

42 Pampaloni, G.; Koelle, U. *J*. *Organomet*. *Chem*. **1994**, *481*, 1.

43 Robinson, R. E.; Holovics, T. C.; Deplazes, S. F.; Powell, D. R.; Lushington, G. H.; Thompson, W. H.; Barybin, M. V. *Organometallics* **2005,** *24*, 2386-2397.

44 See Chapter I of this Dissertation for more details.

45 Lippard, S.; Carnahan, E. *Acc*. *Chem*. *Res*. **1993**, *26*, 90-97.

46 Barybin, M. V.; Meyers, Jr., J. J.; Neal, B. M. Renaissance of Isocyanoarenes as Ligands in Low-Valent Organometallics. In *Isocyanide Chemistry - Applications in Synthesis and Material Science*. Nenajdenko, V. G., Ed. Wiley–VCH: Weinheim, **2012**; pp 493-529.

47 Mathieson, T.; Schier, A.; Schmidbaur, H. *J*. *Chem*. *Soc*. *Dalton Trans*. **2001**, 1196.

48 Malatesta, L.; Bonati, M. Isocyanide Complexes of Metals; John Wiley & Sons: London, 1969.

49 Margulieux, G. W.; Weidemann, N.; Lacy, D. C.; Moore, C. E.; Rheingold, A. L.; Figueroa, J. S. *J*. *Am*. *Chem*. *Soc*. **2010**, *132*, 5033-5035.

CHAPTER III

Isocyanobiazulene Ligands Featuring the 2',6-Biazulenic and Related Motifs: Synthesis, Redox Characteristics, and Homoleptic Complexation with Low-Valent Chromium Centers

III.1 Introduction

The organometallic chemistry of isocyanides has been explored for applications in synthesis, catalysis, and materials science.[1] Recently, there has been an increased interest in the coordination chemistry of linear isocyanoarenes for materials applications[2] with the idea of charge transport mediated by the π-system of the aromatic framework.[3] This can be accomplished by transferring electron density from a metal center through the π-system of the aryl substituent via π-backbonding with the isocyanide junction group.

Unpaired electron spin delocalization into the π-system of a benzenoid isocyanoarene, namely CNXyl (Xyl = xylyl), has already been documented.[4] This unpaired electron in this case originates from the low-spin (S = ½) chromium(I) center of the paramagnetic, homoleptic complex $Cr(CNXyl)_6^+$ and is delocalized throughout all of the CNXyl ligands as determined spectroscopically. The observed hydrogen (from ^1H NMR) and carbon (from ^{13}C NMR) nuclei resonances were paramagnetically shifted with respect to the resonances observed in the diamagnetic, chromium(0) precursor (Table III.1). The quantity Δδ is the shift in value between the respective resonances in the paramagnetic and the diamagnetic complexes.

Table III.1 NMR data reflecting paramagnetic shifts (δ_{para}) of ^1H and ^{13}C resonances due to a delocalized unpaired electron spin in $Cr(CNXyl)_6^+$.[4]

Resonating nucleus	δ_{para} (ppm)	$\Delta\delta_{Observed}$ ($\Delta\delta_{Expected}$)[a]
o-C<u>H</u>$_3$	8.74	+ (+)
o-<u>C</u>H$_3$	-0.8	- (-)
o-C	224.2	+ (+)
m-H	12.53	+ (+)
m-C	90.6	- (-)
p-H	-1.48	- (-)
p-C	179.6	+ (+)
i-C	-32.9	- (-)

[a] The + and – denote downfield and upfield shifts, respectively.

Two methods exist through which a paramagnetic metal center could cause a shift in nuclear resonances: Pseudocontact and Fermi contact[5,6]. Pseudocontact can be considered a "through space" interaction and is therefore attenuated with increasing distance from the paramagnetic metal center.[6] The Fermi contact results from when an unpaired electron originating at a metal center is delocalized throughout the π-systems of the ligands, while alternating spin (i.e., S = ± ½) with respect to the external magnet at every nucleus (Figure III.1). The spin of the electron (spin up or spin down) will either effectively increase of decrease the local magnetic field that each nucleus experiences, thus shifting the resonance downfield or upfield, respectively. It is important to note that while this electron cannot directly affect the carbon nuclei during delocalization due to an orbital (2p) node at the carbon nuclei, it can indirectly change the environment of each nuclei through spin polarization of the bonded electron pair, via the atomic coupling exchange mechanism[7]. Given that all of the hydrogen and carbon resonances in $Cr(CNXyl)_6^+$ exhibit substantial shifts (Table III.I) that do not attenuate with distance from the metal center, the unpaired electron spin density can be concluded to interact with the ligand through Fermi contact. This result signifies that the unpaired electron is delocalized through the π*-system of the CNXyl ligands.

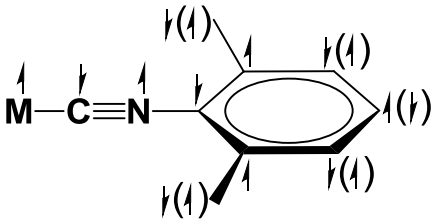

Figure III.1 A diagram detailing the expected alternation of unpaired electron spin delocalized throughout the π-system of a single CNXyl ligand in $Cr(CNXyl)_6^+$. Spin denoted in parentheses resides on the hydrogen atom at the corresponding carbon atom.

In bond polarization, the unpaired electron will interact with C(2p) orbitals associated with the π-system of the aromatic ligand during delocalization. The unpaired electron in the

C(2p) orbital will create a local magnetic field to which the electrons in the C(sp^2)-H(1s) bond will respond by polarizing (Figure III.2). Electron 1, the electron in the localized bonding pair that is closer to the carbon atom, will pair parallel with respect to the unpaired, delocalized electron. Electron 2, the electron closer to the H nucleus, will pair anti with respect to the unpaired, delocalized electron.[7] This event leaves spin aligned against the external magnetic field at the carbon nucleus and spin aligned with the external magnetic field at the hydrogen nucleus. The result detracts from the magnetic field the carbon nucleus "feels," effectively decreasing the energy required for nuclear resonance and shifting the resonance upfield (i.e., to lower ppm). On the other hand, the excess spin about the hydrogen atom effectively increases the magnetic field the hydrogen "feels" and increases the energy required for nuclear resonance, shifting the resonance downfield. This polarization stemming from the atomic exchange coupling mechanism[7] is confirmed by the opposing shifts observed in bonded C and H atoms (e.g., *m*-C/*m*-H or *p*-C/*p*-H) in $Cr(CNXyl)_6^+$ (Table III.1).

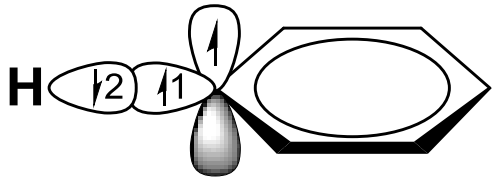

Figure III.2 The polarization of the bonded electron pair in a C(sp^2)-H(1s) bond due to delocalized electron spin.

The work of Barybin *et al*. has led to the synthesis and exploration of nonbenzenoid isocyanoarenes that can participate in charge transport and electron delocalization.[1] Specifically, azulene, the non-benzenoid analog of naphthalene, is particularly attractive. First, azulene has been observed as a defect in carbon nanotubes and, therefore, thought to contribute to the electrical properties of the allotrope.[8] Second, the aromatic delocalization energy of azulene is approximately one-fifth the energy of benzene.[9] This low energy should allow for a more facile

delocalization throughout the π-system of azulene relative to benzene. Third, azulene possesses a complementary nature between the highest occupied molecular orbital (HOMO) and lowest unoccupied molecular orbital (LUMO) leading to unique physicochemical properties[10] that could be advantageously manipulated for materials.[1]

Similar to isocyanoxylene (i.e. CNXyl) in $Cr(CNXyl)_6^+$, isocyanoazulenes can effectively delocalize unpaired spin density through the π-systems thereof.[11] Cyclic voltammetric experiments can be employed to probe the quantitative π-accepting/σ-donating ratio of the azulene moieties.[1] Notably, even-substituted isocyanoazulenes exhibit larger π-accepting/σ-donating ratios (more positive reduction potentials) than their odd-substituted counterparts (more negative reduction potentials) in the respective homoleptic chromium complexes as determined from the reduction potential of the $Cr(CN^xAz)_6^{0/+}$ (x = 2, 4, 6) couple. Monoazulenes published to date that have been shown to allow for electron delocalization are CN^xAz (x = 1, 2, 4, 6), where x is the number of the carbon atom to which the isocyanide is attached, as well as 5-isocyano-1,3-di(*t*-butyl)azulene.[12] An example ^1H NMR spectrum of $Cr(CN^1Az)_6^+$ can be seen in Figure I.18. The ^1H resonance shifts with respect to its diamagnetic counterpart are displayed in Table III.2. The observed proton resonances of the paramagnetic $Cr(CN^1Az)_6^+$ complex are in line with the expected resonances predicted by the atomic coupling exchange mechanism. The correspondence of observed and expected shifts is indicative of delocalized unpaired electron spin present in the CN^1Az ligands.

Table III.2 NMR data reflecting paramagnetic shifts (δ_{para}) of ^{1}H resonances in $Cr(CN^1Az)_6^+$ vs. diamagnetic shifts (δ_{diam}) of $Cr(CN^1Az)_6$.[12]

Resonating nucleus	δ_{para} (ppm)	δ_{diam} (ppm)	$\Delta\delta_{Observed}$ ($\Delta\delta_{Expected}$)[a]
2-H	-2.69	7.72	- (-)
3-H	8.20	7.21	+ (+)
4-H	11.35	8.11	+ (+)
5-H	-4.81	6.93	- (-)
6-H	12.21	7.27	+ (+)
7-H	-6.38	6.37	- (-)
8-H	13.58	8.81	+ (+)

[a] The + and – denote downfield and upfield shifts, respectively.

For nanoelectronic application purposes, control of orientation of the molecular dipole of azulene (1.08 D) between two metal centers or surfaces (Figure III.3) through 2,6-substitution should allow for charge transport.[13] A recent theoretical study suggested azulene-like molecules could be highly conductive and probed the correlation of the molecular dipole to the rectification capabilities within 2,6-substituted azulenic and azulene-like molecules.[14] 2- and 6-substituted azulenes are seemingly beneficial for charge transport or electron delocalization due to the correspondence of these even numbered positions with the vacant LUMO of azulene. Unpaired electron density, then, could pass through the LUMO with minimal repulsion/interference.

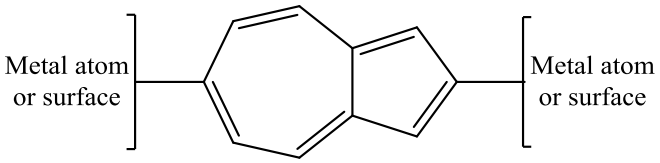

Figure III.3 The generic coordination of a 2,6-substituted azulenic framework.[1]

While the class of monoazulenes has expanded nicely over the past ten years, the chemistry of linear biazulenes (i.e. two coupled azulenes) is still limited.[15] Three different types of biazulenes (Figure III.4) can be envisioned: a) the symmetric 6,6'-biazulene; b) the symmetric

2,2’-biazulene; and c) the asymmetric 2,6’-biazulene. A 2,2’-diisocyano-6,6’-biazulene[16] recently came to light, but asymmetric 2,6’-biazulenes have yet to be explored. The precursor to 2-isocyano-2’,6-biazulene (i.e., 2-amino-1,3-diethoxycarbonyl-2’,6-biazulene) was published in 2002 by Murafuji, Sugihara, et al.[15c] Although the lack of a junction group at the 6’-position prohibits the communication of two metal centers or surfaces, the 2,6’-biazulenyl framework could serve as a terminal ligand through which to delocalize unpaired electron density.

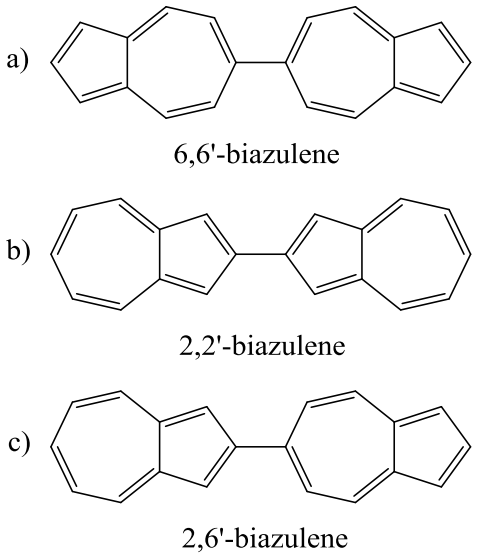

Figure III.4 Molecular structures of the three possible 2,6-coupled biazulenes: a) symmetric 6,6’-biazulene; b) symmetric 2,2’-biazulene; and c) asymmetric 2,6’-biazulene.[16]

III.2 Work Described in Chapter III

In this Chapter, the syntheses and coordination chemistry of two novel 2-isocyano-substituted 2',6-biazulenes are discussed. The characterization of these ligands and their homoleptic complexes of chromium(0) and chromium(I) includes multinuclear and multidimensional NMR spectroscopy, magnetic susceptibility measurements, cyclic voltammetry, and electron paramagnetic resonance (EPR) spectroscopy. Unpaired electron spin delocalization in the Cr(I) complexes of the isocyanobiazulenic ligands is compared and contrasted with that occurring in the homoleptic Cr(I) complexes of related 2-isocyanoazulene derivatives featuring just one azulenic moiety.

III.3 Experimental Section

III.3.1 General Procedures, Starting Materials, and Equipment

Unless specified otherwise, all operations were performed under an argon atmosphere of 99.5% argon further purified by passage through columns of activated BASF catalyst and molecular sieves. All connections involving the gas purification systems were made of glass, metal, or other materials impermeable to air. Solutions were transferred via stainless steel cannulas whenever possible. Standard Schlenk techniques were employed with a double manifold vacuum line. Both CH_2Cl_2 and CD_2Cl_2 were distilled over CaH_2. THF, diethyl ether, and toluene were distilled over Na/benzophenone. Pentane was distilled over Na/benzophenone dissolved in a minimal amount of diglyme. Diisopropylamine was distilled over sodium hydroxide. Following purification, all distilled solvents were stored under argon.

Solution infrared spectra were recorded on a PerkinElmer Spectrum 100 FTIR spectrometer with samples sealed in 0.1 mm gas tight NaCl cells. NMR samples were analyzed using Bruker DRX-400 and Bruker Avance 500 spectrometers. ^{1}H and ^{13}C chemical shifts are given with reference to residual ^{1}H and ^{13}C solvent resonances relative to Me_4Si. ^{14}N NMR chemical shifts are referenced to liquid ammonia at 25 °C. A solution of N,N-dimethylformamide in CD_2Cl_2 was used as an external ^{14}N reference ($\delta(^{14}N)$ = 103.8 ppm vs. liquid NH_3 at 25 °C). Two-dimensional techniques (^{1}H-^{1}H COSY, ^{1}H-^{13}C HSQC) were used to obtain unambiguous assignments of ^{1}H, and ^{13}C in some cases, NMR resonances. Electron paramagnetic resonance (EPR) spectra were recorded in CH_2Cl_2 or CH_2Cl_2/toluene on a Bruker EMXplus EPR spectrometer at 5 K. Mass spectral analyses were performed on a JEOL GCmate in the MS laboratory of Nihon University (Japan).

Solid-state volume magnetic susceptibilities (χ_v) were measured on a Johnson Matthey MSB-1 balance at ambient temperature and converted into the corresponding molar susceptibilities (χ_M) in the usual manner.[17] Samples were packed into gastight tubes (0.400 cm o.d. x 0.324 cm i.d.) to a depth of ca. 2.5 cm in a drybox. The air correction of 0.029×10^{-6} was applied to χ_v values of all samples packed under argon. Diamagnetic corrections applied to the χ_M values of the paramagnetic Cr(I) substances are reported as χ_{diam}. These corrections were obtained by adding contributions from the $[BF_4]^-$ (-39.0×10^{-6} cm^3 mol^{-1}) or $[SbF_6]^-$ (-80.0×10^{-6} cm^3 mol^{-1}) ions to either experimentally determined χ_M values for the corresponding diamagnetic, low-spin d^6 homoleptic chromium(0) complexes or χ_M values for the appropriate $[Cr(CNR)_6]$ units calculated from Pascal's constants[17].

Cyclic voltammetric (CV) experiments on 2×10^{-3} M solutions of selected compounds in CH_2Cl_2 were conducted at room temperature using an EPSILON (Bioanalytical Systems, INC., West Lafayette, IN) electrochemical workstation. The electrochemical cell was placed in an argon-filled Vacuum Atmospheres dry-box. Tetrabutylammonium hexafluorophosphate (0.1 M solution in CH_2Cl_2) was used as the supporting electrolyte. CV data was recorded at room temperature using a three-component system consisting of a platinum working electrode, platinum wire auxillary electrode, and a glass encased non-aqueous silver/silver chloride reference electrode with a scan rate of 100 mV/s. The reference Ag/Ag^+ electrode was monitored with the ferrocenium/ferrocene couple. IR compensation was achieved prior to each CV scan by measuring the uncompensated solution resistance followed by incremental compensation and circuit stability testing. Background CV scans of the electrolyte solution were recorded before adding the analytes. The half-wave potentials ($E_{1/2}$) were determined as

averages of the cathodic and anodic peak potentials of reversible couples and are referenced to an external ferrocene/ferrocenium couple.[18]

Electronic absorption (UV-Vis) spectra were recorded in CH_2Cl_2 at 24 °C using a CARY 100 spectrophotometer. Melting points are uncorrected and were determined for samples in capillary tubes sealed under argon. Elemental analyses were carried out by Columbia Analytical Services, Tucson, Arizona.

Compounds 2-amino-1,3-diethoxycarbonyl-2',6-biazulene,[15c] acetic formic anhydride,[19] bis(η^6-naphthalene)chromium(0),[20] 2-iodoazulene,[21] 2-amino-1,3-diethoxycarbonyl-6-azulenylacetylene,[22] 2-isocyano-1,3-diethoxycarbonylazulene,[23] and 2-isocyano-1,3-dimethylazulene[24] were prepared according to literature procedures. Other reagents were obtained from commercial sources and used as received.

III.3.2 Synthesis of 2-formamido-1,3-diethoxycarbonyl-2',6-biazulene (3.1).

This procedure was established by Erika Shoji and Shota Suzuki in the School of Pharmacy at Nihon University in Japan (Professor Motohashi's laboratory). 2-Amino-1,3-diethoxycarbonyl-2',6-biazulene (1.0563 g, 2.5547 mmol) in 10 mL of CH_2Cl_2 was added to an excess of neat acetic-formic anhydride. After the reaction mixture was stirred for 21 h at 40 °C, all volatiles were removed under vacuum. The resultant residue was dissolved in CH_2Cl_2, washed with water, brine, and dried over Na_2SO_4. Filtration followed by solvent removal afforded a dark brown solid, which was subjected to column chromatography on silica gel using CH_2Cl_2. The product was further purified through recrystallization from CH_2Cl_2 and hexanes to afford dark green microcrystals of **3.1** (0.6544 g, 1.482 mmol) in a 58% yield. Mp: 220-223 °C. HRMS (ES, positive *m/z*): calcd for $C_{27}H_{23}NO_5$, 441.1576; found, 441.1573. ^{1}H NMR (400

MHz, $CDCl_3$, 25 °C): δ 1.50 (t, 6H, CH_3, $^3J_{HH}$ = 7 Hz), 4.51 (q, 4H, CH_2, $^3J_{HH}$ = 7 Hz), 7.25 (t, 2H, $H^{5',7'}$, $^3J_{HH}$ = 10 Hz), 7.63 (t, 1H, $H^{6'}$, $^3J_{HH}$ = 10 Hz), 7.80 (s, 2H, $H^{1',3'}$), 8.39 (d, 2H, $H^{4',8'}$, $^3J_{HH}$ = 10 Hz), 8.40 (d, 2H, $H^{5,7}$, $^3J_{HH}$ = 11 Hz), 8.70 (s, 1H, C*H*O), 9.45 (d, 2H, $H^{4,8}$, $^3J_{HH}$ = 11 Hz), 10.29 (s, 1H, N*H*) ppm.

III.3.3 Synthesis of 2-isocyano-1,3-diethoxycarbonyl-2',6-biazulene (3.2).

Excess phosphorus oxychloride (0.42 mL, 4.5 mmol) was added to a solution of **3.1** (0.6544 g, 1.482 mmol) and diisopropylamine (1.90 mL, 13.34 mmol) in 50 mL of CH_2Cl_2. After stirring for 19 h, the reaction mixture was quenched by addition to 100 mL of 10% aqueous Na_2CO_3. The organic layer was separated, and the aqueous layer was extracted with 50 mL of CH_2Cl_2. The combined organic fractions were washed with water, brine, and dried over Na_2SO_4. The solvent was removed and the residue was subjected to column chromatography on silica gel using neat CH_2Cl_2. This product was further purified via recrystallization from CH_2Cl_2 and hexanes to afford dark green microcrystals of **3.2** (0.5493 g, 1.297 mmol) in an 88% yield following filtration and drying at 10^{-2} Torr for 2 h. Mp: 185-189 °C. Anal. Calcd for $C_{27}H_{21}NO_4$: C, 76.58; H, 5.00; N, 3.31. Found: C, 76.29; H, 5.61; N, 3.41. IR (CH_2Cl_2): ν_{CN} 2126; ν_{CO} 1691 cm^{-1}. ^1H NMR (400 MHz, CD_2Cl_2, 25 °C): δ 1.50 (t, 6H, CH_3, $^3J_{HH}$ = 7 Hz), 4.47 (q, 4H, CH_2, $^3J_{HH}$ = 7 Hz), 7.19 (t, 2H, $H^{5',7'}$, $^3J_{HH}$ = 10 Hz), 7.61 (t, 1H, $H^{6'}$, $^3J_{HH}$ = 10 Hz), 7.67 (s, 2H, $H^{1',3'}$), 8.30 (d, 2H, $H^{4',8'}$, $^3J_{HH}$ = 10 Hz), 8.32 (d, 2H, $H^{5,7}$, $^3J_{HH}$ = 11 Hz), 9.59 (d, 2H, $H^{4,8}$, $^3J_{HH}$ = 11 Hz) ppm. $^{13}C\{^1H\}$ NMR (125.8 MHz, CD_2Cl_2, 25 °C): δ 14.6 (*C*H_3), 61.3 (*C*H_2), 113.1, 117.0, 125.3, 130.8, 132.0, 139.4, 140.0, 140.1, 140.2, 141.9, 149.7, 151.1 (biazulenic motif *C*), 163.6 (*C*O), 177.8 (*C*N) ppm. ^{14}N NMR (36.2 MHz, CD_2Cl_2, 25 °C): 172.6 ppm. UV-vis (1,2-

dichloroethane, λ (log ε)): 433 (4.83), 367 (4.80), 330 (4.99), 253 (4.80) nm. χ_{diam} = -2.45 x 10^{-4} cm^3 mol^{-1}.

III.3.4 Synthesis of [Cr(3.2)$_6$] (3.3).

An orange-brown solution of **3.2** (0.2296 g, 0.5422 mmol) in 50 mL of THF was added to a brown solution of bis(η^6-naphthalene)chromium(0) (0.0278 g, 0.0902 mmol) in 30 mL of THF. After the reaction mixture was stirred for 17 h, the solution was concentrated. Et_2O (75 mL) was added to crash out the product and the slurry was then filtered through a medium-porosity frit. The black powder was washed with Et_2O (4 × 10 mL) until the washings were colorless and then with pentane (4 x 10 mL). Drying for 3 h at 10^{-2} Torr afforded black **3.3** (0.1976 g, 0.0762 mmol) in 85% yield. MP: No change up to 400 °C. Anal. Calcd for $C_{162}H_{84}O_{24}NCr$: C, 75.04; H, 4.90; N, 3.24. Found: C, 74.45; H, 5.79; N, 3.01. IR (CH_2Cl_2): ν_{CN} 1970 br cm^{-1}. ^{1}H NMR (500 MHz, CD_2Cl_2, 25 °C): δ 0.78 (s, 36H, C*H*$_3$), 4.06 (s, 24H, C*H*$_2$), 7.29 (t, 2H, $H^{5',7'}$, $^3J_{HH}$ = 10 Hz), 7.68 (m, 3H, $H^{1',3',6'}$), 8.45 (d, 2H, $H^{4',8'}$, $^3J_{HH}$ = 10 Hz), 9.15 (d, 2H, $H^{5,7}$, $^3J_{HH}$ = 11 Hz), 9.57 (d, 2H, $H^{4,8}$, $^3J_{HH}$ = 11 Hz) ppm. UV-vis (CH_2Cl_2, λ (log ε)): 913 (4.85), 424 (5.28), 357 (5.25), 336 (5.35), 327 (5.37), 250 (5.20) nm.

III.3.5 Synthesis of [Cr(3.2)$_6$][SbF$_6$] (3.4).

CH_2Cl_2 (60 mL) was added to a solid mixture of **3.3** (0.2389 g, 0.0921 mmol) and $AgSbF_6$ (0.0332 g, 0.097 mmol). The reaction mixture was allowed to stir for 3.5 h and then filtered through a 2 cm plug of Celite. The mixture was concentrated to a volume of 5 mL and heptane (100 mL) was then added. The slurry was filtered, washed with heptane (4 × 5 mL), and dried to give **3.4** (0.2176 g, 0.077 mmol) as a black powder in an 84% yield. This product can be further purified through recrystallization by layering a CH_2Cl_2 solution of **3.4** with pentane. MP:

the product decomposes at 284 °C without melting. Anal. Calcd for $C_{162}H_{84}O_{24}NCrF_6Sb$: C, 68.79; H, 4.49; N, 2.97. Found: C, 69.54; H, 5.15; N, 2.74. IR (CH_2Cl_2): ν_{CN} 2058 s, 1950 w; ν_{CO} 1692 cm^{-1}. ^1H NMR (500 MHz, CD_2Cl_2, 25 °C): δ 0.75 (s, 36H, CH_3), 4.05 (s, 24H, CH_2), 7.29 (t, 2H, $H^{5',7'}$, $^3J_{HH}$ = 10 Hz), 7.67 (m, 3H, $H^{1',3',6'}$), 8.45 (d, 2H, $H^{4',8'}$, $^3J_{HH}$ = 10 Hz), 9.22 (d, 2H, $H^{5,7}$, $^3J_{HH}$ = 11 Hz), 9.57 (d, 2H, $H^{4,8}$, $^3J_{HH}$ = 11 Hz) ppm. $^{13}C\{^1H\}$ NMR (125.8 MHz, CD_2Cl_2, 25 °C): δ 14.5 (*C*H_3), 60.4 (*C*H_2), 118.1, 125.5, 126.4, 130.5, 138.0, 139.1, 139.8, 142.0, 146.4, 147.2, 147.7, 149.6 (*biazulene motif*) ppm (Note: due to poor solubility, not all resonances such as CO or CN are observable). ^{14}N NMR (36.2 MHz, CD_2Cl_2, 25 °C): No resonance observed. μ_{eff} (21 °C): 2.43 μ_B. UV-vis (CH_2Cl_2, λ (log ε)): 864 (4.93), 722 (4.86), 520 (4.95), 422 (5.46), 363 (5.39), 337 (5.50), 326 (5.50), 250 (5.40) nm.

III.3.6 Synthesis of $(OC)_5Cr$(3.2) (3.5).

[$Cr(CO)_5$(THF)] was generated by photolysis of $Cr(CO)_6$ (0.0614 g, 0.2790 mmol) in 125 mL of THF using a Hanovia mercury immersion lamp. The resultant orange solution was added to a yellow-brown solution of **3.2** (0.1772 g, 0.4185 mmol) in 10 mL of THF. After stirring for 20 h, the reaction flask was opened to air and all solvent was removed under vacuum at room temperature. The residue was subjected to column chromatography on silica using neat CH_2Cl_2. The first red-orange band was collected, concentrated, and layered with pentane at -20 °C. Following diffusion, filtration and drying of the solid at 10^{-2} torr for 2 h provided dark red crystals of **3.5** (0.1074 g, 0.1745 mmol) in a 63% yield. MP: no melting at least up to 400 °C. IR (CH_2Cl_2): ν_{CN} 2139 m; ν_{CO} 2048 m, 1959 vs (trans- and cis-CO), 1691 (-CO_2Et) cm^{-1}. ^1H NMR (500 MHz, CD_2Cl_2, 25 °C): δ 1.51 (t, 6H, CH_3, $^3J_{HH}$ = 7 Hz), 4.56 (q, 4H, CH_2, $^3J_{HH}$ = 7 Hz), 7.23 (t, 2H, $H^{5',7'}$, $^3J_{HH}$ = 10 Hz), 7.65 (t, 1H, $H^{6'}$, $^3J_{HH}$ = 10 Hz), 7.75 (s, 2H, $H^{1',3'}$), 8.35 (d, 2H, $H^{4',8'}$, $^3J_{HH}$ = 10 Hz), 8.44 (d, 2H, $H^{5,7}$, $^3J_{HH}$ = 11 Hz), 9.71 (d, 2H, $H^{4,8}$, $^3J_{HH}$ = 11 Hz) ppm.

$^{13}C\{^1H\}$ NMR (125.8 MHz, CD_2Cl_2, 25 °C): δ 15.1 (*C*H_3), 61.3 (*C*H_2), 113.1, 117.0, 125.3, 131.5, 132.4, 139.3, 139.8, 139.9, 140.8, 142.0, 149.9, 150.9 (*biazulene motif*), 163.7 (*C*O_2Et), 182.5 (*C*N), 215.3 (*C*O *cis*), 217.6 (*C*O *trans*) ppm. UV-vis (CH_2Cl_2, λ (log ε)): 486 (4.66), 413 (4.49), 363 (4.60), 334 (4.72), 243 (4.89) nm.

III.3.7 Synthesis of 2-amino-1,3-diethoxycarbonyl-2',6-biazulenylacetylene (3.6).

Diisopropylamine (19.1 mL, 137 mmol) was added to a mixture of 2-amino-1,3-diethoxycarbonyl-6-azulenylacetylene (0.8919 g, 2.865 mmol), 2-iodoazulene (0.6930 g, 2.728 mmol), cuprous iodide (0.1038 g, 0.5450 mmol), triphenylphosphine (0.1431 g, 0.5456 mmol), and tetrakis(triphenylphosphine)palladium(0) (0.3154 g, 0.2729 mmol) in toluene (125 mL). The reaction mixture was stirred for 24 h and subsequently poured into 150 mL of a 10% aqueous ammonium chloride solution. After extraction of the aqueous phase with CH_2Cl_2 (2 × 25 mL), the organic fractions were combined, dried over Na_2SO_4, filtered, concentrated, and subjected to column chromatography on silica gel. Neat CH_2Cl_2 was first used to elute any remaining starting material followed by 10% ethyl acetate in CH_2Cl_2 to elute the product as a brown band. Solvent removal and drying at 10^{-2} Torr for 3 h provided **3.6** (1.0351 g, 2.3659 mmol) as a brown powder in an 87% yield. Mp: 161-164 °C. IR (CH_2Cl_2): ν_{CC} 2186; ν_{CO} 1676 cm^{-1}. ^1H NMR (400 MHz, $CDCl_3$, 25 °C): δ 1.51 (t, 6H, CH_3, $^3J_{HH}$ = 7 Hz), 4.50 (q, 4H, CH_2, $^3J_{HH}$ = 7 Hz), 7.23 (t, 2H, $H^{5',7'}$, $^3J_{HH}$ = 10 Hz), 7.52 (s, 2H, $H^{1',3'}$), 7.56 (t, 1H, $H^{6'}$, $^3J_{HH}$ = 10 Hz), 7.79 (d, 2H, $H^{5,7}$, ^{3}JHH = 11 Hz), 7.88 (s, 2H, NH_2), 8.26 (d, 2H, $H^{4',8'}$, $^3J_{HH}$ = 10 Hz), 8.99 (d, 2H, $H^{4,8}$, $^3J_{HH}$ = 11 Hz) ppm. $^{13}C\{^1H\}$ NMR (125.8 MHz, $CDCl_3$, 25 °C): δ 14.8 (*C*H_3), 60.2 (*C*H_2), 90.7, 99.5 (*C*≡*C*), 100.8, 121.0, 124.3, 128.0, 129.9, 135.4, 135.6, 137.0, 138.0, 140.5, 145.7, 162.8, 166.5 (biazulenic motif *C*) ppm.

III.3.8 Synthesis of 2-formamido-1,3-diethoxycarbonyl-2',6-biazulenylacetylene (3.7).

3.6 (0.5241 g, 1.198 mmol) dissolved in 15 mL of CH_2Cl_2 was added to a solution of freshly prepared acetic-formic anhydride (19.00 mL, 300 mmol) and the reaction mixture was stirred for 5.5 h at ambient atmosphere. All volatiles were removed under vacuum and the resultant residue was dissolved in a minimal amount of CH_2Cl_2 and then stirred with 100 mL of 10% aqueous $NaHCO_3$ to quench any remaining anhydride. After extraction of the aqueous phase with CH_2Cl_2 (3 × 20 mL), the organic fractions were combined and dried over anhydrous Na_2SO_4. The solution of filtered, all volatiles were removed on a rotary evaporator, and the resulting residue was subjected to column chromatography on silica gel using 10% ethyl acetate in CH_2Cl_2. A dark brown band was collected, which gave **3.7** (0.4437 g, 0.9532 mmol) as a brown powder in an 80% yield after solvent removal and drying at 10^{-2} Torr. Mp: 210-214 °C. IR (CH_2Cl_2): ν_{CC} 2189 cm^{-1}; ν_{CO} 1707 cm^{-1}. ^{1}H NMR (400 MHz, $CDCl_3$, 25 °C): δ 1.48 (t, 6H, CH_3, $^3J_{HH}$ = 7 Hz), 4.50 (q, 4H, CH_2, $^3J_{HH}$ = 7 Hz), 7.24 (t, 2H, $H^{5',7'}$, $^3J_{HH}$ = 10 Hz), 7.54 (s, 2H, $H^{1',3'}$), 7.62 (t, 1H, $H^{6'}$, $^3J_{HH}$ = 10 Hz), 7.96 (d, 2H, $H^{5,7}$, $^3J_{HH}$ = 11 Hz), 8.32 (d, 2H, $H^{4',8'}$, $^3J_{HH}$ = 10 Hz), 8.68 (s, 1H, C*H*O), 9.29 (d, 2H, $H^{4,8}$, $^3J_{HH}$ = 11 Hz), 10.32 (s, 1H, N*H*) ppm. ^{13}C{^{1}H} NMR (125.8 MHz, $CDCl_3$, 25 °C): δ 14.6 (*C*H_3), 61.1 (*C*H_2), 93.9, 98.7 (*C*≡*C*), 121.2, 124.6, 128.9, 134.3, 134.6, 136.9, 137.8, 138.6, 138.8, 140.5, 142.1, 165.6 (biazulenic motif *C*) ppm.

III.3.9 Synthesis of 2-isocyano-1,3-diethoxycarbonyl-2',6-biazulenylacetylene (3.8).

Excess phosphorous oxychloride (38.4 μL, 0.4120 mmol) was added to a solution of **3.7** (0.1745 g, 0.3749 mmol) and distilled diisopropylamine (1.31 mL, 9.40 mmol) in 50 mL of dry CH_2Cl_2 at room temperature. The reaction mixture was stirred for 2 h after the addition of $POCl_3$, then opened to air and quenched by addition to 100 mL of 10% aqueous $NaHCO_3$. The aqueous phase was extracted with CH_2Cl_2 (3 × 15 mL) and the organic fractions were combined,

dried over anhydrous Na_2SO_4, and filtered. Following solvent removal, the crude product was subjected to column chromatography on silica gel using 5% ethyl acetate in CH_2Cl_2. The first, dark brown band was collected and afforded forest green **3.8** (0.1478 g, 0.3303 mmol) in an 88% yield following solvent removal and drying at 10^{-2} Torr. Mp: no melting up to at least 400 °C. IR (CH_2Cl_2): ν_{CN} 2125; ν_{CC} 2188; ν_{CO} 1691 cm^{-1}. ^1H NMR (400 MHz, $CDCl_3$, 25 °C): δ 1.53 (t, 6H, CH_3, $^3J_{HH}$ = 7 Hz), 4.52 (q, 4H, CH_2, $^3J_{HH}$ = 7 Hz), 7.20 (t, 2H, $H^{5',7'}$, $^3J_{HH}$ = 10 Hz), 7.45 (s, 2H, $H^{1',3'}$), 7.61 (t, 1H, $H^{6'}$, $^3J_{HH}$ = 10 Hz), 7.95 (d, 2H, $H^{5,7}$, $^3J_{HH}$ = 11 Hz), 8.24 (d, 2H, $H^{4',8'}$, $^3J_{HH}$ = 10 Hz), 9.59 (d, 2H, $H^{4,8}$, $^3J_{HH}$ = 11 Hz) ppm. $^{13}C\{^1H\}$ NMR (125.8 MHz, $CDCl_3$, 25 °C): δ 14.6 (*C*H_3), 61.5 (*C*H_2), 96.6, 98.9 (*C*≡*C*), 113.8, 121.7, 125.1, 128.4, 131.3, 135.0, 138.6, 139.1, 139.6, 139.7, 140.8, 140.9 (biazulenic motif *C*), 163.6 (*C*O), 178.5 (*C*N) ppm. ^{14}N NMR (36.2 MHz, CD_2Cl_2, 25 °C): δ 172.8 ppm. UV-vis (CH_2Cl_2, λ (log ε)): 452 (4.84), 434 (4.76), 368 (4.37), 329 (4.80), 279 (4.43), 253 (4.62) nm.

III.3.10 Synthesis of [Cr(3.8)$_6$] (3.9).

A yellow-brown solution of **3.8** (0.2010 g, 0.4492 mmol) in 30 mL of THF was added to a brown solution of Cr(η^6-naphthalene)$_2$ (0.0230 g, 0.0746 mmol) in 20 mL of THF at room temperature. After the reaction mixture was stirred for 17 h, the solution was concentrated. Diethyl ether (125 mL) was added to crash out the product and the slurry was then filtered through a medium-porosity frit. The black filtercake was washed with Et_2O (4 × 10 mL) until the washings were colorless and then with pentane (3 × 10 mL). Drying for 3 h at 10^{-2} Torr afforded black **3.9** (0.1095 g, 0.0400 mmol) in a 54% yield. IR (CH_2Cl_2): ν_{CN} 1971 br; ν_{CO} 1684 cm^{-1}. ^1H NMR (400 MHz, CD_2Cl_2, 25 °C): δ 1.03 (t, 36H, CH_3, $^3J_{HH}$ = 7 Hz), 4.14 (s, 24H, CH_2, $^3J_{HH}$

= 7 Hz), 7.24 (t, 2H, $H^{5',7'}$, $^3J_{HH}$ = 10 Hz), 7.55 (s, 12H, $H^{1',3'}$), 7.61 (t, 6H, $H^{6'}$, $^3J_{HH}$ = 10 Hz), 7.85 (d, 12H, $H^{5,7}$, $^3J_{HH}$ = 11 Hz), 9.36 (d, 12H, $H^{4,8}$, $^3J_{HH}$ = 11 Hz) ppm.

III.3.11 Synthesis of [Cr(3.8)$_6$][SbF$_6$] (3.10).

Dichloromethane (50 mL) was added to a solid mixture of **3.9** (0.1341 g, 0.04900 mmol) and $AgSbF_6$ (0.0177 g, 0.0515 mmol). The reaction mixture was allowed to stir for 4 h at room temperature and then filtered through a 3 cm plug of Celite. All volatiles were removed under vacuum. The residue was dissolved in a minimum amount of CH_2Cl_2 and the resulting solution was layered with pentane to recrystallize the product. The precipitate was filtered, washed with pentane (3 × 5 mL), and dried under vacuum to afford **3.10** (0.1023 g, 0.03441 mmol) as dark microcrystals in a 70% yield. IR (CH_2Cl_2): ν_{CN} 2058 s, 1979 m; ν_{CO} 1693 cm^{-1}. ^{1}H NMR (400 MHz, CD_2Cl_2, 25 °C): δ 0.74 (s, 36H, CH_3), 4.01 (s, 24H, CH_2), 7.29 (t, 12H, $H^{5',7'}$, $^3J_{HH}$ = 10 Hz), 7.51 (s, 12H, $H^{1',3'}$), 7.66 (t, 6H, $H^{6'}$, $^3J_{HH}$ = 10 Hz), 8.36 (d, 12H, $H^{4',8'}$, $^3J_{HH}$ = 10 Hz), 8.82 (d, 12H, $H^{5,7}$, $^3J_{HH}$ = 11 Hz), 9.52 (d, 12H, $H^{4,8}$, $^3J_{HH}$ = 11 Hz) ppm.

III.3.12 Synthesis of [Cr(2-isocyano-1,3-diethoxycarbonylazulene)$_6$] (3.11).

Bis(η^6-naphthalene)chromium(0) (0.0547 g, 0.1774 mmol) and 2-isocyano-1,3-diethoxycarbonylazulene (0.3174 g, 1.068 mmol) were dissolved in 100 mL of THF. After the reaction mixture was stirred for 17 h, all volatiles were removed under vacuum. The residue was redissolved in a minimum amount of CH_2Cl_2 and the resulting solution was layered with pentane to recrystallize the product. Filtration followed by drying afforded dark blue microcrystals of **3.11** (0.2605 g, 0.1419 mmol) in an 80% yield. IR (CH_2Cl_2): ν_{CN} 1969; ν_{CO} 1681 cm^{-1}. ^{1}H NMR (500 MHz, CD_2Cl_2, 25 °C): δ 0.92 (t, 36H, CH_3, $^3J_{HH}$ = 7 Hz), 4.06 (q, 24H, CH_2, $^3J_{HH}$ = 7 Hz), 7.64 (t, 6H, H^6, $^3J_{HH}$ = 10 Hz), 7.71 (t, 12H, $H^{5,7}$, $^3J_{HH}$ = 10 Hz), 9.41 (d, 12H, $H^{4,8}$, $^3J_{HH}$ =

10 Hz) ppm. $^{13}C\{^{1}H\}$ NMR (125.8 MHz, CD_2Cl_2, 25 °C): δ 14.7 (CH_3), 60.6 (CH_2), 131.3, 137.1, 139.0, 139.1, 139.8, 141.0 (*azulene motif*), 162.3 (CO_2Et), 211.4 (*C*N) ppm. ^{14}N NMR (36.2 MHz, CD_2Cl_2, 25 °C): no resonance was observed. χ_{diam} = -8.38 x 10^{-4} cm^3 mol^{-1}.

III.3.13 Synthesis of [Cr(2-isocyano-1,3-diethoxycarbonylazulene)$_6$][SbF_6] (3.12).

CH_2Cl_2 (75 mL) was added to a solid mixture of **3.11** (0.1644 g, 0.08955 mmol) and $AgSbF_6$ (0.0323 g, 0.0940 mmol). The reaction mixture was allowed to stir for 3 h, filtered through a 3 cm plug of Celite, and then all volatiles were removed under vacuum. The residue was dissolved in a minimum amount of CH_2Cl_2 and the resulting solution was layered with pentane to recrystallize the product. The precipitate was filtered off and dried under vacuum to afford dark purple microcrystals of **3.12** (0.1322 g, 0.06382 mmol) in a 71% yield. IR (CH_2Cl_2): ν_{CN} 2059 s, 1977 w; ν_{CO} 1693 cm^{-1}. ^{1}H NMR (400 MHz, CD_2Cl_2, 25 °C): δ 0.64 (t, 36H, CH_3, $^{3}J_{HH}$ = 7 Hz), 3.92 (q, 24H, CH_2, $^{3}J_{HH}$ = 7 Hz), 7.04 (t, 6H, H^{6}, $^{3}J_{HH}$ = 10 Hz), 8.81 (t, 12H, $H^{5,7}$, $^{3}J_{HH}$ = 10 Hz), 8.92 (d, 12H, $H^{4,8}$, $^{3}J_{HH}$ = 10 Hz) ppm. $^{13}C\{^{1}H\}$ NMR (125.8 MHz, CD_2Cl_2, 25 °C): δ 14.7 (CH_3), 60.4 (CH_2), 124.9, 126.9, 137.1, 139.0, 147.2, 149.7, 153.3 (*azulene motif*), 218.5 (*C*N) ppm. ^{14}N NMR (36.2 MHz, CD_2Cl_2, 25 °C): no resonance was observed. μ_{eff} (21 °C): 2.55 μ_B.

III.3.14 Synthesis of [Cr(2-isocyano-1,3-dimethylazulene)$_6$] (3.13).

Bis(η^6-naphthalene)chromium(0) (0.0562 g, 0.1823 mmol) and 2-isocyano-1,3-dimethylazulene (1.0981 g, 0.542 mmol) were dissolved in 75 mL of THF and allowed to stir for 17 h. The solution was concentrated and pentane (75 mL) was added to crash out the product. After filtering the slurry through a medium-porosity frit, the collected purple powder was washed with pentane (3 × 10 mL) until the washings were colorless. Drying for 2.5 h at 10^{-2} Torr

afforded purple **3.13** (0.1581 g, 0.1388 mmol) in a 76% yield. IR (THF): ν_{CN} 1968 s sh, 1944 vs br cm^{-1}.

III.3.15 Synthesis of [Cr(2-isocyano-1,3-dimethylazulene)$_6$][SbF_6] (3.14).

CH_2Cl_2 (50 mL) was added to a solid mixture of **3.13** (0.1550 g, 0.1360 mmol) and $AgSbF_6$ (0.0491 g, 0.1429 mmol). The reaction mixture was allowed to stir for 15 h and then filtered through a 3 cm plug of Celite. All volatiles were removed under vacuum and the dark-colored powder was dried for 1 h. The product was recrystallized by layering a purple CH_2Cl_2 solution of **3.14** with pentane. The precipitated product was filtered off, washed with pentane (3 × 5 mL) and dried at 10^{-2} Torr to give dark purple microcrystals of **3.14** (0.1566 g, 0.1139 mmol) in an 84% yield. IR (CH_2Cl_2): ν_{CN} 2049 cm^{-1}. ^{1}H NMR (500 MHz, CD_2Cl_2, 25 °C): δ 1.50 (t, 1H, H^6, $^3J_{HH}$ = 10 Hz), 3.05 (d, 2H, $H^{4,8}$, $^3J_{HH}$ = 10 Hz), 9.65 (s, 6H, CH_3), 10.35 (t, 2H, $H^{5,7}$, $^3J_{HH}$ = 10 Hz) ppm. ^{14}N NMR (36.2 MHz, CD_2Cl_2, 25 °C): δ 895.41 ppm. μ_{eff} (21 °C): 1.90 μ_B. UV-vis (CH_2Cl_2, λ (log ε)): 588 (4.44), 526 (4.57), 457 (4.59), 342 (4.89), 298 (5.31), 239 (4.93) nm.

III.4 Results and Discussion

The synthesis of the first isocyano-2,6'-biazulene (Scheme III.1) begins with the formylation of the already known 2-amino-1,3-diethoxycarbonyl-2,6'-biazulene[15c]. This formylation to produce 2-formamido-1,3-diethoxycarbonyl-2',6-biazulene (**3.1**) was completed by our collaborators in the laboratory of Professor Shigeyasu Motohashi at Nihon University. Contrary to the procedure established for the formylation of other 2-aminoazulenes[12,25], the starting amine is treated only with excess acetic-formic anhydride instead of a combination of acetic-formic anhydride and excess formic acid. The presence of excess formic acid appears to be destructive to the 2',6-biazulenic motif. Compound **3.1** can be isolated in a 58% yield as dark green microcrystals following purification of the crude product via column chromatography and subsequent recrystallization from CH_2Cl_2/hexanes. As is the case of other 2-formamidoazulenes featuring diethoxycarbonyl (referred to as diester from hereon) substituents at the 1- and 3-carbon atoms, only the *trans* rotamer was observed in the ^1H NMR spectrum of the product in $CDCl_3$.[25] The two-dimensional NMR technique COSY was used to unambiguously assign ^1H resonances for **3.1,** as was done for all other biazulenic compounds discussed in this Chapter.

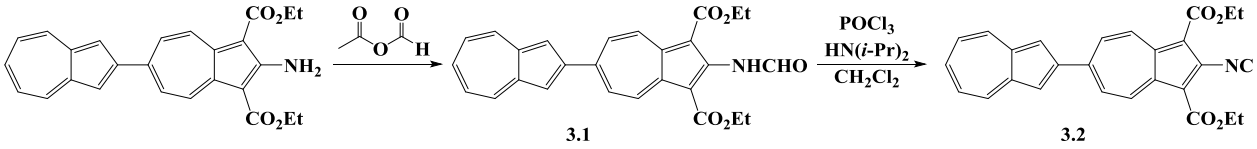

Scheme III.1

The dehydration of formamide **3.1** (Scheme III.1) with phosphorous oxychloride in the presence of diisopropylamine in CH_2Cl_2 yields 2-isocyano-1,3-diester-2',6-biazulene (**3.2**). Following purification via column chromatography and recrystallization from CH_2Cl_2/hexanes, **3.2** is isolated in an 88% yield as dark green microcrystals. The assignments of the proton

resonances are shown in Figure III.5 and were determined through two-dimensional (COSY) NMR. Unambiguous and complete assignments of all ^{1}H NMR resonances for **3.2** are important for the analysis of unpaired electron spin delocalization in paramagnetic complexes of this isocyanobiazulene ligand (*vide infra*). In CD_2Cl_2, the ^{13}C NMR resonance for the isocyanide carbon atom is found at 177.8 ppm whereas the ^{14}N NMR resonance for the nitrogen atom is at 172.6 ppm. These values are typical for ^{13}C and ^{14}N NMR shifts for the isocyanide group in 2-isocyanoazulene derivatives.[12] The presence of the isocyano group in **3.2** , however, was best confirmed by the ν_{CN} band at 2126 cm^{-1} in the FTIR spectrum of **3.2** in CH_2Cl_2

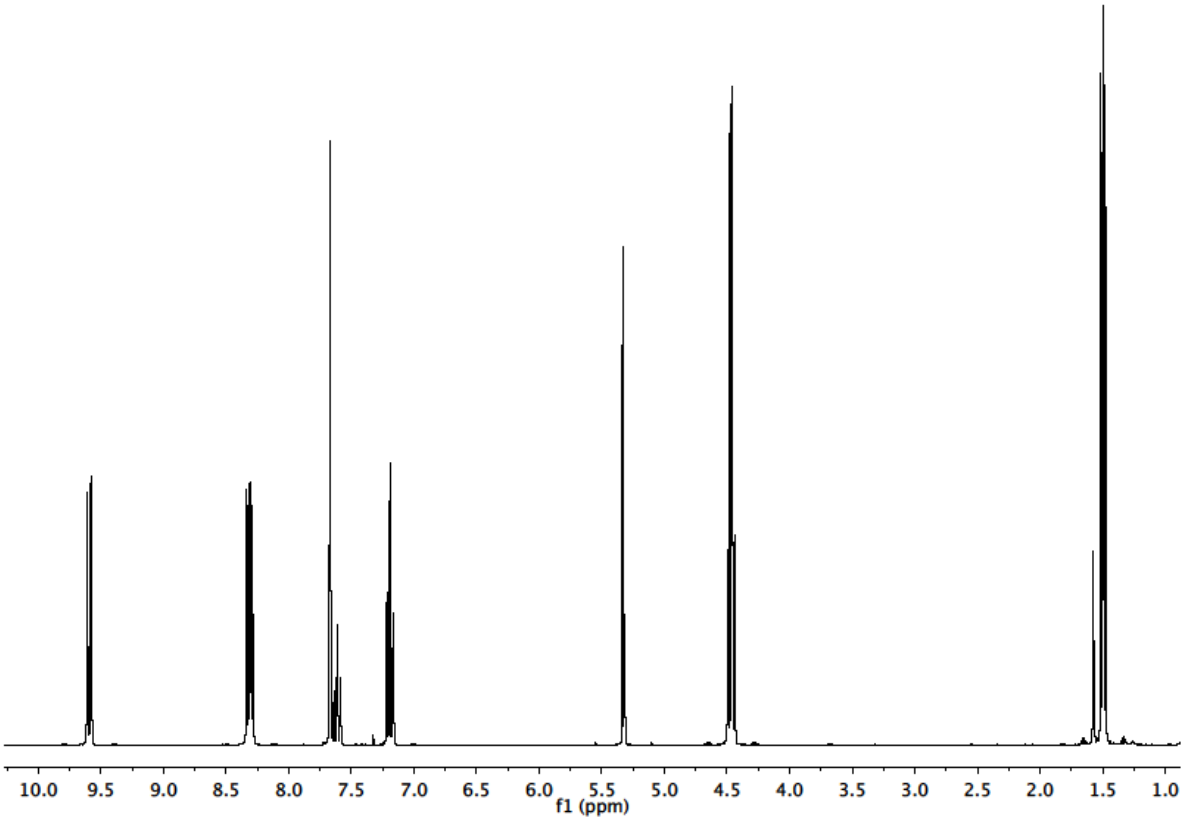

Figure III.5 The ^{1}H NMR spectrum of **3.2** in CD_2Cl_2.

The electronic absorption spectrum of **3.2** in dichloroethane (Figure III.6) shows four absorption bands, where the $S_0 \rightarrow S_1$ (presumably, HOMO→LUMO) transition occurs at 433

nm. This energy is higher than that documented for the $S_0 \rightarrow S_1$ excitation of symmetric biazulene derivatives 2,2'-diisocyano-1,1',3,3'-tetraester-6,6'-biazulene (**3.2b**)[16] and 2,2'-diisocyano-1,1',3,3'-tetraester-6,6'-biazulenylacetylene (**3.2c**)[22] shown in Figure III.7.

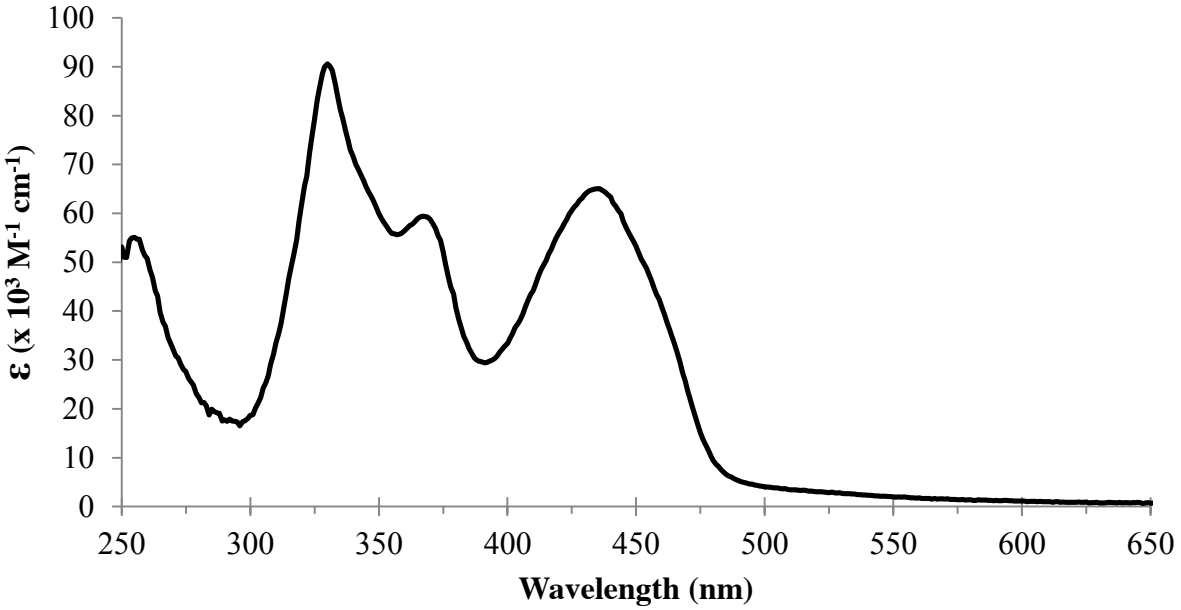

Figure III.6 Electronic absorption spectrum of **3.2** in dichloroethane.

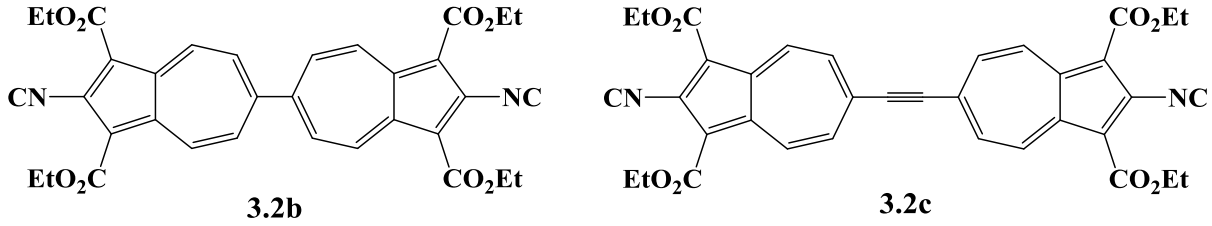

Figure III.7 Molecular structures of symmetric, diisocyanide-substituted biazulenes.

The larger HOMO-LUMO gap of **3.2** relative to those of **3.2b,c** is also suggested by the $E_{½}$ potentials corresponding to the reduction of these compounds, as determined from cyclic voltammetry (Figure III.8, Table III.3). The more negative potentials observed for the reduction of **3.2** relative to **3.2b,c** corroborate the results of the electronic absorption studies. The reduction waves in **3.2** and **3.2c** correspond to two sequential, one-electron redox processes

where as the one reduction wave in **3.2b** corresponds to a two-electron reduction. The observed reversibility ($i_c/i_a \approx 1$) in **3.2**, **3.2b**, and **3.2c** is unique to biazulenes and not seen in monoazulenes. Notably, a monoazulene analogue of **3.2** (i.e., 2-isocyanoazulene) exhibits no reversible reduction or oxidation with the reduction potential of -1.86 V and the oxidation potential of 0.92 V.[12] The stability of the reduced biazulenes is due to the resultant closed-shell configuration for the dianions not obtainable for a monoazulene.[16]

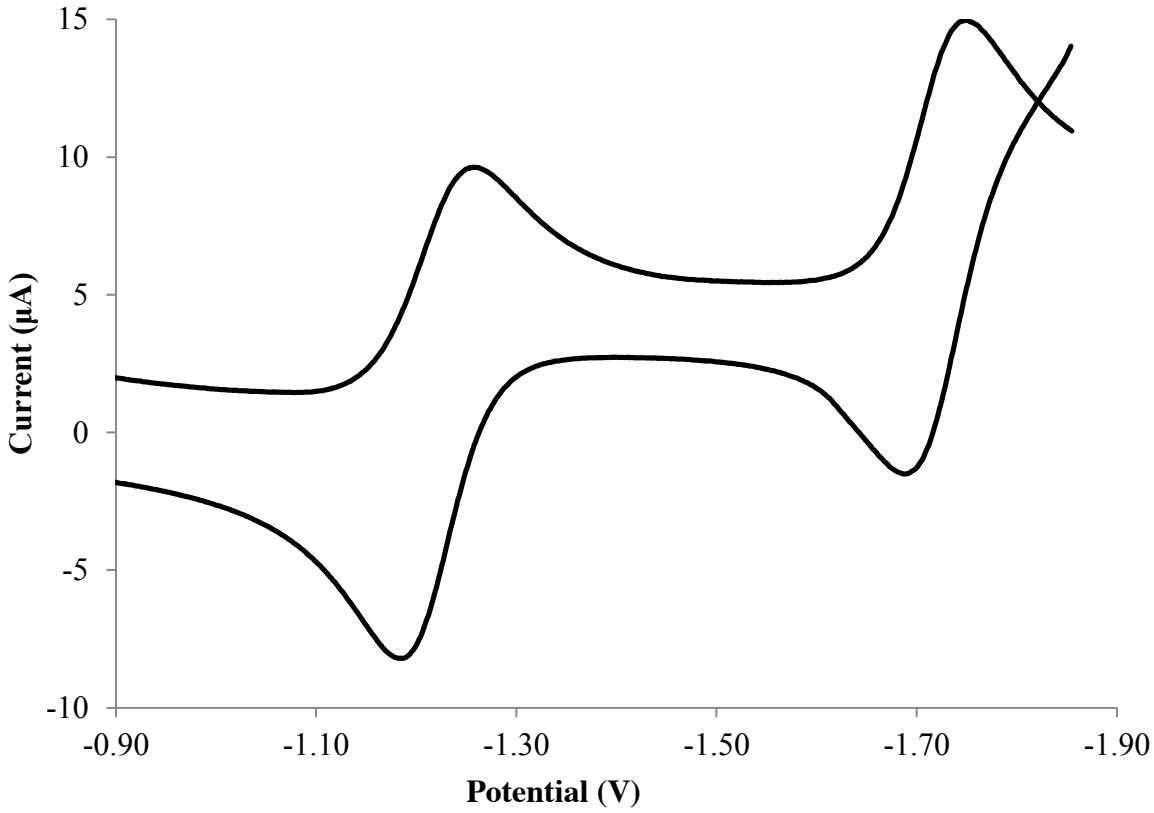

Figure III.8 Cyclic voltammogram of **3.2** in CH_2Cl_2 versus ferrocene/ferrocenium.

Table III.3 A comparison of half-wave ($E_{1/2}$) potentials of asymmetric and symmetric biazulenes.

Compound	$E_{½,\,1}$ (V)	$E_{½,\,2}$ (V)	$\Delta E_{½}$ (V)
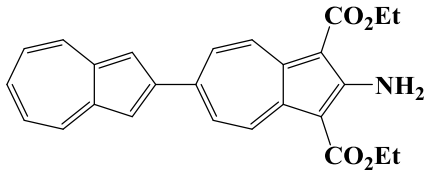	-1.66	-1.98	0.32
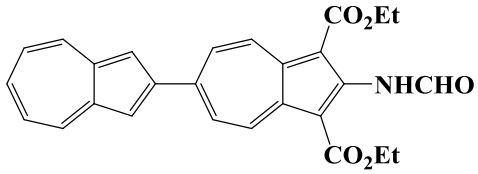 **3.1**	-1.45	-1.82	0.37
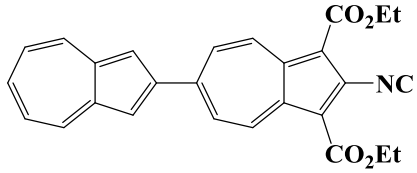 **3.2**	-1.22	-1.72	0.50
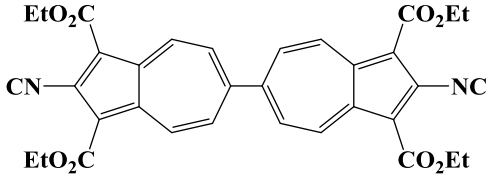 **3.2b**	-1.02	-	-
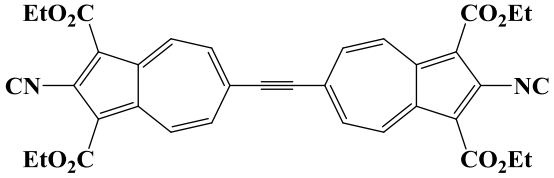 **3.2c**	-0.98	-1.06	0.08

As can also be seen in Table III.3, the redox potentials of 2-amino-1,3-diester-2',6-biazulene, **3.1**, and **3.2** become more positive when progressing from the electron-donating amino substituent to the electron-withdrawing substituent group. This is in line with the tunability of the HOMO-LUMO gap of azulene due to the complementary nature of the electron distribution within the frontier molecular orbitals.[10] The change in substituent from electron-donating to electron-withdrawing causes a decrease in the energy of the LUMO such that the

addition of an electron during reduction becomes more facile and occurs at a more positive potential.

The reaction of six equivalents of **3.2** with one equivalent of bis(η^6-naphthalene)chromium(0) in THF provided the diamagnetic, homoleptic chromium(0) complex **3.3** shown in Scheme III.2. Precipitation of the product from the reaction mixture with excess pentane followed by filtration and washing with diethyl ether provided **3.3** as a black powder in 85% yield. FT-IR analysis in CH_2Cl_2 revealed a band at 1969 cm^{-1}, which was assigned as the CN stretching frequency and is in line with other isocyanide complexes of chromium(0). For example, the homoleptic complexes $Cr(CNPh)_6$ (Ph = phenyl)[26] and $Cr(CNFc)_6$ (Fc = ferrocenyl)[27] exhibit bands attributed to isocyanide stretching at 1950 cm^{-1} and 1971 cm^{-1}, respectively (Table III.4). This large decrease in the stretching frequency of **3.3** relative to uncomplexed **3.2** signifies a large extent of π-backbonding from the electron-rich metal center into the π^* orbitals of the isocyanide junction group. The sharp hydrogen resonances in the ^1H NMR spectrum of **3.3** are located between 1-10 ppm, indicative of a diamagnetic complex. The hydrogen resonances corresponding to the 1,3-diester substituents, while not greatly shifted, appear as broad singlets instead of the expected quartet ($-CO_2CH_2CH_3$) and triplet ($-CO_2CH_2CH_3$) as observed in the free ligand. This result suggests hindered mobility of the 1,3-diester substituents due to steric crowding at the metal center.

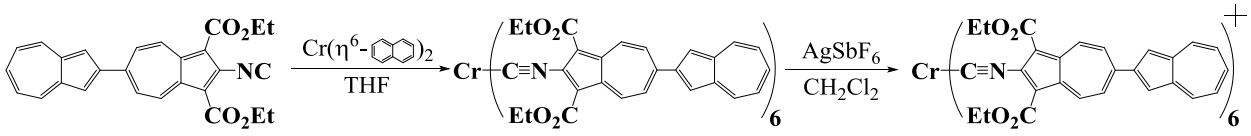

ν_{CN} = 2126 cm^{-1} — **3.2**

ν_{CN} = 1970 cm^{-1} — **3.3**

ν_{CN} = 2058 cm^{-1} — **3.4**

Scheme III.2

Table III.4 Isocyanide stretching frequencies (ν_{CN}) in free **3.2**, CNPh, and CNFc as well as in $Cr(Ar)_6^{0/+}$ (Ar = **3.2**, CNPh, CNFc) complexes.

Compound	ν_{CN} (cm^{-1})	Reference
3.2	2126	-
3.3	1970	-
3.4	2058	-
$Cr(CNPh)_6$	1950	28
$Cr(CNPh)_6^+$	2056	26
CNFc	2122	27
$Cr(CNFc)_6$	1971	27
$Cr(CNFc)_6^+$	2053	27

The subsequent one-electron oxidation of **3.3** with $AgSbF_6$ in CH_2Cl_2 afforded the low-spin, d^5 chromium(I) complex **3.4** (Scheme III.2) as a black powder in 84% yield. Recrystallization of this powder in CH_2Cl_2/pentane provided dark microcrystals of **3.4**. Multiple attempts to grow crystals suitable for X-ray diffraction studies were unsuccessful. While pure microcrystals do indeed grow, all batches provided long, but thin, needles. The isocyanide stretching frequency of **3.4** is observed at 2058 cm^{-1} in CH_2Cl_2. While still lower in energy than the stretching frequency found for **3.2** (ν_{CN} = 2126 cm^{-1}) due to the isocyanide participating in π-backbonding, this stretching frequency is 89 cm^{-1} higher in energy than exhibited by **3.3**. The oxidation from Cr(0) in **3.3** to Cr(I) in **3.4** decreases the amount of electron density present on the metal center and, thus, strengthens the CN bond by reducing the extent of π-backdonation. The isocyanide stretching frequency seen in **3.4** is in line with other homoleptic isocyanide complexes of chromium(I). For example, the homoleptic complexes $Cr(CNPh)_6^+$ (Ph = phenyl)[26]

and $Cr(CNFc)_6^+$ (Fc = ferrocenyl)[27] exhibit bands attributed to isocyanide stretching at 2056 cm^{-1} and 2053 cm^{-1}, respectively (Table III.4).

Electronic absorption studies of **3.2** and the chromium(0/I) complexes thereof in CH_2Cl_2 revealed interesting spectra (Figure III.9). Compound **3.2** absorbs in the blue region of the UV-visible region (λ_{max} ~ 250 - 450 nm) with molar absorptivities approaching 1 x 10^5 M^{-1} cm^{-1}. Compound **3.3** exhibits broad absorption in the UV, visible, and near IR regions with a lowest energy MLCT transition at 913 nm. The molar absorptivities corresponding to azulene($\pi \rightarrow \pi^*$) transitions in **3.3** increase with respect to **3.2**. Compound **3.4** displays absorption bands with similar molar absorptivities and in the same regions as **3.3**. The lowest energy transition of **3.4** shifted hypsochromically to 864 nm.

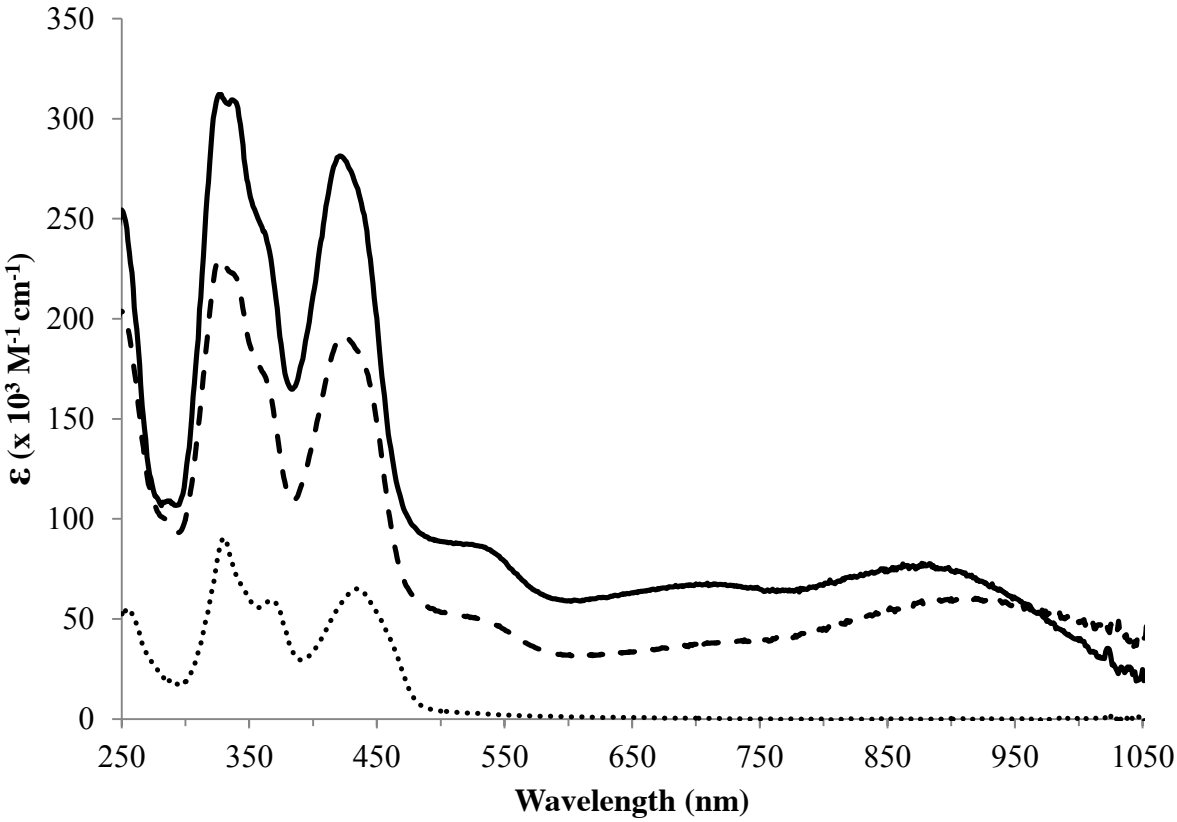

Figure III.9 Electronic absorption spectra of **3.2** (dotted line), **3.3** (dashed line), and **3.4** (solid line) in CH_2Cl_2.

Electrochemical analysis of **3.4** via cyclic voltammetry revealed two partially reversible $E_{½}$ potentials at -0.29 V and -0.63 V (vs. the ferrocene/ferrocenium couple) belonging to the $Cr^{+/2+}$ and $Cr^{0/+}$ redox processes, respectively. The relative potentials of these metal-based redox processes represent the σ-donating/π-accepting ratios of the complex ligands themselves. As shown by Barybin *et al*.[1,12], a more negative reduction potential indicates an increased σ-donor/π-acceptor ratio such that the ligand is a better electron-donating framework. Conversely, a more positive redox potential indicates a decreased σ-donor/π-acceptor (or increased π-acceptor/σ-donor) ratio such that the ligand is more capable of accepting, and presumably delocalizing, electron density. Relative to Cr(2-isocyanoazulene)$_6^+$ [12] and Cr(2-isocyano-1,3-diesterazulene)$_6^+$ [29], **3.4** presents with similar $E_{½}$ values for the $Cr^{0/+}$ and $Cr^{+/2+}$ redox processes (Table III.5). Cr(2-isocyano-1,3-diesterazulene)$_6^+$ can be regarded as the monoazulene congener of **3.4**. The similar values of these metal-based redox processes, especially the $Cr^{0/+}$ process, suggest the 1,3-substituents do not affect the π-accepting/σ-donating ratio of a given ligand. While this seems unintuitive, this observation is logical based on the complementary nature of the frontier molecular orbitals of azulene. During reduction, the 2-isocyanoazulene (or any even-carbon, isocyanide-substituted azulene) accepts an electron into the LUMO via the isocyanide junction group. Due to the lack of electron density at the 1,3-carbon atoms of azulene in the LUMO, a 1,3-substitution should not affect the energy of this orbital and, therefore, cannot affect the π-acceptor/σ-donor.

Table III.5 Half-wave ($E_{½}$) potentials of selected $Cr^{z/z+1}$ (z = 0, 1) redox processes.

Compound	$E_{½}$ {$Cr^{0/+}$} (V)	$E_{½}$ {$Cr^{+/2+}$} (V)	Reference
3.4	-0.63	-0.29	-
Cr(2-isocyano-1,3-diesterazulene)$_6^+$	-0.67	-0.14	29
Cr(2-isocyanoazulene)$_6^+$	-0.69	-0.16	12

Interestingly, the ^{1}H NMR spectrum (Figure III.10) of **3.4** in CD_2Cl_2 features sharp resonances resembling a diamagnetic complex, despite the fact that this complex is paramagnetic. That is, the proton resonances fall in the 0-10 ppm range without following predicted shifts according to the atomic exchange coupling mechanism (Table III.6). Opposed to other paramagnetic, homoleptic chromium(I) complexes – e.g., $Cr(CN^{1}Az)_6^{+}$ (Figure I.18) or $Cr(CN^{2}Az)_6^{+}$ [12] – the proton resonances of **3.4** are not shifted as would be expected if unpaired electron spin density was being delocalized through the π-system of the biazulenic moieties. In fact, the ^{1}H NMR spectra of the paramagnetic, Cr(I) complex **3.4** is similar to its diamagnetic, Cr(0) precursor **3.3**. A ^{14}N NMR experiment revealed no signal even though the ^{14}N resonance is expected in the 800-900 ppm range as seen in other homoleptic Cr(I) complexes of azulene. For instance, the ^{14}N resonances of $Cr(CN^{1}Az)_6^{+}$ and $Cr(CN^{2}Az)_6^{+}$ in CD_2Cl_2 are found at 813.5 and 859.6 ppm.[12]

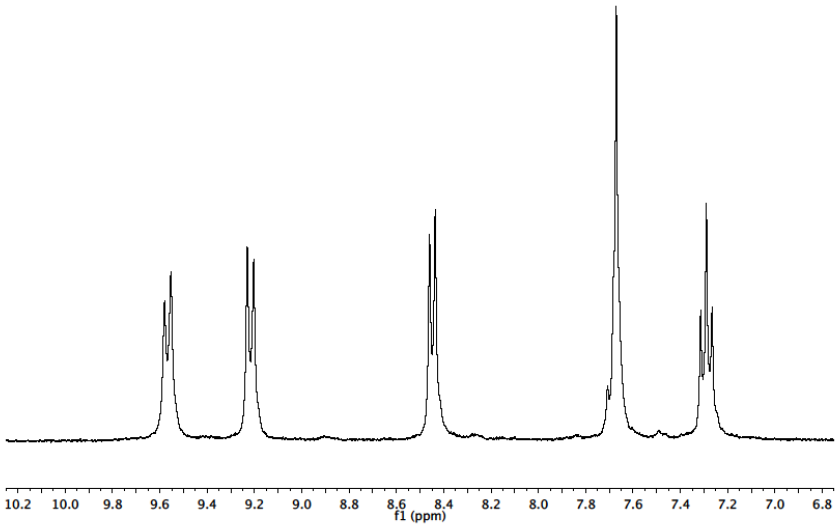

Figure III.10 The diamagnetic-like ^{1}H NMR spectrum of paramagnetic **3.4** in CD_2Cl_2 (Focused on aromatic region).

Table III.6 NMR data reflecting paramagnetic shifts (δ_{para}) of ^{1}H resonances in **3.4** vs. diamagnetic shifts (δ_{diam}) of uncomplexed **3.2**.

Resonating nucleus	δ_{para} (ppm)	δ_{diam} (ppm)	$\Delta\delta_{Observed}$ ($\Delta\delta_{Expected}$)[a]
4,8-H	9.57	9.59	- (-)
5,7-H	9.22	8.32	+ (+)
$CO_2C\underline{H}_2CH_3$	4.05	4.47	- (+)
$CO_2CH_2C\underline{H}_3$	0.75	1.50	- (-)
1',3'-H	7.67	7.67	0 (-)
4',8'-H	8.45	8.30	+ (-)
5',7'-H	9.22	7.19	+ (+)
6'-H	7.67	7.61	+ (-)

[a] The + and – denote downfield and upfield shifts, respectively.

Electron paramagnetic resonance (EPR) experiments of **3.4** in CH_2Cl_2 at 5 K revealed one narrow feature with an observed g-value of 2.080 (Figure III.11). This symmetrical, isotropic feature is characteristic of a complex with local octahedral symmetry. An octahedral geometry is supported by the IR, which shows one band attributed to CN stretching, and NMR, which shows one ligand environment, spectroscopies. One isotropic, narrow feature suggests the unpaired electron spin is metal-centered and is not delocalized through the π-system of the biazulene ligands. If the unpaired electron was delocalized over the ligands and not metal-centered, the EPR spectra would expectedly contain hyperfine-coupling, possibly presented as a broader signal in the solid-state, due to interactions with nuclei possessing angular momentum ($I > 0$) such as the nitrogen atoms of the isocyanide junction groups, $I(^{14}N) = 1$, or the hydrogen atoms of the ligands, $I(^1H) = ½$.

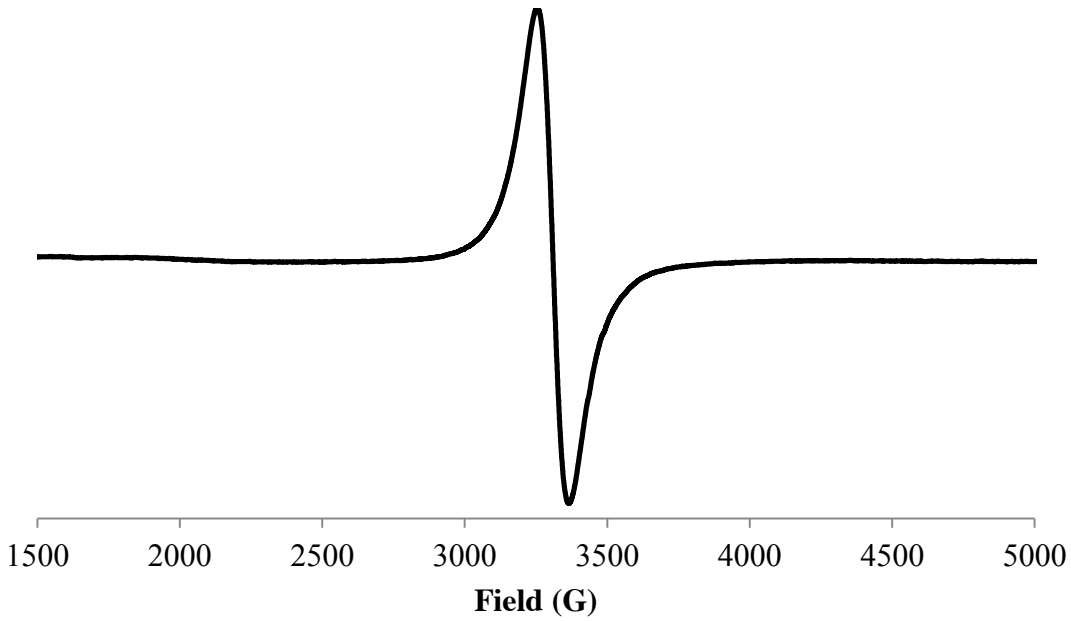

Figure III.11 EPR spectrum of **3.4** in CH_2Cl_2 at 5 K featuring a symmetric, isotropic signal.

A metal-centered unpaired electron can further be corroborated by solid-state magnetic susceptibility measurements. The theoretical, spin-only (i.e., in the absence of spin-orbit coupling) effective magnetic moment of a low-spin, d^5 complex (S = ½) is 1.73 μ_B. The experimental solid-state effective magnetic moment of **3.4** was determined to be 2.43 μ_B at 21 °C. Other examples of homoleptic Cr(I) complexes of azulene, in which there is delocalized unpaired electron spin, exhibit the expected spin-only effective magnetic moments and range from 1.71 – 2.07 μ_B.[12] Noteworthy, $Cr(CN^2Az)_6^+$ exhibits the exact predicted spin-only effective magnetic moment of 1.73 μ_B. The large deviation in **3.4** implies extensive spin-orbit coupling of the unpaired electron at the metal center as spin-orbit coupling is expected to be effectively quenched through π-backbonding during delocalization.[17b] Therefore, the unpaired electron cannot be delocalized and must be metal-centered. Indeed, a paramagnetic, Cr(I) complex

containing a single, unpaired *d*-electron in an octahedral ligand field is predicted to have a magnetic moment of approximately 2.7 μB when spin-orbit coupling is taken into account.[30]

In an attempt to obtain structural data of the first asymmetric 2',6-biazulene, **3.2** was complexed with $Cr(CO)_5(THF)$ following a photolysis of $Cr(CO)_6$ in THF. Subjecting the crude product to column chromatography and recrystallization from CH_2Cl_2/pentane afforded $Cr(CO)_5$(2-isocyano-1,3-diester-2',6-biazulene) (**3.5**) as dark red microcrystals in 63% yield. Unfortunately, multiple attempts to grow X-ray diffraction quality crystals were unsuccessful, affording only small, long needles. IR analysis of **3.5** in CH_2Cl_2 revealed one stretching frequency attributed to the complexed isocyanide junction group (ν_{CN} = 2139 cm^{-1}) and two stretching frequencies corresponding to the *trans*- and *cis*-carbonyls at 2048 and 1959 cm^{-1}, respectively. The third expected IR-active band for the carbonyls in this C_{4v} symmetric motif coincidently overlaps with the band at 1959 cm^{-1} as is observed elsewhere[31]. Although this complex contains an electron-rich Cr(0) metal center, the isocyanide stretching frequency shifted to higher energy relative to **3.2** indicates that the isocyanide acts as a σ-donor while the carbonyls dominantly participate in π-backbonding. The electronic absorption spectrum of **3.5** in CH_2Cl_2 shown in Figure III.12 exhibits five bands with molar absorptivities ranging from approximately 4.50 x 10^4 - 7.75 x 10^4 M^{-1} cm^{-1}.

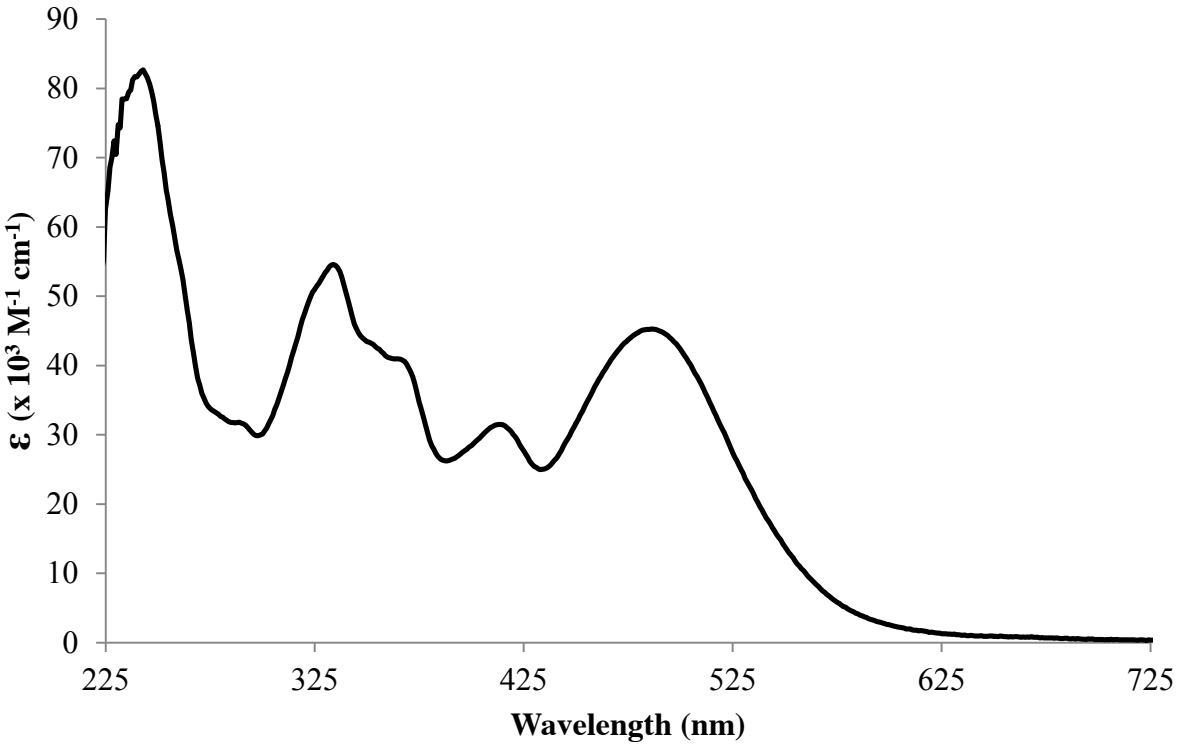

Figure III.12 Electronic absorption spectrum of **3.5** in CH_2Cl_2.

From the above experiments relating to **3.4**, it seems that compound **3.2** was unable to effectively delocalize unpaired electron density. Multiple experiments of **3.4** resulted in 1) diamagnetic-like shifts in the ^{1}H NMR spectrum, 2) lack of resonance in the ^{14}N NMR spectrum, 3) a narrow and symmetrical feature in the EPR spectrum, and 4) a large deviation from the expected spin-only effective magnetic moment.

In order to increase delocalization within the 2',6-biazulenic framework, an acetylene "spacer" group was chosen to be installed between the 6- and 2'-carbon atoms to remove steric interactions between the 5,7-hydrogen atoms of the seven-membered and the 1',3'-hydrogen atoms of the five-membered ring. This acetylene spacer group forces the two azulenic moieties to become co-planar, thereby aligning the π-systems of the two azulenes and increasing π-conjugation. The synthesis of 2-amino-1,3-diester-2',6-biazulenylacetylene (**3.6**), shown in

Scheme III.3, is achieved from the Sonogashira cross-coupling reaction of 2-iodoazulene[21] and 2-amino-1,3-diester-6-azulenylacetylene[22] in 87% yield. The presence of the acetylene spacer in **3.6** is confirmed by IR (ν_{CC}, in CH_2Cl_2 = 2186 cm^{-1}) and ^{13}C NMR (δ, in $CDCl_3$ = 90.7, 99.5 ppm) analyses. The formylation of **3.6** with excess acetic-formic anhydride yields 2-formamido-1,3-diester-2',6-biazulenylacetylene (**3.7**) in 80% yield. As seen in **3.1**, the ^1H NMR spectrum of **3.7** in $CDCl_3$ exhibits only one set of resonances corresponding to the *trans*-rotamer of the NHCHO unit.

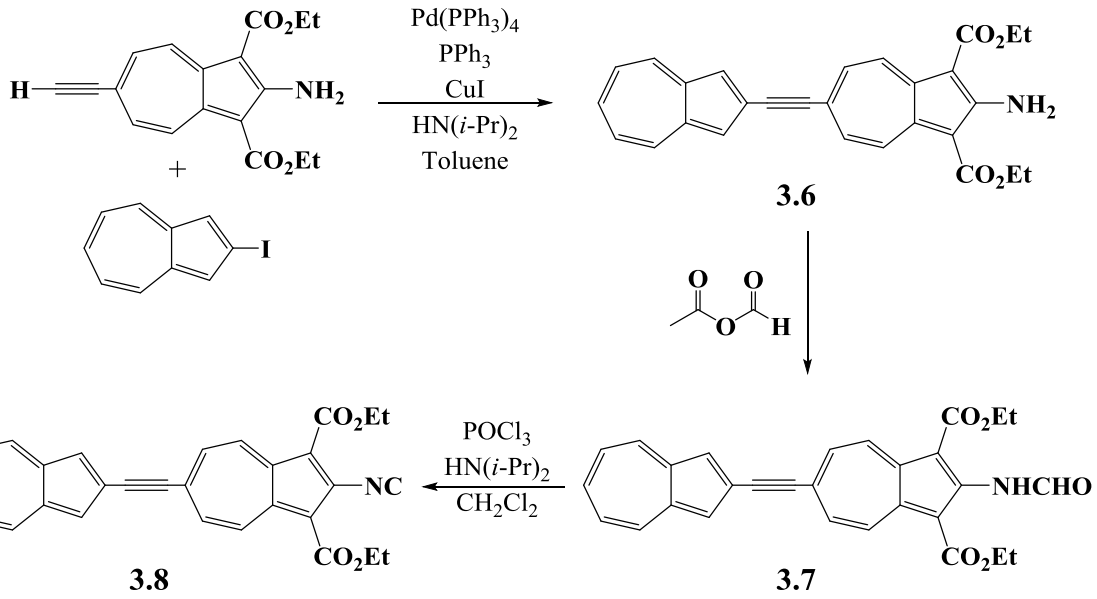

Scheme III.3

The compound 2-isocyano-1,3-diester-2',6-biazulenylacetylene (**3.8**), which is the acetylene-containing analog of **3.2** and the asymmetric analog of **3.2c**, is obtained following dehydration of **3.7** with phosphorous oxychloride. Purification via column chromatography yields **3.8** as a forest green powder in 88% yield. IR analysis of **3.8** in CH_2Cl_2 reveals isocyanide and alkyne stretching frequencies at 2125 and 2188 cm^{-1}, respectively (Figure III.13). The ^{13}C NMR spectrum confirm the presence of the alkyne (δ, in $CDCl_3$ = 96.6, 98.9 ppm). Similar to **3.2**, the ^{14}N resonance of the isocyanide nitrogen atom and the ^{13}C resonance of the isocyanide

carbon atom in **3.8** are observed at 172.8 ppm (in CD_2Cl_2) and 178.5 ppm (in $CDCl_3$), respectively.

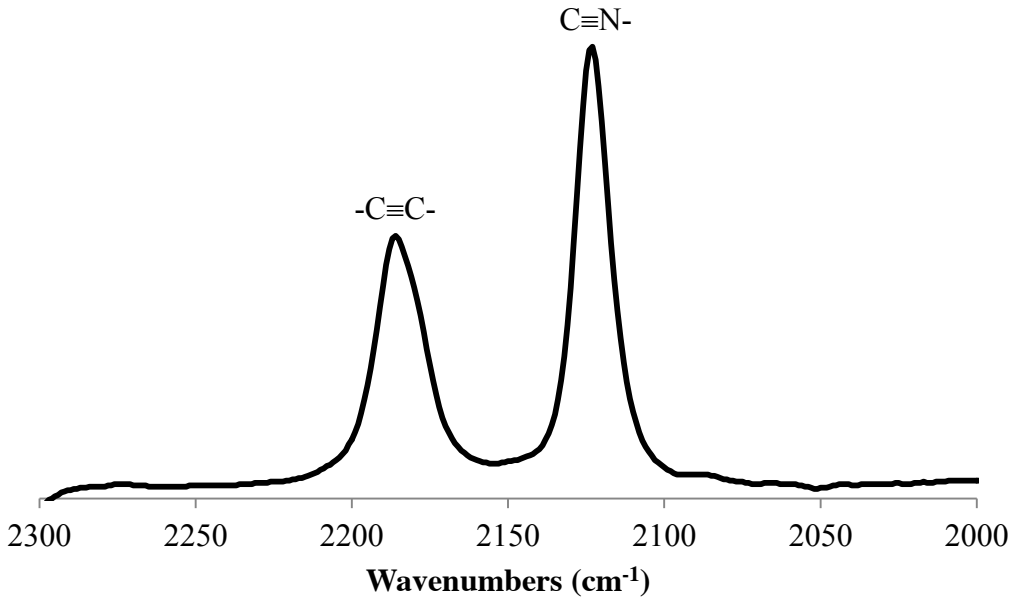

Figure III.13 FT-IR spectrum of **3.8** in CH_2Cl_2.

Indeed, the insertion of an acetylene spacer between the two azulenic moieties does increase π-conjugation across the biazulenic framework as noted by the electronic absorption spectrum of **3.8** in CH_2Cl_2 (Figure III.14). The $S_0 \rightarrow S_1$ transition (presumably corresponding to the HOMO-LUMO transition) in **3.8** occurs at lower energy (452 nm, $\varepsilon = 6.92 \times 10^4$ M^{-1} cm^{-1}) than that in **3.2** (433 nm, $\varepsilon = 6.52 \times 10^4$ M^{-1} cm^{-1}). The cyclic voltammogram of **3.8** shows two, one-electron redox processes (Figure III.15), which is similar to **3.2** (Figure III.8). The $E_{½}$ potentials of **3.8**, however, are at more positive potentials (-1.20 and -1.66 V vs. ferrocene/ferrocenium) implying a more easily reduced species relative to **3.2**. This correlates well with the electronic absorption spectrum that shows a more π-conjugated and, thus, lower LUMO energy.

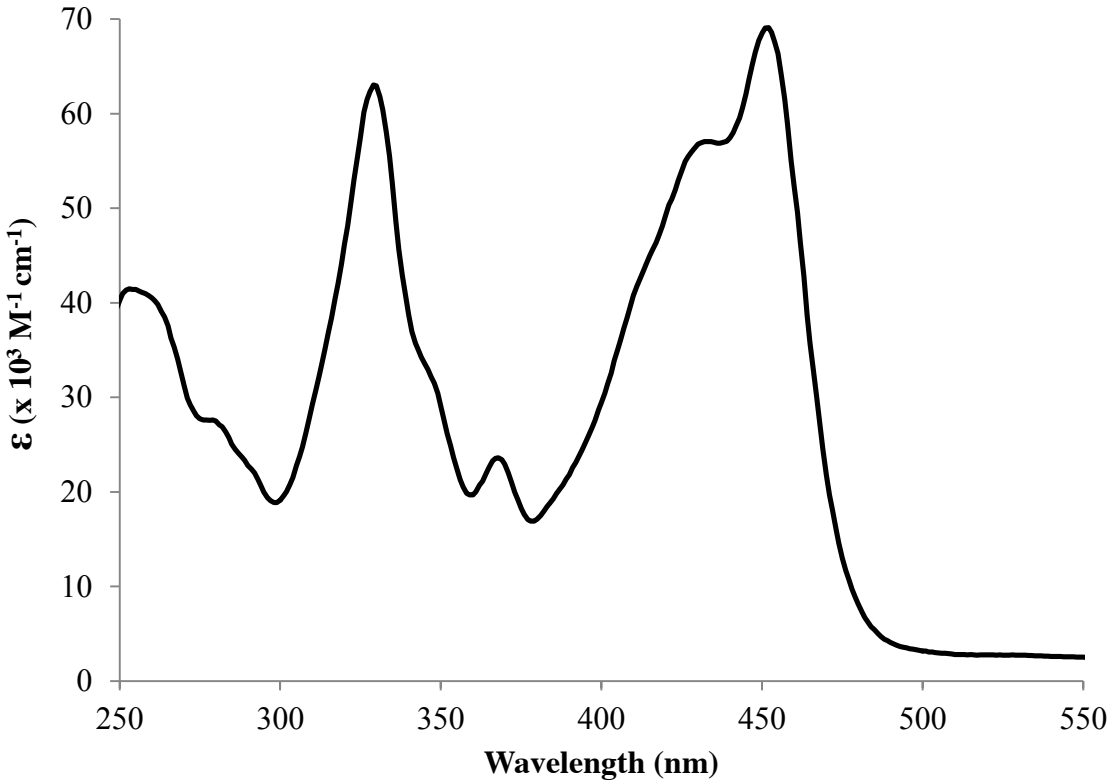

Figure III.14 Electronic absorption spectrum of **3.8** in CH_2Cl_2.

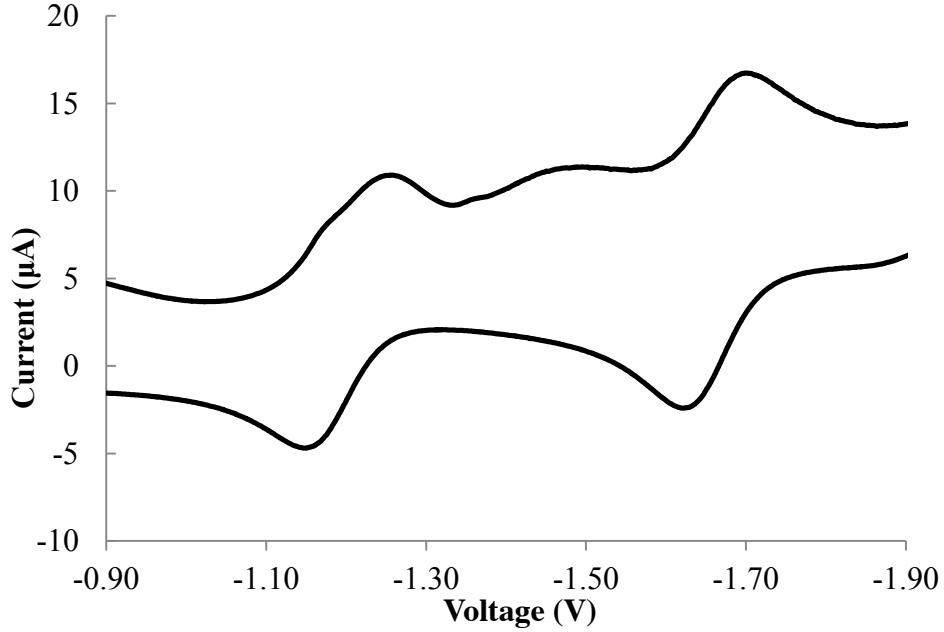

Figure III.15 Cyclic voltammogram of **3.8** in CH_2Cl_2 versus ferrocene/ferrocenium.

In a fashion similar to the complexation of **3.2**, six equivalents of **3.8** were stirred with one equivalent of bis(η^6-naphthalene)chromium(0) in THF. Following removal of all volatiles from the reaction mixture and recrystallization from CH_2Cl_2/pentane, the diamagnetic, homoleptic chromium(0) complex **3.9** was isolated in 54% yield (Scheme III.4). The IR spectrum of **3.9** in CH_2Cl_2 shows one isocyanide stretching frequency at 1971 cm^{-1}, suggesting a local octahedral metal environment. This depression in frequency indicates the isocyanide junction groups are bound to an electron-rich metal and participating in π-backbonding. The ^1H NMR spectrum of **3.9** exhibits discernible coupling in the resonances of the diester substituents, contrary to the analogous **3.4** that exhibits broad singlets for these resonances. It is possible, then, that the co-planar azulenic moieties of the biazulene ligands may play a role in the ordering of the environment about the metal center such that the diester substituents have freedom to rotate and interact less with the neighboring ligands.

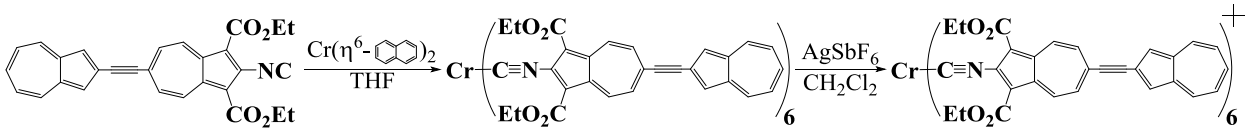

ν_{CN} = 2125 cm^{-1} — **3.8**

ν_{CN} = 1971 cm^{-1} — **3.9**

ν_{CN} = 2058 cm^{-1} — **3.10**

Scheme III.4

The one-electron oxidation of one equivalent of **3.9** with one equivalent of $AgSbF_6$ in CH_2Cl_2 provided the paramagnetic, low-spin, d^5 homoleptic Cr(I) complex **3.10** shown in Scheme III.4. Following recrystallization from CH_2Cl_2/pentane, **3.10** was isolated in 70% yield. IR analysis in CH_2Cl_2 shows one band attributed to isocyanide stretching at 2058 cm^{-1}. This shift of stretching frequency to higher energy by 87 cm^{-1} relative to **3.9** is similar to that observed in **3.4** and implies a decrease in π-backdonation from the less electron-rich Cr(0) center. Also similar to **3.4** are the sharp, diamagnetic-like shifts observed in the ^1H NMR spectrum in CD_2Cl_2.

The hydrogen atom resonances of the diester substituents, however, now appear as broad singlets where they appeared as a discernible quartet and triplet in the precursor **3.9**. This broadening suggests limited ability to rotate and, thus, a more sterically crowded local environment – a result of the decrease in atomic size of chromium upon oxidation. Given that the IR analysis confirms the presence of a Cr(I) metal center, it appears that **3.8** does not effectively delocalize unpaired electron spin. Therefore, the extent of π-conjugation within the biazulenic motif does not seemingly control delocalization.

Since the attempts to grow X-ray diffraction quality crystals of **3.4** and **3.10** failed to provide any structural data to assist in understanding the lack of electron delocalization through the novel 2',6-biazulenic π-systems, a model homoleptic Cr(I) complex of a monoazulene was synthesized and characterized (Scheme III.5). The chosen 2-isocyano-1,3-diesterazulene[23] can be considered the monoazulene congener of **3.2** and **3.8**. The ^{14}N NMR spectrum of this monoazulene exhibits one resonance at 172.8 ppm in CD_2Cl_2 due to the isocyanide nitrogen atom. Complexation of six equivalents of 2-isocyano-1,3-diesterazulene with one equivalent of bis(η^6-naphthalene)chromium(0) in THF provided the diamagnetic, homoleptic Cr(0) complex **3.11**. Following recrystallization from CH_2Cl_2/pentane, **3.11** was afforded in 80% yield. The IR spectrum of **3.11** in CH_2Cl_2 revealed one isocyanide stretching frequency at 1969 cm^{-1}, similar to that observed in **3.3** and **3.9**. The one-electron oxidation with one equivalent of $AgSbF_6$ provided the paramagnetic, homoleptic Cr(I) complex (**3.12**) shown in Scheme III.5, which is akin to **3.4** and **3.10**. Compound **3.12** can be purified via recrystallization from CH_2Cl_2/pentane and isolated in a 70% yield. IR analysis of **3.12** in CH_2Cl_2 provided the isocyanide stretching frequency (ν_{CN} = 2059 cm^{-1}), which is in line with other homoleptic, Cr(I) complexes. While the

electrochemistry of **3.12** was first reported elsewhere[29], this Dissertation reports a straightforward synthesis and further characterization.

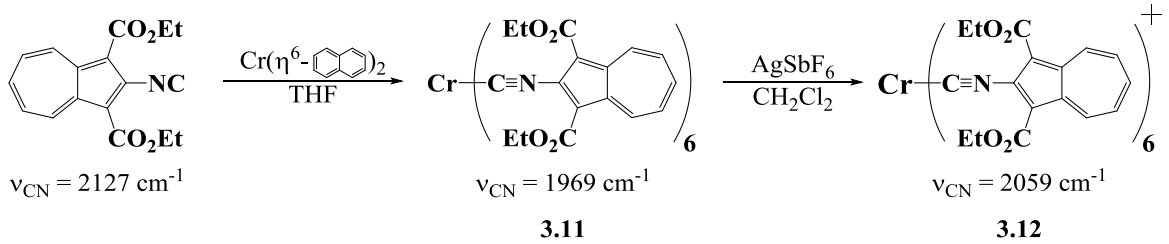

Scheme III.5

Similar to **3.4**, compound **3.12** presents with 1) diamagnetic-like resonances in the ^{1}H NMR spectrum, indicating no unpaired electron density in the π-system of the azulene moiety; 2) a lack of nitrogen resonance in the ^{14}N NMR spectrum; and 3) a solid-state effective magnetic moment of 2.55 μ_B, suggesting extensive spin-orbit coupling of metal-based unpaired electron spin (theoretical spin-only magnetic moment = 1.73 μ_B). The solid-state EPR spectrum of **3.12** in CH_2Cl_2 (1 equiv.)/toluene (2 equiv.) at 5 K shown in Figure III.16 varies from that of **3.4**. The features are reminiscent of a rhombic, S = ½ system. The observed g-values are 2.22, 2.10 and 1.93 for the positive, derivative, and negative features, respectively. Even though the EPR spectrum of **3.12** varies from that of **3.4** due to a possible distortion from perfect octahedral symmetry in the solid-state, the narrow, symmetrical features and lack of hyperfine coupling in Figure III.16 seemingly corroborate the finding of metal-centered unpaired electron spin from the magnetic susceptibility measurements.

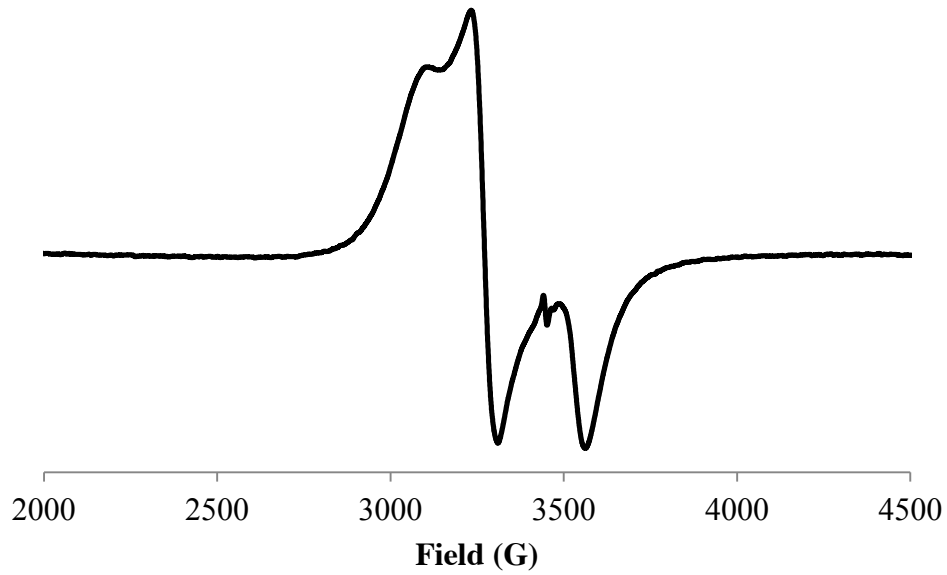

Figure III.16 EPR spectrum of **3.12** in CH_2Cl_2/toluene at 5 K.

Fortunately, structural details of **3.12** were obtained via X-ray crystallographic analysis, which provided structural information relating to homoleptic Cr(I) complexes of 1,3-diester-substituted 2-isocyanoazulenes. X-ray diffraction quality crystals were grown as black needles by allowing a layer of pentane to diffuse into a solution of **3.12** in CH_2Cl_2 at -15 °C. Compound **3.12** crystallizes in the triclinic space group $P\bar{1}$ with three independent Cr(I) cations, three disordered SbF_6^- anions, and 1.67 CH_2Cl_2 molecules within the unit cell. Two different views of the crystal structure of **3.12** are shown in Figure III.13. Figure III.13a elucidates the local octahedral metal environment, confirming the spectroscopic (^{1}H NMR, ^{13}C NMR, and IR) evidence. Figure III.13b demonstrates the orientation of the six azulene moieties coordinated to the Cr(I) center.

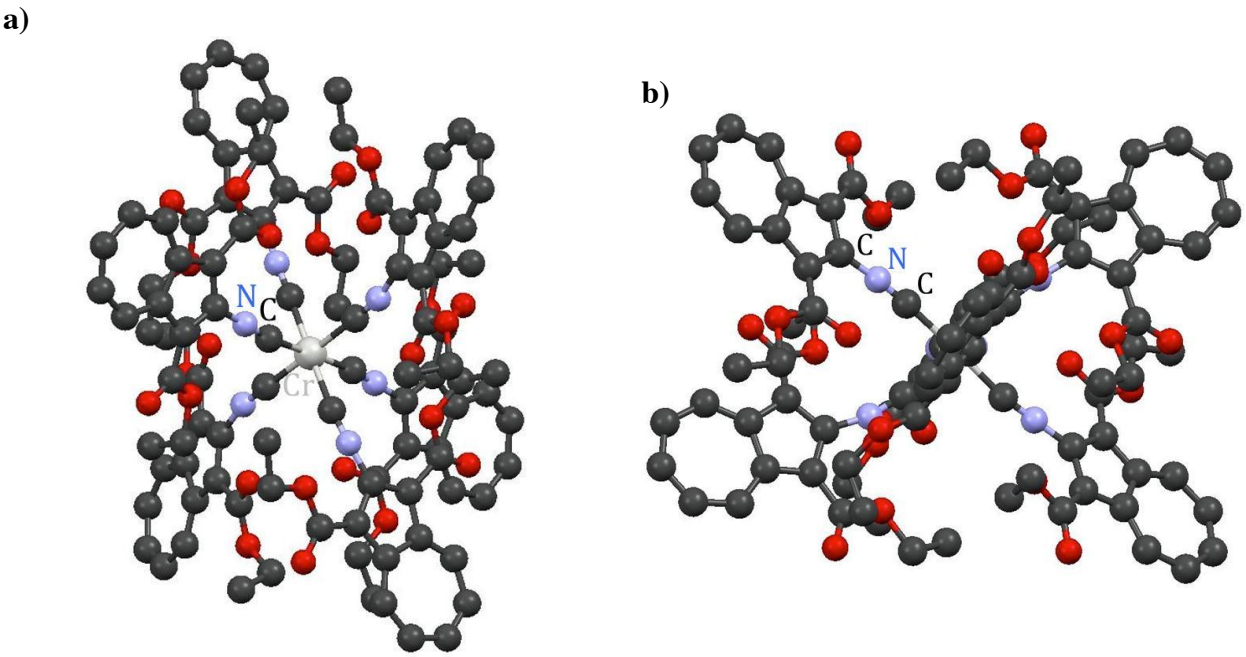

Figure III.17 X-ray crystallographic structure of **3.12** highlighting a) the local octahedral geometry of the Cr(I) metal center and b) 1,3-disubstituted monoazulene ligands.

In **3.12**, the two azulenes of each *trans* pair lie coplanar with respect to one another. The average Cr-C and isocyanide C-N bond lengths are 1.99(2) Å and 1.15(3) Å, respectively. Figure III.18 shows one of the cations of **3.12** without the 1,3-diester substituents and hydrogen atoms for clarity. Of the three *trans* pairs, none of the π-systems of the monoazulene ligands appear to align with the *d*-orbitals of the Cr(I) center. Furthermore, at least one *trans* pair in each of the three independent cations exhibits "bent" C-N-C bond angles ranging from 163(2)° to 169° ($\angle$C-N-C_{avg} = 166(2)°). These bent C-N-C bond angles are statistically different from the more "linear" C-N-C angles that range from 174(2) to 177(2)° ($\angle$C-N-C_{avg} = 175(2)°). Given that other homoleptic Cr(I) complexes of monoazulenes with 1,3-dihydrogen substituents have exhibited unpaired electron density in the π-systems of the azulene ligands, the diester substituents must play a dominant role in effectively curtailing delocalization. That is, the steric crowding about the metal center due to the bulky 1,3-diester substituents disrupts overlap of the

π-system of the azulene frameworks with the Cr(dπ) orbitals by forcing the azulenic π*-system to cant with respect to the metal-based orbitals.

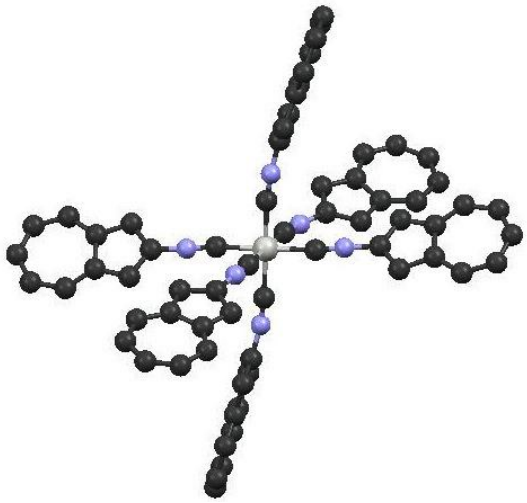

Figure III.18 Structural view of **3.12** depicting the arrangement of the three *trans* pairs of monoazulene ligands. All hydrogen atoms and the 1,3-diester substituents have been removed for clarity.

To prove that electron delocalization can be sterically controlled via 1,3-diester substituents (e.g., in **3.2**, **3.8**, and 2-isocyano-1,3-diesterazulene) in paramagnetic homoleptic Cr(I) complexes, the steric bulk of the 1,3-disubstituent was reduced. The compound 2-isocyano-1,3-dimethylazulene[24] was chosen for this purpose. Six equivalents of 2-isocyano-1,3-dimethylazulene were reacted with one equivalent of bis(η^6-naphthalene)chromium(0) in THF to give the diamagnetic, homoleptic Cr(0) complex thereof (**3.13**) in 76% yield (Scheme III.6). The IR spectrum of **3.13** in CH_2Cl_2 exhibits a strong band at 1944 cm^{-1} with a shoulder at 1968 cm^{-1}.

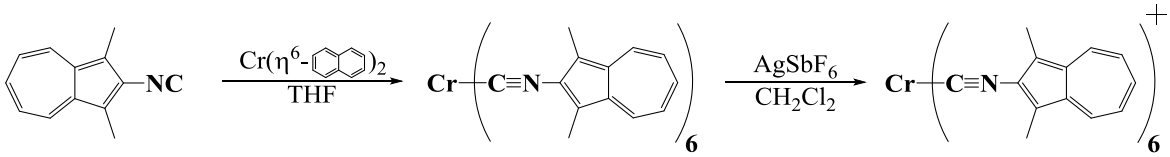

ν_{CN} = 2115 cm^{-1} ν_{CN} = 1943, 1968 cm^{-1} ν_{CN} = 2049 cm^{-1}

3.13 **3.14**

Scheme III.6

The one-electron oxidation of **3.13** with $AgSbF_6$ provided the paramagnetic, homoleptic Cr(I) complex of 2-isocyano-1,3-dimethylazulene (**3.14**) in 84% yield. IR analysis of **3.14** in CH_2Cl_2 revealed one band attributed to isocyanide stretching at 2049 cm^{-1}. The electronic absorption spectrum of **3.14** presents five bands (Figure III.19), which are in the UV region and span across the entire visible region (i.e., 400 - 700 nm). The molar absorptivities range from 0.2 x 10^6 – 8.4 x 10^6 M^{-1} cm^{-1} and 2.8 x 10^5 – 7.8 x 10^5 M^{-1} cm^{-1} in the UV and visible regions, respectively. The cyclic voltammogram of **3.14** in CH_2Cl_2 revealed two, one-electron redox processes (Figure III.20). These two quasi-reversible processes occur at -0.12 V and -0.74 V (vs. ferrocene/ferrocenium) and are attributed to the metal-centered $Cr^{+/2+}$ and $Cr^{0/+}$ reductions, respectively. These values are practically the same as observed in other homoleptic chromium complexes of 2-isocyanoazulenes.[12] This reinforces the fact that the π-acceptor/σ-donor ratio of these azulene motifs is a product of the position of the isocyanide substituent and is not affected by 1,3-substituents.

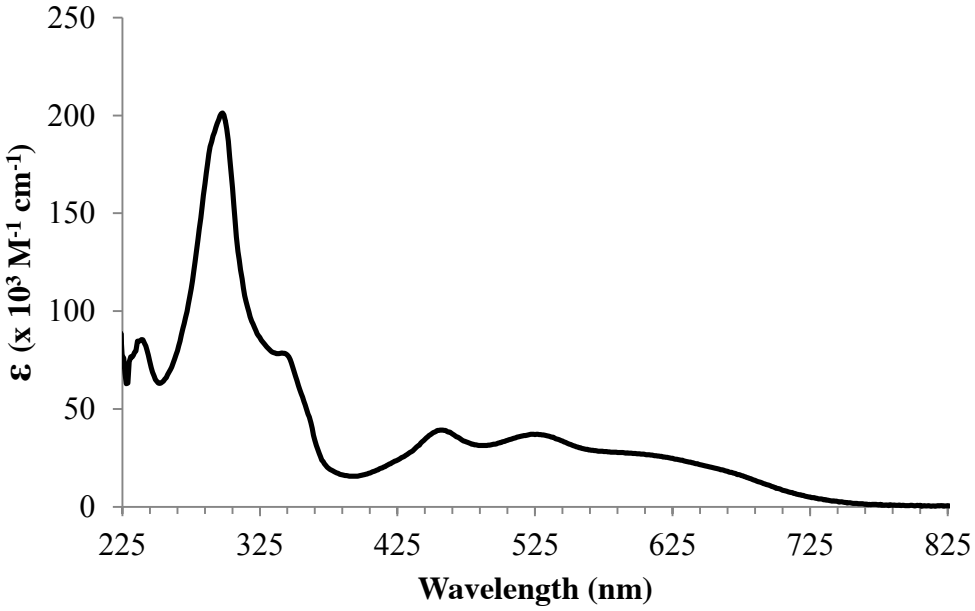

Figure III.19 Electronic absorption spectrum of **3.14** in CH_2Cl_2.

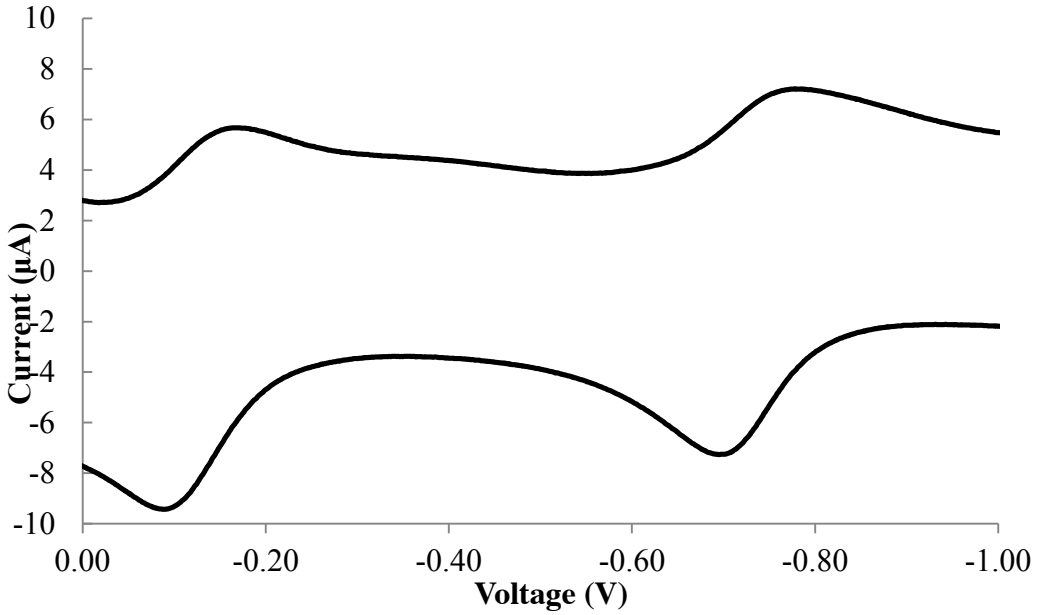

Figure III.20 Cyclic voltammogram of **3.14** in CH_2Cl_2 versus ferrocene/ferrocenium.

Interestingly, the ^{1}H NMR spectrum of **3.14** in CD_2Cl_2 (Figure III.21) exhibits paramagnetic-like shifts contrary to **3.4** and **3.10**. Table III.7 highlights the change in hydrogen atom resonance shifts ($\Delta\delta$) between the paramagnetic complex **3.14** and the free ligand 2-isocyano-1,3-dimethylazulene. Indeed, the observed hydrogen atom resonance shifts occur in the expected directions in accordance with the atomic exchange coupling mechanism[7] and are similar in sign and magnitude to the paramagnetic $Cr(CNXyl)_6^+$,[4] the benzenoid-containing congener of **3.14**. The assignments of the resonances in the ^{1}H NMR spectrum were confirmed via the two-dimensional, ^{1}H-^{1}H NMR technique COSY. Furthermore, the paramagnetic effect of unpaired electron spin on the nuclei of the aromatic azulene moiety is observed in the ^{13}C NMR spectra as the ^{13}C resonances are expectedly shifted with respect to the free ligand due to a delocalized[5] unpaired electron. The ^{14}N NMR spectrum of **3.14** in CD_2Cl_2 revealed one nitrogen resonance at 895.4 ppm. Moreover, the solid-state effective magnetic moment of **3.14** was determined to be 1.90 μ_B, which is in line with the theoretical spin-only magnetic moment of a S

= ½ system of 1.73 μ_B. For comparison, the complex Cr(2-isocyanoazulene)$_6^+$ (without 1,3-substituents) exhibits a resonance in the ^{14}N NMR spectrum at 859.6 ppm and a solid-state effective magnetic moment of 1.73 μ_B.[12]

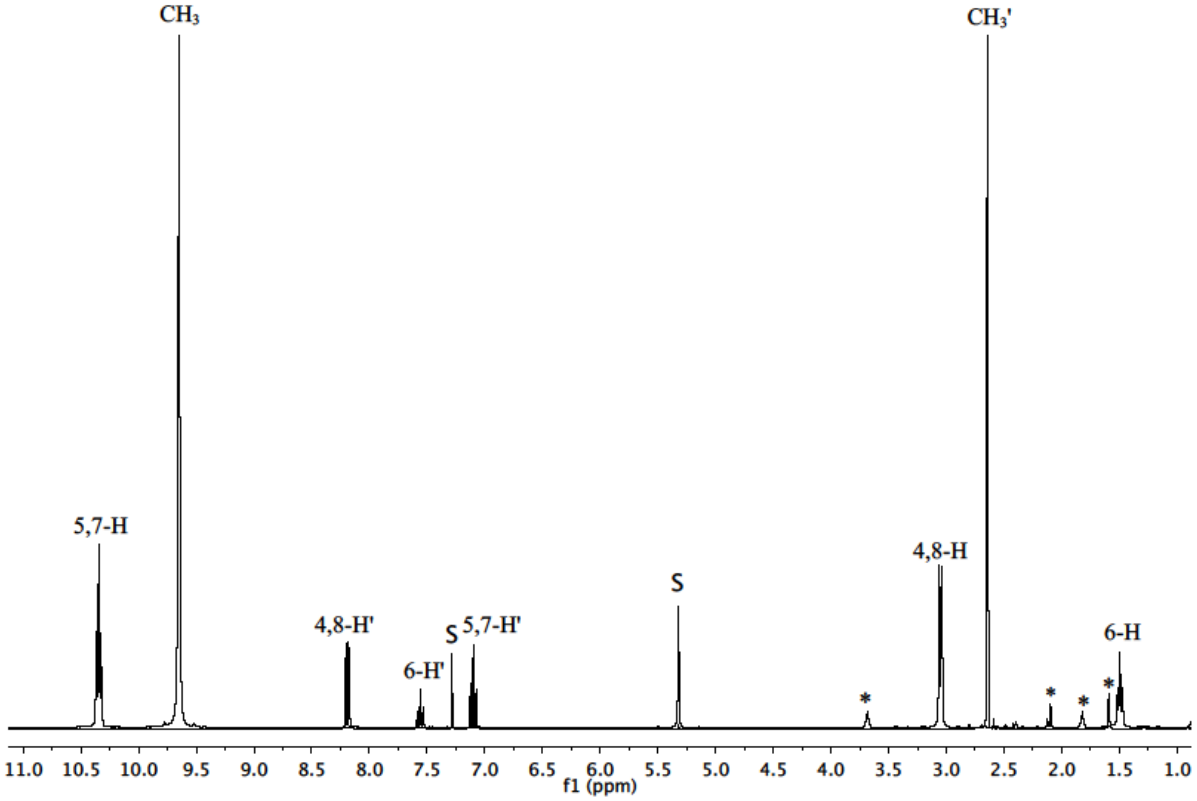

Figure III.21 The ^{1}H NMR spectra of **3.14** in CD_2Cl_2 and 2-isocyano-1,3-dimethylazulene (denoted by prime) in $CDCl_3$ (S = residual solvent; * = solvent impurity).

Table III.7 NMR data reflecting paramagnetic shifts (δ_{para}) of ^{1}H resonances in **3.14** vs. diamagnetic shifts (δ_{diam}) of 2-isocyano-1,3-dimethylazulene.[24]

Resonating nucleus	δ_{para} (ppm)	δ_{diam} (ppm)	$\Delta\delta_{Observed}$ ($\Delta\delta_{Expected}$)[a]
C<u>H</u>$_3$	9.65	2.64	+ (+)
4,8-H	3.05	8.18	- (-)
5,7-H	10.35	7.09	+ (+)
6-H	1.50	7.55	- (-)

[a] The + and – denote downfield and upfield shifts, respectively.

The EPR spectrum of **3.14** in CH_2Cl_2 at 5 K is shown in Figure III.22. The isotropic feature has an observed g-value of 2.08. More importantly, the feature is asymmetric unlike the resonances of **3.4** and **3.12**. Close observation reveals the lower-field portion of the feature to be wider than the higher-field portion. This asymmetry could be a result of a delocalized unpaired electron due to coupling with nuclei of the ligands possessing nuclear spin (e.g., $I(^{14}N) = 1$; $I(^{1}H) = ½$). Attempts to resolve hyperfine coupling by recording the EPR spectrum of **3.14** in a glassing solvent proved unsuccessful.

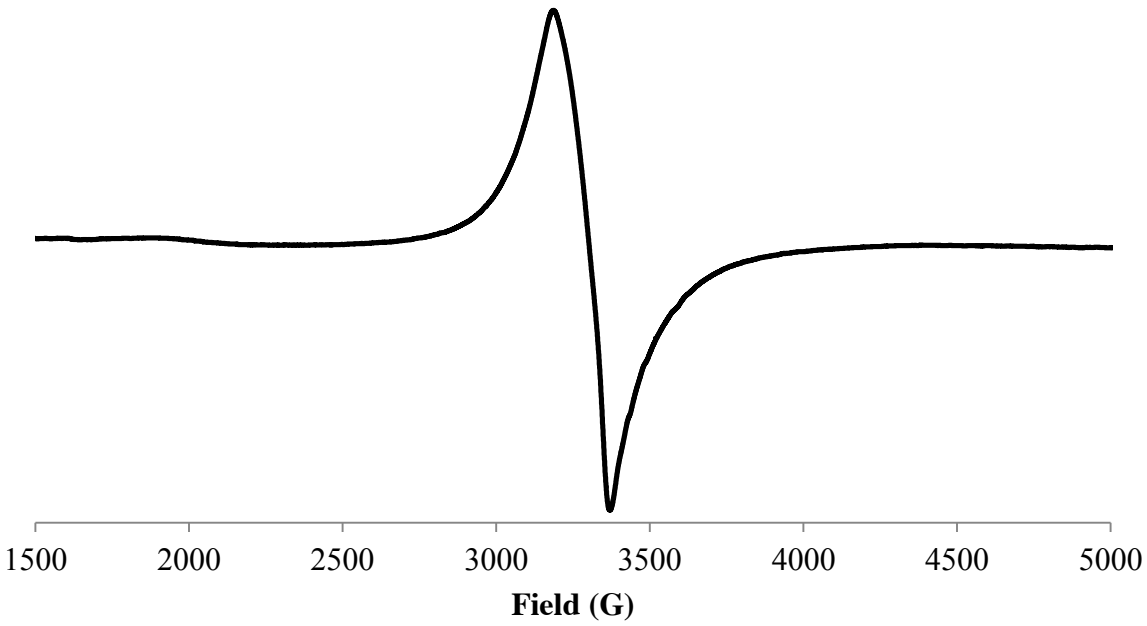

Figure III.22 EPR spectrum of **3.14** in CH_2Cl_2 at 5 K.

Table III.8 summarizes the experimental results and observations of the paramagnetic, homoleptic Cr(I) complexes of **3.2**, **3.8**, 2-isocyano-1,3-diesterazulene, 2-isocyano-1,3-dimethylazulene, and 2-isocyanoazulene; these Cr(I) complexes are identified as **3.4**, **3.10**, **3.12**, **3.14**, and $Cr(2\text{-isocyanoazulene})_6^{+\,12}$, respectively. The compounds **3.4**, **3.10**, and **3.12**, which contain 1,3-diester substituents, all exhibit diamagnetic-like resonances in their ^{1}H and ^{13}C NMR

spectra, indicating no delocalization of unpaired electron density throughout the azulene-based π-systems. The inability to delocalize is paired with a lack of observed resonance in the ^{14}N NMR spectrum as well as solid-state effective magnetic moments of approximately 2.5 μ_B. Both **3.14** and Cr(2-isocyanoazulene)$_6^+$, on the other hand, lack sterically bulky 1,3-substituents and exhibit paramagnetic-like resonances in their ^1H and ^{13}C NMR spectra, the shifts of which do not attenuate with increasing distance from the metal center. This indicates direct contact of the unpaired electron density with the nuclei of the azulene frameworks that is only possible through delocalization. The effective magnetic moments of **3.14** and Cr(2-isocyanoazulene)$_6^+$ are 1.90 and 1.73 μ_B, respectively, which is in line with a spin-only magnetic moment.

Table III.8 Comparison of selected experimental data of various homoleptic Cr(I) complexes.

Compound	$^1H/^{13}C$ Shifts	^{14}N Shift (ppm)	EPR	μ_{eff} (μ_B)	$E_{½}$ {$Cr^{0/+}$} (V)
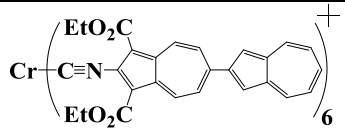 **3.4**	Diamagnetic	Not observed	Isotropic, Symmetric	2.43	-0.63
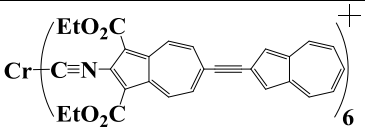 **3.10**	Diamagnetic	N/A	N/A	N/A	N/A
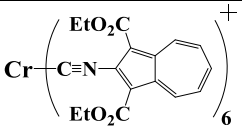 **3.12**	Diamagnetic	Not observed	Rhombic	2.55	-0.67
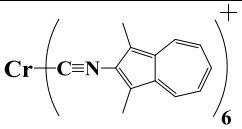 **3.14**	Paramagnetic	895.4	Isotropic, Asymmetric	1.90	-0.74
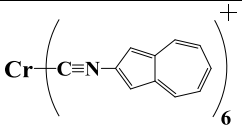	Paramagnetic	859.6	N/A	1.73	-0.69

Furthermore, the EPR spectra of **3.4** and **3.12** exhibit symmetric isotropic and rhombic features where **3.14** presents with an asymmetric, isotropic feature. The isotropic/rhombic features are reasonable in light of the expected octahedral metal geometries determined from the X-ray crystallographic studies of **3.12** and Cr(2-isocyanoazulene)$_6^{+}$ [12]. The symmetry and asymmetry of the features may seemingly reflect the metal-based and delocalized unpaired electron density, respectively. The $E_{½}$ potentials determined from cyclic voltammetry are the only similarity between all homoleptic Cr(I) compounds. With an average potential for the $Cr^{0/+}$ and $Cr^{+/2+}$ reductions at -0.68 and -0.18 V, respectively, the 1,3-substituents do not affect the π-acceptor/σ-donor ratio of the 2-isocyanoazulenes. The steric bulk of the 1,3-substituents, however, does affect the electron delocalization through the azulene framework.

III.5 Conclusions and Outlook

Two novel 2-isocyano-2,6'-biazulenes were prepared and characterized. The asymmetric biazulenes were used to form homoleptic, chromium(I) complexes to ultimately study the extent of electron delocalization through the π-system of the biazulenic frameworks. Various physical characterization methods including NMR ($^{1}H/^{13}C/^{14}N$), EPR, and magnetic susceptibility measurements suggest a lack of electron delocalization throughout the 1,3-diester-substituted 2,'6-biazulenes. An analogous Cr(I) complex of a 1,3-diester-substituted 2-isocyanoazulene was employed as a model. Exhibiting similar spectroscopic properties as the biazulenic analogues, X-ray diffraction studies revealed that the 1,3-dieser substituents of the mono- and biazulenes inhibit electron delocalization due to a steric strain disrupting overlap between M(dπ) and azulene(pπ*) orbitals. A separate model complex featuring the less sterically bulky methyl group as the 1,3-substitutents gave rise to delocalization; conceivably by reducing steric crowding about the metal center and allowing for the necessary orbital overlap. This delocalization is apparent in the NMR ($^{1}H/^{13}C/^{14}N$) spectra as well as the magnetic susceptibility measurements. Cyclic voltammetric measurements reinforced that a 2-isocyanide-substituted azulene possesses practically the same π-acceptor/σ-donor ratio despite 1,3-substituents and a mono- or biazulenic framework. With this, future work will be aimed at the synthesis and characterization of asymmetric 2,6'-biazulenes featuring sterically unencumbering 1,3-substituents (e.g., 2-isocyano-2',6-biazulene and 2-isocyano-2',6-biazulenylacetylene) and the homoleptic Cr(I) complexes thereof. Detailed electronic absorption studies will be undertaken to probe the Cr(dπ)-Azulene(pπ*) interactions. Surface studies, especially conductance measurements, of this current and future 2,'6-biazulene family are warranted.

III.6 References

1 Barybin, M. V. *Coord*. *Chem*. *Rev*. **2010**, *254*, 1240–1252.

2 Lazar, M.; Angelici, R.J. Isocyanide binding modes on metal surfaces and in metal complexes. In *Modern Surface Organometallic Chemistry*; Basset, J.-M.; Psaro, R.; Roberto, D.; Ugo, R., Eds. Wiley-VCH: Weinheim, 2009; pp. 513–556.

3 Representative examples: (a) Choi, S. H.; Kim, B.; Frisbie, C. D. *Science* **2008**, *320*, 1482–1486, (b) Chu, C.; Ayres, J. A.; Stefanescu, D. M.; Walker, B. R.; Gorman, C. B.; Parsons, G. N. J. *Phys*. *Chem*. *C* **2007**, *111*, 8080– 8085, (c) Kim, B.; Beebe, J. M.; Jun, Y.; Zhu, X.-Y.; Frisbie, C. D. *J*. *Am*. *Chem*. *Soc*. **2006**, *128*, 4970–4971, (d) Murphy, K. L.; Tysoe, W. T.; Bennett, D.W. *Langmuir* **2004**, *20*, 1732–1738, (e) Hong, S.; Reifenberger, R.; Tian, W.; Datta, S.; Henderson, J.; Kubiak, C. P. *Superlattices Microstruct*. **2000**, *28*, 289–303.

4 Barybin, M. V.; Young, V. G.; Ellis, J. E. *J*. *Am*. *Chem*. *Soc*. **2000**, *122*, 4678–4691.

5 Fermi, E. *Z*. *Physik*. **1930**, *60*, 320.

6 Satterlee, J. D. *Concepts Magn*. *Res*. **1990**, *2*, 69–79.

7 (a) McConnell, H. M. *J*. *Chem*. *Phys*. **1956**, *24*, 764–766; (b) McConnell, H. M.; Chesnut, D. B. *J*. *Chem*. *Phys*. **1958**, *28*, 107–117.

8 *Carbon Nanotubes: Preparation and Properties*; Ebbesen, T. W., Ed. CRC Press Inc.: Boca Raton, FL, 1997.

9 Dewar, M. J. S. *The Molecular Orbital Theory of Organic Chemistry*. McGraw-Hill: New York, 1969.

10 Liu, R. S. H. *J*. *Chem*. *Ed*. **2002**, *79*, 183-185.

11 See section I.3 of this Dissertation for more information.

12 Robinson, R. E.; Holovics, T. C.; Deplazes, S. F.; Powell, D. R.; Lushington, G. H.; Thompson, W. H.; Barybin, M. V. *Organometallics* **2005**, *24*, 2386–2397.

13 Treboux, G.; Lapstun, P.; Silverbrook, K. *J*. *Phys*. *Chem*. *B* **1998**, *102*, 8978.

14 Zhou, K.-G.; Zhang, Y.-H.; Wang, L.-J.; Xie, K.-F.; Xiong, Y.-Q.; Zhang, H.-L.; Wang, C.-W. *Phys*. *Chem*. *Chem*. *Phys*. **2011**, *13*, 15882–15890.

15 (a) Ito, S.; Terazono, T.; Kubo, T.; Okujima, T.; Morita, N.; Murafuji, T.; Sugihara, Y.; Fujimori, K.; Kawakami, J.; Tajiri, A. *Tetrahedron* **2004**, *60*, 5357–5366, (b) Ito, S.; Okujima, T.; Morita, N. J. *Chem*. *Soc*., *Perkin Trans*. *1* **2002**, 1896–1905, (c) Kurotobi, K.;

Tabata, H.; Miyauchi, M.; Murafuji, T.; Sugihara, Y. *Synthesis* **2002**, *8*, 1013–1016, (d) Morita, T.; Takase, K. *Bull*. *Chem*. *Soc*. *Jpn*. **1982**, *55*, 1144–1152, (e) Hanke, M.; Jutz, C. *Synthesis* **1980**, 31–32.

16 Maher, T. R.; Spaeth, A. D.; Neal, B. M.; Berrie, C. L.; Thompson, W. H.; Day, V. W.; Barybin, M. V. *J*. *Am*. *Chem*. *Soc*. **2010**, *132*, 15924–15926.

17 a) Earnshaw, A. *Introduction to Magnetochemistry*; Academic Press: New York, 1968. b) Kahn, O. *Molecular Magnetism*; VCH: New York 1993.

18 Connelly, N. G.; Geiger, W. *Chem*. *Rev*. **1996**, *96*, 877.

19 Krimen, K. I. *Org*. *Synth*. **1970**, *50*, 1.

20 Pomije, M. K.; Kurth, C. J.; Ellis, J. E.; Barybin, M. V. *Organometallics* **1997**, *16*, 3582.

21 Nozoe, T.; Seto, S.; Matsumura, S. *Bull*. *Chem*. *Soc*. *Jpn*. **1962**, *35*, 1990.

22 McGinnis, D. Synthesis and Coordination Chemistry of Azulene- and Ferrocene-Based Isocyanide Ligands. Ph.D. Dissertation, University of Kansas, Lawrence, KS, 2011.

23 DuBose, D. L.; Robinson, R. E.; Holovics, T. C.; Moody, D. R.; Weintrob, E. C.; Berrie, C. L.; Barybin, M. V. *Langmuir* **2006**, *22*, 4599.

24 See Chapter II, Section II.3.8 (specifically compound II.4) of this Dissertation for synthetic details and additional information.

25 Holovics, T. C.; Robinson, R. E.; Weintrob, E.; Toriyama, M.; Lushington, G. H.; Barybin, M. V. *J*. *Am*. *Chem*. *Soc*. **2006**, *128*, 2300.

26 Bohling, D. A.; Mann, K. R. *Inorg*. *Chem*. **1984**, *23*, 1426-1432.

27 Holovics, T. C.; Deplazes, S. F.; Toriyama, M.; Powell, D. R.; Lushington, G. H.; Barybin, M. V. *Organometallics* **2004**, *23*, 2927-2938.

28 Ljungström, E. *Acta Chem*. *Scand*. **1978**, *32A*, 47-50

29 Deplazes, S. F. Ligand design, coordination, and electrochemistry of nonbenzenoid aryl isocyanides. Ph.D. Dissertation, University of Kansas, Lawrence, KS, 2008.

30 König, E.; König, G. Magnetic Properties of Coordination and Organometallic Transition Metal Compounds: Magnetic Susceptibilities. In *Numerical Data and Functional Relationships in Science and Technology, Vol*. *12*; Hellwege, K.-H., Madelung, O., Eds.; Springer-Verlag: Berlin-Heidelberg, 1984.

31 Darensbourg, M. Y. *Prog*. *Inorg*. *Chem*. **1985**, *33*, 221.

CHAPTER IV

Toward Two-dimensional Metal Organic Frameworks Incorporating Linear Azulenic and Biazulenic Motifs

IV.1 Introduction

Reports on metal-organic frameworks have drastically increased since the 1990s.[1] By definition, a metal-organic framework (MOF) features metal centers linked by organic-based bridges, usually via a junction group (e.g., a carboxylate, R-C(O)O$^-$, unit). The increased interest in MOFs stems from their versatility and tunability. As a result of the infinite amount of possible compositions, and thus three-dimensional (3D) structures, MOFs offer opportunities in many potential applications and encompass a multidisciplinary reach covering catalysis[2], gas separation[3] and storage[4], small-molecule sensing[5], and organometallic crystal engineering[6].

A two-dimensional metal-organic framework (2D-MOF) such as a "molecular rectangle" or "molecular square" constitutes a molecular architecture that possesses less dimensionality, and thus complexity, than extended 3D frameworks while still offering interesting properties. For example, Hupp *et al*. reported on molecular rectangles that exhibit full valence delocalization.[7] As shown in Figure IV.1, a molecular square can be envisioned as an organometallic framework in which four metal centers, or "corner pieces," are connected by the same bridging ligands, or "edge pieces." In a molecular rectangle, the opposing edge pieces are comprised of ligands of different lengths. Such architectures, however, require controlled synthetic installation and, thus, selective building blocks need to be employed. For example, linear heterocyclic amines, such as pyrazine and 4,4'-bipyridine, and benzenoid diisocyanoarenes, such as 1,4-diisocyanobenzene and 1,4-diisocyanodurene (durene = 2,3,5,6-tetramethylbenzene), could be used as bridging ligands of varying sizes.

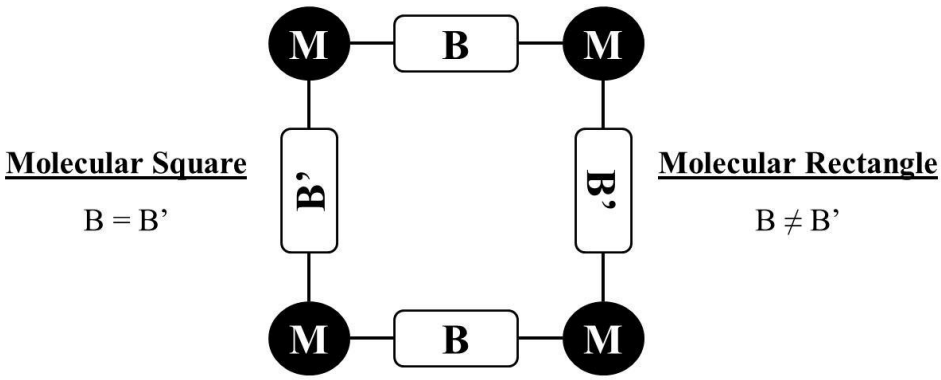

Figure IV.1 A generic representation of a 2D-MOF where M is a metal-based corner piece and B is a bridging edge piece.

Yamamoto *et al*. reported on the use of commercially available starting materials, such as heterocyclic amines and benzenoid diisocyanoarenes, for edge pieces in conjunction with quasi-octahedral [Cp*Cl_2M] (M = Ir(III), Rh(III); Cp* = pentamethylcyclopentadienyl) corner pieces to afford novel, molecular rectangles as shown in Figure IV.2.[8] In that work, two [Cp*Cl_2M] corner pieces were bridged with either the heterocyclic amine or diisocyanoarene (L) to form the dinuclear edge piece [Cp*Cl_2Ir]$_2$(μ-η^1:η^1-L). A coordination site can be opened at both metal centers via halide abstraction. The tetranuclear molecular squares or rectangles are then formed by bridging the corner pieces via coordination of an additional heterocyclic amine or diisocyanoarene. Interestingly, an X-ray structural analysis revealed that the planes of the aromatic bridging ligands are perpendicular to the plane of the tetranuclear framework in the molecular rectangles. This arrangement could be taken advantage of in a sensing application wherein a guest molecule (i.e., an extraneous molecule of interest) in the cavity of the 2D-MOF (i.e., the host) interacts with the π-system of the edge piece. This interaction could lead to detectable changes in the optical properties (e.g., electronic absorption spectrum) of the molecular rectangle.

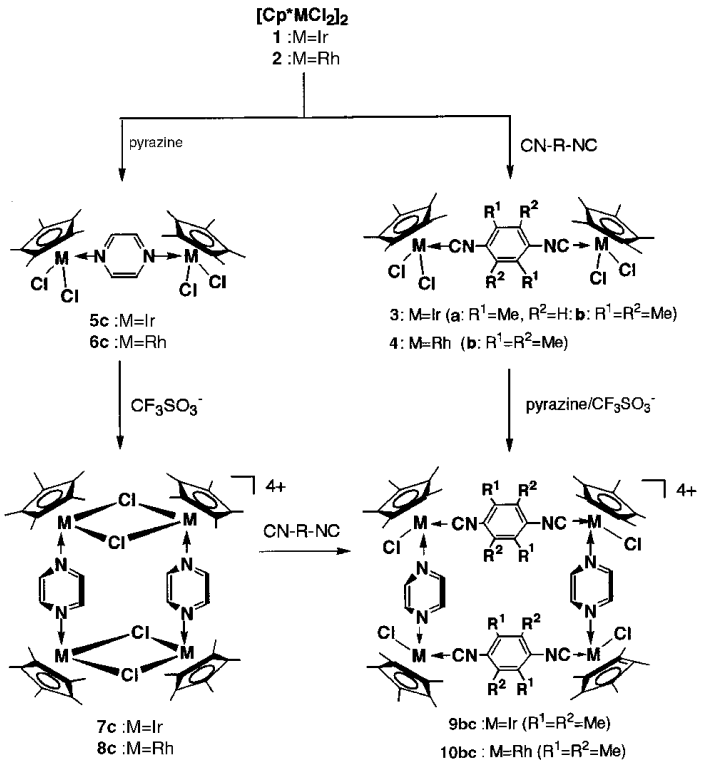

Figure IV.2 Synthetic route to form the molecular rectangle $[(Cp^*ClIr)_4(\mu\text{-}CN\text{-}C_6Me_4\text{-}NC)_2(\mu\text{-pyrazine})_2][OTf]_4$ (OTf = triflate, $CF_3SO_3^-$) from commercially available $[Cp^*Cl_2Ir]_2$, pyrazine, and 1,4-diisocyanodurene (durene = 2,3,5,6-tetramethylbenzene) starting materials.[8]

In fact, shifts in fluorescence emission wavelengths and intensities have been used to detect small molecules through host-guest interactions.[9] For example, fluorescence quenching of a zinc(II)-based MOF was used to sense dinitrotoluene – a volatile nitroaromatic that often accompanies trinitrotoluene.[10] The molecular rectangle displayed in Figure IV.2 or an analogue thereof could therefore play a role in sensing as isocyanide-containing organometallic complexes of Ir(III) have been shown to exhibit luminescent properties.[11] The potential to use 2D-MOFs for sensing applications further extends to Re(III)-based molecular squares. Hupp *et al*. showed that thin-films of tetrarhenium molecular squares incorporating pyrazine or 4,4'-bipyridine edges readily absorbed and selectively sensed volatile organic compounds via non-covalent interactions.[12]

Given the use of aromatic heterocyclic amines and benzenoid diisocyanoarenes to form 2D-MOFs with desirable properties, the linear 2,6-diisocyanoazulene is an attractive candidate to function as an edge piece (Figure IV.3). As a nonbenzenoid aromatic hydrocarbon ($C_{10}H_8$), azulene possesses unique properties relative to its benzenoid counterparts (e.g., its isomer naphthalene). For example, the aromatic delocalization energy of azulene is approximately one-seventh the energy of naphthalene.[13] This suggests any host-guest interaction would more strongly induce a change in the π-system of azulene (i.e., more polarizable π-system) than in naphthalene (i.e., less polarizable π-system). A greater interaction as described could reasonably yield larger changes in optical spectra for easier detection.

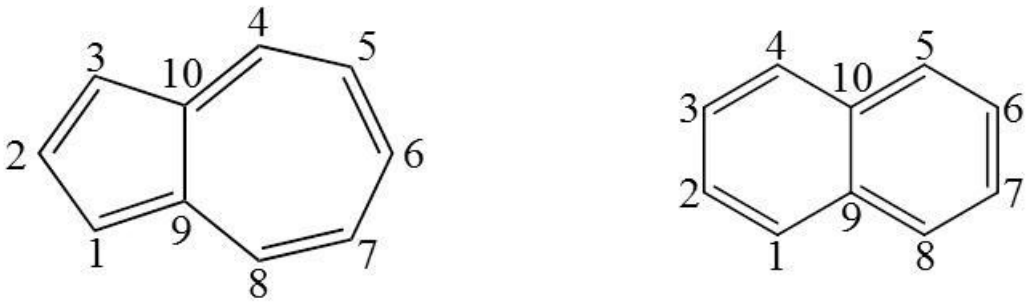

Figure IV.3 The molecular structures of azulene (left) and naphthalene (right) with numbering schemes.

To date, the only azulene-based MOF has been described by Yaghi *et al*. and features the symmetric 1,3-azulenyldicarboxylate as the organic bridge between zinc(II) centers (Figure IV.4).[14] Interestingly, reports on azulene-containing compounds and materials typically feature 1,3-disubstituted azulenes. Separate reports feature azulenes bound to metal centers in a multihapto fashion that effectively destroys aromaticity.[15] This leaves room, then, to take advantage of the linear 2,6-disubstituted framework for materials applications (e.g., molecular rectifier or sensor). Linear diisocyanobenzenes have been shown to participate in charge transport on the molecular level and the isocyanide junction group has been reported to exhibit

better conduction than other junction groups.[16] The incorporation of the linear 2,6-disubstituted azulene moiety, however, requires controlling the orientation of the dipole along the molecular axis.

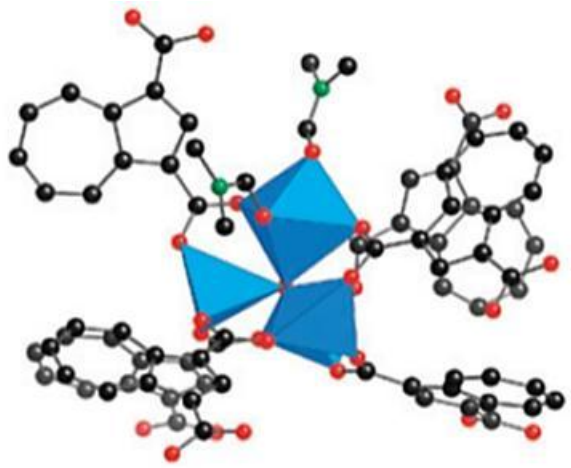

Figure IV.4 Framework structure of the Zn-(1,3-azulenyldicarboxylate) MOF reported by Yaghi *et al*.[13]

Barybin *et al*. have used various synthetic means and junction groups (e.g., carboxylate, $C(O)O^-$, and isocyanide, R-N≡C) to functionalize azulene at the 2- and 6-carbon atoms, which allows for the linear orientation of the molecular axis within complexes and on surfaces.[15] The work involving isocyanide junction groups has also allowed for the regioselective complexation of different metal centers (Scheme I.12).[17] In a similar vein, 2,6-diisocyano-1,3-diethoxycarbonylazulene can be coordinated to a metal carbonyl fragment, $M(CO)_5$ (M = Cr, W), at one isocyanide and then subsequently complexed to a different metal carbonyl fragment (or even metal surface[18]). This gives three possible compounds: an azulene-bridged dinuclear complex or two mononuclear isomers where there is one metal carbonyl fragment bound at either the 2- or 6-isocyanide (Scheme IV.1). These mononuclear complexes have a free isocyanide that could be coordinated to a different metal center, which gives rise to controlled orientation of the 2,6-diisocyanoazulene molecular axis within extended or 2D MOFs. The linear 2,2'-diisocyano-

6,6'-biazulene (i.e., two 2-isocyanoazulenes coupled linearly through the seven-membered ring) has been employed as a bridge between metal carbonyl fragments[19] and could be imagined to be a symmetric bridge in a 2D-MOF. Interestingly, the above 6,6'-biazulenic framework undergoes reversible one- and two-electron reductions, which could provide for adjusting the overall charge of 2D-MOFs in which this motif is incorporated.

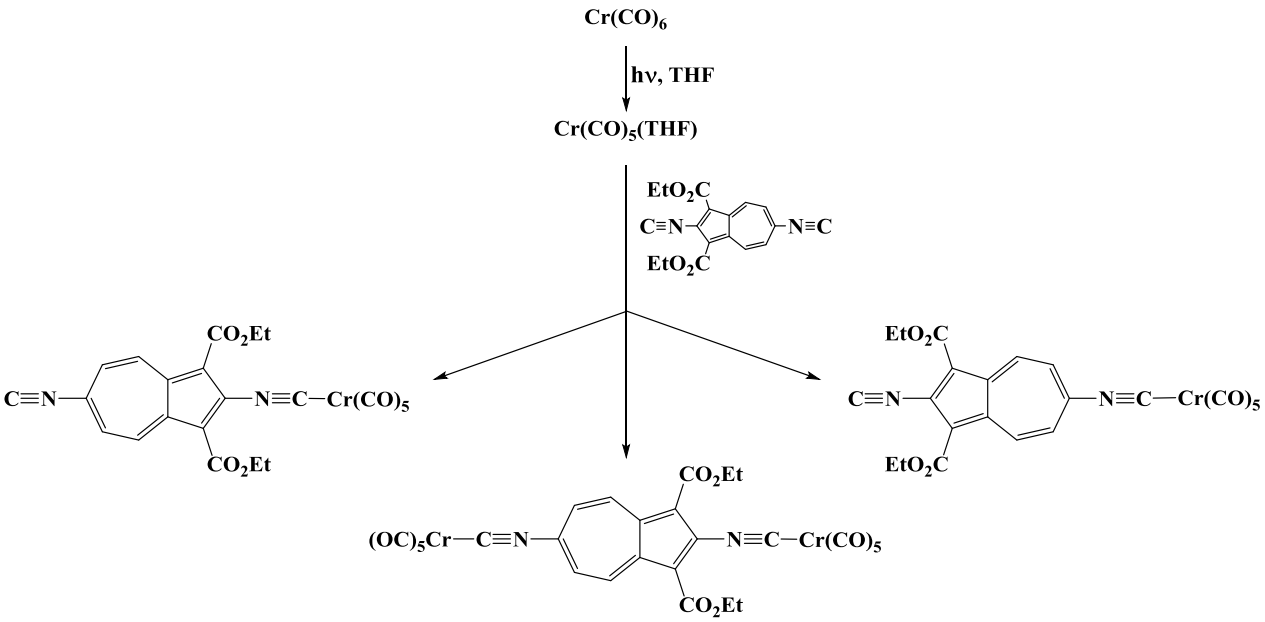

Scheme IV.1

IV.2 Work Described in Chapter IV

The work described herein concerns the author's efforts toward the preparation and isolation of diisocyanoazulene- and diisocyanobiazulene-based MOFs, namely molecular rectangles and heterotetrametallic molecular frameworks. The synthesis and characterization of an asymmetric edge piece featuring 2,6-diisocyano-1,3-diethoxycarbonylazulene, its symmetric biazulene-containing analogs, as well as the tetrairidium molecular rectangles incorporating the above motifs, are presented. The synthetic routes to control orientation of the molecular dipole of the 2,6-diisocyanoazulene moiety within metal-organic frameworks featuring a metal carbonyl end cap are discussed.

IV.3 Experimental Section

IV.3.1 General Procedures, Starting Materials, and Equipment

All operations were performed under ambient atmosphere. Solution infrared spectra were recorded on a PerkinElmer Spectrum 100 FTIR spectrometer with samples sealed in 0.1 mm gas tight NaCl cells. NMR samples were analyzed using Bruker DRX-400 and Bruker Avance 500 spectrometers. ^{1}H and ^{13}C chemical shifts are given with reference to residual ^{1}H and ^{13}C solvent resonances relative to Me_4Si. Two-dimensional techniques (^{1}H-^{1}H COSY, ^{1}H-^{13}C HSQC) were used to obtain unambiguous assignments of ^{1}H and ^{13}C NMR resonances, where necessary.

Electronic absorption (UV-Vis) spectra were recorded in CH_2Cl_2 at 24 °C using a CARY 100 spectrophotometer. Melting points are uncorrected and were determined for samples in sealed capillary tubes. Elemental analyses were carried out by Columbia Analytical Services, Tucson, Arizona. Electrospray ionization (ESI) mass spectroscopy was performed on a Waters Corp. LCT Premier instrument in the mass spectrometry lab at the University of Kansas.

Compounds 2,6-diisocyano-1,3-diethoxycarbonylazulene,[17] 2,2'-diisocyano-1,1',3,3'-tetraethoxycarbonyl-6,6'-biazulene,[19] 2,2'-diisocyano-1,1',3,3'-tetraethoxycarbonyl-6,6'-biazulenylacetylene,[20] $(Cp^*Cl_2Ir)_2(\mu\text{-pyrazine})$[8], $\{(OC)_5Cr\}$(2,6-diisocyano-1,3-diethoxycarbonylazulene-$\kappa(^{2}CN)$},[17] $\{(OC)_5Cr\}$ {2,6-diisocyano-1,3-diethoxycarbonylazulene-$\kappa(^{6}CN)$},[17] 1,4-diisocyano-2,3,5,6-tetramethylbenzene (1,4-diisocyanodurene),[21] and $(Cp^*Cl_2Ir)_2(\mu\text{-}\eta^1\text{:}\eta^1\text{-1,4-diisocyanodurene})$[8] were prepared according to literature procedures. Other reagents were obtained from commercial sources and used as received.

IV.3.2 Synthesis of [(Cp*Cl_2Ir)$_2$(μ-η^1:η^1-2,6-diisocyano-1,3-diethoxycarbonylazulene)] (4.1a).

A solution of 2,6-diisocyano-1,3-diethoxycarbonylazulene (0.042 g, 0.130 mmol) in 20 mL of CH_2Cl_2 was added to a solution of [Cp*Cl_2Ir]$_2$ (0.101 g, 0.126 mmol) in 20 mL of CH_2Cl_2. After the reaction mixture was stirred for 0.5 h, the solution was concentrated at room temperature and layered with pentane. Following diffusion, the mixture was filtered and the resulting solid was dried at 10^{-2} Torr to afford red, crystalline **4.1a** (0.136 g, 0.122 mmol) in a 96% yield. Mp: the product decomposed without melting at 205°C. Anal. Calcd for $C_{38}H_{44}O_4N_2Ir_2Cl_4$: C, 40.80; H, 3.96; N, 2.50. Found: C, 41.52; H, 4.29; N, 2.49. IR (CH_2Cl_2): ν_{CN} 2148, 2127 cm^{-1}. ^{1}H NMR (400 MHz, $CDCl_3$, 25 °C): δ 1.50 (t, 6H, CH_3, $^3J_{HH}$ = 7 Hz), 1.94 (s, 15H, *Cp**), 1.95 (s, 15H, *Cp*'), 4.65 (q, 4H, CH_2, $^3J_{HH}$ = 7 Hz), 7.79 (d, 2H, $H^{5,7}$, $^3J_{HH}$ = 12 Hz), 9.73 (d, 2H, $H^{4,8}$, $^3J_{HH}$ = 12 Hz) ppm. ^{13}C{^{1}H} NMR (125.8 MHz, $CDCl_3$, 25 °C): 9.3 (*C*H_3 of Cp*), 9.5 (*C*H_3 of Cp*'), 15.0 (*C*H_3), 61.9 (*C*H_2), 96.5 (*Cp**), 96.9 (*Cp*'), 116.1, 129.6, 134.5, 137.5, 137. 9, 139.3, 140.1, 141.3 (2,6-diisocyanoazulene motif), 162.8 (*C*O_2Et) ppm. UV-vis (CH_2Cl_2, λ): 482 sh, 422, 346, 312, 232 nm.

IV.3.3 Synthesis of [(Cp*Cl_2Ir)$_2$(μ-η^1:η^1-2,2'-diisocyano-1,1',3,3'-tetraethoxycarbonyl-6,6'-biazulene)] (4.1b).

Compound **4.1b** (0.0743 g, 0.0535 mmol) was obtained in a 68% yield from [(Cp*)Cl_2Ir]$_2$ (0.0623 g, 0.0782 mmol) and 2,2'-diisocyano-1,1',3,3'-tetraethoxycarbonyl-6,6'-biazulene (0.0468 g, 0.0790 mmol) by a procedure similar to that described for **4.1a**. IR (CH_2Cl_2): ν_{CN} 2147 cm^{-1}. ^{1}H NMR (400 MHz, $CDCl_3$, 25 °C): δ 1.52 (t, 12H, CH_3, $^3J_{HH}$ = 7 Hz), 1.96 (s, 30H, *Cp**), 4.67 (q, 8H, CH_2, $^3J_{HH}$ = 7 Hz), 8.04 (d, 4H, $H^{5,7}$, $^3J_{HH}$ = 11 Hz), 9.90 (d, 4H, $H^{4,8}$, $^3J_{HH}$ = 11 Hz) ppm.

IV.3.4 Synthesis of [(Cp*Cl_2Ir)$_2$(μ-η^1:η^1-2,2'-diisocyano-1,1',3,3'-tetraethoxycarbonyl-6,6'-biazulenylacetylene)] (4.1c).

Compound **4.1c** (0.141 g, 0.0998 mmol) was obtained in a 78% yield from [(Cp*)Cl_2Ir]$_2$ (0.102 g, 0.128 mmol) and 2,2'-diisocyano-1,1',3,3'-tetraethoxycarbonyl-6,6'-biazulenylacetylene (0.081 g, 0.131 mmol) by a procedure similar to that described for **4.1a**. IR (CH_2Cl_2): ν_{CC} ~2190, ν_{CN} 2147 cm^{-1}. ^{1}H NMR (400 MHz, $CDCl_3$, 25 °C): δ 1.51 (t, 12H, C*H*$_3$, $^3J_{HH}$ = 7 Hz), 1.96 (s, 30H, *Cp**), 4.66 (q, 8H, C*H*$_2$, $^3J_{HH}$ = 7 Hz), 8.04 (d, 4H, *H*^{5,7}, $^3J_{HH}$ = 11 Hz), 9.73 (d, 4H, *H*^{4,8}, $^3J_{HH}$ = 11 Hz) ppm.

IV.3.5 Synthesis of [(Cp*ClIr)$_4$(μ-η^1:η^1-2,6-diisocyano-1,3-diethoxycarbonylazulene)$_2$(μ-pyrazine)$_2$][SbF_6]$_4$ (4.2a.1).

A solution of $AgSbF_6$ (0.0240 g, 0.0698 mmol) in 5 mL of acetonitrile was added to an orange-red solution of **4.1a** (0.0381 g, 0.034 mmol) in 25 mL of CH_2Cl_2. After stirring for 1 h in the absence of light, pyrazine (0.0028 g, 0.035 mmol) was added and the reaction mixture was stirred for an additional 1 h. The tan reaction mixture was then filtered through a Celite plug and the filtrate was concentrated. Pentane was added to precipitate the product, which after filtration and drying afforded 0.0572 g of yellow-tan **4.2a.1**. IR (CH_2Cl_2): ν_{CN} 2193, 2159 cm^{-1}.

IV.3.6 Synthesis of [(Cp*ClIr)$_4$(μ-η^1:η^1-2,6-diisocyano-1,3-diethoxycarbonylazulene)$_2$(μ-4,4'-bipyridine)$_2$][OTf]$_4$ (4.2a.2).

Compound **4.2a.2** (0.0743 g) was obtained as a tan powder from **4.1a** (0.0497 g, 0.0444 mmol), 4,4'-bipyridine (0.0071 g, 0.045 mmol), and AgOTf (0.0231 g, 0.0899 mmol) by a procedure similar to that described for **4.2a.1**. IR (CH_2Cl_2): ν_{CN} 2179, 2157cm^{-1}.

IV.3.7 Synthesis of [(Cp*ClIr)$_4$(μ-η^1:η^1-2,2'-diisocyano-1,1',3,3'-tetraethoxycarbonyl-6,6'-biazulene)$_2$(μ-pyrazine)$_2$][OTf]$_4$ (4.2b).

Compound **4.2b** (0.0274 g) was obtained as a tan powder from **4.1b** (0.0313 g, 0.0225 mmol), pyrazine (0.0040 g, 0.045 mmol), and AgOTf (0.0064 g, 0.023 mmol) by a procedure similar to that described for **4.2a.1**. IR (CH_2Cl_2): ν_{CN} 2172 cm^{-1}.

IV.3.8 Synthesis of [(Cp*ClIr)$_4$(μ-η^1:η^1-2,2'-diisocyano-1,1',3,3'-tetraethoxycarbonyl-6,6'-biazulenylacetylene)$_2$(μ-pyrazine)$_2$][OTf]$_4$ (4.2c).

Compound **4.2c** (0.0197 g) was obtained as a tan powder from **4.1c** (0.0224 g, 0.0158 mmol), pyrazine (0.0028 g, 0.035 mmol), and AgOTf (0.0045 g, 0.018 mmol) by a procedure similar to that described for **4.2a.1**. IR (CH_2Cl_2): ν_{CN} 2171 cm^{-1}.

IV.3.9 Synthesis of [(Cp*ClIr)$_4$(μ-η^1:η^1-2,6-diisocyano-1,3-diethoxycarbonylazulene)$_2$(μ-η^1:η^1-1,4-diisocyanodurene)$_2$][SbF$_6$]$_4$ (4.3a).

Compound **4.3a** (0.0538 g, 0.0158 mmol) was obtained as a tan powder in an 80% yield from **4.1a** (0.0440 g, 0.0393 mmol), 1,4-diisocyanodurene (0.0074 g, 0.040 mmol), and $AgSbF_6$ (0.0277 g, 0.0806 mmol) by a procedure similar to that described for **4.2a.1**. IR (CH_2Cl_2): ν_{CN} 2202, 2167 cm^{-1}. ^{1}H NMR (400 MHz, CD_2Cl_2, 25 °C): δ 1.40 (m br, 12H, C*H*$_3$-ethoxycarbonyl), 2.18 (m, 60H, *Cp**), 2.45 (s, 24H, C*H*$_3$-durene), 4.44 (m br, 8H, C*H*$_2$), 7.98 (m br, 4H, *H*^{5,7}), 9.83 (m br, 4H, *H*^{4,8}) ppm.

IV.3.10 Synthesis of $[(Cp^*ClIr)_4(\mu\text{-}\eta^1\text{:}\eta^1\text{-}2,2'\text{-diisocyano-}1,1',3,3'\text{-tetraethoxycarbonyl-}6,6'\text{-biazulene})_2(\mu\text{-}\eta^1\text{:}\eta^1\text{-}1,4\text{-diisocyanodurene})_2][SbF_6]_4$ (4.3b).

Compound **4.3b** (0.0908 g, 0.0230 mmol) was obtained as a brown powder in a 88% yield from **4.1b** (0.0730 g, 0.0525 mmol), 1,4-diisocyanodurene (0.0099 g, 0.054 mmol), and $AgSbF_6$ (0.0370 g, 0.108 mmol) by a procedure similar to that described for **4.2a.1**. IR (CH_2Cl_2): ν_{CN} 2205, 2177 cm^{-1}. ^1H NMR (400 MHz, CD_2Cl_2, 25 °C): δ 1.43 (m br, 24H, C*H*$_3$-ethyoxycarbonyl), 2.20 (m, 60H, *Cp**), 2.48 (s, 24H, C*H*$_3$-durene), 4.47 (m br, 16H, C*H*$_2$), 8.20 (d, 8H, $H^{5,7}$, $^3J_{HH}$ = 11 Hz), 9.87 (m, 8H, $H^{4,8}$) ppm. MS (ESI, positive *m*/*z*): 751.4 $(M^{4+} + 1)^{4+}$, 1018.6 $(M^{4+}$ - durene + $SbF_6^-)^{3+}$, 1079.9 $(M^{4+} + SbF_6^-)^{3+}$.

IV.3.11 Synthesis and thermally-controlled isomerism of $[(Cp^*Cl_2Ir)(\eta^1\text{-}2,6\text{-diisocyano-}1,3\text{-diethoxycarbonylazulene})]$ (4.4).

An orange solution of $[(Cp^*)Cl_2Ir]_2$ (0.0598 g, 0.0751 mmol) in 30 mL of CH_2Cl_2 was added dropwise to a purple solution of 2,6-diisocyano-1,3-diethoxycarbonylazulene (0.0490 g, 0.152 mmol) in 15 mL of CH_2Cl_2. After stirring for 1 h at room temperature, the reaction mixture was concentrated and pentane (40 mL) was added to precipitate the product. IR (CH_2Cl_2): ν_{CN} 2147 sh, 2126, 2116 sh cm^{-1}. ^1H NMR (400 MHz, CD_2Cl_2, 25 °C): isomer one – δ 1.48 (t, C*H*$_3$, $^3J_{HH}$ = 7 Hz), 1.89 (s, *Cp**), 4.59 (q, C*H*$_2$, $^3J_{HH}$ = 7 Hz), 7.81 (d, $H^{5,7}$, $^3J_{HH}$ = 11 Hz), 9.74 (d, $H^{4,8}$, $^3J_{HH}$ = 11 Hz) ppm; isomer two – δ 1.46 (t, C*H*$_3$, $^3J_{HH}$ = 7 Hz), 1.87 (s, *Cp**), 4.50 (q, C*H*$_2$, $^3J_{HH}$ = 7 Hz), 7.81 (d, $H^{5,7}$, $^3J_{HH}$ = 11 Hz), 9.70 (d, $H^{4,8}$, $^3J_{HH}$ = 11 Hz) ppm; isomer one/isomer two ratio (following room temperature synthesis) ≈ 1.67:1.

The above sample was then subjected to reflux conditions at 66 °C in 30 mL of THF for 1 h. The product was precipitated with pentane, filtered and dried. ^{1}H NMR (400 MHz, CD_2Cl_2, 25 °C): isomer one/isomer two ratio ≈ 2.5:1.

The sample was then subjected to reflux conditions at 84 °C in 30 mL of 1,2-dichloroethane for 1 h. The product was precipitated with pentane, filtered and dried. ^{1}H NMR (400 MHz, CD_2Cl_2, 25 °C): isomer one/isomer two ratio ≈ 3.75:1.

The sample was then subjected to reflux conditions at 84 °C in 30 mL of 1,2-dichloroethane for an additional 3 h. The product was precipitated with pentane, filtered and dried to give **4.4** as a red-brown powder (0.0598 g, 0.0830 mmol). IR (CH_2Cl_2): ν_{CN} 2147 sh, 2126 cm^{-1}. ^{1}H NMR (400 MHz, CD_2Cl_2, 25 °C): Isomer one/isomer two ratio = Immeasurable (i.e., only one isomer present).

IV.3.12 Synthesis of [(Cp*Cl$_2$Ir)(μ-η^1:η^1-2,6-diisocyano-1,3-diethoxycarbonylazulene){Cr(CO)$_5$}] (4.5a).

A solution of $[Cp^*Cl_2Ir]_2$ (0.0431 g, 0.0541 mmol) in 12.5 mL of CH_2Cl_2 was added to a raspberry-colored solution of {$(OC)_5Cr$} {2,6-diisocyano-1,3-diethoxycarbonylazulene-κ(^{2}*CN*)} (0.0563 g, 0.110 mmol) in 25 mL of CH_2Cl_2. After the reaction mixture was stirred for 1 h, the solution was concentrated at room temperature and pentane (75 mL) was added with vigorous stirring. The resultant precipitate was filtered, washed with pentane (3 × 2 mL), and dried at 10^{-2} Torr to afford **4.5a** (0.0920 g, 0.101 mmol) in a 93% yield as a purple-red powder. Mp: the product decomposed without melting at 135°C. IR (CH_2Cl_2): ν_{CN} 2129 cm^{-1}; ν_{CO} 2042, 1962 cm^{-1}. ^{1}H NMR (500 MHz, $CDCl_3$, 25 °C): δ 1.51 (t, 6H, C*H*$_3$, $^3J_{HH}$ = 7 Hz), 1.95 (s, 15H, *Cp**), 4.59 (q, 4H, C*H*$_2$, $^3J_{HH}$ = 7 Hz), 7.80 (d, 2H, *H*^{5,7}, $^3J_{HH}$ = 11 Hz), 9.74 (d, 2H, *H*^{4,8}, $^3J_{HH}$ = 11 Hz)

ppm. $^{13}C\{^1H\}$ NMR (125.8 MHz, $CDCl_3$, 25 °C): 9.5 (*C*H_3 of Cp*), 14.8 (*C*H_3), 61.6 (*C*H_2), 96.8 (*Cp**), 114.9, 129.8, 133.2, 137.0, 137.5, 138.6, 141.3, 163.0, 186.6 (2,6-diisocyanoazulene motif), 214.4 (*C*O *cis*), 215.1 (*C*O *trans*) ppm. UV-vis (CH_2Cl_2, λ (log ε)): 504 (4.44), 362 (4.50), 312 (4.79), 237 (4.87) nm.

IV.3.13 Synthesis of [(Cp*Cl_2Ir)(μ-η^1:η^1-2,6-diisocyano-1,3-diethoxycarbonylazulene){$Cr(CO)_5$}] (4.5b).

Compound **4.5b** (0.0641 g, 0.0703 mmol) was obtained as a light red powder in an 83% yield from [Cp*Cl_2Ir]$_2$ (0.0339 g, 0.0425 mmol) and {$(OC)_5$Cr}{2,6-diisocyano-1,3-diethoxycarbonylazulene-κ(^{6}*CN)*} (0.0443 g, 0.0862 mmol) by a procedure similar to that described for **4.5a**. Mp: the product decomposed without melting at 194°C. IR (CH_2Cl_2): ν_{CN} 2147, 2122 cm^{-1}; ν_{CO} 2032, 1966 cm^{-1}. ^{1}H NMR (500 MHz, $CDCl_3$, 25 °C): δ 1.50 (t, 6H, C*H*$_3$, $^3J_{HH}$ = 7 Hz), 1.95 (s, 15H, *Cp**), 4.65 (q, 4H, C*H*$_2$, $^3J_{HH}$ = 7 Hz), 7.69 (d, 2H, *H*^{5,7}, $^3J_{HH}$ = 11 Hz), 9.73 (d, 2H, *H*^{4,8}, $^3J_{HH}$ = 11 Hz) ppm. $^{13}C\{^1H\}$ NMR (125.8 MHz, $CDCl_3$, 25 °C): 9.3 (*C*H_3 of Cp*), 15.0 (*C*H_3), 61.8 (*C*H_2), 96.3 (*Cp**), 115.9, 129.0, 133.9, 137.8, 139.4, 139.8, 140.8, 162.9, 181.7 (2,6-diisocyanoazulene motif), 213.8 (*C*O *cis*), 215.4 (*C*O *trans*) ppm. UV-vis (CH_2Cl_2, λ (log ε)): 496 (4.54), 316 (4.71), 240 (4.87) nm.

IV.3.14 Synthesis of [(Cp*ClIr)$_2$(μ-η^1:η^1-1,4-diisocyanodurene)(μ-η^1:η^1-2,6-diisocyano-1,3-diethoxycarbonylazulene)$_2${$Cr(CO)_5$}$_2$][SbF_6]$_2$ (4.6a).

Compound **4.6a** (0.0486 g, 0.0202 mmol) was obtained as a purple powder in a 73% yield from **4.5a** (0.0503 g, 0.0551 mmol), 1,4-diisocyanodurene (0.0052 g, 0.028 mmol), and $AgSbF_6$ (0.0194 g, 0.0565 mmol) by a procedure similar to that described for **4.2a.1**. IR (CH_2Cl_2): ν_{CN} 2199, 2166, 2131; ν_{CO} 2041, 1963 cm^{-1}. ^{1}H NMR (400 MHz, $CDCl_3$, 25 °C): δ

1.49 (m br, 12H, CH_3-ethoxycarbonyl), 2.18 (m, 30H, *Cp**), 2.44 (m, 12H, CH_3-durene), 4.56 (m br, 8H, CH_2), 7.91 (d, 4H, $H^{5,7}$, $^3J_{HH}$ = 10 Hz), 9.83 (m, 4H, $H^{4,8}$) ppm.

IV.3.15 Synthesis of [(Cp*ClIr)$_2$(μ-η^1:η^1-1,4-diisocyanodurene)(μ-η^1:η^1-2,6-diisocyano-1,3-diethoxycarbonylazulene)$_2${Cr(CO)$_5$}$_2$][SbF$_6$]$_2$ (4.6b).

Compound **4.6b** (0.0499 g, 0.0207 mmol) was obtained as a purple powder in a 85% yield from **4.5b** (0.0447 g, 0.0489 mmol), 1,4-diisocyanodurene (0.0046 g, 0.025 mmol), and $AgSbF_6$ (0.0173 g, 0.0503 mmol) by a procedure similar to that described for **4.2a.1**. IR (CH_2Cl_2): ν_{CN} 2205, 2175, 2121; ν_{CO} 2028, 1968 cm^{-1}. ^{1}H NMR (400 MHz, $CDCl_3$, 25 °C): δ 1.44 (m br, 12H, CH_3-ethoxycarbonyl), 2.19 (s, 30H, *Cp**), 2.44 (s, 12H, CH_3-durene), 4.49 (m br, 8H, CH_2), 7.78 (d, 4H, $H^{5,7}$, $^3J_{HH}$ = 10 Hz), 9.71 (m, 4H, $H^{4,8}$) ppm.

IV.3.16 Synthesis of [(Cp*ClIr)$_2$(μ-4,4'-bipyridine)(μ-η^1:η^1-2,6-diisocyano-1,3-diethoxycarbonylazulene)$_2${Cr(CO)$_5$}$_2$][OTf]$_2$ (4.7a).

Compound **4.7a** (0.0470 g) was obtained as a purple powder from **4.5a** (0.0508 g, 0.0557 mmol), 4,4'-bipyridine (0.0045 g, 0.029 mmol), and AgOTf (0.0147 g, 0.0572 mmol) by a procedure similar to that described for **4.2a.1**. IR (CH_2Cl_2): ν_{CN} 2153, 2133; ν_{CO} 2042, 1961 cm^{-1}.

IV.4 Results and Discussion

The synthesis of the two-dimensional metal-organic frameworks, specifically the "molecular rectangles," featuring symmetric and asymmetric azulenes begins with the respective diiridium "edge" pieces. Compound **4.1a**, the first azulene-containing edge of a metal-organic framework, was synthesized from the combination of one equivalent of $[Cp^*Cl_2Ir]_2$ and one equivalent of 2,6-diisocyano-1,3-diethoxycarbonylazulene in CH_2Cl_2 (Scheme IV.2). The asymmetry of this complex is noted by two distinct isocyanide stretching (ν_{CN}) bands revealed by the FTIR analysis in CH_2Cl_2 (Figure IV.5). Upon complexation, the stretching frequencies of the 2-isocyanide (uncomplexed ν_{CN} = 2126 cm^{-1}) and 6-isocyanide (uncomplexed ν_{CN} = 2116 cm^{-1}) are found at 2148 and 2127 cm^{-1}, respectively. These shifts to higher energy correspond with the isocyanides acting more as σ-donors than π-acceptors to stabilize the high-valent Ir(III) metal centers. The lone pair on the carbon atom of the isocyanide has antibonding character with respect to the C≡N bond such that donation of said lone pair will strengthen the bond and require higher energy to induce a vibration.

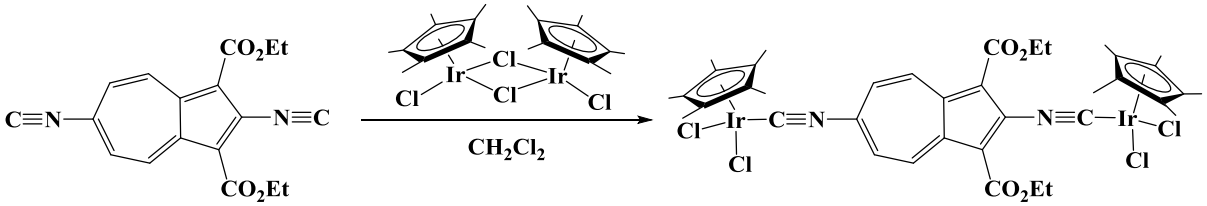

ν_{CN} = 2125, 2116 cm^{-1}

ν_{CN} = ~2148, 2127 cm^{-1}

4.1a

Scheme IV.2

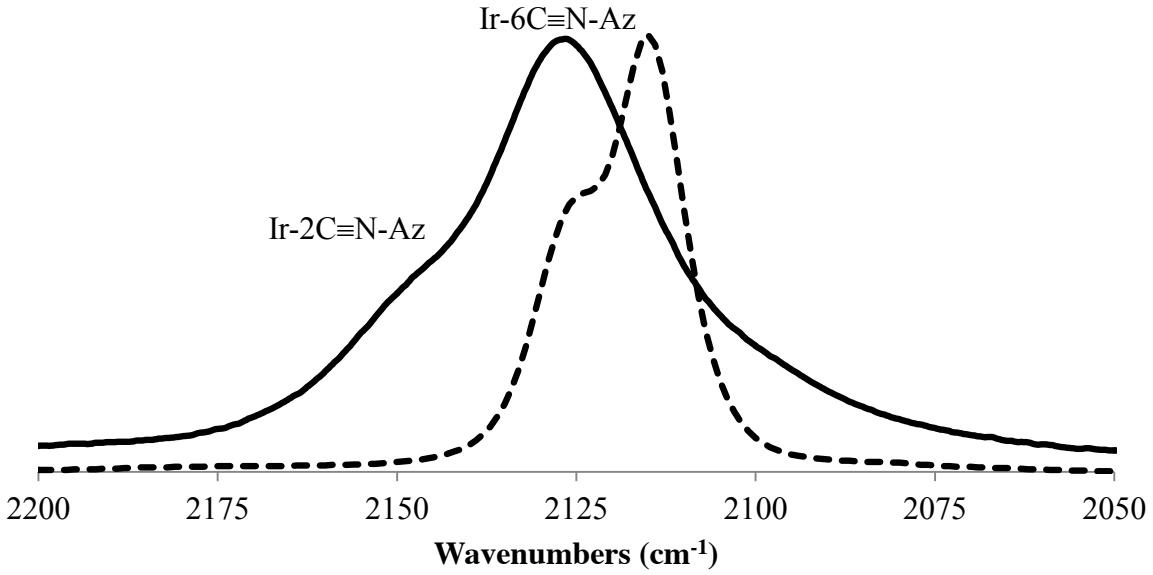

Figure IV.5 FTIR spectra of **4.1a** (solid line) and free 2,6-diisocyano-1,3-diethoxycarbonylazulene (dashed line) in CH_2Cl_2.

X-ray analysis of **4.1a** provided the first structural data of an azulene-containing edge piece, the crystal structure of which is shown in Figure IV.6. Compound **4.1a** crystallizes in the orthorhombic space group $P2_12_12_1$. The ^{1}H NMR spectrum of **4.1a** shows two distinct aromatic environments belonging to the $H^{4,8}$ and $H^{5,7}$ hydrogen nuclei as well as one intense resonance belonging to the ^{1}H nuclei of the Cp* methyl groups.

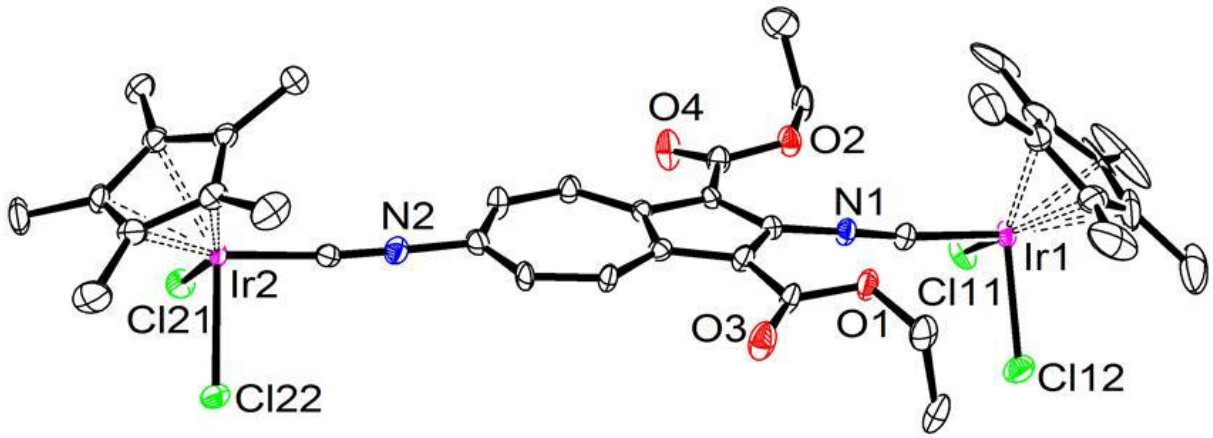

Figure IV.6 Molecular structure of **4.1a** (50% thermal ellipsoids).

The coupling of two azulenic motifs can be envisioned to produce three different biazulenic motifs that could be used as π-bridges in molecular rectangles.[22] The 2,2'-biazulene and the 6,6'-biazulene represent symmetric variations while the 2,6'-biazulene constitutes an asymmetric variation. The symmetric azulene-containing edge pieces can be synthesized from 6,6'-biazulenes, namely 2,2'-diisocyano-1,1',3,3'-tetraethoxycarbonyl-6,6'-biazulene[19] and bis(2-isocyano-1,3-diethoxycarbonyl-6-azulenyl)acetylene[20]. The syntheses of these symmetric diiridium edges are shown in Scheme IV.3. Compound **4.1b** (68% yield) features the non-planar biazulene motif and **4.1c** (78% yield) contains the planar biazulene motif supported by an acetylene spacer. Both **4.1b** and **4.1c** exhibit isocyanide stretching bands in their respective FTIR spectra at 2147 cm^{-1} in CH_2Cl_2, whereas the isocyanide stretching frequencies of the uncomplexed ligands appear at around 2125 cm^{-1}, similar to other 2-isocyanoazulenes. Interestingly, the alkyne stretching frequency ($\nu_{C\equiv C}$) of **4.1c** presents as a shoulder in CH_2Cl_2 at 2190 cm^{-1}, which is relatively unchanged from the uncomplexed biazulene ($\nu_{C\equiv C}$ = 2189 cm^{-1}) in CH_2Cl_2.

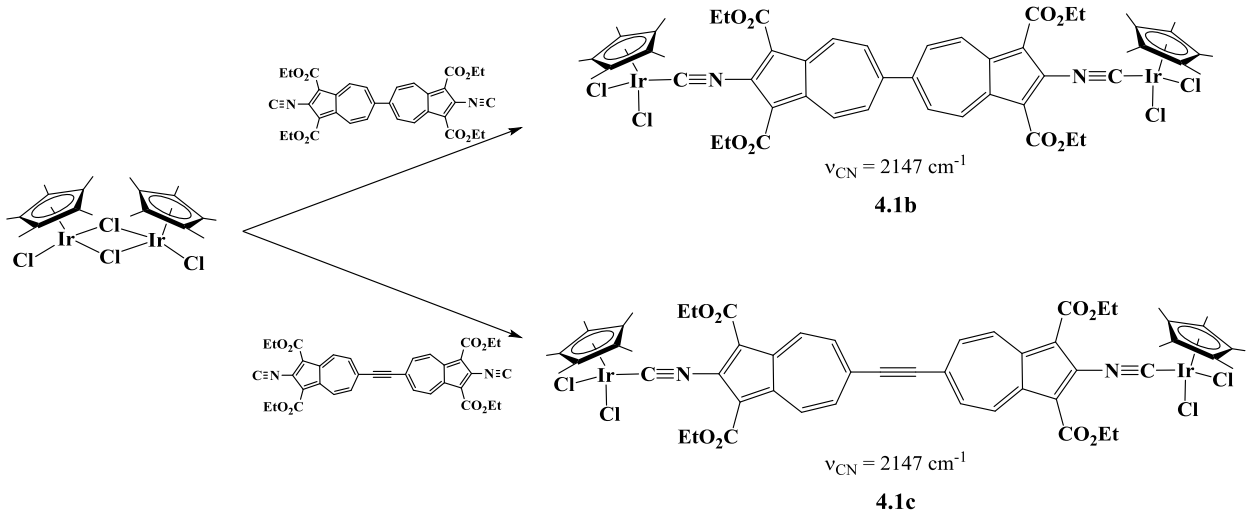

Scheme IV.3

The Cp^*Cl_2Ir corner piece is an attractive building block for metal-organic frameworks because of the ability to connect two ligands or bridges at a 90° angle. Once the first bridge is installed, a coordination site at the iridium center can be opened via halide abstraction with a Ag(I) salt thereby leaving room for the second bridge to coordinate. Yamamoto *et al*. demonstrated this versatility in their tetrairidium frameworks by using diisocyanodurene and pyrazine or bipyridine to link four {Cp*ClIr} corner pieces (Figure IV.2).[8] As shown in Scheme IV.4, a similar approach was taken with the 2,6-diisocyano-1,3-diethoxycarbonylazulene bridge.

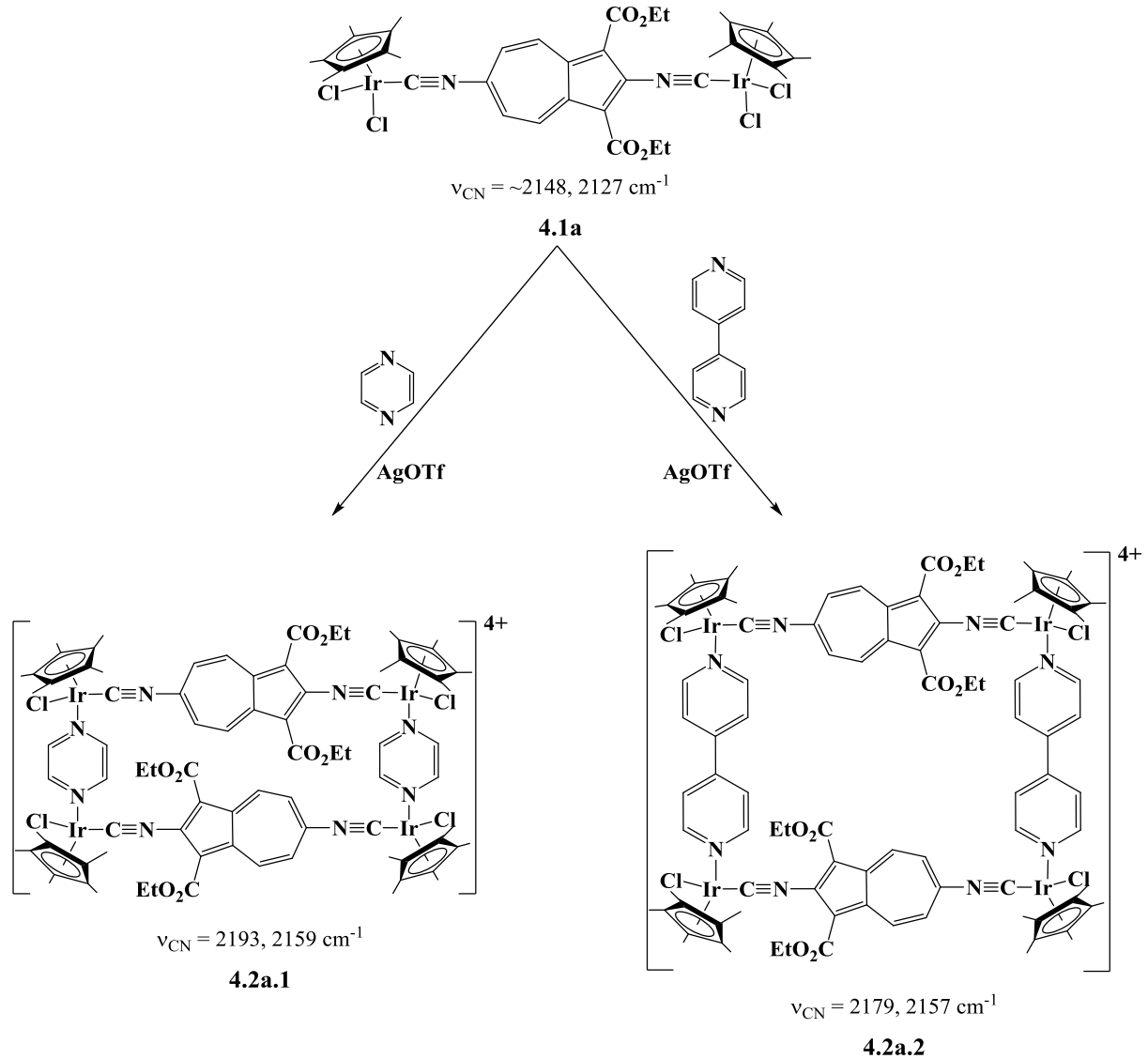

Scheme IV.4

Halide abstraction of one chloride ligand from both Ir(III) centers in **4.1a** with two equivalents of AgOTf opens one coordination site at each corner piece. Filtration of the AgCl precipitate and subsequent treatment of the intermediate with one equivalent of pyrazine or 4,4'-bipyridine should yield two possible azulene-based metal-organic frameworks **4.2a.1** and **4.2a.2**, respectively (Scheme IV.4). The use of two bridging heterocyclic amines of different lengths allows for tunability of the framework in terms of edge length and cavity area. Given the different distances between the nitrogen atoms (d_{N-N}) of the heterocyclic amines pyrazine (d_{N-N} ~ 2.7 Å) and 4,4'-bipyridine (d_{N-N} ~ 6.9 Å), these substitutions should lend toward straightforward alterations.

IR analysis of **4.2a.1** revealed two isocyanide stretching bands in CH_2Cl_2 at 2193 and 2159 cm^{-1} corresponding to the bound 2- and 6-isocyanides, respectively. The IR spectrum of **4.2a.2** exhibits a similar pattern with two isocyanide stretching bands at 2179 and 2156 cm^{-1}. This shift in isocyanide stretching frequency to higher energy upon going from the diiridium edge to the tetrairidium framework implies an increase of σ-donation of the isocyanide to stabilize the now formally $[Cp^*ClIr]^+$ cation following the halide abstraction. In fact, the observed isocyanide stretching frequencies of **4.2a.1** and **4.2a.2** correspond nicely to that documented for the tetrairidium framework $[(Cp^*ClIr)_4(\mu\text{-diisocyanodurene})_2(\mu\text{-pyrazine})_2]^{4+}$ (ν_{CN} = 2176 cm^{-1}) by Yamamoto *et al.*[8]

Due to the asymmetry of the monoazulenic bridge, two isomers of a given framework are possible: parallel and antiparallel. In the parallel isomer, the dipoles of the azulenic moieties align in the same direction such that the 5-membered ring of one azulenic core resides next to the 5-membered ring of the neighboring azulene bridge. In the antiparallel isomer, the dipoles of the azulene motifs align in a head-to-tail fashion such that a 5-membered ring of one azulene resides

next to the 7-membered ring of the adjacent azulene. Unfortunately, the ^{1}H NMR spectra of **4.2a.1** and **4.2a.2** are complex and feature more multiplets than expected in the aromatic region should just two of these isomers co-exist. This result suggests that heterocyclic amines are not feasible bridges in the presence of the 2,6-diisocyanoazulene, leading to possible oligimerization.

To test the possibility that the order of addition of reagents is relevant, **4.2a.1** was produced in an alternate fashion (Route B) as shown in Scheme IV.5. The symmetric, pyrazine-bridged diiridium edge piece $(Cp^*Cl_2Ir)_2(\mu$-pyrazine) was synthesized according to literature procedures.[8] Following halide abstraction, the symmetric edge pieces were conjoined with the 2,6-diisocyano-1,3-diethoxycarbonylazulene bridge. The ^{1}H NMR and IR spectra of the product of Route B are identical to those spectra observed for the product synthesized by Route A as discussed above, reinforcing an incompatibility between the 2,6-diisocyanoazulene and heterocyclic amine bridges.

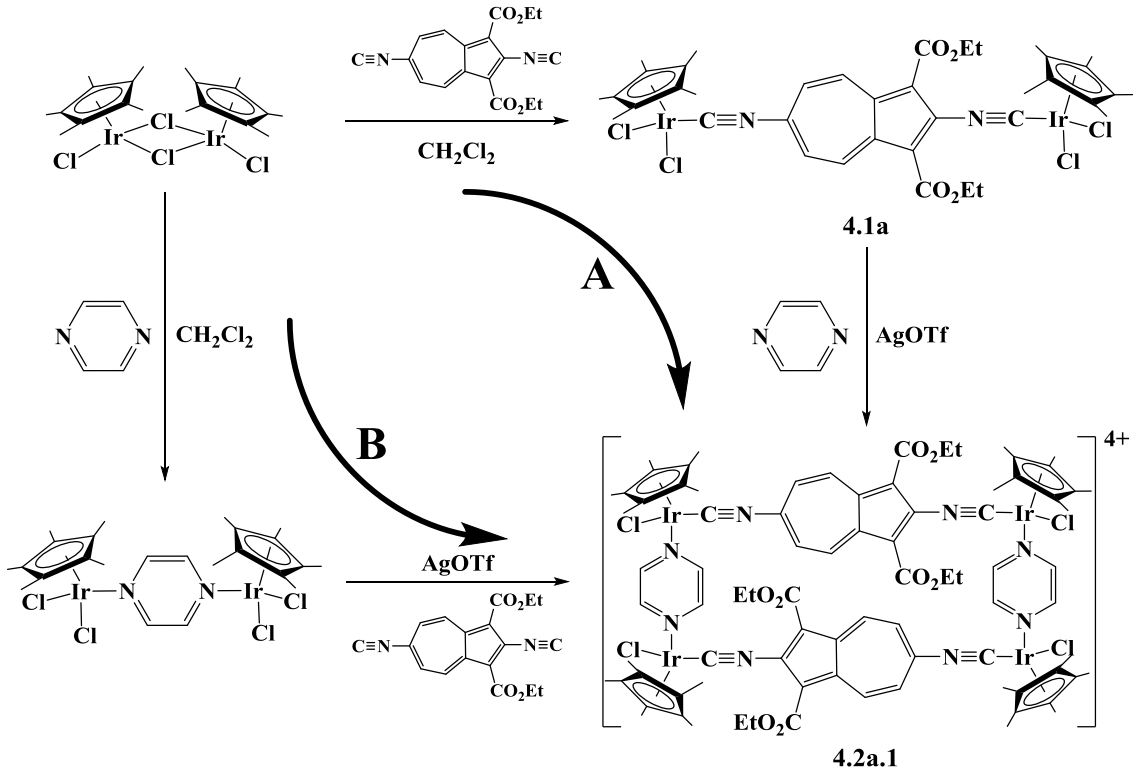

Scheme IV.5

To alleviate the issue of two possible molecular rectangle isomers, the asymmetric 2,6-diisocyanoazulene was replaced with a symmetric diisocyanobiazulene. In a synthetic vein similar to **4.2a.1**, the symmetric molecular rectangles **4.2b** and **4.2c** were produced from the symmetric diiridium edges **4.1b** and **4.1c**, respectively. Scheme IV.6 shows the synthesis of **4.2b**. Following halide abstraction from each iridium center, the diiridium edges were connected with pyrazine. The IR spectra of both **4.2b** and **4.2c** both reveal an isocyanide stretch at 2171 cm^{-1} in CH_2Cl_2. Similar to **4.2a.1** and **4.2a.2**, the ^1H NMR spectra of the symmetric molecular rectangles are exceedingly ambiguous and feature many more aromatic environments than expected. An alternate synthesis to molecular rectangles **4.2b** and **4.2c** in a fashion similar to Route B in Scheme IV.5 was undertaken and provided the same products as in the first route described above.

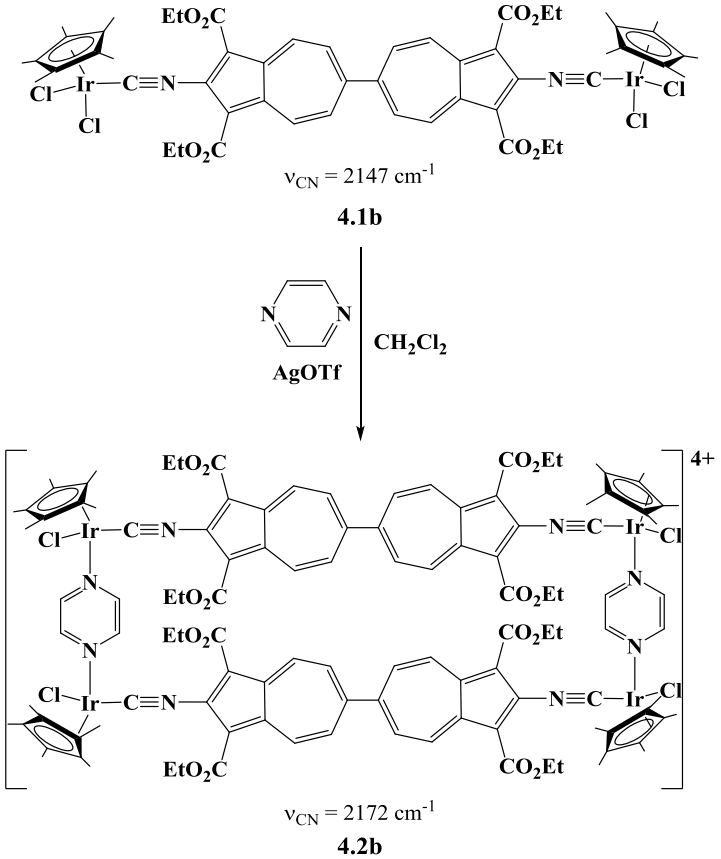

Scheme IV.6

The unexpected and ambiguous multiplets observed in the ^{1}H NMR spectra of **4.2a.1**, **4.2a.2**, **4.2b** and **4.2c** confirm that heterocyclic amines are incompatible with the linear, isocyanide-terminated, nonbenzenoid azulene and biazulenes despite the fact that the IR spectra of these four compounds suggest the tetrairidium frameworks may have been formed. The spectroscopic data feasibly suggests linear or branched coordination oligo- or polymers, which are inseparable due to similar solubility profiles. This incompatibility is attributed to the nature of bond formation between the Ir(III) centers and bridges. Isocyanides bond to metal centers under kinetic control only if the metal center is electron-rich. This is due to the formation of the M(dπ)→CNAr(pπ*) backbond that strengthens the Ir-CN bond. On the other hand, isocyanides and the heterocyclic amines bond to electron-poor metals under thermodynamic control. That is, the Ir-N or Ir-CN bonds can continuously be broken and remade until the most stable configuration (e.g., sterically favored) is achieved as π-backbonding will not occur to such an extent in the electron-poor case as it would in the electron-rich case. Such a rearrangement, or scrambling, in solution can lead to the undesired exchange of edge pieces in a molecular rectangle. To account for the complex ^{1}H NMR spectra of **4.2a.1**, **4.2a.2**, **4.2b**, and **4.2c**, scrambling must be occurring when the combination of heterocyclic amines and nonbenzenoid isocyanides are used as edge pieces.

An alternative bridge to a heterocyclic amine is a benzenoid diisocyanoarene, such as 1,4-diisocyanodurene (durene = 2,3,5,6-tetramethylbenzene). Compound **4.1a** was subjected to halide abstraction and then treated with two equivalents of diisocyanodurene to connect the two diiridium edge pieces (Scheme IV.7, Route A). The resultant molecular rectangle, **4.3a**, was isolated in an 80% yield. FTIR analysis of **4.3a** in CH_2Cl_2 revealed a pattern with two isocyanide stretching bands (Figure IV.7). The isocyanide stretch associated with the Ir-C≡N-

durene bond occurs at 2201 cm^{-1}, while the stretches associated with the Ir-C≡N-azulene bonds coincidentally overlap at 1966 cm^{-1}. Compound **4.3a** can also be produced following Route B as shown in Scheme IV.7.

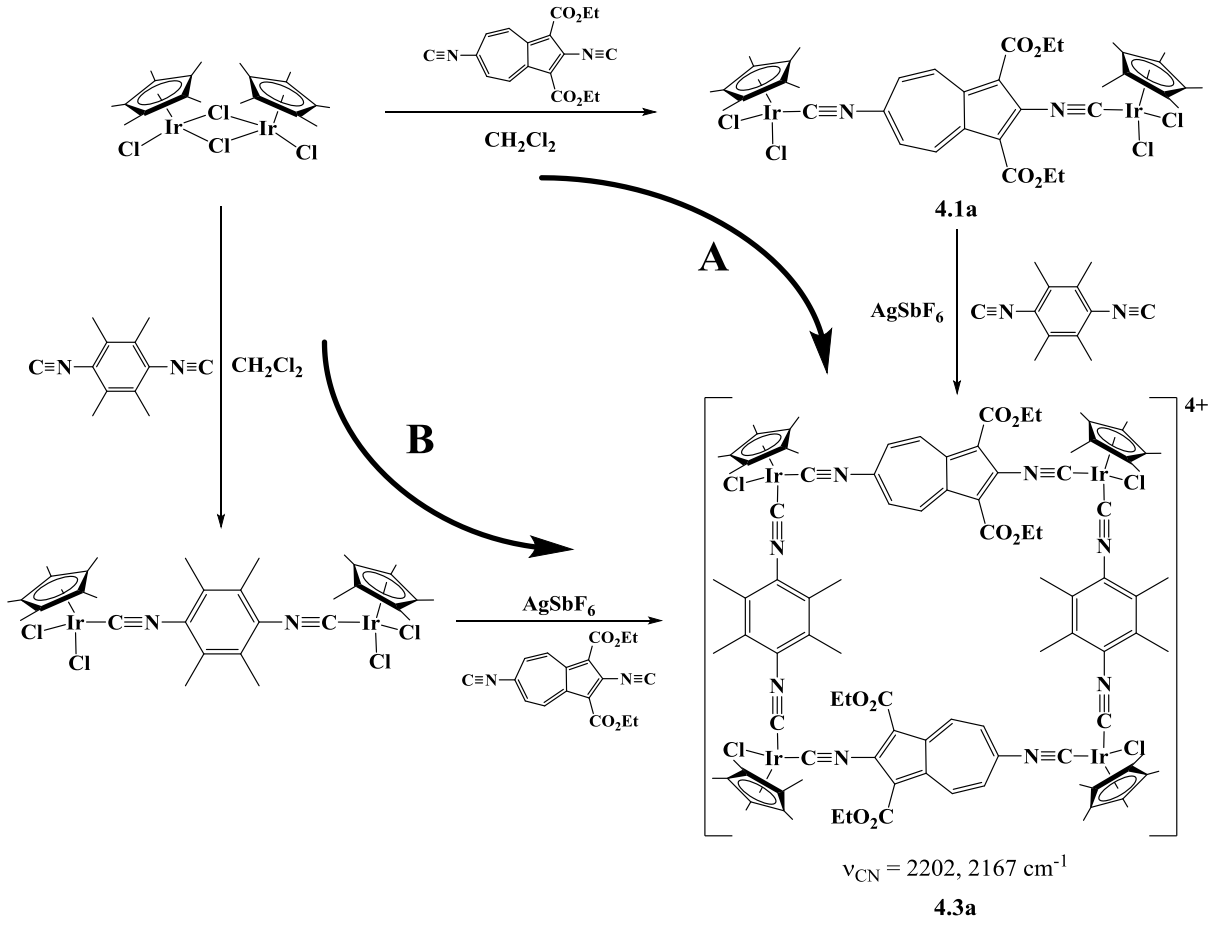

Scheme IV.7

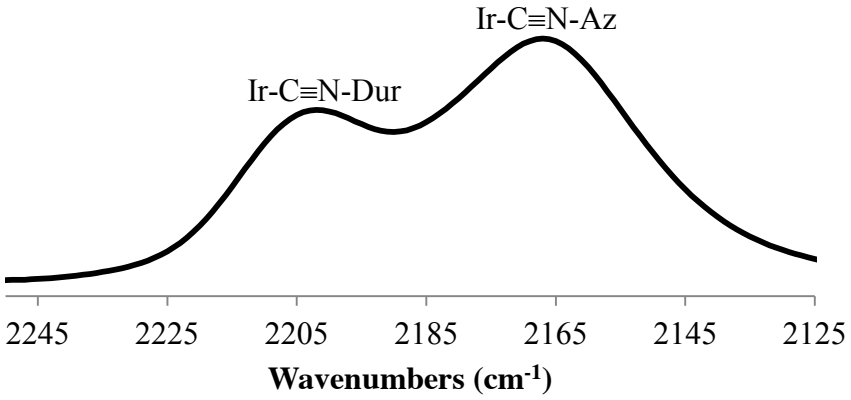

Figure IV.7 FTIR spectrum of **4.3a** in CH_2Cl_2.

Encouragingly, the ^{1}H NMR spectrum of **4.3a** is representative of the expected set of resonances. As can be seen in Figure IV.8, the aromatic region in the ^{1}H NMR spectrum of **4.3a** exhibits two coupled resonances corresponding to the $H^{4,8}$ and $H^{5,7}$ azulenic hydrogen nuclei as determined by the two-dimensional NMR technique COSY. The same region of **4.2a.2** is ambiguous. The broad resonances are explainable based on hindered rotation of the azulenic motifs within the cavity, presumably due to the presence of the bulky 1,3-diethoxycarbonyl substituents. Indeed, the resonances corresponding to the $-CH_2-$ and $-CH_3$ units of the ethoxycarbonyl groups are broadened as well. Furthermore, the integration agrees nicely with the expected formulation of two monoazulenic bridges (two aromatic multiplets, each integrated to four protons), two durene bridges (one aliphatic resonance, 24 protons), and four Cp* units (aliphatic multiplet, 60 protons).

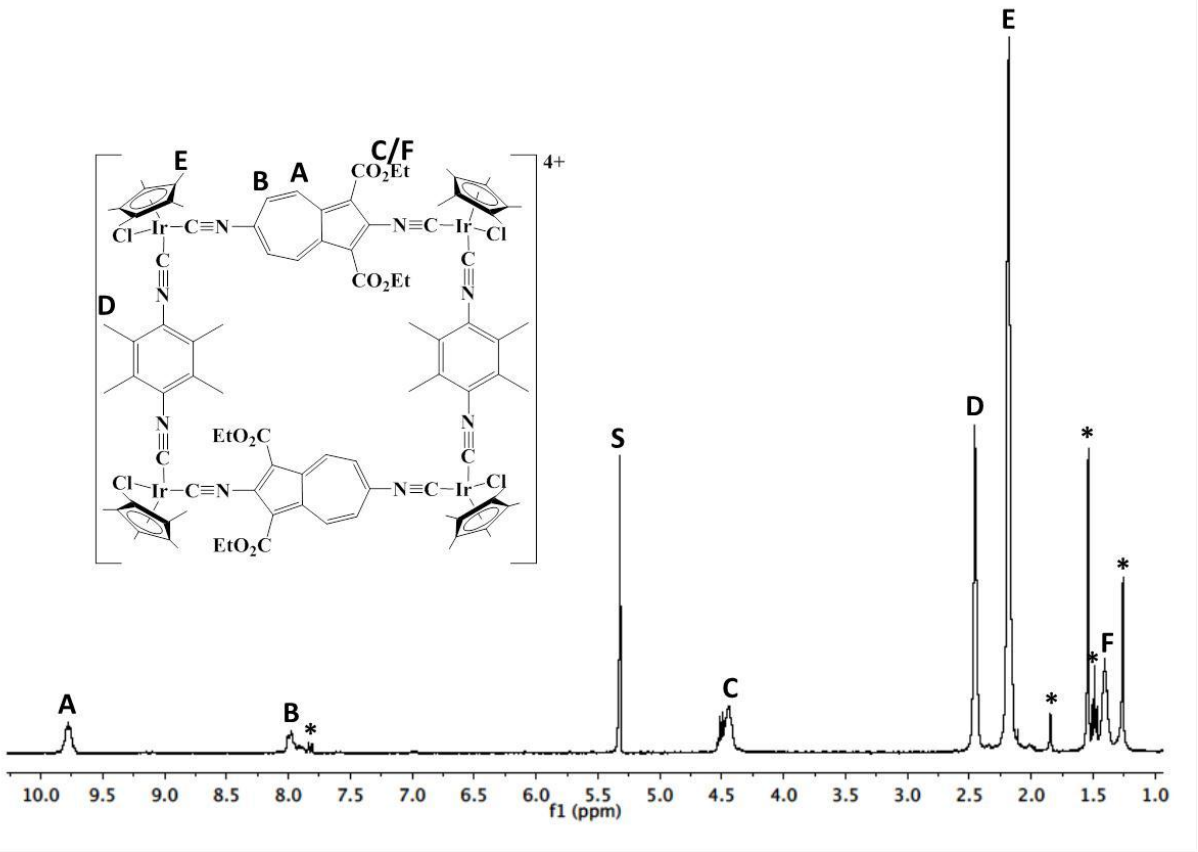

Figure IV.8 ^{1}H NMR spectrum of **4.3a** in CD_2Cl_2 (* = impurity; S = residual solvent).

Similarly, the molecular rectangle featuring the symmetric biazulene bridge 2,2'-diisocyano-1,1',3,3'-tetraethoxycarbonyl-6,6'-biazulene was prepared as shown in Scheme IV.8. Combining one equivalent of **4.1b** with two equivalents of $AgSbF_6$ in the presence of one equivalent of diisocyanodurene in a CH_2Cl_2/acetonitrile mixture formed compound **4.3b** in an 88% yield. The FTIR spectrum of **4.3b** in CH_2Cl_2 (Figure IV.9) showed two isocyanide stretching bands: the Ir-C≡N-durene stretch (ν_{CN} = 2205 cm^{-1}) and the Ir-C≡N-biazulene stretch (ν_{CN} = 2177 cm^{-1}). These observed stretching frequencies are similar to those documented for **4.3a**. According to the ^1H NMR spectrum of **4.3b** in CD_2Cl_2, this compound appears to be a symmetric molecular rectangle with resolved doublets in the aromatic region (Figure IV.10) as opposed to the heterocyclic amine-containing **4.2b**. The resonances corresponding to the ethoxycarbonyl groups are broad as is seen in the ^1H NMR spectrum for **4.3a**, presumably due to sterically hindered rotation within the cavity.

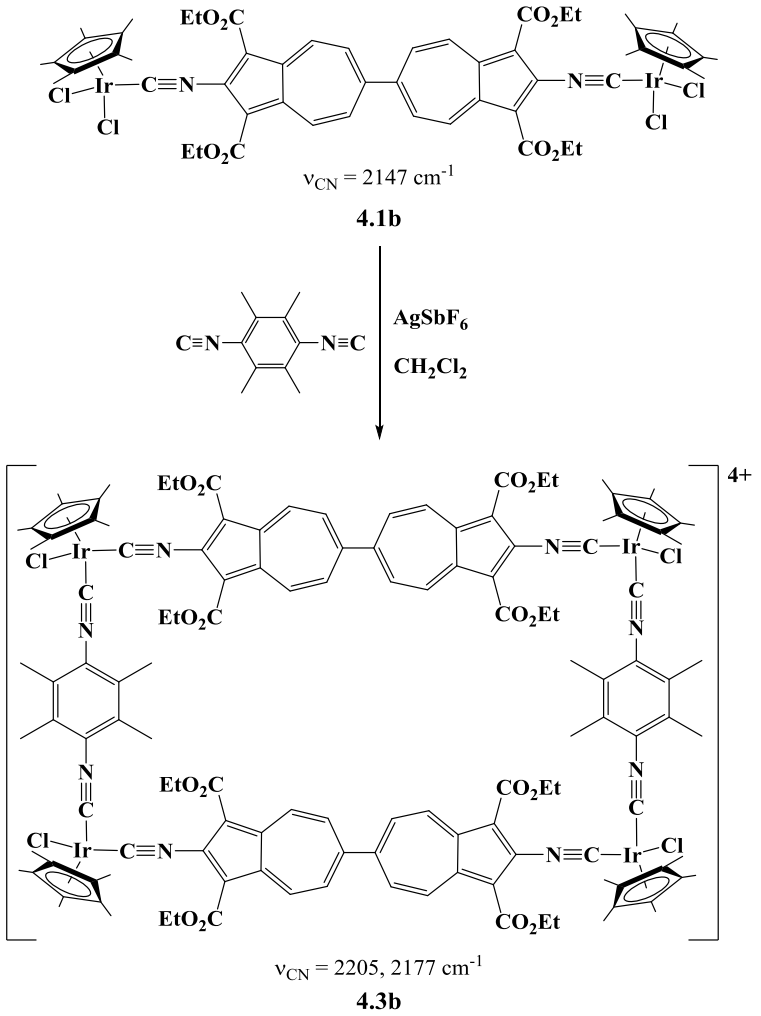

Scheme IV.8

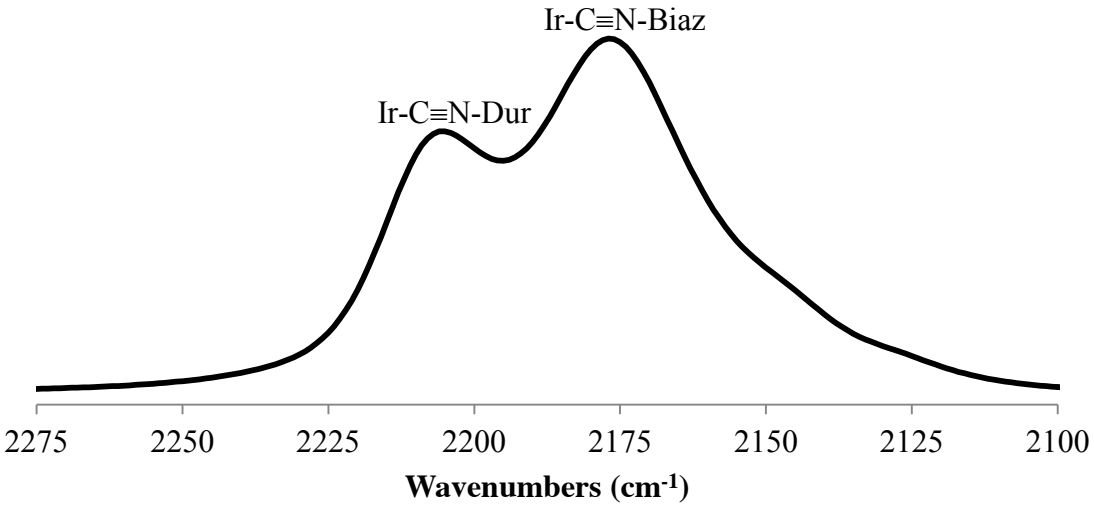

Figure IV.9 The FTIR spectrum of **4.3b** in CH_2Cl_2.

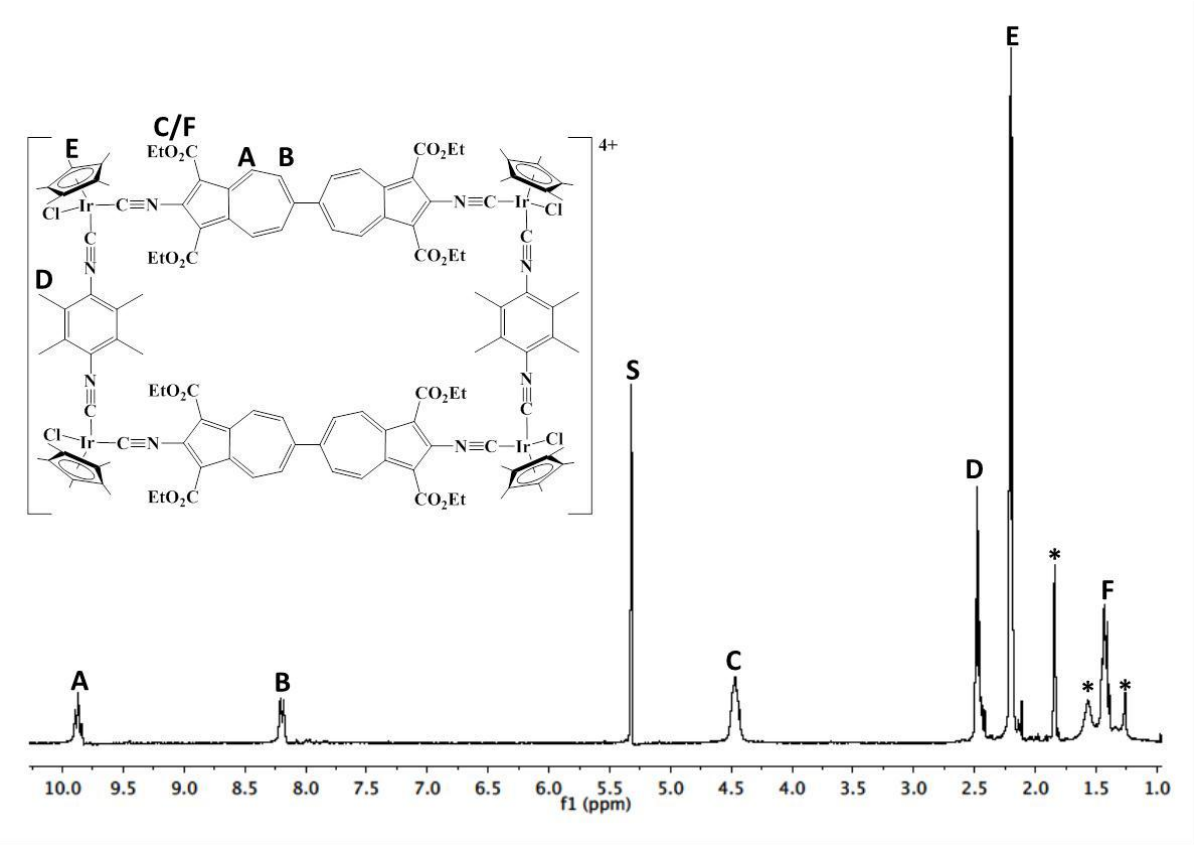

Figure IV.10 ^{1}H NMR spectrum of **4.3b** in CD_2Cl_2 (* = impurity; S = residual solvent).

Furthermore, the mass spectrum of **4.3b** confirms the presence of the tetrairidium molecular rectangle as opposed to an oligomeric structure. The tetracation of **4.3b** $(M^{4+} + 1)^{4+}$ appears at m/z = 751.4 (exact mass = 3005.76 g/mol). Due to the nature of the interactions within **4.3b** (e.g., multiple metal-isocyanoazulene and metal-isocyanodurene bonds, and multiple cation-anion interactions), the mass spectrum revealed many fragments. Some of the more obvious fragments, their masses, overall charges, and the corresponding expected versus found m/z values are listed in Table IV.1.

Table IV.1 Selected fragment contributions in the mass spectrum of **4.3b**.

Fragment	Exact mass (g/mol); overall charge	$m/z_{expected}$	m/z_{found}
$M^{4+} + 1$	3005.76; 4+	751.4	751.4
$M^{4+} + SbF_6^-$	3239.66; 3+	1079.9	1079.9
M^{4+} – durene + SbF_6^-	3055.56; 3+	1018.5	1018.6

While Yamamoto *et al*. showed that heterocyclic amines can act as bridges in the presence of benzenoid diisocyanoarenes in molecular rectangles[8], this is not the case for the nonbenzenoid 2,6-diisocyanoazulene and 2,2'-diisocyano-6,6'-biazulene. Fortunately, the use of the combination of benzenoid and nonbenzenoid isocyanoarenes as bridges prevents ligand scrambling and reduces the amount of possible products to the parallel and antiparallel isomers in **4.3a** and the desired symmetric molecular rectangle in **4.3b**.

Due to the similar molecular shapes of the parallel and antiparallel isomers of **4.3a**, the two isomers are virtually inseparable. An attempt was made to control the orientation of the dipole of the azulenic bridge. In line with precedence established by Barybin *et al*., the 2,6-diisocyanoazulene motif can be complexed to one metal center at either the 2- or 6-isocyanide and subsequently coordinated to a second metal center via the free isocyanide (Scheme IV.1).[17] Alternatively, this can also be regioselectively achieved through the coordination of a 2-formamide-6-isocyanoazulene, followed by a dehydration of the formamide group to create the second, unbound isocyanide for further reactivity (Scheme I.12). Unfortunately, the dehydration conditions are incompatible with the Cp^*Cl_2Ir corner piece, which does not appear to survive after multiple attempts.

An alternative path is to complex only one of the isocyanides with a Cp^*Cl_2Ir corner piece, then coordinate a different metal center (e.g., a $[Cr(CO)_5]$ or $[(Ph_3P)Au]^+$ fragment). The addition of two equivalents of 2,6-diisocyano-1,3-diethoxycarbonylazulene to one equivalent of $[Cp^*Cl_2Ir]_2$ provided two possible mononuclear edge precursors consisting of one Cp^*Cl_2Ir corner piece and one diisocyanoazulene bridge (**4.4**) as shown in Scheme IV.9. An IR analysis of **4.4** in CH_2Cl_2 (Figure IV.11, solid line) revealed a broad isocyanide stretching band centered at 2126 cm^{-1} with two shoulders at ~2146 and ~2116 cm^{-1}.

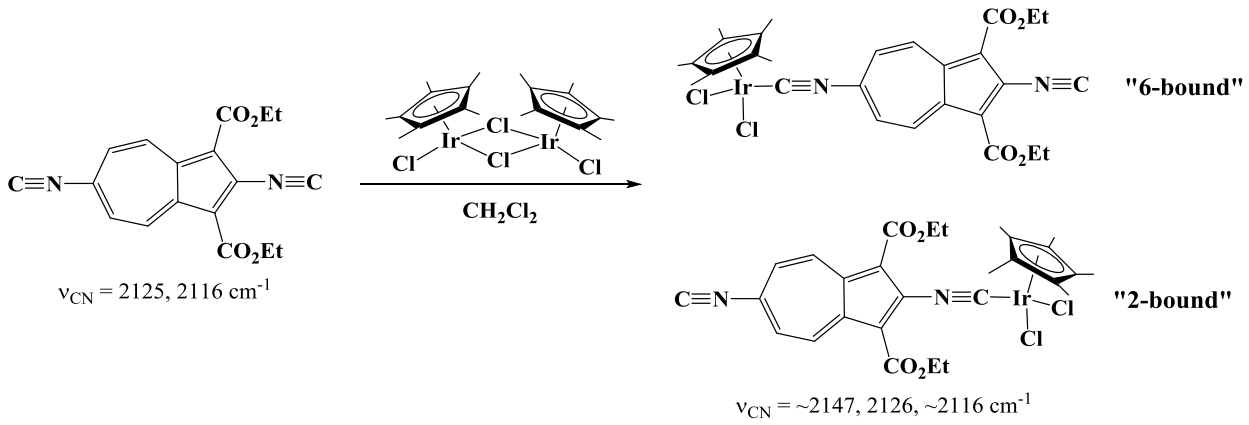

4.4

Scheme IV.9

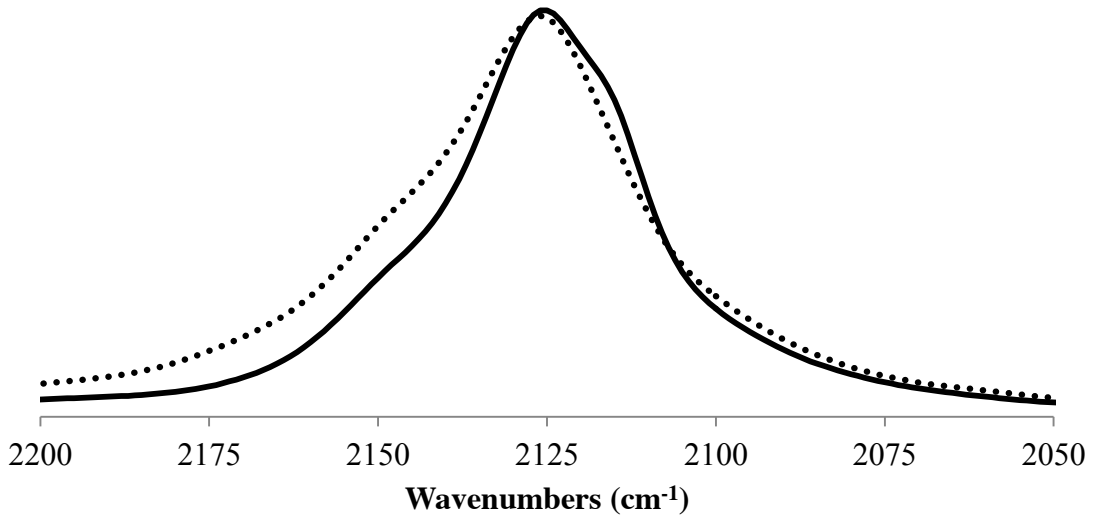

Figure IV.11 FTIR spectrum of **4.4** in CH_2Cl_2 before (solid) and after (dashed) DCE reflux.

The isocyanide stretching bands for **4.4** at 2146 cm^{-1} and 2126 cm^{-1} correspond to the 2-isocyano and the 6-isocyano groups, respectively, bound to the iridium(III) center of a Cp^*Cl_2Ir corner piece. These values are similar to those documented for **4.1a**. In addition, the ν_{CN} peaks at 2126 and 2116 cm^{-1} could be attributed to the uncomplexed (or free) 2-isocyano or 6-isocyano termini as was observed for the corresponding isocyano groups in 2,6-diisocyano-1,3-diethoxycarbonylazulene[17]. The broad asymmetric ν_{CN} band at *ca*. 2126 cm^{-1} (Figure IV.11, solid line) observed for **4.4**, then, suggests a mixture of isomers containing 2,6-diisocyano-1,3-

diethoxycarbonylazulene bound to Cp^*Cl_2Ir via one or the other of its isocyano termini. Indeed, the ^1H NMR spectrum of **4.4** in CD_2Cl_2 shows a 1:1 mixture of two azulenic environments assigned as the 2-bound and 6-bound isomers (Figure IV.12A).

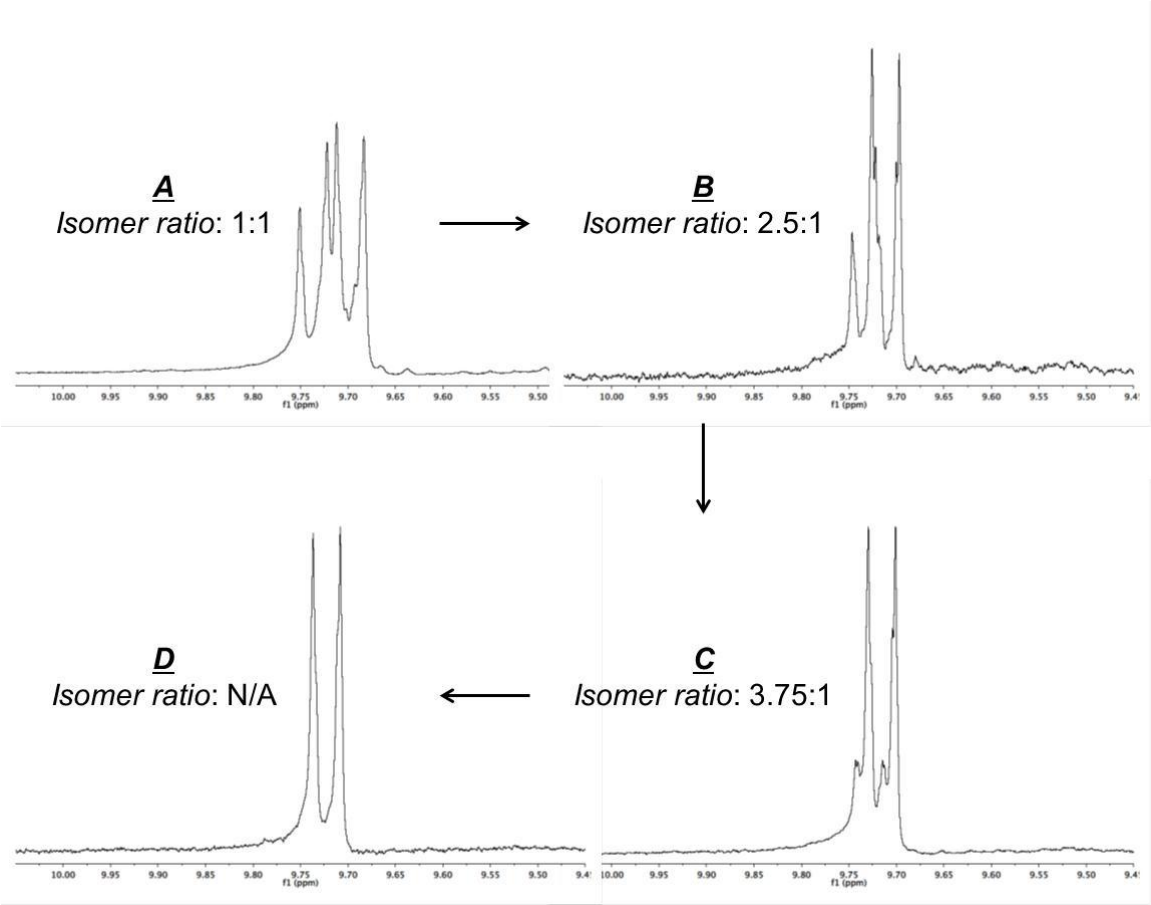

Figure IV.12 Aromatic region of ^1H NMR spectra of **4.4** in CD_2Cl_2 after heating at various temperatures: A) RT for 1 h, B) 66 °C for 1 h, C) 84 °C for 1 h, and D) 84 °C for 4 h.

In order to convert the mixture of presumably kinetic products in **4.4** to the thermodynamically favored isomer, a THF solution of **4.4** was refluxed at 66 °C for one hour. The ^1H NMR spectrum of **4.4** following this reflux showed a change in the composition of the isomeric mixture, giving a new isomer ratio of 2.5:1 (Figure IV.12B). A second refluxing of **4.4** in 1,1'-dichloroethane (DCE) at 84 °C for one hour yielded an isomer ratio of 3.75:1 (Figure IV.12C). Further reflux of **4.4** in DCE for a total of four hours resulted in essentially complete

disappearance of one of the isomers, as judged by ^{1}H NMR. (Figure IV.12D). The observed ^{1}H NMR resonances did not correlate to either free 2,6-diisocyano-1,3-diethoxycarbonylzulene or **4.1a** (the 2,6-diisocyanoazulene linker complexed to two [Cp*Cl_2Ir] units), which suggests the successful formation of the thermodynamically-favored isomer via thermal control. The disappearance of a shoulder at 2116 cm^{-1} in the FTIR spectrum (Figure IV.11, dashed line) implies the uncomplexed 6-isocyano junction ends up binding to the iridium corner piece. Unfortunately, attempts to attach the unbound isocyanide to either the metal carbonyl motif [$Cr(CO)_5$] or the [$(Ph_3P)Au]^+$ unit proved unsuccessful. Similar attempts involving the symmetric biazulene bridges did not yield a well-defined product either.

Provided that the attempts to control the orientation of the 2,6-diisocyanoazulene bridge did not work with an iridium cap or thermal control, a different route was taken where the 2- or 6-isocyanide terminus was capped with the metal carbonyl unit [$Cr(CO)_5$]. As shown in Scheme IV.1, the complexation of 2,6-diisocyano-1,3-diethoxycarbonylazulene with $Cr(CO)_5$(THF) proceeds under kinetic control and produces three products: the dinuclear chromium(0) complex, the mononuclear chromium(0) complex bound through the 2-isocyanide junction group (2-bound chromium(0) isomer), and the mononuclear chromium(0) complex bound through the 6-isocyanide junction group (6-bound chromium(0) isomer).[17] These three complexes are isolable in reasonable yield and stable under ambient conditions. While the dinuclear chromium(0) complex is a "dead end" piece due to the relatively unreactive nature of the remaining Cr-CO bonds following substitution of one of the CO ligands in $Cr(CO)_6$, the mononuclear chromium(0) isomers constitute stable and straightforward alternatives to controlling the dipole orientation of the azulenic scaffold. In fact, the $Cr(CO)_5$ unit serves as a protective "end cap." The FTIR spectrum of the mononuclear chromium(0) complex of 2,6-diisocyano-1,3-

diethoxycarbonylazulene bound to the Cr(0) center via the 2-isocyanide terminus is shown in Figure IV.13.

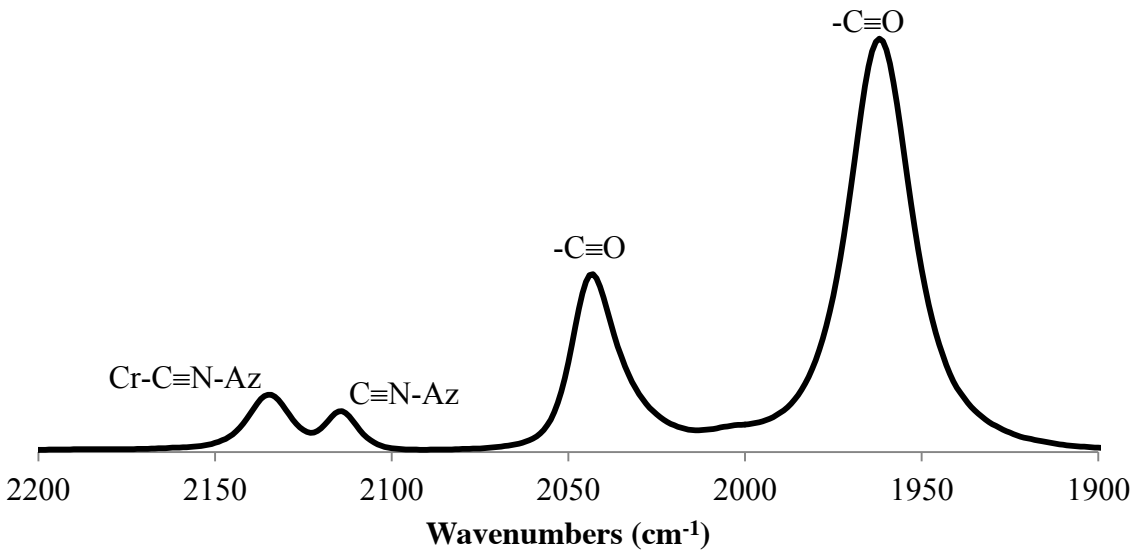

Figure IV.13 FTIR spectrum of the mononuclear Cr(0) complex $\{(OC)_5Cr\}$(2,6-diisocyano-1,3-diethoxycarbonylazulene-κ(*^{2}CN)*}[17] in CH_2Cl_2.

The addition of one equivalent of $[(Cp^*)Cl_2Ir]_2$ to two equivalents of either mononuclear Cr(0) complex (2-bound or 6-bound) in CH_2Cl_2 provided the two azulene-bridged heteronuclear Cr(0)/Ir(III) isomers **4.5a** in a 93% yield and **4.5b** in a 83% yield (Scheme IV.10). In **4.5a**, the 2-isocyanide terminus is bound to the $[Cr(CO)_5]$ end cap while the 6-isocyanide group is bound to the Cp^*Cl_2Ir corner piece; the reverse is true in **4.5b**. The IR spectrum of **4.5a** in CH_2Cl_2 (Figure IV.14, left) presents with three stretching bands: 1) the isocyanide ν_{CN} peaks coincidentally overlap at 2129 cm^{-1}; and 2) the carbonyl ν_{CO} bands appear at 2042 and 1962 cm^{-1}. From the IR spectrum of **4.5b** in CH_2Cl_2 (Figure IV.14, right), the isocyanide stretching frequencies are at 2147 (Ir-2-isocyanide) and 2123 (Cr-6-isocyanide) cm^{-1} while the carbonyl stretching frequencies are at 2032 and 1965 cm^{-1}. The ^1H NMR spectra of both **4.5a** and **4.5b** in

$CDCl_3$ suggest one Cp* environment for every one azulene fragment, which is in accord with their molecular formula.

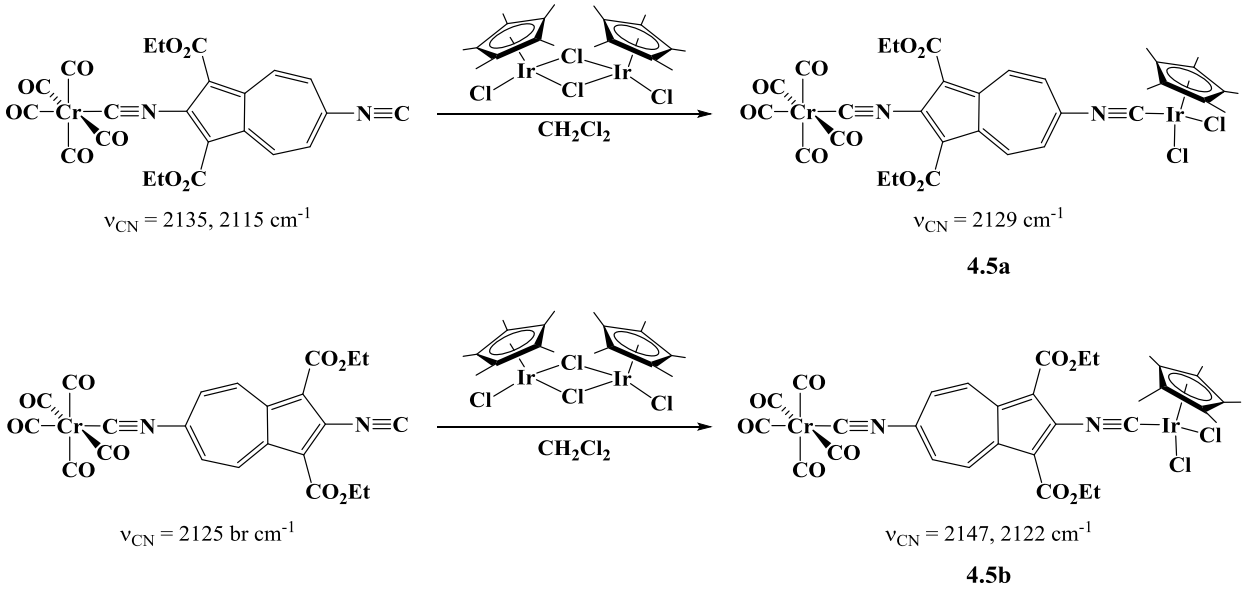

Scheme IV.10

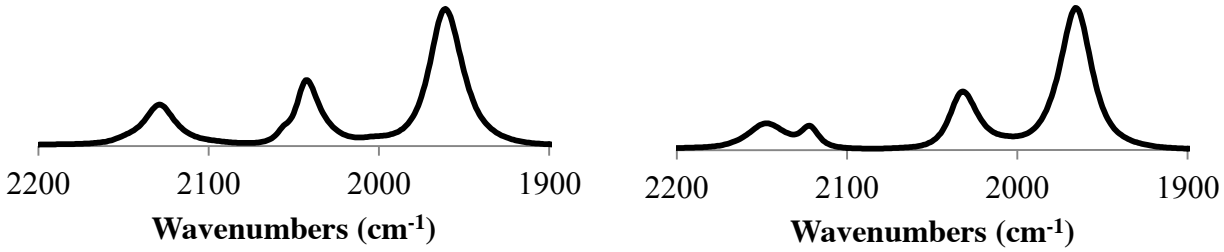

Figure IV.14 FTIR spectra of **4.5a** (left) and **4.5b** (right) in CH_2Cl_2.

The electronic absorption spectra of **4.5a** and **4.5b** in CH_2Cl_2 (Figure IV.15) revealed the metal-to-ligand charge transfer (MLCT) bands at 504 and 496 nm, respectively. The molar absorptivities of the transitions in **4.5a** and **4.5b** range from approximately 3×10^4 to 7×10^4 M^{-1} cm^{-1}. In both cases, the MLCT transitions occur at lower energies than the corresponding transition documented for **4.1a** (482 nm), but at higher energies than that observed for the dinuclear chromium(0) (522 nm) and tungsten(0) (515 nm) complexes of 2,6-diisocyano-1,3-

diethoxycarbonylazulene.[17] The MLCT transition in the related dinuclear tungsten(0) complex of 1,4-diisocyanobenzene occurs at significantly higher energy (370 nm).[23] The lower energy MLCT transitions of these diisocyanoazulene-bridged dinuclear complexes imply a greater delocalization/ involvement of the nonbenzenoid π-system of azulene than the benzenoid π-system of benzene.

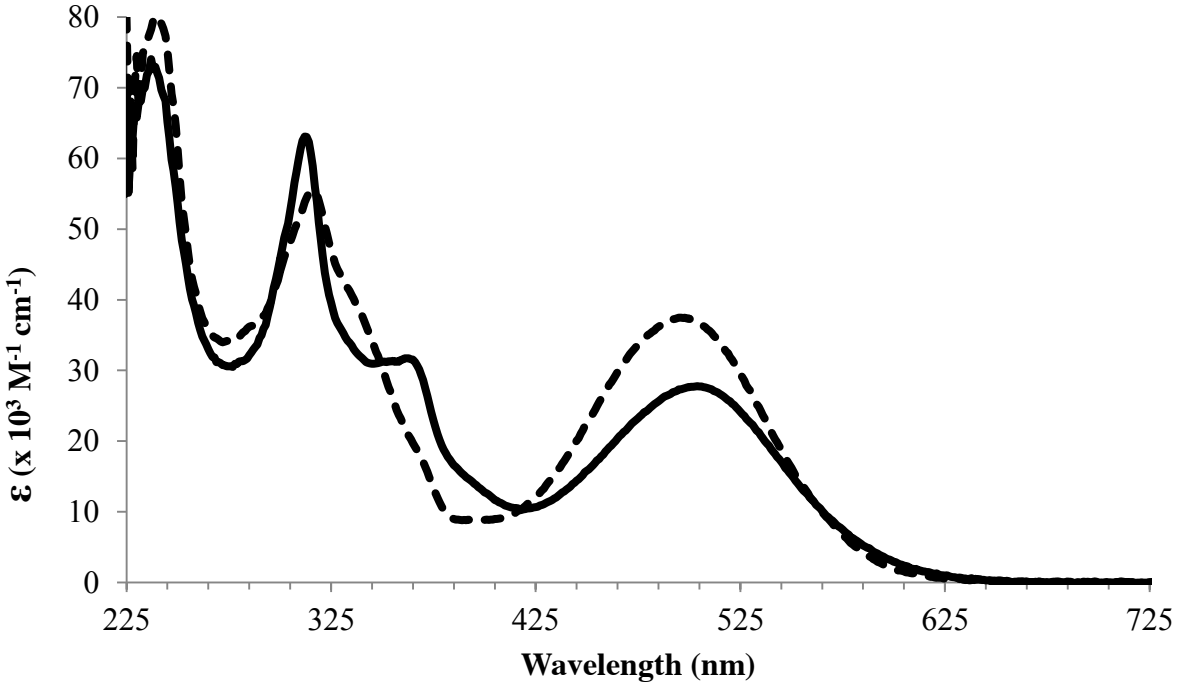

Figure IV.15 Electronic absorption spectra of **4.5a** (solid) and **4.5b** (dashed) in CH_2Cl_2.

With the Cp*Cl_2Ir corner piece in place, halide abstraction in **4.5a** and **4.5b** with $AgSbF_6$ opened a coordination site allowing for the coordination of a bridging ligand to form a heterotetrametallic molecular framework (Scheme IV.11). A benzenoid isocyanoarene, namely diisocyanodurene, was used as the bridge between the iridium centers to give **4.6a** in a 73% yield and **4.6b** in an 85% yield. The IR analysis of **4.6a** in CH_2Cl_2 (Figure IV.16) showed three distinct bands attributable to isocyanide stretching vibrations (2199, 2167, and 2132 cm^{-1}) and two bands associated with carbonyl stretching modes (2041 and 1963 cm^{-1}). The ν_{CN} band for

the isocyanodurene unit attached to the Ir(III) centers occurs at 2199 cm^{-1}, the 6-isocyanide terminus of the diisocyanoazulene ligand bound to the iridium(III) center has the ν_{CN} value of 2167 cm^{-1}, and the 2-isocyanide end of the diisocyanoazulene unit bound to the chromium(0) center corresponds to the ν_{CN} band at 2132 cm^{-1}.

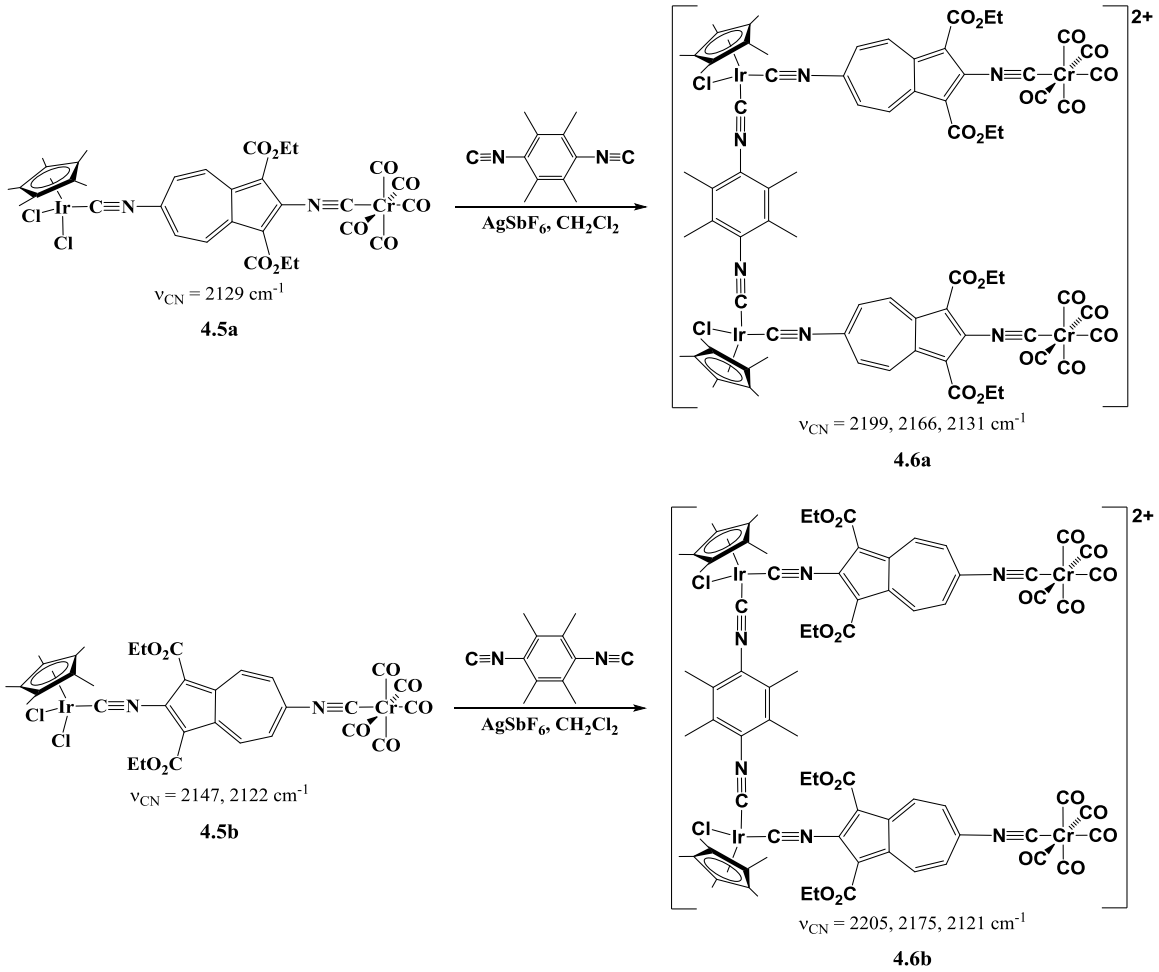

Scheme IV.11

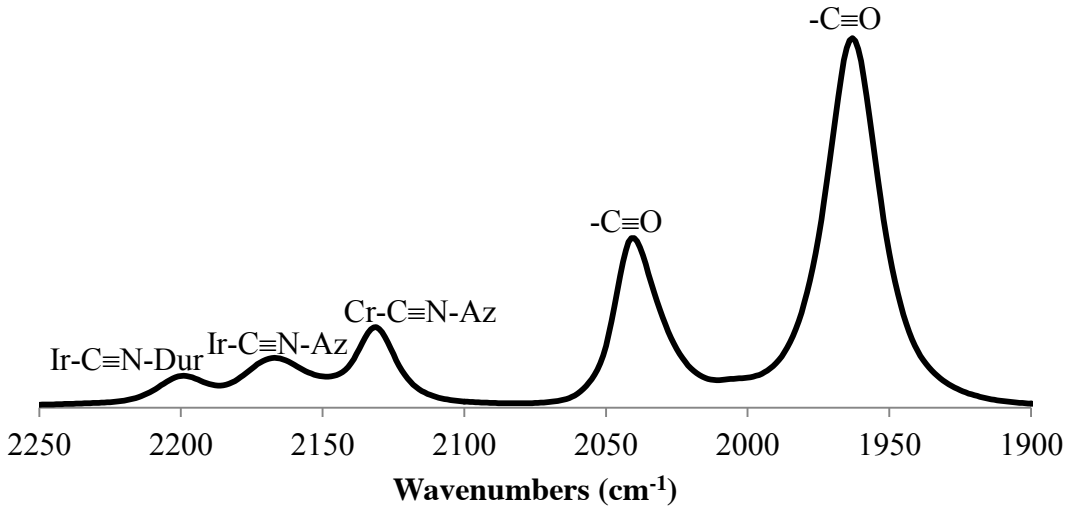

Figure IV.16 FTIR spectrum of **4.6a** in CH_2Cl_2.

The IR analysis of **4.6b** in CH_2Cl_2 (Figure IV.17) showed three distinct bands attributable to isocyanide stretching vibrations (2205, 2175, and 2121 cm^{-1}) and two bands associated with carbonyl stretching modes (2027 and 1968 cm^{-1}). The ν_{CN} band for the isocyanodurene unit attached to the Ir centers occurs at 2205 cm^{-1}, the 2-isocyanide terminus of the diisocyanoazulene ligand bound to the iridium(III) center has the ν_{CN} value of 2175 cm^{-1}, and the 6-isocyanide end of the diisocyanoazulene unit bound to the chromium(0) center corresponds to the ν_{CN} band at 2121 cm^{-1}. The ^1H NMR spectra of **4.6a** and **4.6b** are very similar to each other, reflecting common fragments used to assemble these polynuclear isomeric structures. In the ^1H NMR spectrum of **4.6b** shown in Figure IV.18, the resonances marked by asterisks (*) correspond to either the starting material or solvent impurities.

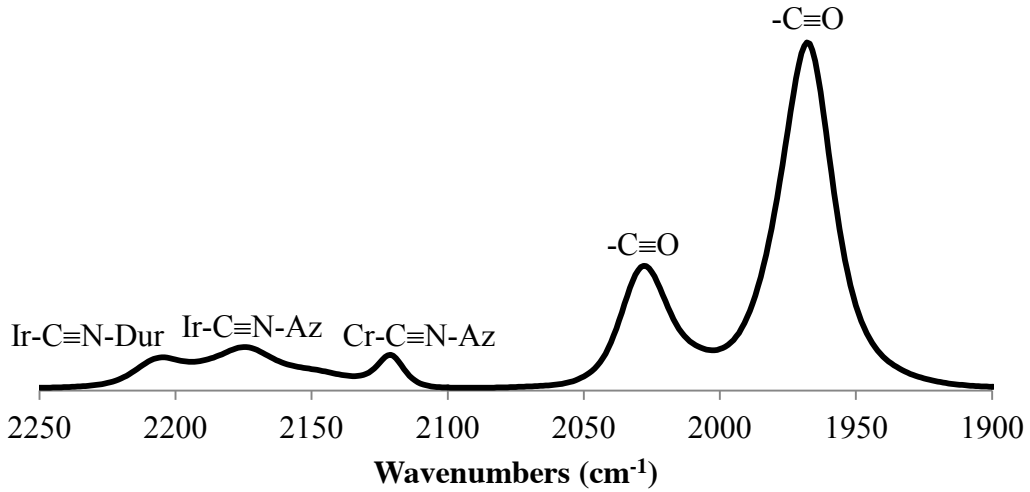

Figure IV.17 FTIR spectrum of **4.6b** in CH_2Cl_2.

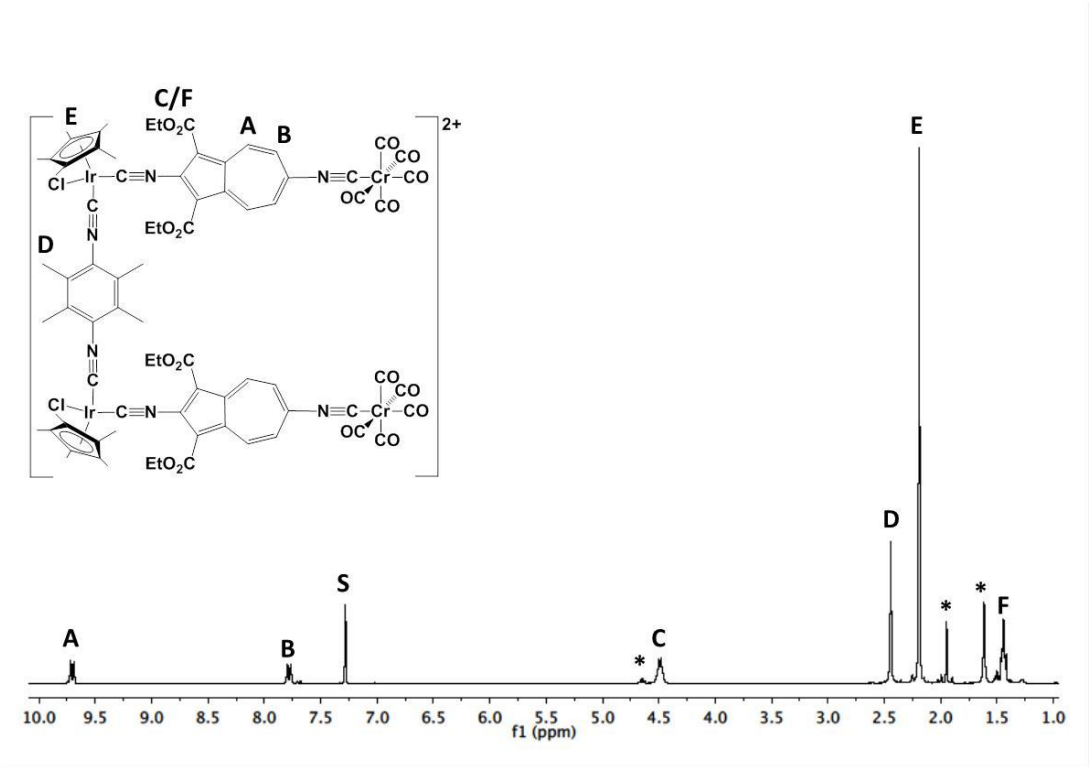

Figure IV.18 ^{1}H NMR spectrum of **4.6b** in $CDCl_3$ (* = impurity, S = residual solvent).

While the use of two different diisocyanide linkers successfully provided a heterotetrametallic molecular framework, which resembles three out of four edges of a molecular

rectangle, the use of the combination of heterocyclic amines (e.g., 4,4'-bipyridine) and diisocyanoazulenes as bridge between the iridium centers as in **4.7a** gave unexpected and incomprehensible signals tentatively ascribed to scrambling as seen in **4.2a.1** and **4.2a.2.** The $[Cr(CO)_5]$ end caps, however, present a challenge at this stage for closing these polymetallic structures to form a molecular rectangle.

IV.5 Conclusions and Outlook

The work in this Chapter described the synthesis and characterization of diisocyanoazulene- and diisocyanobiazulene-containing 2D-MOFs, specifically molecular rectangles and heterotetrametallic molecular frameworks. The asymmetric diiridium edge piece $[Cp^*Cl_2Ir]_2(\mu\text{-}\eta^1\text{:}\eta^1$-2,6-diisocyano-1,3-diethoxycarbonylazulene) (**4.1a**) was structurally characterized. The analogous symmetric biazulene-containing edge pieces were also synthesized and displayed spectroscopic properties similar to the monoazulene edge piece. The isolation of the tetrairidium molecular rectangles containing asymmetric 2,6-diisocyano-1,3-diethoxycarbonylazulene (**4.3a**) and symmetric 2,2'-diisocyano-1,1',3,3'-tetraethoxycarbonyl-6,6'-biazulene (**4.3b**) were confirmed via ^{1}H NMR and IR spectroscopy as well as mass spectrometry for the symmetric molecular rectangle. In addition, metal carbonyl fragments were employed successfully as end caps to control the orientation of the 2,6-diisocyanoazulene framework in heterotetrametallic molecular frameworks (**4.6a** and **4.6b**). When used as bridges, heterocyclic amines such as pyrazine and 4,4'-bipyridine were found to promote scrambling in the presence of diisocyanoazulenes leading to a mixture of products according to ^{1}H NMR studies. The use of 1,4-diisocyanodurene as a bridge in lieu of a heterocyclic amine resolved this incompatibility. It would be interesting to examine the effect of decreasing the bulk of the 1,3-substituents in reducing any steric repulsion within the cavity of the molecular rectangles as well as the sensitivity of their optical properties to volatile organic compounds via electronic absorption studies. In addition, the incorporation of a redox-active 6,6'-biazulenic bridge in 2D-MOFs could allow for adjusting the overall charge. X-ray structural characterization of these systems would provide valuable insight into guest-host interactions.

IV.6 References

1 Zhou, H.-C.; Long, J. R.; Yaghi, O. M. *Chem*. *Rev*. **2012**, *112*, 673 (Note: This is an opening editorial for a thematic issue on metal-organic frameworks, which includes many detailed reviews).

2 Lee, J.; Farha, O. K.; Roberts, J.; Scheidt, K. A.; Nguyen, S. T.; Hupp, J. T. *Chem*. *Soc*. *Rev*. **2009**, *38*, 1450.

3 Li, J.-R.; Sculley, J.; Zhou, H.-C. *Chem*. *Rev*. **2012**, *112*, 869.

4 a) Murray, L. J.; Dinca, M.; Long, J. R. *Chem*. *Soc*. *Rev*. **2009**, *38*, 1294; b) Suh, M. P.; Park, H. J.; Prasad, T. K.; Lim, D.-W. *Chem*. *Rev*. **2012**, *112*, 782.

5 Kreno, L. E.; Leong, K.; Farha, O. K.; Allendorf, M.; Duyne, R. P. Van; Hupp, J. T. *Chem*. *Rev*. **2012**, *112*, 1105.

6 a) Zhang, J.-P.; Zhang, Y.-B.; Lin, J.-B.; Chen, X. M. *Chem*. *Rev*. **2012**, *112*, 1001; b) Maher, T. R.; Meyers, J. J., Jr.; Spaeth, A. D.; Lemley, K. R.; Barybin, M. V. *Dalton Trans*. **2012**, *41*, 7845.

7 Dinolfo, P. H.; Hupp, J. T. *J*. *Am*. *Chem*. *Soc*. **2004**, *126*, 16814.

8 Yamamoto, Y.; Suzuki, H.; Tajima, N.; Tatsumi, K. *Chem*. *Eur*. *J*. **2002**, *8*, 372.

9 Cui, Y.; Yue, Y.; Qian, G.; Chen, B. *Chem*. *Rev*. **2012**, *112*, 1126.

10 Lan, A.; Li, K.; Wu, H.; Olson, D. H.; Emge, T. J.; Ki, W.; Hong, M.; Li, J. *Angew*. *Chem*. *Int*. *Ed*. *Engl*. **2009**, *48*, 2334.

11 a) Dedeian, K.; Shi, J.; Forsythe, E.; Morton, D. C. *Inorg*. *Chem*. **2007**, *46*, 1603; b) Shavaleev, N. M.; Monti, F.; Costa, R. D.; Scopelliti, R.; Bolink, H. J.; Ortí, E.; Accorsi, G.; Armaroli, N.; Baranoff, E.; Grätzel, M.; Nazeeruddin, M. K. *Inorg*. *Chem*. **2012**, *51*, 2263; c) Harvey, P. D.; Clement, S.; Knorr, M.; Husson, J. Luminescent organometallic coordination polymers built on isocyanide bridging ligands. In *Macromolecules Containing Metal and Metal-Like Elements* Volume 10; Aziz, A.S.A.-E., Carraher, C. E., Harvey, P. D., Pittman, C. U., Zeldin, M., Eds. John Wiley & Sons: Hoboken, 2010; pp. 45-87.

12 Keefe, M. H.; Slone, R. V; Hupp, J. T.; Czaplewski, K. F.; Snurr, R. Q.; Stern, C. L. *Langmuir* **2000**, *16*, 3964.

13 Dewar, M. J. S. The Molecular Orbital Theory of Organic Chemistry; McGraw-Hill: New York, 1969.

14 Barman, S.; Furukawa, H.; Blacque, O.; Venkatesan, K.; Yaghi, O. M.; Berke, H. *Chem*. *Commun*. **2010**, *46*, 7981.

15 Barybin, M. V. *Coord*. *Chem*. *Rev*. **2010**, *254*, 1240.

16 Selected articles: a) McCreery, R. L. Chem. Mater. 2004, 16, 4477; b) Chu, C.; Ayres, J. A.; Stefanescu, D. M.; Walker, B. R.; Gorman, C. B.; Parsons, G. N. *J*. *Phys*. *Chem*. *C* **2007**, *111*, 8080.

17 Holovics, T. C.; Robinson, R. E.; Weintrob, E.; Toriyama, M.; Lushington, G. H.; Barybin, M. V. *J*. *Am*. *Chem*. *Soc*. **2006**, *128*, 2300.

18 DuBose, D. L.; Robinson, R. E.; Holovics, T. C.; Moody, D. R.; Weintrob, E. C.; Berrie, C. L.; Barybin, M. V. *Langmuir* **2006**, *22*, 4599.

19 Maher, T. R.; Spaeth, A. D.; Neal, B. M.; Berrie, C. L.; Thompson, W. H.; Day, V. W.; Barybin, M. V. *J*. *Am*. *Chem*. *Soc*. **2010**, *132*, 15924.

20 McGinnis, D. Synthesis and Coordination Chemistry of Azulene- and Ferrocene-Based Isocyanide Ligands. Ph.D. Dissertation, University of Kansas, Lawrence, KS, 2011.

21 Swanson, S. A.; McClain, R.; Lovejoy, K. S.; Alamdari, N. B.; Hamilton, J. S.; Scott, J. C. *Langmuir* **2005**, *21*, 5034.

22 See Figure III.4 for the molecular structures of the three possible biazulenic frameworks.

23 Grubisha, D. S.; Rommel, J. S.; Lane, T. M.; Tysoe, W. T.; Bennett, D. W. *Inorg*. *Chem*. **1992**, *31*, 5022.

Appendix 1

Crystallographic Data for Compound 2.4

Table 1 Crystal data and structure refinement for **2.4**.

Empirical formula	$C_{13}H_{11}N$	
Formula weight	181.23	
Temperature	100(2) K	
Wavelength	0.71073 Å	
Crystal system	Orthorhombic	
Space group	Pbca - D_{2h}^{15} (No. 61)	
Unit cell dimensions	**a** = 13.789(3) Å	α = 90.000°
	b = 9.154(2) Å	β = 90.000°
	c = 15.737(3) Å	γ = 90.000°
Volume	1986.3(6) $Å^3$	
Z	8	
Density (calculated)	1.212 Mg/m^3	
Absorption coefficient	0.071 mm^{-1}	
F(000)	768	
Crystal size	0.35 x 0.11 x 0.03 mm^3	
Theta range for data collection	3.70 to 30.10°	
Index ranges	$-19 \le h \le 19$, $-12 \le k \le 12$, $-22 \le l \le 20$	
Reflections collected	20632	
Independent reflections	2903 [R_{int} = 0.070]	
Completeness to theta = 30.10°	99.2 %	
Absorption correction	Multi-scan	
Max. and min. transmission	1.000 and 0.978	
Refinement method	Full-matrix least-squares on F^2	
Data / restraints / parameters	2903 / 0 / 171	
Goodness-of-fit on F^2	1.014	
Final R indices [I>2sigma(I)]	R_1 = 0.058, wR_2 = 0.140	
R indices (all data)	R_1 = 0.094, wR_2 = 0.155	
Largest diff. peak and hole	0.44 and -0.18 $e^-/Å^3$	

$R_1 = \Sigma \, ||F_o| - |F_c|| \, / \, \Sigma \, |F_o|$

$wR_2 = \{ \Sigma \, [w(F_o^2 - F_c^2)^2] \, / \, \Sigma \, [w(F_o^2)^2] \}^{1/2}$

Table 2 Atomic coordinates (x 10^4) and equivalent isotropic displacement parameters ($Å^2$ x 10^3) for **2.4**. U(eq) is defined as one third of the trace of the orthogonalized U_{ij} tensor.

	x	y	z	U(eq)
N	1031(1)	1774(1)	3736(1)	35(1)
C(1)	1299(1)	4424(2)	3824(1)	30(1)
C(2)	1109(1)	3068(2)	4198(1)	29(1)
C(3)	1022(1)	3139(1)	5083(1)	28(1)
C(4)	1155(1)	5155(2)	6122(1)	30(1)
C(5)	1295(1)	6585(2)	6402(1)	35(1)
C(6)	1485(1)	7825(2)	5918(1)	36(1)
C(7)	1595(1)	7976(2)	5049(1)	35(1)
C(8)	1532(1)	6915(2)	4416(1)	31(1)
C(9)	1346(1)	5431(2)	4495(1)	27(1)
C(10)	1165(1)	4606(2)	5303(1)	26(1)
C(11)	1422(1)	4715(2)	2898(1)	43(1)
C(12)	976(1)	697(2)	3350(1)	47(1)
C(13)	871(1)	1877(2)	5667(1)	35(1)

Table 3 Bond lengths [Å] for **2.4**.

N-C(12)	1.161(2)
N-C(2)	1.394(2)
C(1)-C(2)	1.398(2)
C(1)-C(9)	1.403(2)
C(1)-C(11)	1.491(2)
C(2)-C(3)	1.400(2)
C(3)-C(10)	1.401(2)
C(3)-C(13)	1.490(2)
C(4)-C(10)	1.383(2)
C(4)-C(5)	1.394(2)
C(4)-H(4)	0.97(2)
C(5)-C(6)	1.392(2)
C(5)-H(5)	0.97(2)
C(6)-C(7)	1.382(2)
C(6)-H(6)	0.96(2)
C(7)-C(8)	1.394(2)
C(7)-H(7)	0.97(2)
C(8)-C(9)	1.388(2)
C(8)-H(8)	0.96(2)
C(9)-C(10)	1.499(2)
C(11)-H(11A)	0.95(2)
C(11)-H(11B)	0.93(3)
C(11)-H(11C)	0.91(2)
C(13)-H(13A)	0.99(2)
C(13)-H(13B)	0.96(2)
C(13)-H(13C)	0.96(2)

Table 4 Bond angles [°] for **2.4**.

C(12)-N-C(2)	179.3(2)	C(9)-C(8)-C(7)	129.0(1)
C(2)-C(1)-C(9)	106.0(1)	C(9)-C(8)-H(8)	115(1)
C(2)-C(1)-C(11)	126.2(1)	C(7)-C(8)-H(8)	116(1)
C(9)-C(1)-C(11)	127.9(1)	C(8)-C(9)-C(1)	125.7(1)
N-C(2)-C(1)	123.4(1)	C(8)-C(9)-C(10)	126.8(1)
N-C(2)-C(3)	123.5(1)	C(1)-C(9)-C(10)	107.5(1)
C(1)-C(2)-C(3)	113.1(1)	C(4)-C(10)-C(3)	125.2(1)
C(2)-C(3)-C(10)	106.2(1)	C(4)-C(10)-C(9)	127.5(1)
C(2)-C(3)-C(13)	126.1(1)	C(3)-C(10)-C(9)	107.2(1)
C(10)-C(3)-C(13)	127.6(1)	C(1)-C(11)-H(11A)	111(2)
C(10)-C(4)-C(5)	129.3(1)	C(1)-C(11)-H(11B)	113(2)
C(10)-C(4)-H(4)	115(1)	H(11A)-C(11)-H(11B)	95(2)
C(5)-C(4)-H(4)	116(1)	C(1)-C(11)-H(11C)	117(2)
C(6)-C(5)-C(4)	128.2(1)	H(11A)-C(11)-H(11C)	112(2)
C(6)-C(5)-H(5)	119(1)	H(11B)-C(11)-H(11C)	107(2)
C(4)-C(5)-H(5)	113(1)	C(3)-C(13)-H(13A)	110(1)
C(7)-C(6)-C(5)	130.1(1)	C(3)-C(13)-H(13B)	110(1)
C(7)-C(6)-H(6)	117(1)	H(13A)-C(13)-H(13B)	111(2)
C(5)-C(6)-H(6)	114(1)	C(3)-C(13)-H(13C)	113(1)
C(6)-C(7)-C(8)	129.1(1)	H(13A)-C(13)-H(13C)	108(2)
C(6)-C(7)-H(7)	116(1)	H(13B)-C(13)-H(13C)	105(2)
C(8)-C(7)-H(7)	115(1)		

Table 5 Anisotropic displacement parameters ($Å^2 \times 10^3$)for **2.4**. The anisotropic displacement factor exponent takes the form: $-2\pi^2[h^2 a^{*2} U_{11} + ... + 2 h k a^* b^* U_{12}]$

	U_{11}	U_{22}	U_{33}	U_{23}	U_{13}	U_{12}
N	36(1)	34(1)	34(1)	-6(1)	-2(1)	2(1)
C(1)	28(1)	35(1)	26(1)	1(1)	0(1)	2(1)
C(2)	28(1)	29(1)	30(1)	-4(1)	-2(1)	2(1)
C(3)	28(1)	25(1)	30(1)	1(1)	-1(1)	2(1)
C(4)	32(1)	31(1)	27(1)	2(1)	0(1)	2(1)
C(5)	38(1)	36(1)	31(1)	-6(1)	-1(1)	2(1)
C(6)	38(1)	28(1)	42(1)	-7(1)	-1(1)	0(1)
C(7)	32(1)	26(1)	45(1)	3(1)	0(1)	-2(1)
C(8)	29(1)	30(1)	33(1)	7(1)	1(1)	0(1)
C(9)	26(1)	29(1)	26(1)	2(1)	0(1)	1(1)
C(10)	24(1)	26(1)	26(1)	2(1)	1(1)	2(1)
C(11)	50(1)	52(1)	26(1)	2(1)	0(1)	-3(1)
C(12)	54(1)	45(1)	42(1)	-10(1)	0(1)	-1(1)
C(13)	44(1)	26(1)	36(1)	6(1)	-1(1)	1(1)

Table 6 Hydrogen coordinates (x 10^4) and isotropic displacement parameters (Å^2 x 10^3) for **2.4**.

H(4)	1009(11)	4443(17)	6560(10)	32(4)
H(5)	1258(12)	6685(19)	7012(11)	48(5)
H(6)	1558(12)	8694(18)	6250(11)	45(5)
H(7)	1738(11)	8959(18)	4850(10)	40(4)
H(8)	1645(11)	7239(16)	3847(10)	37(4)
H(11A)	1950(18)	5360(30)	2799(15)	107(9)
H(11B)	1690(20)	3930(30)	2600(20)	147(12)
H(11C)	886(17)	4990(30)	2609(16)	97(8)
H(13A)	540(15)	1070(20)	5363(12)	66(6)
H(13B)	1477(14)	1550(20)	5894(13)	64(6)
H(13C)	486(14)	2119(18)	6158(12)	61(5)

Table 7 Torsion angles [°] for **2.4**.

C(12)-N-C(2)-C(1)	74(13)	C(7)-C(8)-C(9)-C(10)	0.0(2)
C(12)-N-C(2)-C(3)	-105(13)	C(2)-C(1)-C(9)-C(8)	179.2(1)
C(9)-C(1)-C(2)-N	-178.6(1)	C(11)-C(1)-C(9)-C(8)	-0.9(2)
C(11)-C(1)-C(2)-N	1.6(2)	C(2)-C(1)-C(9)-C(10)	-0.4(1)
C(9)-C(1)-C(2)-C(3)	0.4(2)	C(11)-C(1)-C(9)-C(10)	179.5(1)
C(11)-C(1)-C(2)-C(3)	-179.5(1)	C(5)-C(4)-C(10)-C(3)	179.5(1)
N-C(2)-C(3)-C(10)	178.7(1)	C(5)-C(4)-C(10)-C(9)	0.7(2)
C(1)-C(2)-C(3)-C(10)	-0.3(2)	C(2)-C(3)-C(10)-C(4)	-179.0(1)
N-C(2)-C(3)-C(13)	2.2(2)	C(13)-C(3)-C(10)-C(4)	-2.5(2)
C(1)-C(2)-C(3)-C(13)	-176.8(1)	C(2)-C(3)-C(10)-C(9)	0.0(1)
C(10)-C(4)-C(5)-C(6)	0.0(2)	C(13)-C(3)-C(10)-C(9)	176.5(1)
C(4)-C(5)-C(6)-C(7)	-0.9(3)	C(8)-C(9)-C(10)-C(4)	-0.4(2)
C(5)-C(6)-C(7)-C(8)	1.0(3)	C(1)-C(9)-C(10)-C(4)	179.2(1)
C(6)-C(7)-C(8)-C(9)	-0.4(2)	C(8)-C(9)-C(10)-C(3)	-179.4(1)
C(7)-C(8)-C(9)-C(1)	-179.5(1)	C(1)-C(9)-C(10)-C(3)	0.2(1)

Appendix 2

Crystallographic Data for Compound 3.12

Table 1 Crystal data and structure refinement for **3.12**.

Empirical formula	$3(C_{102}\ H_{90}\ Cr\ N_6\ O_{24})^+\ 3(Sb\ F_6)^-\cdot 1.67(C\ H_2\ Cl_2)$	
	$C_{307.67}\ H_{273.33}\ Cl_{3.33}\ Cr_3\ F_{18}\ N_{18}\ O_{72}\ Sb_3$	
Formula weight	6356.10	
Crystal system	triclinic	
Space group	$P\bar{1}$	
Unit cell dimensions	a = 12.686(3) Å	α = 76.794(5)°
	b = 18.687(4) Å	β = 87.395(5)°
	c = 32.513(8) Å	γ = 77.216(6)°
Volume	7318(3) Å^3	
Z, Z'	1, 1.5	
Density (calculated)	1.442 Mg/m^3	
Wavelength	0.71073 Å	
Temperature	100(2) K	
F(000)	3265	
Absorption coefficient	0.508 mm^{-1}	
Absorption correction	Semi-empirical from equivalents	
Max. and min. transmission	0.970 and 0.792	
Theta range for data collection	1.646 to 16.516°	
Reflections collected	28825	
Independent reflections	7822 [R(int) = 0.1346]	
Data / restraints / parameters	7822 / 3454 / 2004	
$wR(F^2$ all data)	$wR2$ = 0.2427	
R(F obsd data)	$R1$ = 0.0951	
Goodness-of-fit on F^2	1.065	
Observed data [I > 2σ(I)]	4791	
Extinction coefficient	n/a	
Largest and mean shift / s.u.	0.003and 0.000	
Largest diff. peak and hole	0.920 and -0.762 e/Å^3	

$wR2 = \{ \Sigma\ [w(F_o^2 - F_c^2)^2] / \Sigma\ [w(F_o^2)^2] \}^{1/2}$

$R1 = \Sigma\ ||F_o| - |F_c|| / \Sigma\ |F_o|$

Table 2 Atomic coordinates and equivalent isotropic displacement parameters for **3.12**. U(eq) is defined as one third of the trace of the orthogonalized U_{ij} tensor.

	x	y	z	U(eq)
Sb(1A)	0.12722(16)	0.69952(11)	0.15784(6)	0.0675(8)
F(1A)	0.1173(13)	0.6461(8)	0.1165(4)	0.086(4)
F(2A)	0.0844(15)	0.6239(7)	0.1987(4)	0.082(4)
F(3A)	0.2725(6)	0.6529(9)	0.1663(5)	0.071(3)
F(4A)	0.1349(13)	0.7540(8)	0.1989(4)	0.081(4)
F(5A)	0.1650(15)	0.7773(7)	0.1161(4)	0.074(3)
F(6A)	-0.0184(7)	0.7493(9)	0.1478(5)	0.083(3)
F(1A')	0.131(2)	0.6384(15)	0.1194(8)	0.086(5)
F(2A')	0.162(3)	0.6134(11)	0.2018(7)	0.079(4)
F(3A')	0.2748(9)	0.697(2)	0.1492(10)	0.068(4)
F(4A')	0.124(2)	0.7602(15)	0.1966(8)	0.081(5)
F(5A')	0.093(3)	0.7854(11)	0.1142(7)	0.078(4)
F(6A')	-0.0196(9)	0.700(2)	0.1674(10)	0.082(4)
Sb(1B)	0.5000	0.0000	0.5000	0.0414(9)
F(1B)	0.6245(7)	0.0344(7)	0.4796(4)	0.088(5)
F(2B)	0.4470(11)	0.0220(8)	0.4449(3)	0.113(6)
F(3B)	0.4330(9)	0.0969(4)	0.5057(4)	0.079(5)
Cr(1)	0.1699(3)	0.18139(19)	0.16623(12)	0.0307(11)
O(1A)	0.3829(11)	0.1125(7)	0.0687(4)	0.032(4)
O(2A)	0.4223(11)	0.1530(7)	0.0005(4)	0.033(4)
O(3A)	0.4211(13)	0.3436(8)	0.1443(5)	0.043(5)
O(4A)	0.5253(13)	0.4140(8)	0.1030(5)	0.059(5)
N(1A)	0.3661(13)	0.2294(9)	0.1139(5)	0.024(4)
C(1A)	0.4866(10)	0.3128(7)	0.0798(4)	0.025(4)
C(2A)	0.4372(10)	0.2505(8)	0.0825(4)	0.023(4)
C(3A)	0.4696(10)	0.2152(7)	0.0495(4)	0.020(4)
C(4A)	0.5923(12)	0.2372(9)	-0.0118(5)	0.029(6)
C(5A)	0.6650(12)	0.2699(9)	-0.0392(5)	0.040(7)
C(6A)	0.7046(13)	0.3318(9)	-0.0369(5)	0.030(6)
C(7A)	0.6820(12)	0.3744(10)	-0.0072(5)	0.032(6)
C(8A)	0.6165(11)	0.3688(8)	0.0280(5)	0.020(5)
C(9A)	0.5530(10)	0.3168(7)	0.0435(4)	0.023(4)
C(10A)	0.5421(10)	0.2546(7)	0.0240(4)	0.019(4)
C(11A)	0.2981(16)	0.2085(12)	0.1339(7)	0.032(5)
C(12A)	0.4210(16)	0.1549(10)	0.0412(5)	0.020(6)
C(13A)	0.3724(18)	0.0953(11)	-0.0095(6)	0.039(7)
C(14A)	0.385(2)	0.0971(14)	-0.0546(6)	0.061(9)
C(15A)	0.4756(18)	0.3546(11)	0.1127(6)	0.033(7)
C(16A)	0.5096(19)	0.4637(12)	0.1322(8)	0.070(9)
C(17A)	0.408(2)	0.5181(14)	0.1213(9)	0.086(9)

O(1B)	-0.0502(13)	0.2422(8)	0.2639(5)	0.057(5)
O(2B)	-0.0902(13)	0.2010(9)	0.3320(5)	0.064(5)
O(3B)	-0.0754(16)	0.0150(10)	0.1832(5)	0.074(6)
O(4B)	-0.1506(12)	-0.0694(8)	0.2270(5)	0.051(5)
N(1B)	-0.0229(13)	0.1280(9)	0.2169(5)	0.031(5)
C(1B)	-0.1380(11)	0.0399(8)	0.2492(5)	0.040(6)
C(2B)	-0.0963(10)	0.1053(8)	0.2472(5)	0.036(4)
C(3B)	-0.1301(10)	0.1373(8)	0.2816(5)	0.036(5)
C(4B)	-0.2453(12)	0.1054(10)	0.3443(5)	0.044(7)
C(5B)	-0.3105(12)	0.0643(10)	0.3708(6)	0.046(7)
C(6B)	-0.3430(13)	0.0008(10)	0.3678(6)	0.042(7)
C(7B)	-0.3186(13)	-0.0396(10)	0.3367(6)	0.044(7)
C(8B)	-0.2564(12)	-0.0269(9)	0.3009(5)	0.037(6)
C(9B)	-0.2008(10)	0.0306(8)	0.2865(5)	0.035(5)
C(10B)	-0.1958(10)	0.0923(8)	0.3073(5)	0.035(5)
C(11B)	0.0431(17)	0.1547(13)	0.1972(7)	0.036(6)
C(12B)	-0.0868(19)	0.1989(11)	0.2918(6)	0.043(7)
C(13B)	-0.048(2)	0.2570(13)	0.3475(9)	0.088(8)
C(14B)	-0.125(3)	0.3274(14)	0.3424(11)	0.142(12)
C(15B)	-0.1192(19)	-0.0026(11)	0.2166(6)	0.042(7)
C(16B)	-0.128(2)	-0.1191(11)	0.1976(7)	0.069(9)
C(17B)	-0.184(2)	-0.1822(13)	0.2145(9)	0.101(12)
O(1C)	0.1768(13)	0.0932(9)	0.2994(4)	0.050(5)
O(2C)	0.2430(12)	0.0430(9)	0.3651(4)	0.057(5)
O(3C)	0.5429(15)	-0.1364(9)	0.2171(5)	0.079(6)
O(4C)	0.4638(12)	-0.0173(7)	0.1896(4)	0.041(4)
N(1C)	0.2974(13)	0.0493(9)	0.2337(5)	0.030(5)
C(1C)	0.4332(11)	-0.0670(8)	0.2615(5)	0.041(6)
C(2C)	0.3539(11)	-0.0038(8)	0.2667(5)	0.035(5)
C(3C)	0.3346(11)	-0.0039(8)	0.3092(5)	0.044(6)
C(4C)	0.4097(14)	-0.0909(10)	0.3770(6)	0.053(7)
C(5C)	0.4756(14)	-0.1544(11)	0.4021(6)	0.057(7)
C(6C)	0.5495(14)	-0.2111(11)	0.3900(7)	0.057(8)
C(7C)	0.5809(14)	-0.2224(10)	0.3505(6)	0.051(7)
C(8C)	0.5440(13)	-0.1770(9)	0.3113(6)	0.049(6)
C(9C)	0.4662(11)	-0.1094(8)	0.3029(5)	0.044(6)
C(10C)	0.4028(11)	-0.0691(8)	0.3332(5)	0.042(5)
C(11C)	0.254(2)	0.0967(12)	0.2076(6)	0.040(6)
C(12C)	0.2447(16)	0.0495(12)	0.3236(6)	0.043(7)
C(13C)	0.1598(18)	0.0980(14)	0.3802(7)	0.072(9)
C(14C)	0.173(2)	0.0857(17)	0.4260(7)	0.107(10)
C(15C)	0.4854(16)	-0.0785(10)	0.2220(5)	0.034(6)
C(16C)	0.5161(16)	-0.0225(11)	0.1492(6)	0.036(6)
C(17C)	0.5955(18)	0.0269(13)	0.1412(8)	0.061(8)
O(1D)	0.1476(11)	0.2681(7)	0.0314(4)	0.035(4)
O(2D)	0.1015(11)	0.3364(8)	-0.0328(4)	0.040(4)

O(3D)	-0.2260(12)	0.4895(8)	0.1183(5)	0.049(5)
O(4D)	-0.1299(11)	0.3725(7)	0.1446(4)	0.041(4)
N(1D)	0.0397(14)	0.3147(10)	0.0989(5)	0.036(5)
C(1D)	-0.1070(11)	0.4257(7)	0.0731(5)	0.029(4)
C(2D)	-0.0191(10)	0.3680(7)	0.0668(5)	0.024(4)
C(3D)	0.0022(10)	0.3734(7)	0.0239(5)	0.022(4)
C(4D)	-0.0810(13)	0.4616(9)	-0.0423(5)	0.034(6)
C(5D)	-0.1522(13)	0.5223(9)	-0.0673(6)	0.036(6)
C(6D)	-0.2342(13)	0.5732(10)	-0.0545(6)	0.038(7)
C(7D)	-0.2678(14)	0.5774(9)	-0.0141(6)	0.039(6)
C(8D)	-0.2279(12)	0.5318(8)	0.0243(6)	0.031(6)
C(9D)	-0.1423(11)	0.4689(8)	0.0323(5)	0.028(5)
C(10D)	-0.0726(11)	0.4360(8)	0.0007(5)	0.023(4)
C(11D)	0.0854(17)	0.2694(11)	0.1264(6)	0.024(4)
C(12D)	0.0914(15)	0.3209(11)	0.0082(5)	0.027(5)
C(13D)	0.1791(19)	0.2848(12)	-0.0523(6)	0.060(8)
C(14D)	0.176(2)	0.3141(16)	-0.0978(6)	0.095(10)
C(15D)	-0.1599(17)	0.4338(11)	0.1129(5)	0.038(7)
C(16D)	-0.1727(17)	0.3736(11)	0.1867(6)	0.041(7)
C(17D)	-0.2544(18)	0.3267(14)	0.1964(7)	0.064(9)
O(1E)	-0.0679(11)	0.2209(8)	-0.0032(4)	0.038(4)
O(2E)	-0.0652(11)	0.1765(7)	0.0674(4)	0.029(4)
O(3E)	0.3379(11)	-0.1041(8)	0.0705(5)	0.048(4)
O(4E)	0.2376(11)	-0.0589(7)	0.1210(4)	0.034(4)
N(1E)	0.1383(13)	0.0922(9)	0.0983(5)	0.024(4)
C(1E)	0.1937(10)	0.0042(8)	0.0515(5)	0.028(5)
C(2E)	0.1273(10)	0.0694(8)	0.0616(5)	0.021(5)
C(3E)	0.0604(10)	0.1102(7)	0.0275(5)	0.024(5)
C(4E)	0.0316(13)	0.0952(10)	-0.0451(5)	0.047(7)
C(5E)	0.0495(14)	0.0599(10)	-0.0791(6)	0.036(6)
C(6E)	0.1213(13)	-0.0058(10)	-0.0820(6)	0.044(7)
C(7E)	0.1936(14)	-0.0540(10)	-0.0528(5)	0.037(6)
C(8E)	0.2151(13)	-0.0508(9)	-0.0119(5)	0.034(5)
C(9E)	0.1666(11)	0.0050(8)	0.0095(5)	0.031(5)
C(10E)	0.0818(11)	0.0722(8)	-0.0059(5)	0.031(6)
C(11E)	0.1515(17)	0.1208(11)	0.1251(6)	0.023(5)
C(12E)	-0.0281(15)	0.1767(10)	0.0286(5)	0.026(5)
C(13E)	-0.1643(15)	0.2317(11)	0.0714(6)	0.041(7)
C(14E)	-0.1971(18)	0.2151(13)	0.1158(6)	0.053(8)
C(15E)	0.2648(16)	-0.0566(10)	0.0802(5)	0.028(5)
C(16E)	0.2912(17)	-0.1216(10)	0.1536(5)	0.034(6)
C(17E)	0.2449(19)	-0.1092(13)	0.1947(6)	0.055(8)
O(1F)	0.4754(16)	0.1143(9)	0.3081(5)	0.083(6)
O(2F)	0.4202(11)	0.1788(9)	0.2435(5)	0.053(5)
O(3F)	0.0453(14)	0.4282(9)	0.3024(5)	0.071(5)
O(4F)	0.0917(12)	0.4036(8)	0.2392(4)	0.047(4)

N(1F)	0.2129(13)	0.2638(10)	0.2361(5)	0.034(5)
C(1F)	0.1879(11)	0.3234(8)	0.2982(5)	0.046(5)
C(2F)	0.2437(11)	0.2705(8)	0.2753(5)	0.037(5)
C(3F)	0.3253(11)	0.2181(8)	0.3003(5)	0.041(6)
C(4F)	0.3918(15)	0.1980(10)	0.3739(5)	0.054(6)
C(5F)	0.3968(17)	0.2114(12)	0.4142(6)	0.086(10)
C(6F)	0.3332(16)	0.2679(12)	0.4307(7)	0.086(10)
C(7F)	0.2494(16)	0.3248(12)	0.4121(6)	0.062(8)
C(8F)	0.2055(16)	0.3413(11)	0.3718(6)	0.066(7)
C(9F)	0.2362(12)	0.3037(8)	0.3389(5)	0.049(6)
C(10F)	0.3239(12)	0.2366(9)	0.3403(5)	0.046(6)
C(11F)	0.1907(18)	0.2404(12)	0.2084(6)	0.028(5)
C(12F)	0.4153(16)	0.1660(12)	0.2848(6)	0.045(7)
C(13F)	0.5080(15)	0.1325(12)	0.2244(8)	0.057(8)
C(14F)	0.5980(16)	0.1704(13)	0.2137(8)	0.060(8)
C(15F)	0.1029(17)	0.3879(11)	0.2818(6)	0.051(7)
C(16F)	0.0134(18)	0.4702(11)	0.2190(6)	0.055(8)
C(17F)	0.0327(18)	0.4808(11)	0.1728(6)	0.046(7)
Cr(2)	0.5000	0.5000	0.5000	0.0350(16)
O(1G)	0.2703(15)	0.3250(12)	0.5178(6)	0.093(7)
O(2G)	0.1554(15)	0.2594(9)	0.5509(5)	0.079(5)
O(3G)	0.3154(14)	0.5310(9)	0.6135(5)	0.066(5)
O(4G)	0.2798(14)	0.4714(10)	0.6794(5)	0.077(6)
N(1G)	0.3181(14)	0.4357(10)	0.5550(5)	0.036(5)
C(1G)	0.2201(11)	0.4323(8)	0.6221(5)	0.050(7)
C(2G)	0.2500(11)	0.4059(8)	0.5850(5)	0.038(5)
C(3G)	0.1998(11)	0.3467(8)	0.5839(4)	0.037(6)
C(4G)	0.0742(12)	0.2809(9)	0.6316(6)	0.037(6)
C(5G)	0.0100(13)	0.2656(11)	0.6672(6)	0.063(8)
C(6G)	-0.0100(13)	0.2988(10)	0.7010(6)	0.050(8)
C(7G)	0.0300(13)	0.3573(10)	0.7085(6)	0.056(8)
C(8G)	0.1002(12)	0.3960(10)	0.6835(5)	0.044(7)
C(9G)	0.1494(10)	0.3887(8)	0.6450(5)	0.034(5)
C(10G)	0.1363(10)	0.3339(8)	0.6203(5)	0.028(5)
C(11G)	0.3790(19)	0.4615(13)	0.5323(7)	0.040(7)
C(12G)	0.209(2)	0.3133(13)	0.5466(6)	0.060(8)
C(13G)	0.176(2)	0.2135(12)	0.5194(7)	0.085(7)
C(14G)	0.189(3)	0.1357(12)	0.5409(9)	0.110(10)
C(15G)	0.2756(19)	0.4827(12)	0.6365(6)	0.054(7)
C(16G)	0.341(2)	0.5169(15)	0.6956(7)	0.091(8)
C(17G)	0.331(3)	0.4975(17)	0.7425(7)	0.104(9)
O(1H)	0.1052(15)	0.7975(9)	0.4874(6)	0.084(6)
O(2H)	0.1956(13)	0.6781(9)	0.4987(5)	0.063(5)
O(3H)	0.4551(13)	0.6269(9)	0.3675(5)	0.063(5)
O(4H)	0.3810(14)	0.7069(10)	0.3091(5)	0.076(6)
N(1H)	0.3592(15)	0.6438(10)	0.4431(6)	0.049(6)

C(1H)	0.3072(11)	0.7268(8)	0.3739(5)	0.046(5)
C(2H)	0.2920(11)	0.7054(8)	0.4181(5)	0.035(5)
C(3H)	0.2094(11)	0.7563(8)	0.4320(5)	0.049(6)
C(4H)	0.0839(13)	0.8739(9)	0.3982(7)	0.060(7)
C(5H)	0.0356(15)	0.9337(10)	0.3657(7)	0.069(8)
C(6H)	0.0626(15)	0.9446(11)	0.3241(7)	0.072(8)
C(7H)	0.1391(15)	0.9035(10)	0.3026(7)	0.057(6)
C(8H)	0.2149(15)	0.8365(10)	0.3174(6)	0.067(7)
C(9H)	0.2296(12)	0.7948(8)	0.3593(5)	0.050(5)
C(10H)	0.1674(11)	0.8134(8)	0.3965(5)	0.048(6)
C(11H)	0.4082(19)	0.5930(12)	0.4660(7)	0.038(7)
C(12H)	0.1655(19)	0.7466(11)	0.4754(6)	0.058(8)
C(13H)	0.154(2)	0.6610(15)	0.5412(6)	0.084(10)
C(14H)	0.071(2)	0.6170(17)	0.5442(10)	0.116(13)
C(15H)	0.3900(16)	0.6844(11)	0.3515(6)	0.039(6)
C(16H)	0.454(2)	0.6615(16)	0.2847(7)	0.093(11)
C(17H)	0.414(3)	0.6833(19)	0.2408(7)	0.131(14)
O(1I)	0.2210(13)	0.5895(9)	0.3423(5)	0.066(5)
O(2I)	0.2450(11)	0.5191(8)	0.4078(5)	0.048(5)
O(3I)	0.6414(14)	0.2694(9)	0.3627(6)	0.087(6)
O(4I)	0.5795(13)	0.2931(9)	0.4249(4)	0.057(5)
N(1I)	0.4591(15)	0.4344(10)	0.4232(5)	0.033(5)
C(1I)	0.4951(11)	0.3708(8)	0.3631(5)	0.045(5)
C(2I)	0.4358(11)	0.4267(8)	0.3832(5)	0.048(6)
C(3I)	0.3592(11)	0.4774(8)	0.3559(5)	0.045(6)
C(4I)	0.3035(15)	0.4928(11)	0.2819(6)	0.065(6)
C(5I)	0.3013(16)	0.4780(11)	0.2416(6)	0.072(6)
C(6I)	0.3684(16)	0.4185(11)	0.2287(7)	0.072(7)
C(7I)	0.4492(16)	0.3616(11)	0.2488(6)	0.058(6)
C(8I)	0.4889(15)	0.3465(11)	0.2899(6)	0.068(7)
C(9I)	0.4539(12)	0.3875(9)	0.3213(5)	0.051(6)
C(10I)	0.3673(12)	0.4553(9)	0.3166(5)	0.052(5)
C(11I)	0.4728(18)	0.4555(12)	0.4525(6)	0.029(6)
C(12I)	0.2689(17)	0.5349(11)	0.3671(6)	0.050(7)
C(13I)	0.1519(17)	0.5669(12)	0.4232(8)	0.071(9)
C(14I)	0.079(2)	0.5206(16)	0.4440(10)	0.108(11)
C(15I)	0.5805(16)	0.3088(11)	0.3822(6)	0.043(6)
C(16I)	0.651(2)	0.2260(13)	0.4474(7)	0.080(10)
C(17I)	0.616(2)	0.2132(14)	0.4921(7)	0.077(9)
Cl(1T)	0.5691(11)	0.7504(7)	0.1575(4)	0.061(4)
C(2T)	0.500(3)	0.726(2)	0.1187(11)	0.053(13)
Cl(3T)	0.5785(12)	0.6505(8)	0.1000(5)	0.077(5)
Cl(4T)	0.8891(16)	0.0937(12)	0.4286(6)	0.073(7)
C(5T)	0.890(4)	0.048(3)	0.4823(11)	0.08(2)
Cl(6T)	0.998(2)	-0.0299(11)	0.4947(8)	0.106(9)

Table 3 Bond lengths [Å] and angles [°] for **3.12**.

Sb(1A)-F(3A)	1.859(7)	C(9A)-C(10A)	1.480(15)
Sb(1A)-F(2A)	1.863(7)	C(13A)-C(14A)	1.461(16)
Sb(1A)-F(4A)	1.870(6)	C(13A)-H(13A)	0.9900
Sb(1A)-F(1A)	1.873(6)	C(13A)-H(13B)	0.9900
Sb(1A)-F(5A)	1.880(7)	C(14A)-H(14A)	0.9800
Sb(1A)-F(6A)	1.881(7)	C(14A)-H(14B)	0.9800
Sb(1A)-F(5A')	1.866(7)	C(14A)-H(14C)	0.9800
Sb(1A)-F(1A')	1.870(7)	C(16A)-C(17A)	1.453(17)
Sb(1A)-F(6A')	1.871(7)	C(16A)-H(16A)	0.9900
Sb(1A)-F(4A')	1.872(7)	C(16A)-H(16B)	0.9900
Sb(1A)-F(3A')	1.873(7)	C(17A)-H(17A)	0.9800
Sb(1A)-F(2A')	1.876(7)	C(17A)-H(17B)	0.9800
Cr(1)-C(11B)	1.957(19)	C(17A)-H(17C)	0.9800
Cr(1)-C(11C)	1.97(2)	O(1B)-C(12B)	1.219(14)
Cr(1)-C(11D)	1.977(19)	O(2B)-C(12B)	1.314(15)
Cr(1)-C(11E)	1.992(19)	O(2B)-C(13B)	1.467(16)
Cr(1)-C(11A)	1.992(19)	O(3B)-C(15B)	1.208(14)
Cr(1)-C(11F)	2.00(2)	O(4B)-C(15B)	1.357(15)
O(1A)-C(12A)	1.213(14)	O(4B)-C(16B)	1.457(15)
O(2A)-C(12A)	1.329(14)	N(1B)-C(11B)	1.162(14)
O(2A)-C(13A)	1.467(15)	N(1B)-C(2B)	1.385(14)
O(3A)-C(15A)	1.216(14)	C(1B)-C(9B)	1.418(15)
O(4A)-C(15A)	1.364(14)	C(1B)-C(2B)	1.423(15)
O(4A)-C(16A)	1.451(15)	C(1B)-C(15B)	1.448(16)
N(1A)-C(11A)	1.141(14)	C(2B)-C(3B)	1.392(15)
N(1A)-C(2A)	1.378(14)	C(3B)-C(10B)	1.422(15)
C(1A)-C(9A)	1.416(14)	C(3B)-C(12B)	1.487(16)
C(1A)-C(2A)	1.423(14)	C(4B)-C(10B)	1.377(15)
C(1A)-C(15A)	1.445(15)	C(4B)-C(5B)	1.390(16)
C(2A)-C(3A)	1.386(14)	C(4B)-H(4B)	0.9500
C(3A)-C(10A)	1.422(14)	C(5B)-C(6B)	1.365(16)
C(3A)-C(12A)	1.479(15)	C(5B)-H(5B)	0.9500
C(4A)-C(10A)	1.372(15)	C(6B)-C(7B)	1.381(16)
C(4A)-C(5A)	1.394(15)	C(6B)-H(6B)	0.9500
C(4A)-H(4A)	0.9500	C(7B)-C(8B)	1.382(16)
C(5A)-C(6A)	1.377(16)	C(7B)-H(7B)	0.9500
C(5A)-H(5A)	0.9500	C(8B)-C(9B)	1.396(15)
C(6A)-C(7A)	1.368(16)	C(8B)-H(8B)	0.9500
C(6A)-H(6A)	0.9500	C(9B)-C(10B)	1.477(15)
C(7A)-C(8A)	1.383(15)	C(13B)-C(14B)	1.437(18)
C(7A)-H(7A)	0.9500	C(13B)-H(13C)	0.9900
C(8A)-C(9A)	1.390(15)	C(13B)-H(13D)	0.9900
C(8A)-H(8A)	0.9500	C(14B)-H(14D)	0.9800

C(14B)-H(14E)	0.9800	O(1D)-C(12D)	1.204(14)
C(14B)-H(14F)	0.9800	O(2D)-C(12D)	1.306(14)
C(16B)-C(17B)	1.496(17)	O(2D)-C(13D)	1.450(15)
C(16B)-H(16C)	0.9900	O(3D)-C(15D)	1.226(14)
C(16B)-H(16D)	0.9900	O(4D)-C(15D)	1.349(15)
C(17B)-H(17D)	0.9800	O(4D)-C(16D)	1.450(15)
C(17B)-H(17E)	0.9800	N(1D)-C(11D)	1.155(14)
C(17B)-H(17F)	0.9800	N(1D)-C(2D)	1.380(14)
O(1C)-C(12C)	1.219(15)	C(1D)-C(2D)	1.412(14)
O(2C)-C(12C)	1.326(15)	C(1D)-C(9D)	1.420(15)
O(2C)-C(13C)	1.455(16)	C(1D)-C(15D)	1.455(15)
O(3C)-C(15C)	1.203(14)	C(2D)-C(3D)	1.394(14)
O(4C)-C(15C)	1.354(15)	C(3D)-C(10D)	1.418(14)
O(4C)-C(16C)	1.456(15)	C(3D)-C(12D)	1.478(15)
N(1C)-C(11C)	1.135(14)	C(4D)-C(10D)	1.372(15)
N(1C)-C(2C)	1.385(14)	C(4D)-C(5D)	1.398(16)
C(1C)-C(2C)	1.409(14)	C(4D)-H(4D)	0.9500
C(1C)-C(9C)	1.427(15)	C(5D)-C(6D)	1.366(16)
C(1C)-C(15C)	1.455(16)	C(5D)-H(5D)	0.9500
C(2C)-C(3C)	1.393(15)	C(6D)-C(7D)	1.376(16)
C(3C)-C(10C)	1.416(15)	C(6D)-H(6D)	0.9500
C(3C)-C(12C)	1.474(16)	C(7D)-C(8D)	1.386(15)
C(4C)-C(10C)	1.391(15)	C(7D)-H(7D)	0.9500
C(4C)-C(5C)	1.397(16)	C(8D)-C(9D)	1.397(15)
C(4C)-H(4C)	0.9500	C(8D)-H(8D)	0.9500
C(5C)-C(6C)	1.369(16)	C(9D)-C(10D)	1.477(15)
C(5C)-H(5C)	0.9500	C(13D)-C(14D)	1.454(17)
C(6C)-C(7C)	1.376(16)	C(13D)-H(13G)	0.9900
C(6C)-H(6C)	0.9500	C(13D)-H(13H)	0.9900
C(7C)-C(8C)	1.394(16)	C(14D)-H(14J)	0.9800
C(7C)-H(7C)	0.9500	C(14D)-H(14K)	0.9800
C(8C)-C(9C)	1.400(15)	C(14D)-H(14L)	0.9800
C(8C)-H(8C)	0.9500	C(16D)-C(17D)	1.479(17)
C(9C)-C(10C)	1.476(16)	C(16D)-H(16G)	0.9900
C(13C)-C(14C)	1.465(17)	C(16D)-H(16H)	0.9900
C(13C)-H(13E)	0.9900	C(17D)-H(17J)	0.9800
C(13C)-H(13F)	0.9900	C(17D)-H(17K)	0.9800
C(14C)-H(14G)	0.9800	C(17D)-H(17L)	0.9800
C(14C)-H(14H)	0.9800	O(1E)-C(12E)	1.216(14)
C(14C)-H(14I)	0.9800	O(2E)-C(12E)	1.325(14)
C(16C)-C(17C)	1.488(17)	O(2E)-C(13E)	1.461(15)
C(16C)-H(16E)	0.9900	O(3E)-C(15E)	1.218(14)
C(16C)-H(16F)	0.9900	O(4E)-C(15E)	1.347(14)
C(17C)-H(17G)	0.9800	O(4E)-C(16E)	1.452(14)
C(17C)-H(17H)	0.9800	N(1E)-C(11E)	1.155(14)
C(17C)-H(17I)	0.9800	N(1E)-C(2E)	1.379(14)

C(1E)-C(2E)	1.417(14)	C(4F)-H(4F)	0.9500
C(1E)-C(9E)	1.420(15)	C(5F)-C(6F)	1.376(17)
C(1E)-C(15E)	1.455(15)	C(5F)-H(5F)	0.9500
C(2E)-C(3E)	1.393(14)	C(6F)-C(7F)	1.375(17)
C(3E)-C(10E)	1.414(15)	C(6F)-H(6F)	0.9500
C(3E)-C(12E)	1.484(15)	C(7F)-C(8F)	1.389(16)
C(4E)-C(10E)	1.384(15)	C(7F)-H(7F)	0.9500
C(4E)-C(5E)	1.396(16)	C(8F)-C(9F)	1.405(16)
C(4E)-H(4E)	0.9500	C(8F)-H(8F)	0.9500
C(5E)-C(6E)	1.378(16)	C(9F)-C(10F)	1.474(16)
C(5E)-H(5E)	0.9500	C(13F)-C(14F)	1.461(17)
C(6E)-C(7E)	1.369(16)	C(13F)-H(13K)	0.9900
C(6E)-H(6E)	0.9500	C(13F)-H(13L)	0.9900
C(7E)-C(8E)	1.388(15)	C(14F)-H(14P)	0.9800
C(7E)-H(7E)	0.9500	C(14F)-H(14Q)	0.9800
C(8E)-C(9E)	1.399(15)	C(14F)-H(14R)	0.9800
C(8E)-H(8E)	0.9500	C(16F)-C(17F)	1.486(17)
C(9E)-C(10E)	1.466(15)	C(16F)-H(16K)	0.9900
C(13E)-C(14E)	1.467(17)	C(16F)-H(16L)	0.9900
C(13E)-H(13I)	0.9900	C(17F)-H(17P)	0.9800
C(13E)-H(13J)	0.9900	C(17F)-H(17Q)	0.9800
C(14E)-H(14M)	0.9800	C(17F)-H(17R)	0.9800
C(14E)-H(14N)	0.9800	Cr(2)-C(11H)	1.987(19)
C(14E)-H(14O)	0.9800	Cr(2)-C(11I)	1.99(2)
C(16E)-C(17E)	1.482(16)	Cr(2)-C(11G)	1.994(19)
C(16E)-H(16I)	0.9900	O(1G)-C(12G)	1.203(15)
C(16E)-H(16J)	0.9900	O(2G)-C(12G)	1.315(15)
C(17E)-H(17M)	0.9800	O(2G)-C(13G)	1.460(16)
C(17E)-H(17N)	0.9800	O(3G)-C(15G)	1.221(15)
C(17E)-H(17O)	0.9800	O(4G)-C(15G)	1.363(15)
O(1F)-C(12F)	1.219(15)	O(4G)-C(16G)	1.465(16)
O(2F)-C(12F)	1.311(15)	N(1G)-C(11G)	1.151(14)
O(2F)-C(13F)	1.459(15)	N(1G)-C(2G)	1.378(14)
O(3F)-C(15F)	1.221(15)	C(1G)-C(2G)	1.410(15)
O(4F)-C(15F)	1.355(15)	C(1G)-C(9G)	1.416(15)
O(4F)-C(16F)	1.452(15)	C(1G)-C(15G)	1.457(16)
N(1F)-C(11F)	1.158(14)	C(2G)-C(3G)	1.400(15)
N(1F)-C(2F)	1.391(14)	C(3G)-C(10G)	1.406(15)
C(1F)-C(2F)	1.417(15)	C(3G)-C(12G)	1.474(16)
C(1F)-C(9F)	1.419(15)	C(4G)-C(10G)	1.375(15)
C(1F)-C(15F)	1.444(16)	C(4G)-C(5G)	1.396(16)
C(2F)-C(3F)	1.398(14)	C(4G)-H(4G)	0.9500
C(3F)-C(10F)	1.419(15)	C(5G)-C(6G)	1.370(16)
C(3F)-C(12F)	1.478(16)	C(5G)-H(5G)	0.9500
C(4F)-C(10F)	1.381(15)	C(6G)-C(7G)	1.374(16)
C(4F)-C(5F)	1.396(16)	C(6G)-H(6G)	0.9500

C(7G)-C(8G)	1.389(16)	C(14H)-H(14V)	0.9800
C(7G)-H(7G)	0.9500	C(14H)-H(14W)	0.9800
C(8G)-C(9G)	1.396(15)	C(14H)-H(14X)	0.9800
C(8G)-H(8G)	0.9500	C(16H)-C(17H)	1.474(17)
C(9G)-C(10G)	1.479(15)	C(16H)-H(16O)	0.9900
C(13G)-C(14G)	1.437(17)	C(16H)-H(16P)	0.9900
C(13G)-H(13M)	0.9900	C(17H)-H(17V)	0.9800
C(13G)-H(13N)	0.9900	C(17H)-H(17W)	0.9800
C(14G)-H(14S)	0.9800	C(17H)-H(17X)	0.9800
C(14G)-H(14T)	0.9800	O(1I)-C(12I)	1.207(15)
C(14G)-H(14U)	0.9800	O(2I)-C(12I)	1.325(15)
C(16G)-C(17G)	1.492(17)	O(2I)-C(13I)	1.458(15)
C(16G)-H(16M)	0.9900	O(3I)-C(15I)	1.207(14)
C(16G)-H(16N)	0.9900	O(4I)-C(15I)	1.352(15)
C(17G)-H(17S)	0.9800	O(4I)-C(16I)	1.437(16)
C(17G)-H(17T)	0.9800	N(1I)-C(11I)	1.145(14)
C(17G)-H(17U)	0.9800	N(1I)-C(2I)	1.393(14)
O(1H)-C(12H)	1.211(15)	C(1I)-C(2I)	1.415(15)
O(2H)-C(12H)	1.314(15)	C(1I)-C(9I)	1.421(15)
O(2H)-C(13H)	1.449(16)	C(1I)-C(15I)	1.441(16)
O(3H)-C(15H)	1.224(14)	C(2I)-C(3I)	1.383(15)
O(4H)-C(15H)	1.348(15)	C(3I)-C(10I)	1.423(15)
O(4H)-C(16H)	1.450(16)	C(3I)-C(12I)	1.482(16)
N(1H)-C(11H)	1.138(14)	C(4I)-C(10I)	1.374(16)
N(1H)-C(2H)	1.384(14)	C(4I)-C(5I)	1.403(16)
C(1H)-C(2H)	1.417(15)	C(4I)-H(4I)	0.9500
C(1H)-C(9H)	1.423(15)	C(5I)-C(6I)	1.377(17)
C(1H)-C(15H)	1.445(16)	C(5I)-H(5I)	0.9500
C(2H)-C(3H)	1.385(14)	C(6I)-C(7I)	1.368(16)
C(3H)-C(10H)	1.412(15)	C(6I)-H(6I)	0.9500
C(3H)-C(12H)	1.479(16)	C(7I)-C(8I)	1.395(16)
C(4H)-C(10H)	1.378(15)	C(7I)-H(7I)	0.9500
C(4H)-C(5H)	1.399(16)	C(8I)-C(9I)	1.410(16)
C(4H)-H(4H)	0.9500	C(8I)-H(8I)	0.9500
C(5H)-C(6H)	1.363(17)	C(9I)-C(10I)	1.466(16)
C(5H)-H(5H)	0.9500	C(13I)-C(14I)	1.442(17)
C(6H)-C(7H)	1.369(17)	C(13I)-H(13Q)	0.9900
C(6H)-H(6H)	0.9500	C(13I)-H(13R)	0.9900
C(7H)-C(8H)	1.399(16)	C(14I)-H(14Y)	0.9800
C(7H)-H(7H)	0.9500	C(14I)-H(14Z)	0.9800
C(8H)-C(9H)	1.402(16)	C(14I)-H(14$)	0.9800
C(8H)-H(8H)	0.9500	C(16I)-C(17I)	1.481(17)
C(9H)-C(10H)	1.481(16)	C(16I)-H(16Q)	0.9900
C(13H)-C(14H)	1.462(18)	C(16I)-H(16R)	0.9900
C(13H)-H(13O)	0.9900	C(17I)-H(17Y)	0.9800
C(13H)-H(13P)	0.9900	C(17I)-H(17Z)	0.9800

C(17I)-H(17$)	0.9800	Cl(4T)-C(5T)	1.76(2)
Cl(1T)-C(2T)	1.76(2)	C(5T)-Cl(6T)	1.76(2)
C(2T)-Cl(3T)	1.76(2)	C(5T)-H(5TA)	0.9899
C(2T)-H(2T1)	0.9900	C(5T)-H(5TB)	0.9900
C(2T)-H(2T2)	0.9900	Cl(6T)-C(5T)#1	1.56(6)

F(3A)-Sb(1A)-F(2A)	92.1(4)	C(11B)-Cr(1)-C(11D)	94.4(9)
F(3A)-Sb(1A)-F(4A)	90.6(4)	C(11C)-Cr(1)-C(11D)	177.4(10)
F(2A)-Sb(1A)-F(4A)	90.4(4)	C(11B)-Cr(1)-C(11E)	90.0(9)
F(3A)-Sb(1A)-F(1A)	90.4(4)	C(11C)-Cr(1)-C(11E)	95.7(9)
F(2A)-Sb(1A)-F(1A)	89.8(4)	C(11D)-Cr(1)-C(11E)	86.9(9)
F(4A)-Sb(1A)-F(1A)	179.0(4)	C(11B)-Cr(1)-C(11A)	179.1(10)
F(3A)-Sb(1A)-F(5A)	90.0(4)	C(11C)-Cr(1)-C(11A)	94.9(10)
F(2A)-Sb(1A)-F(5A)	177.9(4)	C(11D)-Cr(1)-C(11A)	85.2(9)
F(4A)-Sb(1A)-F(5A)	89.9(4)	C(11E)-Cr(1)-C(11A)	89.3(9)
F(1A)-Sb(1A)-F(5A)	89.8(4)	C(11B)-Cr(1)-C(11F)	90.1(9)
F(3A)-Sb(1A)-F(6A)	178.0(4)	C(11C)-Cr(1)-C(11F)	83.0(9)
F(2A)-Sb(1A)-F(6A)	89.9(4)	C(11D)-Cr(1)-C(11F)	94.4(9)
F(4A)-Sb(1A)-F(6A)	89.5(4)	C(11E)-Cr(1)-C(11F)	178.7(9)
F(1A)-Sb(1A)-F(6A)	89.5(4)	C(11A)-Cr(1)-C(11F)	90.6(9)
F(5A)-Sb(1A)-F(6A)	88.0(4)	C(12A)-O(2A)-C(13A)	115.1(13)
F(5A')-Sb(1A)-F(1A')	90.4(4)	C(15A)-O(4A)-C(16A)	116.8(15)
F(5A')-Sb(1A)-F(6A')	90.7(4)	C(11A)-N(1A)-C(2A)	167(2)
F(1A')-Sb(1A)-F(6A')	90.0(4)	C(9A)-C(1A)-C(2A)	107.2(11)
F(5A')-Sb(1A)-F(4A')	90.0(4)	C(9A)-C(1A)-C(15A)	130.2(13)
F(1A')-Sb(1A)-F(4A')	179.6(5)	C(2A)-C(1A)-C(15A)	122.2(12)
F(6A')-Sb(1A)-F(4A')	89.9(4)	N(1A)-C(2A)-C(3A)	125.3(13)
F(5A')-Sb(1A)-F(3A')	90.3(4)	N(1A)-C(2A)-C(1A)	123.8(13)
F(1A')-Sb(1A)-F(3A')	90.2(4)	C(3A)-C(2A)-C(1A)	110.9(12)
F(6A')-Sb(1A)-F(3A')	179.0(5)	C(2A)-C(3A)-C(10A)	107.8(12)
F(4A')-Sb(1A)-F(3A')	89.9(4)	C(2A)-C(3A)-C(12A)	122.8(12)
F(5A')-Sb(1A)-F(2A')	179.7(5)	C(10A)-C(3A)-C(12A)	128.8(12)
F(1A')-Sb(1A)-F(2A')	89.9(4)	C(10A)-C(4A)-C(5A)	131.8(16)
F(6A')-Sb(1A)-F(2A')	89.5(4)	C(10A)-C(4A)-H(4A)	114.1
F(4A')-Sb(1A)-F(2A')	89.8(4)	C(5A)-C(4A)-H(4A)	114.1
F(3A')-Sb(1A)-F(2A')	89.5(4)	C(6A)-C(5A)-C(4A)	127.4(17)
F(2B)-Sb(1B)-F(2B)#2	180.00(19)	C(6A)-C(5A)-H(5A)	116.3
F(2B)-Sb(1B)-F(3B)#2	89.6(4)	C(4A)-C(5A)-H(5A)	116.3
F(2B)-Sb(1B)-F(3B)	90.4(4)	C(7A)-C(6A)-C(5A)	127.8(17)
F(3B)-Sb(1B)-F(3B)#2	180.0(8)	C(7A)-C(6A)-H(6A)	116.1
F(2B)-Sb(1B)-F(1B)	89.9(4)	C(5A)-C(6A)-H(6A)	116.1
F(3B)-Sb(1B)-F(1B)	89.9(4)	C(6A)-C(7A)-C(8A)	131.6(17)
F(2B)-Sb(1B)-F(1B)#2	90.1(4)	C(6A)-C(7A)-H(7A)	114.2
F(3B)-Sb(1B)-F(1B)#2	90.1(4)	C(8A)-C(7A)-H(7A)	114.2
F(1B)-Sb(1B)-F(1B)#2	180.0	C(7A)-C(8A)-C(9A)	129.3(16)
C(11B)-Cr(1)-C(11C)	85.6(10)	C(7A)-C(8A)-H(8A)	115.4

C(9A)-C(8A)-H(8A)	115.4	C(3B)-C(2B)-C(1B)	111.1(12)
C(8A)-C(9A)-C(1A)	127.8(14)	C(2B)-C(3B)-C(10B)	107.6(12)
C(8A)-C(9A)-C(10A)	125.3(13)	C(2B)-C(3B)-C(12B)	123.6(13)
C(1A)-C(9A)-C(10A)	106.9(11)	C(10B)-C(3B)-C(12B)	127.9(13)
C(4A)-C(10A)-C(3A)	125.9(14)	C(10B)-C(4B)-C(5B)	128.9(17)
C(4A)-C(10A)-C(9A)	126.9(13)	C(10B)-C(4B)-H(4B)	115.6
C(3A)-C(10A)-C(9A)	107.2(11)	C(5B)-C(4B)-H(4B)	115.6
N(1A)-C(11A)-Cr(1)	174(2)	C(6B)-C(5B)-C(4B)	130.1(18)
O(1A)-C(12A)-O(2A)	124.0(15)	C(6B)-C(5B)-H(5B)	114.9
O(1A)-C(12A)-C(3A)	122.9(14)	C(4B)-C(5B)-H(5B)	114.9
O(2A)-C(12A)-C(3A)	113.1(13)	C(5B)-C(6B)-C(7B)	128.3(18)
C(14A)-C(13A)-O(2A)	108.9(14)	C(5B)-C(6B)-H(6B)	115.9
C(14A)-C(13A)-H(13A)	109.9	C(7B)-C(6B)-H(6B)	115.9
O(2A)-C(13A)-H(13A)	109.9	C(8B)-C(7B)-C(6B)	129.8(18)
C(14A)-C(13A)-H(13B)	109.9	C(8B)-C(7B)-H(7B)	115.1
O(2A)-C(13A)-H(13B)	109.9	C(6B)-C(7B)-H(7B)	115.1
H(13A)-C(13A)-H(13B)	108.3	C(7B)-C(8B)-C(9B)	129.1(17)
C(13A)-C(14A)-H(14A)	109.3	C(7B)-C(8B)-H(8B)	115.5
C(13A)-C(14A)-H(14B)	109.4	C(9B)-C(8B)-H(8B)	115.5
H(14A)-C(14A)-H(14B)	109.5	C(8B)-C(9B)-C(1B)	125.9(14)
C(13A)-C(14A)-H(14C)	109.7	C(8B)-C(9B)-C(10B)	126.5(14)
H(14A)-C(14A)-H(14C)	109.5	C(1B)-C(9B)-C(10B)	107.6(12)
H(14B)-C(14A)-H(14C)	109.5	C(4B)-C(10B)-C(3B)	125.6(14)
O(3A)-C(15A)-O(4A)	121.6(15)	C(4B)-C(10B)-C(9B)	127.4(14)
O(3A)-C(15A)-C(1A)	125.2(15)	C(3B)-C(10B)-C(9B)	107.0(12)
O(4A)-C(15A)-C(1A)	112.9(13)	N(1B)-C(11B)-Cr(1)	170(2)
O(4A)-C(16A)-C(17A)	107.8(17)	O(1B)-C(12B)-O(2B)	124.8(17)
O(4A)-C(16A)-H(16A)	110.1	O(1B)-C(12B)-C(3B)	120.2(16)
C(17A)-C(16A)-H(16A)	110.1	O(2B)-C(12B)-C(3B)	115.0(15)
O(4A)-C(16A)-H(16B)	110.1	C(14B)-C(13B)-O(2B)	111.7(19)
C(17A)-C(16A)-H(16B)	110.1	C(14B)-C(13B)-H(13C)	109.3
H(16A)-C(16A)-H(16B)	108.5	O(2B)-C(13B)-H(13C)	109.3
C(16A)-C(17A)-H(17A)	109.4	C(14B)-C(13B)-H(13D)	109.3
C(16A)-C(17A)-H(17B)	109.2	O(2B)-C(13B)-H(13D)	109.3
H(17A)-C(17A)-H(17B)	109.5	H(13C)-C(13B)-H(13D)	107.9
C(16A)-C(17A)-H(17C)	109.8	C(13B)-C(14B)-H(14D)	109.3
H(17A)-C(17A)-H(17C)	109.5	C(13B)-C(14B)-H(14E)	109.8
H(17B)-C(17A)-H(17C)	109.5	H(14D)-C(14B)-H(14E)	109.5
C(12B)-O(2B)-C(13B)	121.8(16)	C(13B)-C(14B)-H(14F)	109.3
C(15B)-O(4B)-C(16B)	118.5(14)	H(14D)-C(14B)-H(14F)	109.5
C(11B)-N(1B)-C(2B)	167(2)	H(14E)-C(14B)-H(14F)	109.5
C(9B)-C(1B)-C(2B)	106.6(12)	O(3B)-C(15B)-O(4B)	120.0(16)
C(9B)-C(1B)-C(15B)	130.5(13)	O(3B)-C(15B)-C(1B)	125.7(16)
C(2B)-C(1B)-C(15B)	122.8(13)	O(4B)-C(15B)-C(1B)	114.2(14)
N(1B)-C(2B)-C(3B)	125.7(14)	O(4B)-C(16B)-C(17B)	106.4(16)
N(1B)-C(2B)-C(1B)	122.8(14)	O(4B)-C(16B)-H(16C)	110.4

C(17B)-C(16B)-H(16C)	110.4	O(2C)-C(12C)-C(3C)	113.7(15)
O(4B)-C(16B)-H(16D)	110.4	O(2C)-C(13C)-C(14C)	108.3(18)
C(17B)-C(16B)-H(16D)	110.4	O(2C)-C(13C)-H(13E)	110.0
H(16C)-C(16B)-H(16D)	108.6	C(14C)-C(13C)-H(13E)	110.0
C(16B)-C(17B)-H(17D)	109.2	O(2C)-C(13C)-H(13F)	110.0
C(16B)-C(17B)-H(17E)	109.5	C(14C)-C(13C)-H(13F)	110.0
H(17D)-C(17B)-H(17E)	109.5	H(13E)-C(13C)-H(13F)	108.4
C(16B)-C(17B)-H(17F)	109.7	C(13C)-C(14C)-H(14G)	109.1
H(17D)-C(17B)-H(17F)	109.5	C(13C)-C(14C)-H(14H)	109.5
H(17E)-C(17B)-H(17F)	109.5	H(14G)-C(14C)-H(14H)	109.5
C(12C)-O(2C)-C(13C)	115.3(14)	C(13C)-C(14C)-H(14I)	109.8
C(15C)-O(4C)-C(16C)	118.2(14)	H(14G)-C(14C)-H(14I)	109.5
C(11C)-N(1C)-C(2C)	175(2)	H(14H)-C(14C)-H(14I)	109.5
C(2C)-C(1C)-C(9C)	106.4(12)	O(3C)-C(15C)-O(4C)	120.7(16)
C(2C)-C(1C)-C(15C)	126.1(13)	O(3C)-C(15C)-C(1C)	125.1(16)
C(9C)-C(1C)-C(15C)	126.5(13)	O(4C)-C(15C)-C(1C)	114.2(14)
N(1C)-C(2C)-C(3C)	124.1(13)	O(4C)-C(16C)-C(17C)	108.8(15)
N(1C)-C(2C)-C(1C)	124.2(14)	O(4C)-C(16C)-H(16E)	109.9
C(3C)-C(2C)-C(1C)	111.6(12)	C(17C)-C(16C)-H(16E)	109.9
C(2C)-C(3C)-C(10C)	107.5(12)	O(4C)-C(16C)-H(16F)	109.9
C(2C)-C(3C)-C(12C)	122.7(13)	C(17C)-C(16C)-H(16F)	109.9
C(10C)-C(3C)-C(12C)	129.0(14)	H(16E)-C(16C)-H(16F)	108.3
C(10C)-C(4C)-C(5C)	128.7(18)	C(16C)-C(17C)-H(17G)	109.4
C(10C)-C(4C)-H(4C)	115.7	C(16C)-C(17C)-H(17H)	110.1
C(5C)-C(4C)-H(4C)	115.7	H(17G)-C(17C)-H(17H)	109.5
C(6C)-C(5C)-C(4C)	129.1(19)	C(16C)-C(17C)-H(17I)	108.9
C(6C)-C(5C)-H(5C)	115.5	H(17G)-C(17C)-H(17I)	109.5
C(4C)-C(5C)-H(5C)	115.5	H(17H)-C(17C)-H(17I)	109.5
C(5C)-C(6C)-C(7C)	131.0(19)	C(12D)-O(2D)-C(13D)	119.0(14)
C(5C)-C(6C)-H(6C)	114.5	C(15D)-O(4D)-C(16D)	119.6(14)
C(7C)-C(6C)-H(6C)	114.5	C(11D)-N(1D)-C(2D)	178(2)
C(6C)-C(7C)-C(8C)	128.0(18)	C(2D)-C(1D)-C(9D)	106.5(12)
C(6C)-C(7C)-H(7C)	116.0	C(2D)-C(1D)-C(15D)	126.8(13)
C(8C)-C(7C)-H(7C)	116.0	C(9D)-C(1D)-C(15D)	126.3(13)
C(7C)-C(8C)-C(9C)	128.3(17)	N(1D)-C(2D)-C(3D)	124.6(13)
C(7C)-C(8C)-H(8C)	115.9	N(1D)-C(2D)-C(1D)	124.5(14)
C(9C)-C(8C)-H(8C)	115.9	C(3D)-C(2D)-C(1D)	110.9(12)
C(8C)-C(9C)-C(1C)	124.1(15)	C(2D)-C(3D)-C(10D)	108.4(12)
C(8C)-C(9C)-C(10C)	128.6(14)	C(2D)-C(3D)-C(12D)	122.5(12)
C(1C)-C(9C)-C(10C)	107.3(12)	C(10D)-C(3D)-C(12D)	129.1(13)
C(4C)-C(10C)-C(3C)	126.5(15)	C(10D)-C(4D)-C(5D)	131.2(17)
C(4C)-C(10C)-C(9C)	126.4(14)	C(10D)-C(4D)-H(4D)	114.4
C(3C)-C(10C)-C(9C)	107.1(13)	C(5D)-C(4D)-H(4D)	114.4
N(1C)-C(11C)-Cr(1)	175(2)	C(6D)-C(5D)-C(4D)	128.2(18)
O(1C)-C(12C)-O(2C)	123.8(16)	C(6D)-C(5D)-H(5D)	115.9
O(1C)-C(12C)-C(3C)	122.4(16)	C(4D)-C(5D)-H(5D)	115.9

C(5D)-C(6D)-C(7D)	129.0(18)	C(12E)-O(2E)-C(13E)	116.6(13)
C(5D)-C(6D)-H(6D)	115.5	C(15E)-O(4E)-C(16E)	119.5(13)
C(7D)-C(6D)-H(6D)	115.5	C(11E)-N(1E)-C(2E)	170(2)
C(6D)-C(7D)-C(8D)	129.7(18)	C(2E)-C(1E)-C(9E)	106.4(12)
C(6D)-C(7D)-H(7D)	115.1	C(2E)-C(1E)-C(15E)	126.7(13)
C(8D)-C(7D)-H(7D)	115.1	C(9E)-C(1E)-C(15E)	126.5(13)
C(7D)-C(8D)-C(9D)	129.0(17)	N(1E)-C(2E)-C(3E)	125.9(13)
C(7D)-C(8D)-H(8D)	115.5	N(1E)-C(2E)-C(1E)	123.3(13)
C(9D)-C(8D)-H(8D)	115.5	C(3E)-C(2E)-C(1E)	110.4(12)
C(8D)-C(9D)-C(1D)	124.9(14)	C(2E)-C(3E)-C(10E)	108.6(12)
C(8D)-C(9D)-C(10D)	126.9(14)	C(2E)-C(3E)-C(12E)	125.0(13)
C(1D)-C(9D)-C(10D)	108.1(12)	C(10E)-C(3E)-C(12E)	126.0(13)
C(4D)-C(10D)-C(3D)	128.0(14)	C(10E)-C(4E)-C(5E)	128.3(17)
C(4D)-C(10D)-C(9D)	126.0(14)	C(10E)-C(4E)-H(4E)	115.9
C(3D)-C(10D)-C(9D)	106.0(12)	C(5E)-C(4E)-H(4E)	115.9
N(1D)-C(11D)-Cr(1)	170(2)	C(6E)-C(5E)-C(4E)	128.8(18)
O(1D)-C(12D)-O(2D)	123.7(16)	C(6E)-C(5E)-H(5E)	115.6
O(1D)-C(12D)-C(3D)	122.5(15)	C(4E)-C(5E)-H(5E)	115.6
O(2D)-C(12D)-C(3D)	113.8(14)	C(7E)-C(6E)-C(5E)	129.9(19)
O(2D)-C(13D)-C(14D)	108.9(17)	C(7E)-C(6E)-H(6E)	115.1
O(2D)-C(13D)-H(13G)	109.9	C(5E)-C(6E)-H(6E)	115.1
C(14D)-C(13D)-H(13G)	109.9	C(6E)-C(7E)-C(8E)	130.1(18)
O(2D)-C(13D)-H(13H)	109.9	C(6E)-C(7E)-H(7E)	114.9
C(14D)-C(13D)-H(13H)	109.9	C(8E)-C(7E)-H(7E)	114.9
H(13G)-C(13D)-H(13H)	108.3	C(7E)-C(8E)-C(9E)	127.0(16)
C(13D)-C(14D)-H(14J)	109.1	C(7E)-C(8E)-H(8E)	116.5
C(13D)-C(14D)-H(14K)	109.9	C(9E)-C(8E)-H(8E)	116.5
H(14J)-C(14D)-H(14K)	109.5	C(8E)-C(9E)-C(1E)	123.5(14)
C(13D)-C(14D)-H(14L)	109.4	C(8E)-C(9E)-C(10E)	128.2(14)
H(14J)-C(14D)-H(14L)	109.5	C(1E)-C(9E)-C(10E)	108.3(12)
H(14K)-C(14D)-H(14L)	109.5	C(4E)-C(10E)-C(3E)	126.0(14)
O(3D)-C(15D)-O(4D)	121.6(15)	C(4E)-C(10E)-C(9E)	127.8(14)
O(3D)-C(15D)-C(1D)	125.0(15)	C(3E)-C(10E)-C(9E)	106.3(12)
O(4D)-C(15D)-C(1D)	113.3(14)	N(1E)-C(11E)-Cr(1)	173.3(18)
O(4D)-C(16D)-C(17D)	110.0(16)	O(1E)-C(12E)-O(2E)	124.9(15)
O(4D)-C(16D)-H(16G)	109.7	O(1E)-C(12E)-C(3E)	122.8(15)
C(17D)-C(16D)-H(16G)	109.7	O(2E)-C(12E)-C(3E)	111.9(13)
O(4D)-C(16D)-H(16H)	109.7	O(2E)-C(13E)-C(14E)	107.0(15)
C(17D)-C(16D)-H(16H)	109.7	O(2E)-C(13E)-H(13I)	110.3
H(16G)-C(16D)-H(16H)	108.2	C(14E)-C(13E)-H(13I)	110.3
C(16D)-C(17D)-H(17J)	109.3	O(2E)-C(13E)-H(13J)	110.3
C(16D)-C(17D)-H(17K)	110.0	C(14E)-C(13E)-H(13J)	110.3
H(17J)-C(17D)-H(17K)	109.5	H(13I)-C(13E)-H(13J)	108.6
C(16D)-C(17D)-H(17L)	109.2	C(13E)-C(14E)-H(14M)	109.6
H(17J)-C(17D)-H(17L)	109.5	C(13E)-C(14E)-H(14N)	109.2
H(17K)-C(17D)-H(17L)	109.5	H(14M)-C(14E)-H(14N)	109.5

C(13E)-C(14E)-H(14O)	109.6	C(8F)-C(9F)-C(10F)	126.4(15)
H(14M)-C(14E)-H(14O)	109.5	C(1F)-C(9F)-C(10F)	107.5(13)
H(14N)-C(14E)-H(14O)	109.5	C(4F)-C(10F)-C(3F)	125.9(16)
O(3E)-C(15E)-O(4E)	121.1(15)	C(4F)-C(10F)-C(9F)	127.3(15)
O(3E)-C(15E)-C(1E)	126.6(16)	C(3F)-C(10F)-C(9F)	106.8(13)
O(4E)-C(15E)-C(1E)	112.2(14)	N(1F)-C(11F)-Cr(1)	169(2)
O(4E)-C(16E)-C(17E)	107.5(15)	O(1F)-C(12F)-O(2F)	123.5(17)
O(4E)-C(16E)-H(16I)	110.2	O(1F)-C(12F)-C(3F)	123.2(17)
C(17E)-C(16E)-H(16I)	110.2	O(2F)-C(12F)-C(3F)	113.2(15)
O(4E)-C(16E)-H(16J)	110.2	O(2F)-C(13F)-C(14F)	110.6(16)
C(17E)-C(16E)-H(16J)	110.2	O(2F)-C(13F)-H(13K)	109.5
H(16I)-C(16E)-H(16J)	108.5	C(14F)-C(13F)-H(13K)	109.5
C(16E)-C(17E)-H(17M)	109.4	O(2F)-C(13F)-H(13L)	109.5
C(16E)-C(17E)-H(17N)	109.7	C(14F)-C(13F)-H(13L)	109.5
H(17M)-C(17E)-H(17N)	109.5	H(13K)-C(13F)-H(13L)	108.1
C(16E)-C(17E)-H(17O)	109.4	C(13F)-C(14F)-H(14P)	110.0
H(17M)-C(17E)-H(17O)	109.5	C(13F)-C(14F)-H(14Q)	109.3
H(17N)-C(17E)-H(17O)	109.5	H(14P)-C(14F)-H(14Q)	109.5
C(12F)-O(2F)-C(13F)	118.2(16)	C(13F)-C(14F)-H(14R)	109.1
C(15F)-O(4F)-C(16F)	118.6(14)	H(14P)-C(14F)-H(14R)	109.5
C(11F)-N(1F)-C(2F)	164(2)	H(14Q)-C(14F)-H(14R)	109.5
C(2F)-C(1F)-C(9F)	107.1(13)	O(3F)-C(15F)-O(4F)	119.9(16)
C(2F)-C(1F)-C(15F)	125.9(14)	O(3F)-C(15F)-C(1F)	126.2(17)
C(9F)-C(1F)-C(15F)	126.9(14)	O(4F)-C(15F)-C(1F)	113.8(15)
N(1F)-C(2F)-C(3F)	123.5(13)	O(4F)-C(16F)-C(17F)	106.7(16)
N(1F)-C(2F)-C(1F)	125.4(13)	O(4F)-C(16F)-H(16K)	110.4
C(3F)-C(2F)-C(1F)	110.4(13)	C(17F)-C(16F)-H(16K)	110.4
C(2F)-C(3F)-C(10F)	108.1(13)	O(4F)-C(16F)-H(16L)	110.4
C(2F)-C(3F)-C(12F)	125.7(13)	C(17F)-C(16F)-H(16L)	110.4
C(10F)-C(3F)-C(12F)	124.3(13)	H(16K)-C(16F)-H(16L)	108.6
C(10F)-C(4F)-C(5F)	130.2(19)	C(16F)-C(17F)-H(17P)	109.6
C(10F)-C(4F)-H(4F)	114.9	C(16F)-C(17F)-H(17Q)	109.4
C(5F)-C(4F)-H(4F)	114.9	H(17P)-C(17F)-H(17Q)	109.5
C(6F)-C(5F)-C(4F)	128(2)	C(16F)-C(17F)-H(17R)	109.5
C(6F)-C(5F)-H(5F)	115.9	H(17P)-C(17F)-H(17R)	109.5
C(4F)-C(5F)-H(5F)	115.9	H(17Q)-C(17F)-H(17R)	109.5
C(7F)-C(6F)-C(5F)	129(2)	C(11H)-Cr(2)-C(11H)#3	180.0
C(7F)-C(6F)-H(6F)	115.4	C(11H)-Cr(2)-C(11I)	83.6(9)
C(5F)-C(6F)-H(6F)	115.4	C(11H)-Cr(2)-C(11I)#3	96.4(9)
C(6F)-C(7F)-C(8F)	130(2)	C(11I)-Cr(2)-C(11I)#3	180.0
C(6F)-C(7F)-H(7F)	115.0	C(11H)-Cr(2)-C(11G)	95.9(11)
C(8F)-C(7F)-H(7F)	115.0	C(11I)-Cr(2)-C(11G)	90.2(10)
C(7F)-C(8F)-C(9F)	128.7(19)	C(11H)-Cr(2)-C(11G)#3	84.1(10)
C(7F)-C(8F)-H(8F)	115.7	C(11I)-Cr(2)-C(11G)#3	89.8(10)
C(9F)-C(8F)-H(8F)	115.7	C(11G)-Cr(2)-C(11G)#3	180.0
C(8F)-C(9F)-C(1F)	126.1(16)	C(12G)-O(2G)-C(13G)	116.5(16)

C(15G)-O(4G)-C(16G)	115.7(15)	H(14S)-C(14G)-H(14U)	109.5
C(11G)-N(1G)-C(2G)	175(2)	H(14T)-C(14G)-H(14U)	109.5
C(2G)-C(1G)-C(9G)	107.5(12)	O(3G)-C(15G)-O(4G)	121.3(16)
C(2G)-C(1G)-C(15G)	122.4(13)	O(3G)-C(15G)-C(1G)	125.2(16)
C(9G)-C(1G)-C(15G)	128.5(13)	O(4G)-C(15G)-C(1G)	113.5(15)
N(1G)-C(2G)-C(3G)	126.7(14)	O(4G)-C(16G)-C(17G)	106.3(17)
N(1G)-C(2G)-C(1G)	123.5(14)	O(4G)-C(16G)-H(16M)	110.5
C(3G)-C(2G)-C(1G)	109.8(12)	C(17G)-C(16G)-H(16M)	110.5
C(2G)-C(3G)-C(10G)	108.8(12)	O(4G)-C(16G)-H(16N)	110.5
C(2G)-C(3G)-C(12G)	121.1(13)	C(17G)-C(16G)-H(16N)	110.5
C(10G)-C(3G)-C(12G)	129.8(14)	H(16M)-C(16G)-H(16N)	108.7
C(10G)-C(4G)-C(5G)	130.2(17)	C(16G)-C(17G)-H(17S)	109.9
C(10G)-C(4G)-H(4G)	114.9	C(16G)-C(17G)-H(17T)	109.6
C(5G)-C(4G)-H(4G)	114.9	H(17S)-C(17G)-H(17T)	109.5
C(6G)-C(5G)-C(4G)	130.5(19)	C(16G)-C(17G)-H(17U)	108.9
C(6G)-C(5G)-H(5G)	114.7	H(17S)-C(17G)-H(17U)	109.5
C(4G)-C(5G)-H(5G)	114.7	H(17T)-C(17G)-H(17U)	109.5
C(5G)-C(6G)-C(7G)	128.0(18)	C(12H)-O(2H)-C(13H)	119.1(16)
C(5G)-C(6G)-H(6G)	116.0	C(15H)-O(4H)-C(16H)	116.6(16)
C(7G)-C(6G)-H(6G)	116.0	C(11H)-N(1H)-C(2H)	175(2)
C(6G)-C(7G)-C(8G)	127.8(18)	C(2H)-C(1H)-C(9H)	106.4(12)
C(6G)-C(7G)-H(7G)	116.1	C(2H)-C(1H)-C(15H)	122.8(13)
C(8G)-C(7G)-H(7G)	116.1	C(9H)-C(1H)-C(15H)	130.7(14)
C(7G)-C(8G)-C(9G)	131.9(17)	N(1H)-C(2H)-C(3H)	126.4(14)
C(7G)-C(8G)-H(8G)	114.1	N(1H)-C(2H)-C(1H)	121.8(14)
C(9G)-C(8G)-H(8G)	114.1	C(3H)-C(2H)-C(1H)	111.6(12)
C(8G)-C(9G)-C(1G)	126.8(15)	C(2H)-C(3H)-C(10H)	107.7(13)
C(8G)-C(9G)-C(10G)	125.9(14)	C(2H)-C(3H)-C(12H)	125.2(13)
C(1G)-C(9G)-C(10G)	107.3(12)	C(10H)-C(3H)-C(12H)	126.7(13)
C(4G)-C(10G)-C(3G)	127.7(15)	C(10H)-C(4H)-C(5H)	129.7(18)
C(4G)-C(10G)-C(9G)	125.7(14)	C(10H)-C(4H)-H(4H)	115.2
C(3G)-C(10G)-C(9G)	106.5(12)	C(5H)-C(4H)-H(4H)	115.2
N(1G)-C(11G)-Cr(2)	171(2)	C(6H)-C(5H)-C(4H)	126.4(19)
O(1G)-C(12G)-O(2G)	121.6(17)	C(6H)-C(5H)-H(5H)	116.8
O(1G)-C(12G)-C(3G)	124.9(16)	C(4H)-C(5H)-H(5H)	116.8
O(2G)-C(12G)-C(3G)	112.7(15)	C(5H)-C(6H)-C(7H)	132(2)
C(14G)-C(13G)-O(2G)	108.4(18)	C(5H)-C(6H)-H(6H)	114.1
C(14G)-C(13G)-H(13M)	110.0	C(7H)-C(6H)-H(6H)	114.1
O(2G)-C(13G)-H(13M)	110.0	C(6H)-C(7H)-C(8H)	130.0(19)
C(14G)-C(13G)-H(13N)	110.0	C(6H)-C(7H)-H(7H)	115.0
O(2G)-C(13G)-H(13N)	110.0	C(8H)-C(7H)-H(7H)	115.0
H(13M)-C(13G)-H(13N)	108.4	C(7H)-C(8H)-C(9H)	127.1(18)
C(13G)-C(14G)-H(14S)	108.8	C(7H)-C(8H)-H(8H)	116.5
C(13G)-C(14G)-H(14T)	110.9	C(9H)-C(8H)-H(8H)	116.5
H(14S)-C(14G)-H(14T)	109.5	C(8H)-C(9H)-C(1H)	126.4(16)
C(13G)-C(14G)-H(14U)	108.7	C(8H)-C(9H)-C(10H)	126.5(15)

C(1H)-C(9H)-C(10H)	107.1(12)	C(10I)-C(3I)-C(12I)	123.9(14)
C(4H)-C(10H)-C(3H)	124.2(15)	C(10I)-C(4I)-C(5I)	131.0(19)
C(4H)-C(10H)-C(9H)	128.6(15)	C(10I)-C(4I)-H(4I)	114.5
C(3H)-C(10H)-C(9H)	107.2(13)	C(5I)-C(4I)-H(4I)	114.5
N(1H)-C(11H)-Cr(2)	173(2)	C(6I)-C(5I)-C(4I)	124.6(19)
O(1H)-C(12H)-O(2H)	123.8(18)	C(6I)-C(5I)-H(5I)	117.7
O(1H)-C(12H)-C(3H)	122.1(17)	C(4I)-C(5I)-H(5I)	117.7
O(2H)-C(12H)-C(3H)	114.1(15)	C(7I)-C(6I)-C(5I)	132(2)
O(2H)-C(13H)-C(14H)	111.9(19)	C(7I)-C(6I)-H(6I)	113.8
O(2H)-C(13H)-H(13O)	109.2	C(5I)-C(6I)-H(6I)	113.8
C(14H)-C(13H)-H(13O)	109.2	C(6I)-C(7I)-C(8I)	129.7(19)
O(2H)-C(13H)-H(13P)	109.2	C(6I)-C(7I)-H(7I)	115.1
C(14H)-C(13H)-H(13P)	109.2	C(8I)-C(7I)-H(7I)	115.1
H(13O)-C(13H)-H(13P)	107.9	C(7I)-C(8I)-C(9I)	127.6(18)
C(13H)-C(14H)-H(14V)	110.1	C(7I)-C(8I)-H(8I)	116.2
C(13H)-C(14H)-H(14W)	108.5	C(9I)-C(8I)-H(8I)	116.2
H(14V)-C(14H)-H(14W)	109.5	C(8I)-C(9I)-C(1I)	126.7(15)
C(13H)-C(14H)-H(14X)	109.7	C(8I)-C(9I)-C(10I)	126.0(15)
H(14V)-C(14H)-H(14X)	109.5	C(1I)-C(9I)-C(10I)	107.4(13)
H(14W)-C(14H)-H(14X)	109.5	C(4I)-C(10I)-C(3I)	124.4(16)
O(3H)-C(15H)-O(4H)	120.0(16)	C(4I)-C(10I)-C(9I)	128.8(15)
O(3H)-C(15H)-C(1H)	125.6(16)	C(3I)-C(10I)-C(9I)	106.8(13)
O(4H)-C(15H)-C(1H)	113.8(15)	N(1I)-C(11I)-Cr(2)	175(2)
O(4H)-C(16H)-C(17H)	108.0(19)	O(1I)-C(12I)-O(2I)	123.2(17)
O(4H)-C(16H)-H(16O)	110.1	O(1I)-C(12I)-C(3I)	124.5(17)
C(17H)-C(16H)-H(16O)	110.1	O(2I)-C(12I)-C(3I)	112.3(14)
O(4H)-C(16H)-H(16P)	110.1	C(14I)-C(13I)-O(2I)	108.8(17)
C(17H)-C(16H)-H(16P)	110.1	C(14I)-C(13I)-H(13Q)	109.9
H(16O)-C(16H)-H(16P)	108.4	O(2I)-C(13I)-H(13Q)	109.9
C(16H)-C(17H)-H(17V)	109.2	C(14I)-C(13I)-H(13R)	109.9
C(16H)-C(17H)-H(17W)	109.7	O(2I)-C(13I)-H(13R)	109.9
H(17V)-C(17H)-H(17W)	109.5	H(13Q)-C(13I)-H(13R)	108.3
C(16H)-C(17H)-H(17X)	109.5	C(13I)-C(14I)-H(14Y)	109.9
H(17V)-C(17H)-H(17X)	109.5	C(13I)-C(14I)-H(14Z)	109.3
H(17W)-C(17H)-H(17X)	109.5	H(14Y)-C(14I)-H(14Z)	109.5
C(12I)-O(2I)-C(13I)	118.8(16)	C(13I)-C(14I)-H(14$)	109.2
C(15I)-O(4I)-C(16I)	118.6(15)	H(14Y)-C(14I)-H(14$)	109.5
C(11I)-N(1I)-C(2I)	167(2)	H(14Z)-C(14I)-H(14$)	109.5
C(2I)-C(1I)-C(9I)	107.0(13)	O(3I)-C(15I)-O(4I)	121.9(17)
C(2I)-C(1I)-C(15I)	125.8(14)	O(3I)-C(15I)-C(1I)	124.2(17)
C(9I)-C(1I)-C(15I)	127.2(14)	O(4I)-C(15I)-C(1I)	113.6(14)
C(3I)-C(2I)-N(1I)	124.4(14)	O(4I)-C(16I)-C(17I)	107.3(17)
C(3I)-C(2I)-C(1I)	110.7(13)	O(4I)-C(16I)-H(16Q)	110.3
N(1I)-C(2I)-C(1I)	124.5(14)	C(17I)-C(16I)-H(16Q)	110.3
C(2I)-C(3I)-C(10I)	108.1(13)	O(4I)-C(16I)-H(16R)	110.3
C(2I)-C(3I)-C(12I)	126.8(14)	C(17I)-C(16I)-H(16R)	110.3

H(16Q)-C(16I)-H(16R)	108.5	Cl(3T)-C(2T)-H(2T2)	109.2
C(16I)-C(17I)-H(17Y)	109.5	Cl(1T)-C(2T)-H(2T2)	109.2
C(16I)-C(17I)-H(17Z)	110.0	H(2T1)-C(2T)-H(2T2)	107.9
H(17Y)-C(17I)-H(17Z)	109.5	Cl(4T)-C(5T)-Cl(6T)	112(2)
C(16I)-C(17I)-H(17$)	108.9	Cl(4T)-C(5T)-H(5TA)	112.4
H(17Y)-C(17I)-H(17$)	109.5	Cl(6T)-C(5T)-H(5TA)	112.6
H(17Z)-C(17I)-H(17$)	109.5	Cl(4T)-C(5T)-H(5TB)	105.4
Cl(3T)-C(2T)-Cl(1T)	112(2)	Cl(6T)-C(5T)-H(5TB)	106.0
Cl(3T)-C(2T)-H(2T1)	109.2	H(5TA)-C(5T)-H(5TB)	108.2
Cl(1T)-C(2T)-H(2T1)	109.2	C(5T)#1-Cl(6T)-C(5T)	136.2(18)

Symmetry transformations used to generate equivalent atoms:
#1 -x+2, -y, -z+1 #2 -x+1, -y, -z+1 #3 -x+1, -y+1, -z+1

Table 4 Anisotropic displacement parameters ($Å^2 x\ 10^3$) for **3.12**. The anisotropic displacement factor exponent takes the form: $-2\pi^2[h^2 a^{*2} U_{11} + ... + 2 h k a^* b^* U_{12}]$

	U_{11}	U_{22}	U_{33}	U_{23}	U_{13}	U_{12}
Sb(1A)	77(2)	77(2)	68(2)	-41(1)	45(1)	-41(1)
F(1A)	101(8)	98(8)	83(6)	-51(6)	24(6)	-46(7)
F(2A)	87(6)	88(6)	83(6)	-25(4)	28(6)	-44(5)
F(3A)	84(4)	68(7)	67(7)	-20(5)	23(5)	-31(5)
F(4A)	92(8)	89(8)	80(6)	-48(6)	22(6)	-33(7)
F(5A)	75(6)	78(6)	74(6)	-17(4)	10(6)	-30(5)
F(6A)	80(4)	93(7)	87(7)	-31(5)	21(5)	-34(5)
F(1A')	103(10)	99(8)	83(8)	-55(6)	27(8)	-48(9)
F(2A')	85(7)	87(6)	77(7)	-26(5)	34(7)	-38(7)
F(3A')	73(4)	70(8)	68(8)	-22(6)	22(6)	-30(6)
F(4A')	90(10)	93(8)	81(8)	-53(6)	24(8)	-34(9)
F(5A')	73(7)	89(6)	81(7)	-26(5)	14(7)	-33(7)
F(6A')	78(4)	94(8)	89(8)	-36(6)	27(6)	-42(6)
Sb(1B)	53(2)	35(2)	31(2)	-4(1)	14(2)	-4(1)
F(1B)	80(7)	80(9)	115(10)	-35(8)	51(7)	-34(6)
F(2B)	156(14)	131(15)	50(8)	-25(9)	-25(10)	-19(13)
F(3B)	86(10)	50(7)	91(11)	-26(8)	23(10)	10(8)
Cr(1)	24(3)	23(3)	42(3)	-11(2)	6(2)	3(2)
O(1A)	36(11)	16(10)	43(9)	-5(8)	8(9)	-3(7)
O(2A)	48(11)	24(10)	37(8)	-15(8)	7(10)	-23(8)
O(3A)	69(14)	37(11)	34(11)	-21(9)	19(9)	-27(9)
O(4A)	99(14)	47(12)	52(12)	-30(9)	33(10)	-49(9)
N(1A)	26(7)	16(8)	26(7)	-3(6)	1(5)	2(6)
C(1A)	28(8)	24(8)	25(7)	-10(6)	0(6)	-5(6)
C(2A)	26(8)	16(8)	26(7)	-6(6)	1(6)	1(6)
C(3A)	21(8)	15(7)	23(7)	-5(6)	-1(6)	0(6)
C(4A)	48(18)	22(15)	13(14)	1(10)	0(9)	-3(12)
C(5A)	60(20)	41(18)	20(15)	-14(13)	14(11)	-14(13)
C(6A)	41(17)	37(17)	8(15)	3(11)	-1(12)	-8(13)
C(7A)	43(18)	35(16)	19(17)	-3(11)	0(10)	-15(13)
C(8A)	16(16)	22(13)	27(15)	-16(11)	-4(9)	-4(10)
C(9A)	23(8)	18(8)	29(7)	-8(6)	-1(6)	-3(6)
C(10A)	19(8)	15(8)	23(7)	-5(6)	-2(6)	-2(6)
C(11A)	27(7)	20(15)	51(15)	-12(11)	5(8)	-7(7)
C(12A)	4(14)	20(14)	36(10)	-13(11)	6(13)	1(9)
C(13A)	46(18)	35(16)	57(14)	-42(14)	35(15)	-26(13)
C(14A)	70(20)	80(20)	59(15)	-57(16)	35(17)	-50(18)
C(15A)	60(20)	29(15)	16(15)	-4(12)	0(11)	-21(12)
C(16A)	80(19)	49(18)	100(20)	-57(16)	21(18)	-24(12)

C(17A)	102(16)	72(14)	87(16)	-34(13)	1(13)	-7(10)
O(1B)	52(13)	33(11)	75(11)	10(10)	14(11)	-7(8)
O(2B)	51(12)	96(12)	61(9)	-26(10)	11(11)	-42(10)
O(3B)	106(17)	86(14)	45(12)	-18(11)	29(11)	-54(12)
O(4B)	56(12)	37(11)	56(12)	-10(8)	21(10)	-6(10)
N(1B)	29(7)	25(8)	33(7)	1(6)	2(6)	-1(6)
C(1B)	17(16)	61(16)	51(15)	-21(11)	9(11)	-17(12)
C(2B)	28(8)	37(8)	38(7)	-2(6)	4(6)	-4(6)
C(3B)	30(9)	32(8)	40(7)	-1(6)	7(6)	-2(6)
C(4B)	50(20)	43(17)	38(15)	-7(12)	11(11)	-22(13)
C(5B)	50(20)	54(19)	37(16)	-10(14)	12(11)	-25(14)
C(6B)	31(17)	49(19)	47(17)	-7(13)	9(14)	-17(14)
C(7B)	40(19)	44(18)	53(19)	-9(12)	10(12)	-19(14)
C(8B)	42(19)	47(15)	22(15)	4(12)	-12(10)	-17(12)
C(9B)	28(9)	34(8)	40(8)	-4(6)	4(6)	-3(6)
C(10B)	32(9)	31(8)	37(7)	-1(6)	5(6)	-4(6)
C(11B)	43(11)	49(16)	23(12)	-6(8)	-1(8)	-27(10)
C(12B)	38(18)	30(16)	61(11)	-14(12)	30(16)	-6(12)
C(13B)	91(12)	87(10)	101(11)	-35(8)	-7(8)	-36(7)
C(14B)	153(19)	102(12)	180(20)	-55(15)	3(16)	-13(11)
C(15B)	60(20)	44(15)	24(16)	1(12)	-5(13)	-13(14)
C(16B)	90(20)	30(16)	80(20)	-20(13)	51(19)	-5(15)
C(17B)	110(30)	80(20)	140(30)	-42(19)	30(20)	-54(19)
O(1C)	58(13)	45(13)	37(10)	-4(9)	18(9)	-2(7)
O(2C)	35(11)	69(13)	50(9)	5(10)	7(9)	4(9)
O(3C)	94(18)	40(12)	84(14)	-5(9)	22(11)	11(10)
O(4C)	60(12)	36(10)	25(9)	2(7)	2(8)	-16(9)
N(1C)	27(14)	17(12)	45(10)	-4(8)	0(10)	-10(8)
C(1C)	49(19)	22(14)	39(6)	20(9)	11(10)	-6(8)
C(2C)	39(18)	24(15)	42(8)	-2(10)	-6(12)	-11(8)
C(3C)	37(16)	46(14)	45(8)	-2(10)	-2(12)	-11(8)
C(4C)	48(19)	66(17)	40(7)	8(11)	7(13)	-24(10)
C(5C)	40(20)	84(19)	33(11)	12(10)	5(12)	-20(11)
C(6C)	54(11)	55(10)	60(10)	5(8)	0(8)	-29(7)
C(7C)	45(18)	39(15)	62(11)	-2(11)	-26(13)	2(11)
C(8C)	34(18)	45(16)	62(10)	-1(10)	-30(13)	-2(9)
C(9C)	36(18)	51(16)	39(7)	0(9)	-19(12)	0(9)
C(10C)	41(9)	42(8)	41(6)	2(6)	-4(7)	-17(6)
C(11C)	57(14)	41(11)	13(11)	-13(7)	6(9)	14(10)
C(12C)	43(19)	35(18)	49(10)	2(14)	15(12)	-20(8)
C(13C)	42(19)	100(20)	74(13)	-35(17)	18(15)	-10(14)
C(14C)	107(18)	137(18)	79(12)	-48(14)	5(13)	-8(14)
C(15C)	13(17)	35(14)	43(9)	9(8)	0(12)	-3(12)
C(16C)	43(17)	9(15)	43(11)	2(11)	13(13)	7(11)
C(17C)	54(14)	63(14)	76(15)	-30(12)	33(11)	-24(10)
O(1D)	36(10)	19(9)	46(9)	-2(7)	2(8)	-1(6)

O(2D)	37(11)	38(11)	37(7)	-9(8)	1(8)	11(8)
O(3D)	49(13)	42(11)	55(11)	-21(8)	7(8)	3(8)
O(4D)	46(12)	34(10)	41(8)	-10(7)	17(9)	-9(8)
N(1D)	33(13)	46(13)	30(8)	-10(8)	-10(9)	-5(8)
C(1D)	32(8)	29(8)	33(5)	-15(6)	-2(6)	-8(5)
C(2D)	23(8)	24(8)	30(5)	-5(5)	1(6)	-12(5)
C(3D)	23(8)	18(7)	30(5)	-9(6)	-4(6)	-10(5)
C(4D)	58(18)	8(15)	33(6)	-1(10)	2(11)	-6(10)
C(5D)	12(17)	60(20)	32(12)	11(10)	-1(11)	-14(10)
C(6D)	8(16)	44(17)	48(12)	22(14)	1(13)	-11(10)
C(7D)	43(17)	10(14)	57(13)	7(12)	9(13)	-9(10)
C(8D)	24(16)	23(16)	45(12)	-3(10)	13(11)	-9(7)
C(9D)	25(15)	21(14)	39(6)	-8(8)	3(9)	-9(6)
C(10D)	17(8)	23(8)	31(5)	-3(6)	0(6)	-9(5)
C(11D)	25(8)	20(6)	31(7)	-8(5)	1(6)	-11(6)
C(12D)	21(8)	25(8)	35(7)	-4(7)	3(7)	-7(5)
C(13D)	50(20)	54(19)	62(11)	-17(13)	26(15)	11(14)
C(14D)	106(17)	116(18)	56(10)	-41(12)	20(12)	8(14)
C(15D)	37(19)	35(15)	41(8)	-10(8)	12(12)	-6(11)
C(16D)	60(19)	11(15)	47(9)	-8(11)	25(14)	-3(12)
C(17D)	60(20)	80(20)	63(19)	-30(17)	36(15)	-33(15)
O(1E)	38(11)	30(10)	40(8)	-2(7)	-6(8)	2(7)
O(2E)	44(10)	10(9)	37(8)	-14(8)	10(8)	-9(7)
O(3E)	30(11)	41(10)	70(11)	-20(9)	3(8)	4(6)
O(4E)	38(11)	24(9)	38(7)	-4(7)	-6(7)	-6(7)
N(1E)	21(8)	17(8)	24(7)	3(5)	-1(6)	8(6)
C(1E)	24(15)	29(12)	33(8)	-9(7)	3(10)	-5(7)
C(2E)	16(15)	23(12)	23(11)	1(8)	12(9)	-8(7)
C(3E)	10(13)	33(12)	29(11)	-6(9)	5(8)	-7(7)
C(4E)	45(18)	64(17)	26(13)	-7(11)	2(12)	-2(12)
C(5E)	32(18)	45(17)	37(12)	-9(12)	-4(13)	-19(11)
C(6E)	70(20)	24(17)	46(15)	-5(12)	-7(12)	-23(11)
C(7E)	46(19)	36(16)	32(12)	-9(11)	13(12)	-13(11)
C(8E)	34(9)	32(8)	41(8)	-15(7)	4(7)	-12(6)
C(9E)	19(16)	40(14)	36(10)	-15(9)	5(11)	-7(8)
C(10E)	23(17)	43(15)	26(11)	-7(10)	9(10)	-4(8)
C(11E)	21(9)	16(7)	28(7)	5(6)	-3(7)	-4(6)
C(12E)	22(8)	26(8)	30(8)	-3(6)	3(7)	-6(5)
C(13E)	31(15)	37(17)	64(15)	-28(14)	18(13)	-12(10)
C(14E)	46(18)	60(20)	54(15)	-31(15)	7(13)	16(15)
C(15E)	30(9)	17(8)	40(6)	-8(6)	0(6)	-7(5)
C(16E)	32(9)	24(9)	43(7)	-4(6)	-6(7)	-4(7)
C(17E)	60(20)	80(20)	35(8)	-6(11)	0(13)	-35(17)
O(1F)	116(17)	40(14)	81(12)	-5(10)	-30(12)	8(8)
O(2F)	45(11)	61(13)	55(10)	-20(10)	1(10)	-9(9)
O(3F)	85(14)	68(13)	61(11)	-26(10)	50(11)	-17(8)

O(4F)	64(13)	30(11)	50(9)	-23(9)	14(9)	-9(8)
N(1F)	12(12)	46(13)	51(12)	-16(9)	-1(10)	-12(10)
C(1F)	50(9)	48(8)	50(7)	-15(6)	11(7)	-27(6)
C(2F)	43(17)	34(15)	40(13)	-5(10)	3(10)	-23(7)
C(3F)	52(17)	42(16)	31(11)	3(11)	2(9)	-25(8)
C(4F)	78(19)	63(17)	30(13)	12(13)	-2(12)	-55(10)
C(5F)	80(20)	150(30)	15(14)	-1(16)	22(15)	-16(17)
C(6F)	60(30)	160(30)	60(20)	-32(16)	34(14)	-46(16)
C(7F)	50(20)	100(20)	61(14)	-46(18)	31(14)	-65(14)
C(8F)	70(20)	90(20)	60(15)	-39(15)	26(15)	-55(13)
C(9F)	80(20)	37(17)	41(11)	-7(11)	13(11)	-42(8)
C(10F)	67(19)	47(17)	31(12)	2(12)	6(10)	-39(8)
C(11F)	23(15)	24(12)	34(11)	1(9)	-2(9)	-9(11)
C(12F)	56(18)	30(18)	54(10)	-9(12)	-14(14)	-18(8)
C(13F)	29(16)	70(20)	88(17)	-42(17)	-9(13)	-9(11)
C(14F)	53(17)	50(20)	70(20)	-12(17)	13(16)	-15(14)
C(15F)	56(19)	57(17)	54(10)	-38(13)	7(13)	-16(8)
C(16F)	70(20)	20(15)	85(12)	-17(14)	-1(14)	-19(11)
C(17F)	45(18)	12(15)	82(12)	-2(12)	-6(15)	-13(13)
Cr(2)	33(4)	36(3)	34(4)	-9(3)	5(3)	-3(3)
O(1G)	85(17)	160(20)	83(15)	-84(15)	51(11)	-72(13)
O(2G)	94(9)	84(8)	76(9)	-31(6)	13(7)	-43(7)
O(3G)	72(14)	57(14)	81(12)	-31(11)	40(12)	-32(10)
O(4G)	91(15)	95(15)	68(9)	-43(11)	40(13)	-47(11)
N(1G)	43(14)	27(13)	38(13)	-9(11)	9(9)	-6(9)
C(1G)	70(20)	33(15)	44(12)	-4(11)	22(10)	-20(12)
C(2G)	35(9)	31(8)	41(8)	-2(6)	9(6)	-1(7)
C(3G)	36(17)	46(16)	24(14)	3(11)	0(10)	-8(11)
C(4G)	15(18)	40(17)	52(16)	-6(13)	6(11)	-1(10)
C(5G)	23(18)	120(20)	70(20)	-36(16)	20(14)	-48(16)
C(6G)	60(20)	60(20)	23(16)	17(13)	4(14)	-31(15)
C(7G)	28(19)	70(20)	71(17)	-26(16)	28(13)	-19(14)
C(8G)	43(19)	54(18)	40(14)	-15(13)	12(11)	-20(13)
C(9G)	33(9)	29(8)	31(7)	2(6)	1(6)	1(7)
C(10G)	2(16)	42(16)	36(13)	-7(11)	-2(10)	4(10)
C(11G)	49(17)	35(16)	43(15)	-24(12)	22(12)	-12(13)
C(12G)	70(20)	90(20)	35(17)	-21(15)	8(12)	-37(16)
C(13G)	99(12)	82(9)	86(11)	-36(7)	9(8)	-27(8)
C(14G)	133(19)	79(8)	113(18)	-32(10)	8(15)	-3(14)
C(15G)	54(19)	50(20)	67(10)	-30(13)	37(16)	-17(13)
C(16G)	97(12)	94(11)	93(10)	-33(8)	-4(8)	-32(8)
C(17G)	114(18)	126(18)	93(10)	-46(12)	0(13)	-50(14)
O(1H)	80(17)	76(12)	91(14)	-37(11)	19(11)	7(11)
O(2H)	51(13)	75(12)	50(11)	-8(9)	13(10)	3(11)
O(3H)	53(13)	48(13)	81(12)	-6(9)	4(11)	-2(7)
O(4H)	82(15)	101(16)	45(9)	-8(10)	4(10)	-29(11)

N(1H)	32(16)	57(16)	51(11)	-10(9)	-9(12)	7(9)
C(1H)	35(9)	49(8)	52(7)	-8(6)	-4(7)	-10(6)
C(2H)	24(17)	41(16)	46(8)	-21(8)	-17(10)	-6(8)
C(3H)	40(19)	37(16)	63(9)	-6(9)	5(11)	-1(9)
C(4H)	40(20)	43(18)	89(13)	-10(11)	-12(13)	2(9)
C(5H)	60(20)	69(19)	74(12)	-22(12)	-29(14)	18(12)
C(6H)	66(10)	71(10)	81(10)	-15(8)	-8(8)	-22(7)
C(7H)	54(9)	55(9)	60(8)	3(6)	-11(7)	-25(6)
C(8H)	60(19)	63(17)	68(9)	16(11)	-5(13)	-20(9)
C(9H)	47(9)	42(8)	58(6)	-4(6)	-4(7)	-14(6)
C(10H)	42(19)	33(16)	68(9)	-8(9)	-5(12)	-7(8)
C(11H)	50(20)	43(13)	21(17)	-13(9)	4(12)	3(10)
C(12H)	40(20)	65(16)	59(11)	-20(10)	-1(14)	6(15)
C(13H)	70(20)	110(20)	67(16)	-17(13)	39(18)	-8(16)
C(14H)	90(30)	110(30)	130(30)	10(20)	40(20)	-25(19)
C(15H)	45(19)	33(18)	45(9)	-10(12)	-2(12)	-22(8)
C(16H)	110(30)	130(30)	45(13)	-27(19)	11(15)	-30(20)
C(17H)	190(40)	160(40)	53(15)	-40(20)	-20(20)	-30(30)
O(1I)	70(14)	50(13)	68(11)	9(10)	-12(11)	-14(7)
O(2I)	48(11)	37(11)	53(10)	-13(9)	3(9)	4(8)
O(3I)	86(15)	74(14)	122(14)	-71(12)	75(13)	-22(8)
O(4I)	58(13)	59(12)	58(9)	-34(9)	0(10)	1(9)
N(1I)	32(13)	23(13)	48(12)	-14(8)	12(10)	-11(10)
C(1I)	53(9)	44(8)	48(7)	-20(6)	15(7)	-25(6)
C(2I)	50(18)	40(16)	59(13)	-24(11)	-1(12)	-10(8)
C(3I)	51(18)	44(15)	37(10)	8(10)	20(8)	-23(7)
C(4I)	72(19)	72(17)	69(12)	-20(12)	-15(12)	-48(10)
C(5I)	79(10)	75(9)	63(8)	-16(7)	-7(7)	-18(6)
C(6I)	69(10)	75(9)	75(9)	-15(7)	9(7)	-27(7)
C(7I)	69(9)	61(9)	55(7)	-22(7)	8(7)	-31(6)
C(8I)	80(20)	87(19)	43(12)	-24(12)	21(12)	-33(11)
C(9I)	58(18)	58(16)	55(11)	-24(11)	12(11)	-42(8)
C(10I)	56(9)	56(9)	56(7)	-12(6)	4(7)	-38(6)
C(11I)	20(16)	31(14)	33(12)	-4(12)	11(12)	-6(13)
C(12I)	53(18)	33(17)	59(12)	6(10)	5(14)	-15(8)
C(13I)	60(20)	35(19)	130(20)	-50(17)	24(15)	-8(12)
C(14I)	82(14)	106(17)	122(18)	-9(13)	49(13)	-19(12)
C(15I)	32(17)	55(16)	57(9)	-40(12)	27(11)	-15(8)
C(16I)	80(20)	80(20)	87(13)	-39(15)	-20(17)	13(16)
C(17I)	90(20)	60(20)	78(13)	-20(13)	-31(18)	-8(18)
Cl(1T)	59(10)	54(10)	69(11)	-22(8)	-4(8)	1(8)
C(2T)	60(40)	70(30)	30(30)	-20(20)	20(20)	0(30)
Cl(3T)	70(11)	58(11)	115(14)	-50(9)	24(10)	-13(9)
Cl(4T)	63(16)	126(18)	42(14)	-32(10)	20(11)	-40(13)
C(5T)	90(60)	90(60)	60(30)	-10(40)	30(60)	-40(30)
Cl(6T)	105(10)	105(10)	106(10)	-22(5)	3(4)	-21(5)

Table 5 Hydrogen coordinates and isotropic displacement parameters for **3.12**.

	x	y	z	U(eq)
H(4A)	0.5743	0.1951	-0.0193	0.035
H(5A)	0.6900	0.2469	-0.0621	0.048
H(6A)	0.7536	0.3467	-0.0585	0.036
H(7A)	0.7176	0.4152	-0.0117	0.038
H(8A)	0.6145	0.4059	0.0439	0.024
H(13A)	0.4075	0.0450	0.0072	0.047
H(13B)	0.2947	0.1051	-0.0023	0.047
H(14A)	0.3381	0.0677	-0.0629	0.092
H(14B)	0.4607	0.0753	-0.0603	0.092
H(14C)	0.3658	0.1493	-0.0709	0.092
H(16A)	0.5702	0.4898	0.1300	0.084
H(16B)	0.5070	0.4343	0.1616	0.084
H(17A)	0.3910	0.5479	0.1429	0.129
H(17B)	0.3507	0.4913	0.1201	0.129
H(17C)	0.4147	0.5515	0.0938	0.129
H(4B)	-0.2333	0.1483	0.3527	0.053
H(5B)	-0.3364	0.0835	0.3949	0.055
H(6B)	-0.3882	-0.0179	0.3898	0.050
H(7B)	-0.3491	-0.0827	0.3405	0.053
H(8B)	-0.2507	-0.0623	0.2836	0.045
H(13C)	-0.0287	0.2375	0.3778	0.106
H(13D)	0.0187	0.2655	0.3318	0.106
H(14D)	-0.0906	0.3655	0.3487	0.214
H(14E)	-0.1861	0.3214	0.3616	0.214
H(14F)	-0.1520	0.3433	0.3131	0.214
H(16C)	-0.0491	-0.1387	0.1958	0.082
H(16D)	-0.1556	-0.0916	0.1690	0.082
H(17D)	-0.1630	-0.2206	0.1978	0.151
H(17E)	-0.2625	-0.1629	0.2125	0.151
H(17F)	-0.1633	-0.2045	0.2441	0.151
H(4C)	0.3634	-0.0582	0.3919	0.064
H(5C)	0.4681	-0.1589	0.4317	0.068
H(6C)	0.5852	-0.2490	0.4127	0.068
H(7C)	0.6343	-0.2666	0.3498	0.061
H(8C)	0.5758	-0.1941	0.2873	0.059
H(13E)	0.0873	0.0920	0.3736	0.086
H(13F)	0.1668	0.1496	0.3663	0.086
H(14G)	0.2446	0.0924	0.4321	0.160
H(14H)	0.1661	0.0345	0.4396	0.160
H(14I)	0.1173	0.1220	0.4370	0.160
H(16E)	0.4613	-0.0063	0.1263	0.043

H(16F)	0.5534	-0.0752	0.1499	0.043
H(17G)	0.6260	0.0277	0.1129	0.092
H(17H)	0.6537	0.0081	0.1623	0.092
H(17I)	0.5583	0.0780	0.1429	0.092
H(4D)	-0.0295	0.4332	-0.0579	0.041
H(5D)	-0.1423	0.5290	-0.0970	0.043
H(6D)	-0.2735	0.6109	-0.0764	0.046
H(7D)	-0.3273	0.6176	-0.0122	0.047
H(8D)	-0.2638	0.5453	0.0487	0.037
H(13G)	0.1610	0.2346	-0.0456	0.073
H(13H)	0.2525	0.2795	-0.0413	0.073
H(14J)	0.1720	0.3685	-0.1038	0.142
H(14K)	0.1128	0.3044	-0.1099	0.142
H(14L)	0.2420	0.2894	-0.1103	0.142
H(16G)	-0.2061	0.4260	0.1884	0.049
H(16H)	-0.1132	0.3540	0.2077	0.049
H(17J)	-0.2848	0.3294	0.2244	0.096
H(17K)	-0.2209	0.2743	0.1961	0.096
H(17L)	-0.3121	0.3457	0.1751	0.096
H(4E)	-0.0219	0.1407	-0.0494	0.056
H(5E)	0.0063	0.0845	-0.1035	0.044
H(6E)	0.1206	-0.0199	-0.1083	0.053
H(7E)	0.2356	-0.0962	-0.0620	0.045
H(8E)	0.2686	-0.0910	0.0033	0.041
H(13I)	-0.2216	0.2277	0.0529	0.050
H(13J)	-0.1512	0.2833	0.0631	0.050
H(14M)	-0.2577	0.2550	0.1207	0.080
H(14N)	-0.1359	0.2125	0.1338	0.080
H(14O)	-0.2192	0.1667	0.1226	0.080
H(16I)	0.3700	-0.1240	0.1533	0.041
H(16J)	0.2792	-0.1696	0.1488	0.041
H(17M)	0.2833	-0.1487	0.2176	0.083
H(17N)	0.1681	-0.1107	0.1955	0.083
H(17O)	0.2528	-0.0599	0.1982	0.083
H(4F)	0.4433	0.1556	0.3688	0.065
H(5F)	0.4509	0.1773	0.4326	0.104
H(6F)	0.3495	0.2675	0.4590	0.104
H(7F)	0.2165	0.3579	0.4295	0.074
H(8F)	0.1468	0.3837	0.3656	0.079
H(13K)	0.4814	0.1226	0.1985	0.069
H(13L)	0.5332	0.0835	0.2444	0.069
H(14P)	0.6516	0.1428	0.1971	0.091
H(14Q)	0.6318	0.1726	0.2398	0.091
H(14R)	0.5705	0.2216	0.1972	0.091
H(16K)	0.0230	0.5146	0.2289	0.066
H(16L)	-0.0611	0.4631	0.2257	0.066

H(17P)	-0.0052	0.5313	0.1583	0.070
H(17Q)	0.0056	0.4431	0.1623	0.070
H(17R)	0.1104	0.4749	0.1673	0.070
H(4G)	0.0751	0.2497	0.6122	0.045
H(5G)	-0.0255	0.2255	0.6681	0.075
H(6G)	-0.0573	0.2790	0.7218	0.060
H(7G)	0.0068	0.3731	0.7338	0.067
H(8G)	0.1179	0.4346	0.6947	0.053
H(13M)	0.1151	0.2279	0.4991	0.102
H(13N)	0.2426	0.2214	0.5034	0.102
H(14S)	0.2355	0.1044	0.5239	0.165
H(14T)	0.1190	0.1213	0.5451	0.165
H(14U)	0.2236	0.1284	0.5683	0.165
H(16M)	0.3113	0.5712	0.6843	0.109
H(16N)	0.4180	0.5051	0.6872	0.109
H(17S)	0.2553	0.5117	0.7505	0.155
H(17T)	0.3745	0.5245	0.7551	0.155
H(17U)	0.3577	0.4432	0.7527	0.155
H(4H)	0.0547	0.8752	0.4256	0.072
H(5H)	-0.0216	0.9704	0.3735	0.083
H(6H)	0.0206	0.9887	0.3067	0.086
H(7H)	0.1411	0.9235	0.2730	0.068
H(8H)	0.2615	0.8172	0.2970	0.081
H(13O)	0.1231	0.7086	0.5501	0.101
H(13P)	0.2140	0.6324	0.5608	0.101
H(14V)	0.0430	0.6071	0.5732	0.174
H(14W)	0.1028	0.5691	0.5366	0.174
H(14X)	0.0111	0.6447	0.5247	0.174
H(16O)	0.4562	0.6074	0.2964	0.112
H(16P)	0.5280	0.6701	0.2857	0.112
H(17V)	0.4640	0.6545	0.2235	0.197
H(17W)	0.4099	0.7372	0.2296	0.197
H(17X)	0.3422	0.6725	0.2399	0.197
H(4I)	0.2521	0.5360	0.2859	0.077
H(5I)	0.2500	0.5114	0.2217	0.086
H(6I)	0.3562	0.4166	0.2004	0.086
H(7I)	0.4834	0.3271	0.2323	0.069
H(8I)	0.5463	0.3036	0.2977	0.082
H(13Q)	0.1759	0.5929	0.4432	0.085
H(13R)	0.1143	0.6056	0.3992	0.085
H(14Y)	0.0338	0.5116	0.4231	0.162
H(14Z)	0.0337	0.5463	0.4637	0.162
H(14$)	0.1218	0.4724	0.4597	0.162
H(16Q)	0.7264	0.2324	0.4452	0.096
H(16R)	0.6463	0.1825	0.4355	0.096
H(17Y)	0.6640	0.1681	0.5086	0.115

H(17Z)	0.5416	0.2064	0.4942	0.115
H(17$)	0.6209	0.2569	0.5033	0.115
H(2T1)	0.4322	0.7130	0.1307	0.063
H(2T2)	0.4812	0.7706	0.0948	0.063
H(5TA)	0.8195	0.0358	0.4916	0.095
H(5TB)	0.9036	0.0852	0.4978	0.095

Table 6 Torsion angles [°] for **3.12**.

C(11A)-N(1A)-C(2A)-C(3A)	-35(9)
C(11A)-N(1A)-C(2A)-C(1A)	145(9)
C(9A)-C(1A)-C(2A)-N(1A)	-179.6(12)
C(15A)-C(1A)-C(2A)-N(1A)	7.1(16)
C(9A)-C(1A)-C(2A)-C(3A)	-0.1(3)
C(15A)-C(1A)-C(2A)-C(3A)	-173.3(14)
N(1A)-C(2A)-C(3A)-C(10A)	179.4(12)
C(1A)-C(2A)-C(3A)-C(10A)	-0.1(3)
N(1A)-C(2A)-C(3A)-C(12A)	7.5(15)
C(1A)-C(2A)-C(3A)-C(12A)	-172.0(13)
C(10A)-C(4A)-C(5A)-C(6A)	-1.0(14)
C(4A)-C(5A)-C(6A)-C(7A)	0.3(13)
C(5A)-C(6A)-C(7A)-C(8A)	0.6(14)
C(6A)-C(7A)-C(8A)-C(9A)	-0.3(14)
C(7A)-C(8A)-C(9A)-C(1A)	-179.9(7)
C(7A)-C(8A)-C(9A)-C(10A)	-0.6(12)
C(2A)-C(1A)-C(9A)-C(8A)	179.6(6)
C(15A)-C(1A)-C(9A)-C(8A)	-7.9(18)
C(2A)-C(1A)-C(9A)-C(10A)	0.2(5)
C(15A)-C(1A)-C(9A)-C(10A)	172.8(16)
C(5A)-C(4A)-C(10A)-C(3A)	-179.2(7)
C(5A)-C(4A)-C(10A)-C(9A)	0.4(13)
C(2A)-C(3A)-C(10A)-C(4A)	179.9(6)
C(12A)-C(3A)-C(10A)-C(4A)	-8.8(17)
C(2A)-C(3A)-C(10A)-C(9A)	0.3(6)
C(12A)-C(3A)-C(10A)-C(9A)	171.5(14)
C(8A)-C(9A)-C(10A)-C(4A)	0.7(12)
C(1A)-C(9A)-C(10A)-C(4A)	-179.9(6)
C(8A)-C(9A)-C(10A)-C(3A)	-179.7(6)
C(1A)-C(9A)-C(10A)-C(3A)	-0.3(7)
C(13A)-O(2A)-C(12A)-O(1A)	1(3)
C(13A)-O(2A)-C(12A)-C(3A)	-178.6(16)
C(2A)-C(3A)-C(12A)-O(1A)	-29(3)
C(10A)-C(3A)-C(12A)-O(1A)	160.9(15)
C(2A)-C(3A)-C(12A)-O(2A)	150.1(12)
C(10A)-C(3A)-C(12A)-O(2A)	-20(2)
C(12A)-O(2A)-C(13A)-C(14A)	-176.8(19)
C(16A)-O(4A)-C(15A)-O(3A)	0(3)
C(16A)-O(4A)-C(15A)-C(1A)	174.1(17)
C(9A)-C(1A)-C(15A)-O(3A)	-174.9(17)
C(2A)-C(1A)-C(15A)-O(3A)	-3(3)
C(9A)-C(1A)-C(15A)-O(4A)	11(3)
C(2A)-C(1A)-C(15A)-O(4A)	-177.4(13)

C(15A)-O(4A)-C(16A)-C(17A)	-84(3)
C(11B)-N(1B)-C(2B)-C(3B)	14(9)
C(11B)-N(1B)-C(2B)-C(1B)	-159(8)
C(9B)-C(1B)-C(2B)-N(1B)	174.0(12)
C(15B)-C(1B)-C(2B)-N(1B)	-8.8(17)
C(9B)-C(1B)-C(2B)-C(3B)	0.1(3)
C(15B)-C(1B)-C(2B)-C(3B)	177.3(15)
N(1B)-C(2B)-C(3B)-C(10B)	-173.6(13)
C(1B)-C(2B)-C(3B)-C(10B)	0.1(3)
N(1B)-C(2B)-C(3B)-C(12B)	-3.3(17)
C(1B)-C(2B)-C(3B)-C(12B)	170.4(15)
C(10B)-C(4B)-C(5B)-C(6B)	0.0(14)
C(4B)-C(5B)-C(6B)-C(7B)	0.1(14)
C(5B)-C(6B)-C(7B)-C(8B)	-0.4(14)
C(6B)-C(7B)-C(8B)-C(9B)	0.3(13)
C(7B)-C(8B)-C(9B)-C(1B)	179.8(7)
C(7B)-C(8B)-C(9B)-C(10B)	0.3(13)
C(2B)-C(1B)-C(9B)-C(8B)	-179.8(6)
C(15B)-C(1B)-C(9B)-C(8B)	3.3(19)
C(2B)-C(1B)-C(9B)-C(10B)	-0.2(6)
C(15B)-C(1B)-C(9B)-C(10B)	-177.2(17)
C(5B)-C(4B)-C(10B)-C(3B)	179.8(7)
C(5B)-C(4B)-C(10B)-C(9B)	0.4(13)
C(2B)-C(3B)-C(10B)-C(4B)	-179.7(6)
C(12B)-C(3B)-C(10B)-C(4B)	10.5(18)
C(2B)-C(3B)-C(10B)-C(9B)	-0.2(6)
C(12B)-C(3B)-C(10B)-C(9B)	-170.0(16)
C(8B)-C(9B)-C(10B)-C(4B)	-0.7(12)
C(1B)-C(9B)-C(10B)-C(4B)	179.7(7)
C(8B)-C(9B)-C(10B)-C(3B)	179.9(6)
C(1B)-C(9B)-C(10B)-C(3B)	0.3(7)
C(2B)-N(1B)-C(11B)-Cr(1)	109(12)
C(13B)-O(2B)-C(12B)-O(1B)	-1(4)
C(13B)-O(2B)-C(12B)-C(3B)	178.3(17)
C(2B)-C(3B)-C(12B)-O(1B)	26(3)
C(10B)-C(3B)-C(12B)-O(1B)	-165.3(16)
C(2B)-C(3B)-C(12B)-O(2B)	-152.5(15)
C(10B)-C(3B)-C(12B)-O(2B)	16(3)
C(12B)-O(2B)-C(13B)-C(14B)	83(3)
C(16B)-O(4B)-C(15B)-O(3B)	1(4)
C(16B)-O(4B)-C(15B)-C(1B)	-175.5(19)
C(9B)-C(1B)-C(15B)-O(3B)	170(2)
C(2B)-C(1B)-C(15B)-O(3B)	-6(3)
C(9B)-C(1B)-C(15B)-O(4B)	-13(3)
C(2B)-C(1B)-C(15B)-O(4B)	170.2(13)
C(15B)-O(4B)-C(16B)-C(17B)	-173(2)

C(9C)-C(1C)-C(2C)-N(1C)	-176.4(13)
C(15C)-C(1C)-C(2C)-N(1C)	14.5(17)
C(9C)-C(1C)-C(2C)-C(3C)	-0.2(3)
C(15C)-C(1C)-C(2C)-C(3C)	-169.3(15)
N(1C)-C(2C)-C(3C)-C(10C)	176.1(13)
C(1C)-C(2C)-C(3C)-C(10C)	-0.1(3)
N(1C)-C(2C)-C(3C)-C(12C)	5.4(17)
C(1C)-C(2C)-C(3C)-C(12C)	-170.8(15)
C(10C)-C(4C)-C(5C)-C(6C)	-0.2(14)
C(4C)-C(5C)-C(6C)-C(7C)	0.2(14)
C(5C)-C(6C)-C(7C)-C(8C)	0.3(14)
C(6C)-C(7C)-C(8C)-C(9C)	-0.3(13)
C(7C)-C(8C)-C(9C)-C(1C)	-179.6(6)
C(7C)-C(8C)-C(9C)-C(10C)	-0.4(13)
C(2C)-C(1C)-C(9C)-C(8C)	179.7(6)
C(15C)-C(1C)-C(9C)-C(8C)	-11.2(17)
C(2C)-C(1C)-C(9C)-C(10C)	0.3(6)
C(15C)-C(1C)-C(9C)-C(10C)	169.5(15)
C(5C)-C(4C)-C(10C)-C(3C)	-179.8(7)
C(5C)-C(4C)-C(10C)-C(9C)	-0.5(13)
C(2C)-C(3C)-C(10C)-C(4C)	179.7(6)
C(12C)-C(3C)-C(10C)-C(4C)	-10.3(19)
C(2C)-C(3C)-C(10C)-C(9C)	0.3(6)
C(12C)-C(3C)-C(10C)-C(9C)	170.2(16)
C(8C)-C(9C)-C(10C)-C(4C)	0.9(13)
C(1C)-C(9C)-C(10C)-C(4C)	-179.8(6)
C(8C)-C(9C)-C(10C)-C(3C)	-179.7(7)
C(1C)-C(9C)-C(10C)-C(3C)	-0.4(7)
C(13C)-O(2C)-C(12C)-O(1C)	-6(4)
C(13C)-O(2C)-C(12C)-C(3C)	176.1(19)
C(2C)-C(3C)-C(12C)-O(1C)	6(3)
C(10C)-C(3C)-C(12C)-O(1C)	-162.9(18)
C(2C)-C(3C)-C(12C)-O(2C)	-176.7(14)
C(10C)-C(3C)-C(12C)-O(2C)	15(3)
C(12C)-O(2C)-C(13C)-C(14C)	-177(2)
C(16C)-O(4C)-C(15C)-O(3C)	-3(3)
C(16C)-O(4C)-C(15C)-C(1C)	177.5(15)
C(2C)-C(1C)-C(15C)-O(3C)	-170.4(19)
C(9C)-C(1C)-C(15C)-O(3C)	23(3)
C(2C)-C(1C)-C(15C)-O(4C)	9(2)
C(9C)-C(1C)-C(15C)-O(4C)	-157.9(12)
C(15C)-O(4C)-C(16C)-C(17C)	-111(2)
C(9D)-C(1D)-C(2D)-N(1D)	178.5(13)
C(15D)-C(1D)-C(2D)-N(1D)	-8.5(17)
C(9D)-C(1D)-C(2D)-C(3D)	0.1(3)
C(15D)-C(1D)-C(2D)-C(3D)	173.1(15)

N(1D)-C(2D)-C(3D)-C(10D)	-178.3(13)
C(1D)-C(2D)-C(3D)-C(10D)	0.1(3)
N(1D)-C(2D)-C(3D)-C(12D)	0.6(16)
C(1D)-C(2D)-C(3D)-C(12D)	178.9(13)
C(10D)-C(4D)-C(5D)-C(6D)	0.2(14)
C(4D)-C(5D)-C(6D)-C(7D)	-0.5(13)
C(5D)-C(6D)-C(7D)-C(8D)	0.3(14)
C(6D)-C(7D)-C(8D)-C(9D)	-0.1(13)
C(7D)-C(8D)-C(9D)-C(1D)	179.8(6)
C(7D)-C(8D)-C(9D)-C(10D)	0.3(13)
C(2D)-C(1D)-C(9D)-C(8D)	-179.8(6)
C(15D)-C(1D)-C(9D)-C(8D)	7.1(17)
C(2D)-C(1D)-C(9D)-C(10D)	-0.2(6)
C(15D)-C(1D)-C(9D)-C(10D)	-173.3(15)
C(5D)-C(4D)-C(10D)-C(3D)	179.9(7)
C(5D)-C(4D)-C(10D)-C(9D)	0.4(13)
C(2D)-C(3D)-C(10D)-C(4D)	-179.7(6)
C(12D)-C(3D)-C(10D)-C(4D)	1.5(17)
C(2D)-C(3D)-C(10D)-C(9D)	-0.2(6)
C(12D)-C(3D)-C(10D)-C(9D)	-179.0(15)
C(8D)-C(9D)-C(10D)-C(4D)	-0.6(12)
C(1D)-C(9D)-C(10D)-C(4D)	179.8(6)
C(8D)-C(9D)-C(10D)-C(3D)	179.9(6)
C(1D)-C(9D)-C(10D)-C(3D)	0.3(7)
C(13D)-O(2D)-C(12D)-O(1D)	5(3)
C(13D)-O(2D)-C(12D)-C(3D)	-174.0(18)
C(2D)-C(3D)-C(12D)-O(1D)	4(3)
C(10D)-C(3D)-C(12D)-O(1D)	-177.6(15)
C(2D)-C(3D)-C(12D)-O(2D)	-177.6(12)
C(10D)-C(3D)-C(12D)-O(2D)	1(2)
C(12D)-O(2D)-C(13D)-C(14D)	-180(2)
C(16D)-O(4D)-C(15D)-O(3D)	-3(3)
C(16D)-O(4D)-C(15D)-C(1D)	177.5(15)
C(2D)-C(1D)-C(15D)-O(3D)	169.6(18)
C(9D)-C(1D)-C(15D)-O(3D)	-19(3)
C(2D)-C(1D)-C(15D)-O(4D)	-11(2)
C(9D)-C(1D)-C(15D)-O(4D)	160.7(13)
C(15D)-O(4D)-C(16D)-C(17D)	106(2)
C(11E)-N(1E)-C(2E)-C(3E)	-56(11)
C(11E)-N(1E)-C(2E)-C(1E)	116(11)
C(9E)-C(1E)-C(2E)-N(1E)	-173.0(12)
C(15E)-C(1E)-C(2E)-N(1E)	14.5(16)
C(9E)-C(1E)-C(2E)-C(3E)	0.1(3)
C(15E)-C(1E)-C(2E)-C(3E)	-172.4(14)
N(1E)-C(2E)-C(3E)-C(10E)	172.9(12)
C(1E)-C(2E)-C(3E)-C(10E)	0.0(3)

N(1E)-C(2E)-C(3E)-C(12E)	-14.5(16)
C(1E)-C(2E)-C(3E)-C(12E)	172.6(13)
C(10E)-C(4E)-C(5E)-C(6E)	-0.3(13)
C(4E)-C(5E)-C(6E)-C(7E)	0.2(13)
C(5E)-C(6E)-C(7E)-C(8E)	0.3(14)
C(6E)-C(7E)-C(8E)-C(9E)	-0.8(13)
C(7E)-C(8E)-C(9E)-C(1E)	-179.7(6)
C(7E)-C(8E)-C(9E)-C(10E)	0.7(13)
C(2E)-C(1E)-C(9E)-C(8E)	-179.7(6)
C(15E)-C(1E)-C(9E)-C(8E)	-7.3(16)
C(2E)-C(1E)-C(9E)-C(10E)	-0.1(6)
C(15E)-C(1E)-C(9E)-C(10E)	172.4(14)
C(5E)-C(4E)-C(10E)-C(3E)	-179.9(6)
C(5E)-C(4E)-C(10E)-C(9E)	0.2(13)
C(2E)-C(3E)-C(10E)-C(4E)	180.0(6)
C(12E)-C(3E)-C(10E)-C(4E)	7.5(16)
C(2E)-C(3E)-C(10E)-C(9E)	-0.1(6)
C(12E)-C(3E)-C(10E)-C(9E)	-172.6(14)
C(8E)-C(9E)-C(10E)-C(4E)	-0.3(13)
C(1E)-C(9E)-C(10E)-C(4E)	-179.9(7)
C(8E)-C(9E)-C(10E)-C(3E)	179.7(7)
C(1E)-C(9E)-C(10E)-C(3E)	0.1(7)
C(13E)-O(2E)-C(12E)-O(1E)	3(3)
C(13E)-O(2E)-C(12E)-C(3E)	-169.6(15)
C(2E)-C(3E)-C(12E)-O(1E)	162.5(16)
C(10E)-C(3E)-C(12E)-O(1E)	-26(3)
C(2E)-C(3E)-C(12E)-O(2E)	-25(2)
C(10E)-C(3E)-C(12E)-O(2E)	146.8(12)
C(12E)-O(2E)-C(13E)-C(14E)	173.0(19)
C(16E)-O(4E)-C(15E)-O(3E)	-4(3)
C(16E)-O(4E)-C(15E)-C(1E)	172.3(16)
C(2E)-C(1E)-C(15E)-O(3E)	-163.4(17)
C(9E)-C(1E)-C(15E)-O(3E)	26(3)
C(2E)-C(1E)-C(15E)-O(4E)	20(2)
C(9E)-C(1E)-C(15E)-O(4E)	-150.7(12)
C(15E)-O(4E)-C(16E)-C(17E)	-179.7(18)
C(11F)-N(1F)-C(2F)-C(3F)	40(8)
C(11F)-N(1F)-C(2F)-C(1F)	-130(7)
C(9F)-C(1F)-C(2F)-N(1F)	171.2(13)
C(15F)-C(1F)-C(2F)-N(1F)	-12.6(18)
C(9F)-C(1F)-C(2F)-C(3F)	0.1(3)
C(15F)-C(1F)-C(2F)-C(3F)	176.3(16)
N(1F)-C(2F)-C(3F)-C(10F)	-171.5(13)
C(1F)-C(2F)-C(3F)-C(10F)	-0.2(3)
N(1F)-C(2F)-C(3F)-C(12F)	23.6(17)
C(1F)-C(2F)-C(3F)-C(12F)	-165.1(15)

C(10F)-C(4F)-C(5F)-C(6F)	0.2(13)
C(4F)-C(5F)-C(6F)-C(7F)	0.1(13)
C(5F)-C(6F)-C(7F)-C(8F)	0.1(14)
C(6F)-C(7F)-C(8F)-C(9F)	-0.4(14)
C(7F)-C(8F)-C(9F)-C(1F)	-180.0(7)
C(7F)-C(8F)-C(9F)-C(10F)	0.3(13)
C(2F)-C(1F)-C(9F)-C(8F)	-179.8(6)
C(15F)-C(1F)-C(9F)-C(8F)	4.0(19)
C(2F)-C(1F)-C(9F)-C(10F)	0.0(6)
C(15F)-C(1F)-C(9F)-C(10F)	-176.1(16)
C(5F)-C(4F)-C(10F)-C(3F)	-179.9(7)
C(5F)-C(4F)-C(10F)-C(9F)	-0.6(13)
C(2F)-C(3F)-C(10F)-C(4F)	179.6(6)
C(12F)-C(3F)-C(10F)-C(4F)	-15.2(17)
C(2F)-C(3F)-C(10F)-C(9F)	0.1(6)
C(12F)-C(3F)-C(10F)-C(9F)	165.4(15)
C(8F)-C(9F)-C(10F)-C(4F)	0.3(12)
C(1F)-C(9F)-C(10F)-C(4F)	-179.5(7)
C(8F)-C(9F)-C(10F)-C(3F)	179.7(6)
C(1F)-C(9F)-C(10F)-C(3F)	-0.1(7)
C(2F)-N(1F)-C(11F)-Cr(1)	-25(17)
C(13F)-O(2F)-C(12F)-O(1F)	-5(4)
C(13F)-O(2F)-C(12F)-C(3F)	177.9(16)
C(2F)-C(3F)-C(12F)-O(1F)	-169.2(19)
C(10F)-C(3F)-C(12F)-O(1F)	28(3)
C(2F)-C(3F)-C(12F)-O(2F)	8(3)
C(10F)-C(3F)-C(12F)-O(2F)	-155.1(14)
C(12F)-O(2F)-C(13F)-C(14F)	-96(3)
C(16F)-O(4F)-C(15F)-O(3F)	2(3)
C(16F)-O(4F)-C(15F)-C(1F)	-176.1(17)
C(2F)-C(1F)-C(15F)-O(3F)	170(2)
C(9F)-C(1F)-C(15F)-O(3F)	-14(3)
C(2F)-C(1F)-C(15F)-O(4F)	-12(3)
C(9F)-C(1F)-C(15F)-O(4F)	163.9(13)
C(15F)-O(4F)-C(16F)-C(17F)	170(2)
C(9G)-C(1G)-C(2G)-N(1G)	179.7(13)
C(15G)-C(1G)-C(2G)-N(1G)	-13.2(17)
C(9G)-C(1G)-C(2G)-C(3G)	0.1(3)
C(15G)-C(1G)-C(2G)-C(3G)	167.2(15)
N(1G)-C(2G)-C(3G)-C(10G)	-179.5(14)
C(1G)-C(2G)-C(3G)-C(10G)	0.1(3)
N(1G)-C(2G)-C(3G)-C(12G)	-5.4(19)
C(1G)-C(2G)-C(3G)-C(12G)	174.2(16)
C(10G)-C(4G)-C(5G)-C(6G)	0.2(14)
C(4G)-C(5G)-C(6G)-C(7G)	-0.3(14)
C(5G)-C(6G)-C(7G)-C(8G)	-0.1(13)

C(6G)-C(7G)-C(8G)-C(9G)	0.3(14)
C(7G)-C(8G)-C(9G)-C(1G)	179.7(7)
C(7G)-C(8G)-C(9G)-C(10G)	0.2(13)
C(2G)-C(1G)-C(9G)-C(8G)	-179.7(6)
C(15G)-C(1G)-C(9G)-C(8G)	14.2(19)
C(2G)-C(1G)-C(9G)-C(10G)	-0.2(6)
C(15G)-C(1G)-C(9G)-C(10G)	-166.3(17)
C(5G)-C(4G)-C(10G)-C(3G)	179.9(7)
C(5G)-C(4G)-C(10G)-C(9G)	0.5(13)
C(2G)-C(3G)-C(10G)-C(4G)	-179.7(6)
C(12G)-C(3G)-C(10G)-C(4G)	7(2)
C(2G)-C(3G)-C(10G)-C(9G)	-0.2(6)
C(12G)-C(3G)-C(10G)-C(9G)	-173.7(18)
C(8G)-C(9G)-C(10G)-C(4G)	-0.7(12)
C(1G)-C(9G)-C(10G)-C(4G)	179.8(6)
C(8G)-C(9G)-C(10G)-C(3G)	179.8(6)
C(1G)-C(9G)-C(10G)-C(3G)	0.3(7)
C(13G)-O(2G)-C(12G)-O(1G)	1(4)
C(13G)-O(2G)-C(12G)-C(3G)	-168.7(19)
C(2G)-C(3G)-C(12G)-O(1G)	11(4)
C(10G)-C(3G)-C(12G)-O(1G)	-176(2)
C(2G)-C(3G)-C(12G)-O(2G)	-179.0(16)
C(10G)-C(3G)-C(12G)-O(2G)	-6(3)
C(12G)-O(2G)-C(13G)-C(14G)	135(3)
C(16G)-O(4G)-C(15G)-O(3G)	-4(4)
C(16G)-O(4G)-C(15G)-C(1G)	176(2)
C(2G)-C(1G)-C(15G)-O(3G)	33(3)
C(9G)-C(1G)-C(15G)-O(3G)	-162.6(19)
C(2G)-C(1G)-C(15G)-O(4G)	-146.9(15)
C(9G)-C(1G)-C(15G)-O(4G)	17(3)
C(15G)-O(4G)-C(16G)-C(17G)	178(2)
C(9H)-C(1H)-C(2H)-N(1H)	-175.7(14)
C(15H)-C(1H)-C(2H)-N(1H)	2.8(17)
C(9H)-C(1H)-C(2H)-C(3H)	0.0(3)
C(15H)-C(1H)-C(2H)-C(3H)	178.5(15)
N(1H)-C(2H)-C(3H)-C(10H)	175.5(14)
C(1H)-C(2H)-C(3H)-C(10H)	0.1(3)
N(1H)-C(2H)-C(3H)-C(12H)	-11.3(19)
C(1H)-C(2H)-C(3H)-C(12H)	173.2(17)
C(10H)-C(4H)-C(5H)-C(6H)	0.1(13)
C(4H)-C(5H)-C(6H)-C(7H)	0.2(14)
C(5H)-C(6H)-C(7H)-C(8H)	-0.4(14)
C(6H)-C(7H)-C(8H)-C(9H)	0.2(13)
C(7H)-C(8H)-C(9H)-C(1H)	-179.9(6)
C(7H)-C(8H)-C(9H)-C(10H)	0.0(13)
C(2H)-C(1H)-C(9H)-C(8H)	180.0(6)

C(15H)-C(1H)-C(9H)-C(8H)	1.6(19)
C(2H)-C(1H)-C(9H)-C(10H)	0.0(6)
C(15H)-C(1H)-C(9H)-C(10H)	-178.3(17)
C(5H)-C(4H)-C(10H)-C(3H)	179.8(7)
C(5H)-C(4H)-C(10H)-C(9H)	-0.1(13)
C(2H)-C(3H)-C(10H)-C(4H)	-180.0(6)
C(12H)-C(3H)-C(10H)-C(4H)	7.0(19)
C(2H)-C(3H)-C(10H)-C(9H)	0.0(6)
C(12H)-C(3H)-C(10H)-C(9H)	-173.1(17)
C(8H)-C(9H)-C(10H)-C(4H)	0.0(13)
C(1H)-C(9H)-C(10H)-C(4H)	179.9(7)
C(8H)-C(9H)-C(10H)-C(3H)	-179.9(6)
C(1H)-C(9H)-C(10H)-C(3H)	0.0(7)
C(13H)-O(2H)-C(12H)-O(1H)	1(4)
C(13H)-O(2H)-C(12H)-C(3H)	-177.4(18)
C(2H)-C(3H)-C(12H)-O(1H)	169(2)
C(10H)-C(3H)-C(12H)-O(1H)	-20(3)
C(2H)-C(3H)-C(12H)-O(2H)	-13(3)
C(10H)-C(3H)-C(12H)-O(2H)	158.8(15)
C(12H)-O(2H)-C(13H)-C(14H)	105(3)
C(16H)-O(4H)-C(15H)-O(3H)	-2(4)
C(16H)-O(4H)-C(15H)-C(1H)	-173(2)
C(2H)-C(1H)-C(15H)-O(3H)	0(3)
C(9H)-C(1H)-C(15H)-O(3H)	178.0(18)
C(2H)-C(1H)-C(15H)-O(4H)	170.4(13)
C(9H)-C(1H)-C(15H)-O(4H)	-11(3)
C(15H)-O(4H)-C(16H)-C(17H)	166(2)
C(11I)-N(1I)-C(2I)-C(3I)	-31(10)
C(11I)-N(1I)-C(2I)-C(1I)	141(9)
C(9I)-C(1I)-C(2I)-C(3I)	0.2(3)
C(15I)-C(1I)-C(2I)-C(3I)	-179.5(15)
C(9I)-C(1I)-C(2I)-N(1I)	-173.3(13)
C(15I)-C(1I)-C(2I)-N(1I)	7.1(17)
N(1I)-C(2I)-C(3I)-C(10I)	173.4(13)
C(1I)-C(2I)-C(3I)-C(10I)	-0.1(3)
N(1I)-C(2I)-C(3I)-C(12I)	-18.7(18)
C(1I)-C(2I)-C(3I)-C(12I)	167.8(16)
C(10I)-C(4I)-C(5I)-C(6I)	-0.1(13)
C(4I)-C(5I)-C(6I)-C(7I)	-0.1(14)
C(5I)-C(6I)-C(7I)-C(8I)	0.0(14)
C(6I)-C(7I)-C(8I)-C(9I)	0.2(13)
C(7I)-C(8I)-C(9I)-C(1I)	179.6(7)
C(7I)-C(8I)-C(9I)-C(10I)	-0.1(13)
C(2I)-C(1I)-C(9I)-C(8I)	-179.9(6)
C(15I)-C(1I)-C(9I)-C(8I)	-0.2(18)
C(2I)-C(1I)-C(9I)-C(10I)	-0.1(6)

C(15I)-C(1I)-C(9I)-C(10I)	179.5(16)
C(5I)-C(4I)-C(10I)-C(3I)	-179.7(7)
C(5I)-C(4I)-C(10I)-C(9I)	0.3(14)
C(2I)-C(3I)-C(10I)-C(4I)	180.0(6)
C(12I)-C(3I)-C(10I)-C(4I)	11.6(17)
C(2I)-C(3I)-C(10I)-C(9I)	0.0(6)
C(12I)-C(3I)-C(10I)-C(9I)	-168.3(15)
C(8I)-C(9I)-C(10I)-C(4I)	-0.2(13)
C(1I)-C(9I)-C(10I)-C(4I)	-179.9(7)
C(8I)-C(9I)-C(10I)-C(3I)	179.8(6)
C(1I)-C(9I)-C(10I)-C(3I)	0.1(7)
C(13I)-O(2I)-C(12I)-O(1I)	4(4)
C(13I)-O(2I)-C(12I)-C(3I)	-174.8(17)
C(2I)-C(3I)-C(12I)-O(1I)	160.5(19)
C(10I)-C(3I)-C(12I)-O(1I)	-33(3)
C(2I)-C(3I)-C(12I)-O(2I)	-20(3)
C(10I)-C(3I)-C(12I)-O(2I)	145.7(14)
C(12I)-O(2I)-C(13I)-C(14I)	124(3)
C(16I)-O(4I)-C(15I)-O(3I)	-2(4)
C(16I)-O(4I)-C(15I)-C(1I)	171(2)
C(2I)-C(1I)-C(15I)-O(3I)	-167.3(18)
C(9I)-C(1I)-C(15I)-O(3I)	13(3)
C(2I)-C(1I)-C(15I)-O(4I)	20(2)
C(9I)-C(1I)-C(15I)-O(4I)	-159.9(13)
C(15I)-O(4I)-C(16I)-C(17I)	-167(2)

Symmetry transformations used to generate equivalent atoms:
#1 -x+2, -y, -z+1 #2 -x+1, -y, -z+1 #3 -x+1, -y+1, -z+1

Table 7 Hydrogen bonds for **3.12** [Å and °].

D-H...A	d(D-H)	d(H...A)	d(D...A)	<(DHA)
C(4A)-H(4A)...O(2A)	0.95	2.25	2.90(2)	124.7
C(8A)-H(8A)...O(4A)	0.95	2.20	2.87(2)	126.5
C(4B)-H(4B)...O(2B)	0.95	2.26	2.90(2)	123.8
C(8B)-H(8B)...O(4B)	0.95	2.20	2.88(2)	127.8
C(4C)-H(4C)...O(2C)	0.95	2.18	2.86(2)	127.3
C(8C)-H(8C)...O(3C)	0.95	2.30	2.98(3)	127.9
C(4D)-H(4D)...O(2D)	0.95	2.19	2.88(2)	127.7
C(8D)-H(8D)...O(3D)	0.95	2.29	2.98(2)	128.5
C(4E)-H(4E)...O(1E)	0.95	2.33	2.99(2)	126.9
C(8E)-H(8E)...O(3E)	0.95	2.33	3.01(2)	127.9
C(4F)-H(4F)...O(1F)	0.95	2.27	2.96(3)	128.7
C(8F)-H(8F)...O(3F)	0.95	2.36	3.02(3)	126.7
C(4G)-H(4G)...O(2G)	0.95	2.19	2.86(2)	126.9
C(8G)-H(8G)...O(4G)	0.95	2.30	2.92(2)	121.5
C(4H)-H(4H)...O(1H)	0.95	2.22	2.92(3)	129.6
C(8H)-H(8H)...O(4H)	0.95	2.24	2.89(3)	125.4
C(4I)-H(4I)...O(1I)	0.95	2.26	2.97(3)	130.7
C(8I)-H(8I)...O(3I)	0.95	2.37	3.01(3)	124.3

Appendix 3

Crystallographic Data for Compound 4.1a

Table 1 Crystal data and structure refinement for **4.1a.**

Empirical formula	$C_{38}H_{44}Cl_4Ir_2N_2O_4$	
Formula weight	1118.95	
Temperature	100(2) K	
Wavelength	0.71073 Å	
Crystal system	Orthorhombic	
Space group	$P2_12_12_1 - D_2^4$ (No. 19)	
Unit cell dimensions	**a** = 12.5422(6) Å	α = 90.000°
	b = 15.7507(8) Å	β = 90.000°
	c = 19.5075(10) Å	γ = 90.000°
Volume	3853.7(3) $Å^3$	
Z	4	
Density (calculated)	1.929 Mg/m^3	
Absorption coefficient	7.219 mm^{-1}	
F(000)	2160	
Crystal size	0.26 x 0.16 x 0.12 mm^3	
Theta range for data collection	2.46° to 30.55°.	
Index ranges	$-17 \le h \le 17$, $-22 \le k \le 22$, $-27 \le l \le 27$	
Reflections collected	45283	
Independent reflections	11652 [R_{int} = 0.042]	
Completeness to theta = 30.55°	99.5 %	
Absorption correction	Multi-scan	
Max. and min. transmission	1.000 and 0.510	
Refinement method	Full-matrix least-squares on F^2	
Data / restraints / parameters	11652 / 0 / 463	
Goodness-of-fit on F^2	1.060	
Final R indices [I>2sigma(I)]	R_1 = 0.032, wR_2 = 0.074	
R indices (all data)	R_1 = 0.034, wR_2 = 0.075	
Absolute structure parameter	0.009(6)	
Largest diff. peak and hole	2.75 and -0.93 $e^-/Å^3$	

$R_1 = \Sigma \, ||F_o| - |F_c|| \, / \, \Sigma \, |F_o|$

$wR_2 = \{ \Sigma \, [w(F_o^2 - F_c^2)^2] \, / \, \Sigma \, [w(F_o^2)^2] \}^{1/2}$

Table 2 Atomic coordinates (x 10^4) and equivalent isotropic displacement parameters ($Å^2$ x 10^3) for **4.1a**. U(eq) is defined as one third of the trace of the orthogonalized U_{ij} tensor.

	x	y	z	U(eq)
Ir(1)	6728(1)	2701(1)	6002(1)	18(1)
Ir(2)	3800(1)	2847(1)	-956(1)	15(1)
Cl(11)	5593(1)	1503(1)	6191(1)	26(1)
Cl(12)	5265(1)	3612(1)	6305(1)	29(1)
Cl(21)	2512(1)	1719(1)	-895(1)	23(1)
Cl(22)	2359(1)	3820(1)	-776(1)	23(1)
N(1)	6249(3)	2817(3)	4469(2)	18(1)
N(2)	4413(3)	2787(3)	570(2)	20(1)
O(1)	6530(3)	4486(2)	4203(2)	25(1)
O(2)	6466(3)	1145(2)	4227(2)	24(1)
O(3)	5716(4)	5043(2)	3283(2)	32(1)
O(4)	5572(4)	584(2)	3339(2)	31(1)
C(1)	5929(4)	3541(3)	3373(2)	18(1)
C(2)	6050(4)	2816(3)	3780(2)	17(1)
C(3)	5852(4)	2069(3)	3392(2)	15(1)
C(4)	5315(4)	1794(3)	2179(3)	20(1)
C(5)	4978(4)	1997(3)	1531(3)	23(1)
C(6)	4806(4)	2787(4)	1245(2)	21(1)
C(7)	4967(4)	3590(3)	1517(2)	18(1)
C(8)	5342(4)	3798(3)	2173(2)	18(1)
C(9)	5560(4)	2341(3)	2727(2)	15(1)
C(10)	5604(4)	3261(3)	2710(2)	16(1)
C(14)	5939(4)	1192(3)	3630(3)	21(1)
C(15)	6625(5)	301(3)	4513(3)	28(1)
C(16)	7538(5)	-135(4)	4141(4)	40(2)
C(11)	6036(4)	4431(3)	3598(2)	20(1)
C(12)	6522(5)	5311(3)	4541(3)	27(1)
C(13)	5469(5)	5431(3)	4931(3)	30(1)
C(17)	6357(4)	2763(3)	5048(2)	18(1)
C(18)	4119(4)	2799(3)	0(2)	16(1)
C(21)	8389(4)	2936(4)	5784(3)	25(1)

C(22)	8259(4)	2099(4)	6067(3)	35(1)
C(23)	7901(5)	2233(5)	6779(3)	47(2)
C(24)	7754(5)	3095(5)	6878(3)	43(2)
C(25)	8020(4)	3547(4)	6280(3)	30(1)
C(26)	8806(5)	3166(6)	5090(3)	55(2)
C(27)	8532(5)	1304(4)	5752(6)	72(3)
C(28)	7690(6)	1518(7)	7269(5)	98(5)
C(29)	7349(6)	3532(8)	7532(4)	87(4)
C(30)	8016(6)	4507(4)	6197(5)	61(3)
C(31)	5468(4)	2735(3)	-1228(2)	19(1)
C(32)	4847(4)	2170(3)	-1663(2)	20(1)
C(33)	4134(4)	2689(4)	-2070(2)	22(1)
C(34)	4310(4)	3552(3)	-1897(3)	21(1)
C(35)	5101(4)	3581(3)	-1355(3)	20(1)
C(36)	6343(4)	2475(4)	-762(3)	27(1)
C(37)	4980(5)	1236(3)	-1735(3)	25(1)
C(38)	3405(4)	2350(5)	-2606(3)	34(1)
C(39)	3754(6)	4304(4)	-2203(3)	35(1)
C(40)	5568(5)	4383(3)	-1046(3)	33(1)

Table 3 Bond lengths [Å] **4.1a**.

Ir(1)-C(17)	1.921(4)	C(3)-C(14)	1.462(7)
Ir(1)-C(22)	2.144(5)	C(4)-C(5)	1.372(7)
Ir(1)-C(21)	2.158(5)	C(4)-C(9)	1.407(6)
Ir(1)-C(25)	2.167(5)	C(5)-C(6)	1.380(7)
Ir(1)-C(24)	2.227(6)	C(6)-C(7)	1.387(7)
Ir(1)-C(23)	2.236(5)	C(7)-C(8)	1.403(6)
Ir(1)-Cl(11)	2.392(1)	C(8)-C(10)	1.385(7)
Ir(1)-Cl(12)	2.404(1)	C(9)-C(10)	1.450(6)
Ir(2)-C(18)	1.908(4)	C(15)-C(16)	1.520(9)
Ir(2)-C(35)	2.146(5)	C(12)-C(13)	1.535(8)
Ir(2)-C(31)	2.166(5)	C(21)-C(22)	1.437(8)
Ir(2)-C(32)	2.184(5)	C(21)-C(25)	1.440(8)
Ir(2)-C(33)	2.228(4)	C(21)-C(26)	1.496(8)
Ir(2)-C(34)	2.240(5)	C(22)-C(27)	1.437(9)
Ir(2)-Cl(22)	2.395(1)	C(22)-C(23)	1.474(10)
Ir(2)-Cl(21)	2.405(1)	C(23)-C(24)	1.383(11)
N(1)-C(17)	1.141(6)	C(23)-C(28)	1.500(9)
N(1)-C(2)	1.367(6)	C(24)-C(25)	1.407(9)
N(2)-C(18)	1.172(6)	C(24)-C(29)	1.536(10)
N(2)-C(6)	1.405(6)	C(25)-C(30)	1.521(9)
O(1)-C(11)	1.335(6)	C(31)-C(35)	1.431(7)
O(1)-C(12)	1.457(6)	C(31)-C(32)	1.455(7)
O(2)-C(14)	1.340(6)	C(31)-C(36)	1.483(7)
O(2)-C(15)	1.456(6)	C(32)-C(33)	1.448(7)
O(3)-C(11)	1.211(6)	C(32)-C(37)	1.488(7)
O(4)-C(14)	1.205(6)	C(33)-C(34)	1.418(8)
C(1)-C(2)	1.399(7)	C(33)-C(38)	1.489(7)
C(1)-C(10)	1.427(7)	C(34)-C(35)	1.451(7)
C(1)-C(11)	1.476(7)	C(34)-C(39)	1.499(7)
C(2)-C(3)	1.420(7)	C(35)-C(40)	1.518(7)
C(3)-C(9)	1.414(6)		

Table 4 Bond angles [°] for **4.1a**.

C(17)-Ir(1)-C(22)	107.3(2)	C(18)-Ir(2)-C(33)	155.4(2)
C(17)-Ir(1)-C(21)	92.0(2)	C(35)-Ir(2)-C(33)	64.1(2)
C(22)-Ir(1)-C(21)	39.0(2)	C(31)-Ir(2)-C(33)	64.5(2)
C(17)-Ir(1)-C(25)	113.1(2)	C(32)-Ir(2)-C(33)	38.3(2)
C(22)-Ir(1)-C(25)	65.6(2)	C(18)-Ir(2)-C(34)	139.6(2)
C(21)-Ir(1)-C(25)	38.9(2)	C(35)-Ir(2)-C(34)	38.6(2)
C(17)-Ir(1)-C(24)	150.3(2)	C(31)-Ir(2)-C(34)	64.1(2)
C(22)-Ir(1)-C(24)	63.9(3)	C(32)-Ir(2)-C(34)	63.4(2)
C(21)-Ir(1)-C(24)	63.0(2)	C(33)-Ir(2)-C(34)	37.0(2)
C(25)-Ir(1)-C(24)	37.3(2)	C(18)-Ir(2)-Cl(22)	92.3(1)
C(17)-Ir(1)-C(23)	146.4(3)	C(35)-Ir(2)-Cl(22)	106.4(1)
C(22)-Ir(1)-C(23)	39.3(3)	C(31)-Ir(2)-Cl(22)	144.8(1)
C(21)-Ir(1)-C(23)	63.6(2)	C(32)-Ir(2)-Cl(22)	149.2(1)
C(25)-Ir(1)-C(23)	62.7(2)	C(33)-Ir(2)-Cl(22)	110.9(1)
C(24)-Ir(1)-C(23)	36.1(3)	C(34)-Ir(2)-Cl(22)	91.1(1)
C(17)-Ir(1)-Cl(11)	92.6(2)	C(18)-Ir(2)-Cl(21)	93.6(1)
C(22)-Ir(1)-Cl(11)	100.1(2)	C(35)-Ir(2)-Cl(21)	157.9(1)
C(21)-Ir(1)-Cl(11)	137.8(2)	C(31)-Ir(2)-Cl(21)	126.921)
C(25)-Ir(1)-Cl(11)	153.1(2)	C(32)-Ir(2)-Cl(21)	94.3(1)
C(24)-Ir(1)-Cl(11)	116.5(2)	C(33)-Ir(2)-Cl(21)	95.3(1)
C(23)-Ir(1)-Cl(11)	91.6(2)	C(34)-Ir(2)-Cl(21)	126.8(1)
C(17)-Ir(1)-Cl(12)	91.3(2)	Cl(22)-Ir(2)-Cl(21)	87.62(4)
C(22)-Ir(1)-Cl(12)	158.9(2)	C(17)-N(1)-C(2)	174.3(5)
C(21)-Ir(1)-Cl(12)	133.1(2)	C(18)-N(2)-C(6)	177.6(5)
C(25)-Ir(1)-Cl(12)	98.2(2)	C(11)-O(1)-C(12)	117.0(4)
C(24)-Ir(1)-Cl(12)	94.9(2)	C(14)-O(2)-C(15)	116.8(4)
C(23)-Ir(1)-Cl(12)	122.2(2)	C(2)-C(1)-C(10)	107.1(4)
Cl(11)-Ir(1)-Cl(12)	88.78(5)	C(2)-C(1)-C(11)	126.7(4)
C(18)-Ir(2)-C(35)	102.5(2)	C(10)-C(1)-C(11)	126.1(4)
C(18)-Ir(2)-C(31)	92.0(2)	N(1)-C(2)-C(1)	125.2(5)
C(35)-Ir(2)-C(31)	38.8(2)	N(1)-C(2)-C(3)	123.9(5)
C(18)-Ir(2)-C(32)	118.2(2)	C(1)-C(2)-C(3)	110.7(4)
C(35)-Ir(2)-C(32)	64.9(2)	C(9)-C(3)-C(2)	106.5(4)
C(31)-Ir(2)-C(32)	39.1(2)	C(9)-C(3)-C(14)	126.7(4)

C(2)-C(3)-C(14)	126.8(4)	C(24)-C(23)-C(22)	108.2(5)
C(5)-C(4)-C(9)	128.6(5)	C(24)-C(23)-C(28)	128.6(9)
C(4)-C(5)-C(6)	129.2(5)	C(22)-C(23)-C(28)	123.1(8)
C(5)-C(6)-C(7)	130.2(4)	C(24)-C(23)-Ir(1)	71.6(4)
C(5)-C(6)-N(2)	115.7(5)	C(22)-C(23)-Ir(1)	67.0(3)
C(7)-C(6)-N(2)	114.1(5)	C(28)-C(23)-Ir(1)	124.2(4)
C(6)-C(7)-C(8)	127.6(4)	C(23)-C(24)-C(25)	110.4(6)
C(10)-C(8)-C(7)	128.9(5)	C(23)-C(24)-C(29)	126.9(8)
C(4)-C(9)-C(3)	124.6(4)	C(25)-C(24)-C(29)	122.7(8)
C(4)-C(9)-C(10)	127.1(4)	C(23)-C(24)-Ir(1)	72.3(3)
C(3)-C(9)-C(10)	108.3(4)	C(25)-C(24)-Ir(1)	69.0(3)
C(8)-C(10)-C(1)	124.4(4)	C(29)-C(24)-Ir(1)	124.8(5)
C(8)-C(10)-C(9)	128.2(5)	C(24)-C(25)-C(21)	107.1(5)
C(1)-C(10)-C(9)	107.3(4)	C(24)-C(25)-C(30)	126.1(7)
O(4)-C(14)-O(2)	123.6(5)	C(21)-C(25)-C(30)	126.5(6)
O(4)-C(14)-C(3)	124.9(5)	C(24)-C(25)-Ir(1)	73.7(3)
O(2)-C(14)-C(3)	111.4(4)	C(21)-C(25)-Ir(1)	70.2(3)
O(2)-C(15)-C(16)	109.4(5)	C(30)-C(25)-Ir(1)	125.7(4)
O(3)-C(11)-O(1)	123.4(5)	C(35)-C(31)-C(32)	107.2(4)
O(3)-C(11)-C(1)	125.1(5)	C(35)-C(31)-C(36)	126.9(5)
O(1)-C(11)-C(1)	111.5(4)	C(32)-C(31)-C(36)	125.8(5)
O(1)-C(12)-C(13)	109.9(4)	C(35)-C(31)-Ir(2)	69.9(3)
N(1)-C(17)-Ir(1)	172.7(4)	C(32)-C(31)-Ir(2)	71.1(3)
N(2)-C(18)-Ir(2)	173.6(4)	C(36)-C(31)-Ir(2)	125.9(3)
C(22)-C(21)-C(25)	108.6(5)	C(33)-C(32)-C(31)	107.8(4)
C(22)-C(21)-C(26)	127.5(6)	C(33)-C(32)-C(37)	125.1(5)
C(25)-C(21)-C(26)	123.9(6)	C(31)-C(32)-C(37)	126.9(5)
C(22)-C(21)-Ir(1)	69.9(3)	C(33)-C(32)-Ir(2)	72.5(3)
C(25)-C(21)-Ir(1)	70.9(3)	C(31)-C(32)-Ir(2)	69.8(3)
C(26)-C(21)-Ir(1)	123.9(4)	C(37)-C(32)-Ir(2)	127.6(4)
C(27)-C(22)-C(21)	127.4(7)	C(34)-C(33)-C(32)	108.3(4)
C(27)-C(22)-C(23)	126.9(7)	C(34)-C(33)-C(38)	127.3(5)
C(21)-C(22)-C(23)	105.4(5)	C(32)-C(33)-C(38)	124.2(5)
C(27)-C(22)-Ir(1)	125.0(4)	C(34)-C(33)-Ir(2)	71.9(3)
C(21)-C(22)-Ir(1)	71.0(3)	C(32)-C(33)-Ir(2)	69.2(2)
C(23)-C(22)-Ir(1)	73.7(3)	C(38)-C(33)-Ir(2)	127.6(4)

C(33)-C(34)-C(35)	108.0(4)	C(31)-C(35)-C(34)	108.5(4)
C(33)-C(34)-C(39)	126.2(5)	C(31)-C(35)-C(40)	125.6(5)
C(35)-C(34)-C(39)	125.7(5)	C(34)-C(35)-C(40)	125.4(5)
C(33)-C(34)-Ir(2)	71.0(3)	C(31)-C(35)-Ir(2)	71.4(3)
C(35)-C(34)-Ir(2)	67.2(3)	C(34)-C(35)-Ir(2)	74.2(3)
C(39)-C(34)-Ir(2)	125.8(4)	C(40)-C(35)-Ir(2)	126.7(4)

Table 5 Anisotropic displacement parameters ($Å^2 x\ 10^3$) for **4.1a**. The anisotropic displacement factor exponent takes the form: $-2\pi^2[\ h^2\ a^{*2}U_{11} + ...\ + 2\ h\ k\ a^*\ b^*\ U_{12}\ ]$.

	U_{11}	U_{22}	U_{33}	U_{23}	U_{13}	U_{12}
Ir(1)	19(1)	23(1)	12(1)	2(1)	-1(1)	-4(1)
Ir(2)	18(1)	17(1)	11(1)	0(1)	-1(1)	1(1)
Cl(11)	24(1)	27(1)	26(1)	10(1)	-6(1)	-8(1)
Cl(12)	30(1)	33(1)	25(1)	-3(1)	7(1)	4(1)
Cl(21)	22(1)	22(1)	26(1)	-1(1)	1(1)	-4(1)
Cl(22)	24(1)	23(1)	22(1)	-3(1)	3(1)	7(1)
N(1)	25(2)	18(2)	12(2)	-1(2)	-2(2)	1(2)
N(2)	22(2)	23(2)	16(2)	0(2)	1(2)	-1(2)
O(1)	35(2)	22(2)	18(2)	-7(1)	-8(1)	5(2)
O(2)	34(2)	19(2)	20(2)	1(1)	-8(2)	3(2)
O(3)	55(3)	19(2)	22(2)	-2(2)	-6(2)	4(2)
O(4)	53(3)	14(2)	25(2)	4(1)	-14(2)	-8(2)
C(1)	24(3)	19(2)	13(2)	-2(2)	1(2)	1(2)
C(2)	18(2)	20(2)	14(2)	0(2)	-2(2)	2(2)
C(3)	15(2)	17(2)	13(2)	2(2)	-2(2)	2(2)
C(4)	27(3)	16(2)	18(2)	-2(2)	-4(2)	2(2)
C(5)	30(3)	22(2)	15(2)	-1(2)	-5(2)	-4(2)
C(6)	18(2)	28(3)	15(2)	2(2)	-1(2)	2(2)
C(7)	28(3)	17(2)	10(2)	3(2)	-6(2)	3(2)
C(8)	24(2)	20(2)	10(2)	-2(2)	-1(2)	0(2)
C(9)	13(2)	21(2)	11(2)	2(2)	1(2)	0(2)
C(10)	15(2)	18(2)	16(2)	-1(2)	3(2)	0(2)
C(14)	25(3)	19(2)	18(2)	1(2)	-1(2)	-3(2)
C(15)	51(4)	18(2)	15(2)	3(2)	-12(2)	4(2)
C(16)	46(4)	33(3)	41(4)	6(3)	-3(3)	15(3)
C(11)	32(3)	18(2)	11(2)	-3(2)	0(2)	0(2)
C(12)	37(3)	16(2)	28(3)	-5(2)	-5(2)	-4(2)
C(13)	55(4)	19(3)	16(2)	-4(2)	2(2)	-1(3)
C(17)	23(2)	17(2)	15(2)	0(2)	0(2)	-2(2)
C(18)	15(2)	13(2)	21(2)	-3(2)	-2(2)	0(2)
C(21)	19(2)	35(3)	20(2)	-2(2)	1(2)	0(2)

C(22)	23(3)	29(3)	53(4)	-1(3)	-14(3)	0(2)
C(23)	24(3)	71(5)	45(4)	47(4)	-29(3)	-25(3)
C(24)	29(3)	82(5)	17(3)	-11(3)	-3(2)	-18(3)
C(25)	17(2)	32(3)	39(3)	-10(2)	1(2)	-5(2)
C(26)	24(3)	112(7)	28(3)	13(4)	4(3)	-11(4)
C(27)	24(3)	36(4)	156(10)	-30(5)	-46(5)	8(3)
C(28)	40(4)	138(9)	115(8)	106(8)	-48(5)	-46(5)
C(29)	28(4)	192(12)	42(4)	-49(6)	3(3)	-26(6)
C(30)	33(3)	29(3)	122(8)	-15(4)	-24(4)	-4(3)
C(31)	22(2)	20(2)	14(2)	1(2)	3(2)	2(2)
C(32)	20(2)	21(2)	17(2)	0(2)	3(2)	1(2)
C(33)	21(2)	34(3)	10(2)	-1(2)	1(2)	0(2)
C(34)	23(2)	23(2)	19(2)	7(2)	5(2)	6(2)
C(35)	22(2)	19(2)	20(2)	-1(2)	3(2)	-1(2)
C(36)	22(2)	36(3)	22(2)	-2(2)	-3(2)	4(2)
C(37)	32(3)	20(2)	21(2)	-1(2)	4(2)	2(2)
C(38)	24(3)	62(4)	15(2)	-2(2)	-7(2)	-6(3)
C(39)	46(4)	29(3)	31(3)	12(2)	8(3)	16(3)
C(40)	36(3)	24(2)	40(3)	-8(3)	8(3)	-11(2)

Table 6 Hydrogen coordinates (x 10^4) and isotropic displacement parameters (Å^2 x 10^3) for **4.1a**.

	x	y	z	U(eq)
H(4)	5395	1205	2271	24
H(5)	4843	1528	1237	27
H(7)	4803	4055	1224	22
H(8)	5430	4387	2261	22
H(15A)	5964	-38	4462	33
H(15B)	6791	345	5008	33
H(16A)	7697	-676	4366	60
H(16B)	8170	230	4154	60
H(16C)	7334	-239	3663	60
H(12A)	6603	5766	4195	33
H(12B)	7128	5348	4865	33
H(13A)	5496	5962	5192	45
H(13B)	5362	4953	5245	45
H(13C)	4878	5454	4603	45
H(26A)	9573	3280	5121	82
H(26B)	8438	3674	4924	82
H(26C)	8682	2695	4772	82
H(27A)	9281	1172	5847	109
H(27B)	8424	1344	5256	109
H(27C)	8077	854	5939	109
H(28A)	8284	1471	7592	147
H(28B)	7618	986	7012	147
H(28C)	7029	1631	7521	147
H(29A)	7911	3897	7719	131
H(29B)	7154	3101	7871	131
H(29C)	6722	3878	7422	131
H(30A)	8598	4753	6467	92
H(30B)	7334	4735	6359	92
H(30C)	8113	4653	5713	92
H(36A)	7027	2521	-1002	40

H(36B)	6231	1886	-616	40
H(36C)	6349	2846	-358	40
H(37A)	5254	1105	-2194	37
H(37B)	4290	956	-1670	37
H(37C)	5485	1031	-1389	37
H(38A)	3822	2167	-3004	50
H(38B)	2903	2794	-2746	50
H(38C)	3009	1864	-2422	50
H(39A)	4189	4540	-2574	53
H(39B)	3647	4737	-1849	53
H(39C)	3061	4127	-2386	53
H(40A)	6150	4589	-1336	50
H(40B)	5843	4259	-586	50
H(40C)	5012	4819	-1015	50

Table 7 Torsion angles [°] for **4.1a**.

C(17)-N(1)-C(2)-C(1)	140(5)	C(15)-O(2)-C(14)-O(4)	2.3(8)
C(17)-N(1)-C(2)-C(3)	-35(6)	C(15)-O(2)-C(14)-C(3)	-178.8(5)
C(10)-C(1)-C(2)-N(1)	-173.0(5)	C(9)-C(3)-C(14)-O(4)	-15.7(9)
C(11)-C(1)-C(2)-N(1)	2.8(9)	C(2)-C(3)-C(14)-O(4)	164.7(5)
C(10)-C(1)-C(2)-C(3)	2.3(6)	C(9)-C(3)-C(14)-O(2)	165.5(4)
C(11)-C(1)-C(2)-C(3)	178.0(5)	C(2)-C(3)-C(14)-O(2)	-14.1(7)
N(1)-C(2)-C(3)-C(9)	173.1(4)	C(14)-O(2)-C(15)-C(16)	78.5(6)
C(1)-C(2)-C(3)-C(9)	-2.2(5)	C(12)-O(1)-C(11)-O(3)	10.1(8)
N(1)-C(2)-C(3)-C(14)	-7.2(8)	C(12)-O(1)-C(11)-C(1)	-169.5(5)
C(1)-C(2)-C(3)-C(14)	177.5(5)	C(2)-C(1)-C(11)-O(3)	-163.7(6)
C(9)-C(4)-C(5)-C(6)	1.1(10)	C(10)-C(1)-C(11)-O(3)	11.3(9)
C(4)-C(5)-C(6)-C(7)	3.1(10)	C(2)-C(1)-C(11)-O(1)	15.9(7)
C(4)-C(5)-C(6)-N(2)	-177.3(5)	C(10)-C(1)-C(11)-O(1)	-169.1(5)
C(18)-N(2)-C(6)-C(5)	-111(13)	C(11)-O(1)-C(12)-C(13)	82.6(6)
C(18)-N(2)-C(6)-C(7)	69(13)	C(2)-N(1)-C(17)-Ir(1)	140(4)
C(5)-C(6)-C(7)-C(8)	-0.8(9)	C(22)-Ir(1)-C(17)-N(1)	-37(4)
N(2)-C(6)-C(7)-C(8)	179.5(5)	C(21)-Ir(1)-C(17)-N(1)	-1(4)
C(6)-C(7)-C(8)-C(10)	-2.6(9)	C(25)-Ir(1)-C(17)-N(1)	33(4)
C(5)-C(4)-C(9)-C(3)	176.7(5)	C(24)-Ir(1)-C(17)-N(1)	30(4)
C(5)-C(4)-C(9)-C(10)	-6.2(9)	C(23)-Ir(1)-C(17)-N(1)	-42(4)
C(2)-C(3)-C(9)-C(4)	178.8(4)	Cl(11)-Ir(1)-C(17)-N(1)	-139(4)
C(14)-C(3)-C(9)-C(4)	-0.9(8)	Cl(12)-Ir(1)-C(17)-N(1)	133(4)
C(2)-C(3)-C(9)-C(10)	1.2(5)	C(6)-N(2)-C(18)-Ir(2)	9(17)
C(14)-C(3)-C(9)-C(10)	-178.5(5)	C(35)-Ir(2)-C(18)-N(2)	-21(4)
C(7)-C(8)-C(10)-C(1)	-176.6(5)	C(31)-Ir(2)-C(18)-N(2)	17(4)
C(7)-C(8)-C(10)-C(9)	0.4(9)	C(32)-Ir(2)-C(18)-N(2)	47(4)
C(2)-C(1)-C(10)-C(8)	176.1(5)	C(33)-Ir(2)-C(18)-N(2)	33(4)
C(11)-C(1)-C(10)-C(8)	0.3(8)	C(34)-Ir(2)-C(18)-N(2)	-34(4)
C(2)-C(1)-C(10)-C(9)	-1.4(6)	Cl(22)-Ir(2)-C(18)-N(2)	-128(4)
C(11)-C(1)-C(10)-C(9)	-177.2(5)	Cl(21)-Ir(2)-C(18)-N(2)	144(4)
C(4)-C(9)-C(10)-C(8)	5.2(9)	C(17)-Ir(1)-C(21)-C(22)	-115.4(3)
C(3)-C(9)-C(10)-C(8)	-177.3(5)	C(25)-Ir(1)-C(21)-C(22)	119.0(5)
C(4)-C(9)-C(10)-C(1)	-177.4(5)	C(24)-Ir(1)-C(21)-C(22)	81.1(4)
C(3)-C(9)-C(10)-C(1)	0.1(6)	C(23)-Ir(1)-C(21)-C(22)	40.5(4)

Cl(11)-Ir(1)-C(21)-C(22)	-19.4(4)	C(17)-Ir(1)-C(22)-C(23)	-175.9(4)
Cl(12)-Ir(1)-C(21)-C(22)	151.0(3)	C(21)-Ir(1)-C(22)-C(23)	113.1(5)
C(17)-Ir(1)-C(21)-C(25)	125.5(4)	C(25)-Ir(1)-C(22)-C(23)	76.0(4)
C(22)-Ir(1)-C(21)-C(25)	-119.0(5)	C(24)-Ir(1)-C(22)-C(23)	34.7(4)
C(24)-Ir(1)-C(21)-C(25)	-37.9(4)	Cl(11)-Ir(1)-C(22)-C(23)	-80.0(3)
C(23)-Ir(1)-C(21)-C(25)	-78.5(4)	Cl(12)-Ir(1)-C(22)-C(23)	33.7(7)
Cl(11)-Ir(1)-C(21)-C(25)	-138.4(3)	C(27)-C(22)-C(23)-C(24)	178.2(6)
Cl(12)-Ir(1)-C(21)-C(25)	31.9(4)	C(21)-C(22)-C(23)-C(24)	4.5(6)
C(17)-Ir(1)-C(21)-C(26)	7.0(6)	Ir(1)-C(22)-C(23)-C(24)	-60.0(4)
C(22)-Ir(1)-C(21)-C(26)	122.4(7)	C(27)-C(22)-C(23)-C(28)	-4.9(9)
C(25)-Ir(1)-C(21)-C(26)	-118.5(7)	C(21)-C(22)-C(23)-C(28)	-178.6(5)
C(24)-Ir(1)-C(21)-C(26)	-156.4(7)	Ir(1)-C(22)-C(23)-C(28)	116.9(5)
C(23)-Ir(1)-C(21)-C(26)	163.0(7)	C(27)-C(22)-C(23)-Ir(1)	-121.8(6)
Cl(11)-Ir(1)-C(21)-C(26)	103.0(6)	C(21)-C(22)-C(23)-Ir(1)	64.4(4)
Cl(12)-Ir(1)-C(21)-C(26)	-86.6(6)	C(17)-Ir(1)-C(23)-C(24)	127.0(5)
C(25)-C(21)-C(22)-C(27)	-179.4(6)	C(22)-Ir(1)-C(23)-C(24)	119.9(5)
C(26)-C(21)-C(22)-C(27)	2.1(9)	C(21)-Ir(1)-C(23)-C(24)	79.6(4)
Ir(1)-C(21)-C(22)-C(27)	120.0(6)	C(25)-Ir(1)-C(23)-C(24)	35.8(4)
C(25)-C(21)-C(22)-C(23)	-5.7(6)	Cl(11)-Ir(1)-C(23)-C(24)	-136.0(4)
C(26)-C(21)-C(22)-C(23)	175.8(5)	Cl(12)-Ir(1)-C(23)-C(24)	-46.4(4)
Ir(1)-C(21)-C(22)-C(23)	-66.3(3)	C(17)-Ir(1)-C(23)-C(22)	7.1(6)
C(25)-C(21)-C(22)-Ir(1)	60.6(4)	C(21)-Ir(1)-C(23)-C(22)	-40.3(3)
C(26)-C(21)-C(22)-Ir(1)	-117.9(6)	C(25)-Ir(1)-C(23)-C(22)	-84.1(4)
C(17)-Ir(1)-C(22)-C(27)	-52.0(8)	C(24)-Ir(1)-C(23)-C(22)	-119.9(5)
C(21)-Ir(1)-C(22)-C(27)	-122.9(9)	Cl(11)-Ir(1)-C(23)-C(22)	104.1(3)
C(25)-Ir(1)-C(22)-C(27)	-160.0(8)	Cl(12)-Ir(1)-C(23)-C(22)	-166.3(3)
C(24)-Ir(1)-C(22)-C(27)	158.6(8)	C(17)-Ir(1)-C(23)-C(28)	-108.4(8)
C(23)-Ir(1)-C(22)-C(27)	124.0(9)	C(22)-Ir(1)-C(23)-C(28)	-115.4(10)
Cl(11)-Ir(1)-C(22)-C(27)	44.0(7)	C(21)-Ir(1)-C(23)-C(28)	-155.7(9)
Cl(12)-Ir(1)-C(22)-C(27)	157.6(6)	C(25)-Ir(1)-C(23)-C(28)	160.5(9)
C(17)-Ir(1)-C(22)-C(21)	71.0(3)	C(24)-Ir(1)-C(23)-C(28)	124.7(10)
C(25)-Ir(1)-C(22)-C(21)	-37.1(3)	Cl(11)-Ir(1)-C(23)-C(28)	-11.3(9)
C(24)-Ir(1)-C(22)-C(21)	-78.5(4)	Cl(12)-Ir(1)-C(23)-C(28)	78.2(9)
C(23)-Ir(1)-C(22)-C(21)	-113.1(5)	C(22)-C(23)-C(24)-C(25)	-1.5(7)
Cl(11)-Ir(1)-C(22)-C(21)	166.9(3)	C(28)-C(23)-C(24)-C(25)	-178.2(6)
Cl(12)-Ir(1)-C(22)-C(21)	-79.4(6)	Ir(1)-C(23)-C(24)-C(25)	-58.7(4)

C(22)-C(23)-C(24)-C(29)	177.7(6)	C(26)-C(21)-C(25)-C(30)	-1.8(9)
C(28)-C(23)-C(24)-C(29)	1.1(11)	Ir(1)-C(21)-C(25)-C(30)	-120.3(6)
Ir(1)-C(23)-C(24)-C(29)	120.6(7)	C(22)-C(21)-C(25)-Ir(1)	-60.0(4)
C(22)-C(23)-C(24)-Ir(1)	57.1(4)	C(26)-C(21)-C(25)-Ir(1)	118.5(5)
C(28)-C(23)-C(24)-Ir(1)	-119.5(6)	C(17)-Ir(1)-C(25)-C(24)	-177.7(4)
C(17)-Ir(1)-C(24)-C(23)	-116.7(5)	C(22)-Ir(1)-C(25)-C(24)	-78.3(4)
C(22)-Ir(1)-C(24)-C(23)	-37.6(4)	C(21)-Ir(1)-C(25)-C(24)	-115.5(5)
C(21)-Ir(1)-C(24)-C(23)	-81.5(4)	C(23)-Ir(1)-C(25)-C(24)	-34.6(4)
C(25)-Ir(1)-C(24)-C(23)	-121.0(6)	Cl(11)-Ir(1)-C(25)-C(24)	-16.2(6)
Cl(11)-Ir(1)-C(24)-C(23)	50.9(4)	Cl(12)-Ir(1)-C(25)-C(24)	87.5(4)
Cl(12)-Ir(1)-C(24)-C(23)	142.0(4)	C(17)-Ir(1)-C(25)-C(21)	-62.1(4)
C(17)-Ir(1)-C(24)-C(25)	4.3(7)	C(22)-Ir(1)-C(25)-C(21)	37.2(3)
C(22)-Ir(1)-C(24)-C(25)	83.4(4)	C(24)-Ir(1)-C(25)-C(21)	115.5(5)
C(21)-Ir(1)-C(24)-C(25)	39.5(3)	C(23)-Ir(1)-C(25)-C(21)	80.9(4)
C(23)-Ir(1)-C(24)-C(25)	121.0(6)	Cl(11)-Ir(1)-C(25)-C(21)	99.4(4)
Cl(11)-Ir(1)-C(24)-C(25)	171.9(3)	Cl(12)-Ir(1)-C(25)-C(21)	-157.0(3)
Cl(12)-Ir(1)-C(24)-C(25)	-97.0(4)	C(17)-Ir(1)-C(25)-C(30)	59.2(7)
C(17)-Ir(1)-C(24)-C(29)	120.3(8)	C(22)-Ir(1)-C(25)-C(30)	158.5(7)
C(22)-Ir(1)-C(24)-C(29)	-160.7(9)	C(21)-Ir(1)-C(25)-C(30)	121.4(8)
C(21)-Ir(1)-C(24)-C(29)	155.5(9)	C(24)-Ir(1)-C(25)-C(30)	-123.1(8)
C(25)-Ir(1)-C(24)-C(29)	115.9(10)	C(23)-Ir(1)-C(25)-C(30)	-157.7(7)
C(23)-Ir(1)-C(24)-C(29)	-123.1(10)	Cl(11)-Ir(1)-C(25)-C(30)	-139.3(6)
Cl(11)-Ir(1)-C(24)-C(29)	-72.1(8)	Cl(12)-Ir(1)-C(25)-C(30)	-35.7(6)
Cl(12)-Ir(1)-C(24)-C(29)	19.0(8)	C(18)-Ir(2)-C(31)-C(35)	-107.7(3)
C(23)-C(24)-C(25)-C(21)	-2.0(7)	C(32)-Ir(2)-C(31)-C(35)	117.3(4)
C(29)-C(24)-C(25)-C(21)	178.6(5)	C(33)-Ir(2)-C(31)-C(35)	79.7(3)
Ir(1)-C(24)-C(25)-C(21)	-62.7(4)	C(34)-Ir(2)-C(31)-C(35)	38.4(3)
C(23)-C(24)-C(25)-C(30)	-176.8(6)	Cl(22)-Ir(2)-C(31)-C(35)	-10.9(4)
C(29)-C(24)-C(25)-C(30)	3.9(10)	Cl(21)-Ir(2)-C(31)-C(35)	156.3(2)
Ir(1)-C(24)-C(25)-C(30)	122.6(6)	C(18)-Ir(2)-C(31)-C(32)	135.0(3)
C(23)-C(24)-C(25)-Ir(1)	60.6(5)	C(35)-Ir(2)-C(31)-C(32)	-117.3(4)
C(29)-C(24)-C(25)-Ir(1)	-118.7(6)	C(33)-Ir(2)-C(31)-C(32)	-37.6(3)
C(22)-C(21)-C(25)-C(24)	4.9(6)	C(34)-Ir(2)-C(31)-C(32)	-78.9(3)
C(26)-C(21)-C(25)-C(24)	-176.5(5)	Cl(22)-Ir(2)-C(31)-C(32)	-128.2(3)
Ir(1)-C(21)-C(25)-C(24)	64.9(4)	Cl(21)-Ir(2)-C(31)-C(32)	39.0(3)
C(22)-C(21)-C(25)-C(30)	179.6(6)	C(18)-Ir(2)-C(31)-C(36)	14.0(5)

C(35)-Ir(2)-C(31)-C(36)	121.7(6)	C(31)-C(32)-C(33)-C(38)	176.7(5)
C(32)-Ir(2)-C(31)-C(36)	-121.0(6)	C(37)-C(32)-C(33)-C(38)	2.0(8)
C(33)-Ir(2)-C(31)-C(36)	-158.7(5)	Ir(2)-C(32)-C(33)-C(38)	-122.1(5)
C(34)-Ir(2)-C(31)-C(36)	160.1(5)	C(31)-C(32)-C(33)-Ir(2)	-61.2(3)
Cl(22)-Ir(2)-C(31)-C(36)	110.8(4)	C(37)-C(32)-C(33)-Ir(2)	124.1(5)
Cl(21)-Ir(2)-C(31)-C(36)	-82.0(5)	C(18)-Ir(2)-C(33)-C(34)	-98.0(5)
C(35)-C(31)-C(32)-C(33)	2.1(5)	C(35)-Ir(2)-C(33)-C(34)	-36.9(3)
C(36)-C(31)-C(32)-C(33)	-175.9(4)	C(31)-Ir(2)-C(33)-C(34)	-80.1(3)
Ir(2)-C(31)-C(32)-C(33)	63.0(3)	C(32)-Ir(2)-C(33)-C(34)	-118.5(4)
C(35)-C(31)-C(32)-C(37)	176.7(5)	Cl(22)-Ir(2)-C(33)-C(34)	61.8(3)
C(36)-C(31)-C(32)-C(37)	-1.3(8)	Cl(21)-Ir(2)-C(33)-C(34)	151.2(3)
Ir(2)-C(31)-C(32)-C(37)	-122.5(5)	C(18)-Ir(2)-C(33)-C(32)	20.5(6)
C(35)-C(31)-C(32)-Ir(2)	-60.9(3)	C(35)-Ir(2)-C(33)-C(32)	81.6(3)
C(36)-C(31)-C(32)-Ir(2)	121.2(5)	C(31)-Ir(2)-C(33)-C(32)	38.4(3)
C(18)-Ir(2)-C(32)-C(33)	-170.5(3)	C(34)-Ir(2)-C(33)-C(32)	118.5(4)
C(35)-Ir(2)-C(32)-C(33)	-79.3(3)	Cl(22)-Ir(2)-C(33)-C(32)	-179.7(3)
C(31)-Ir(2)-C(32)-C(33)	-117.2(4)	Cl(21)-Ir(2)-C(33)-C(32)	-90.2(3)
C(34)-Ir(2)-C(32)-C(33)	-36.3(3)	C(18)-Ir(2)-C(33)-C(38)	138.3(5)
Cl(22)-Ir(2)-C(32)-C(33)	0.6(5)	C(35)-Ir(2)-C(33)-C(38)	-160.6(6)
Cl(21)-Ir(2)-C(32)-C(33)	93.1(3)	C(31)-Ir(2)-C(33)-C(38)	156.2(6)
C(18)-Ir(2)-C(32)-C(31)	-53.3(3)	C(32)-Ir(2)-C(33)-C(38)	117.8(6)
C(35)-Ir(2)-C(32)-C(31)	37.9(3)	C(34)-Ir(2)-C(33)-C(38)	-123.7(7)
C(33)-Ir(2)-C(32)-C(31)	117.2(4)	Cl(22)-Ir(2)-C(33)-C(38)	-61.9(5)
C(34)-Ir(2)-C(32)-C(31)	80.9(3)	Cl(21)-Ir(2)-C(33)-C(38)	27.6(5)
Cl(22)-Ir(2)-C(32)-C(31)	117.8(3)	C(32)-C(33)-C(34)-C(35)	-2.7(6)
Cl(21)-Ir(2)-C(32)-C(31)	-149.7(2)	C(38)-C(33)-C(34)-C(35)	-178.9(5)
C(18)-Ir(2)-C(32)-C(37)	68.3(5)	Ir(2)-C(33)-C(34)-C(35)	57.2(3)
C(35)-Ir(2)-C(32)-C(37)	159.4(5)	C(32)-C(33)-C(34)-C(39)	179.1(5)
C(31)-Ir(2)-C(32)-C(37)	121.5(6)	C(38)-C(33)-C(34)-C(39)	2.9(9)
C(33)-Ir(2)-C(32)-C(37)	-121.2(6)	Ir(2)-C(33)-C(34)-C(39)	-121.0(5)
C(34)-Ir(2)-C(32)-C(37)	-157.5(5)	C(32)-C(33)-C(34)-Ir(2)	-59.9(3)
Cl(22)-Ir(2)-C(32)-C(37)	-120.7(4)	C(38)-C(33)-C(34)-Ir(2)	123.9(5)
Cl(21)-Ir(2)-C(32)-C(37)	-28.1(5)	C(18)-Ir(2)-C(34)-C(33)	140.6(3)
C(31)-C(32)-C(33)-C(34)	0.4(5)	C(35)-Ir(2)-C(34)-C(33)	119.9(4)
C(37)-C(32)-C(33)-C(34)	-174.3(5)	C(31)-Ir(2)-C(34)-C(33)	81.3(3)
Ir(2)-C(32)-C(33)-C(34)	61.6(3)	C(32)-Ir(2)-C(34)-C(33)	37.5(3)

Cl(22)-Ir(2)-C(34)-C(33)	-124.6(3)	Ir(2)-C(34)-C(35)-C(31)	63.6(3)
Cl(21)-Ir(2)-C(34)-C(33)	-36.7(3)	C(33)-C(34)-C(35)-C(40)	176.4(5)
C(18)-Ir(2)-C(34)-C(35)	20.6(4)	C(39)-C(34)-C(35)-C(40)	-5.4(8)
C(31)-Ir(2)-C(34)-C(35)	-38.6(3)	Ir(2)-C(34)-C(35)-C(40)	-124.1(5)
C(32)-Ir(2)-C(34)-C(35)	-82.4(3)	C(33)-C(34)-C(35)-Ir(2)	-59.5(4)
C(33)-Ir(2)-C(34)-C(35)	-119.9(4)	C(39)-C(34)-C(35)-Ir(2)	118.7(5)
Cl(22)-Ir(2)-C(34)-C(35)	115.5(3)	C(18)-Ir(2)-C(35)-C(31)	77.3(3)
Cl(21)-Ir(2)-C(34)-C(35)	-156.7(2)	C(32)-Ir(2)-C(35)-C(31)	-38.2(3)
C(18)-Ir(2)-C(34)-C(39)	-97.9(5)	C(33)-Ir(2)-C(35)-C(31)	-80.8(3)
C(35)-Ir(2)-C(34)-C(39)	-118.6(6)	C(34)-Ir(2)-C(35)-C(31)	-116.3(4)
C(31)-Ir(2)-C(34)-C(39)	-157.2(6)	Cl(22)-Ir(2)-C(35)-C(31)	173.5(2)
C(32)-Ir(2)-C(34)-C(39)	159.0(6)	Cl(21)-Ir(2)-C(35)-C(31)	-58.8(5)
C(33)-Ir(2)-C(34)-C(39)	121.5(6)	C(18)-Ir(2)-C(35)-C(34)	-166.5(3)
Cl(22)-Ir(2)-C(34)-C(39)	-3.1(5)	C(31)-Ir(2)-C(35)-C(34)	116.3(4)
Cl(21)-Ir(2)-C(34)-C(39)	84.8(5)	C(32)-Ir(2)-C(35)-C(34)	78.1(3)
C(32)-C(31)-C(35)-C(34)	-3.8(5)	C(33)-Ir(2)-C(35)-C(34)	35.4(3)
C(36)-C(31)-C(35)-C(34)	174.1(5)	Cl(22)-Ir(2)-C(35)-C(34)	-70.2(3)
Ir(2)-C(31)-C(35)-C(34)	-65.4(3)	Cl(21)-Ir(2)-C(35)-C(34)	57.5(5)
C(32)-C(31)-C(35)-C(40)	-176.1(5)	C(18)-Ir(2)-C(35)-C(40)	-43.8(5)
C(36)-C(31)-C(35)-C(40)	1.8(8)	C(31)-Ir(2)-C(35)-C(40)	-121.0(6)
Ir(2)-C(31)-C(35)-C(40)	122.2(5)	C(32)-Ir(2)-C(35)-C(40)	-159.2(5)
C(32)-C(31)-C(35)-Ir(2)	61.7(3)	C(33)-Ir(2)-C(35)-C(40)	158.1(5)
C(36)-C(31)-C(35)-Ir(2)	-120.4(5)	C(34)-Ir(2)-C(35)-C(40)	122.7(6)
C(33)-C(34)-C(35)-C(31)	4.1(6)	Cl(22)-Ir(2)-C(35)-C(40)	52.5(5)
C(39)-C(34)-C(35)-C(31)	-177.7(5)	Cl(21)-Ir(2)-C(35)-C(40)	-179.8(3)